Technical Report GL-94-17
April 1994

US Army Corps
of Engineers
Waterways Experiment
Station

Force Projection Site Evaluation Using the Electric Cone Penetrometer (ECP) and the Dynamic Cone Penetrometer (DCP)

by Steve L. Webster

Randall W. Brown
USAF Academy

Jonathan R. Porter
Wright Laboratory

Approved For Public Release; Distribution Is Unlimited

Prepared for Headquarters, Air Force Civil Engineering Support Agency

PRINTED ON RECYCLED PAPER

Technical Report GL-94-17
April 1994

Force Projection Site Evaluation Using the Electric Cone Penetrometer (ECP) and the Dynamic Cone Penetrometer (DCP)

by Steve L. Webster

U.S. Army Corps of Engineers
Waterways Experiment Station
3909 Halls Ferry Road
Vicksburg, MS 39180-6199

Randall W. Brown

Department of Civil Engineering
USAF Academy, CO 80840

Jonathan R. Porter

Wright Laboratory
Tyndall AFB, FL 32403-6001

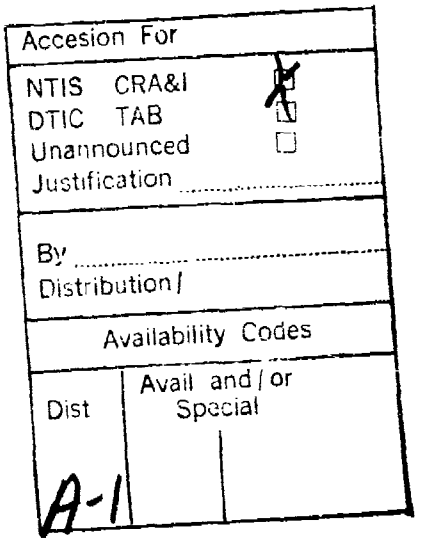

Final Report

Approved for public release; distribution is unlimited

Prepared for U.S. Air Force
Headquarters, Air Force Civil Engineering Support Agency
Tyndall AFB, FL 32403-6001

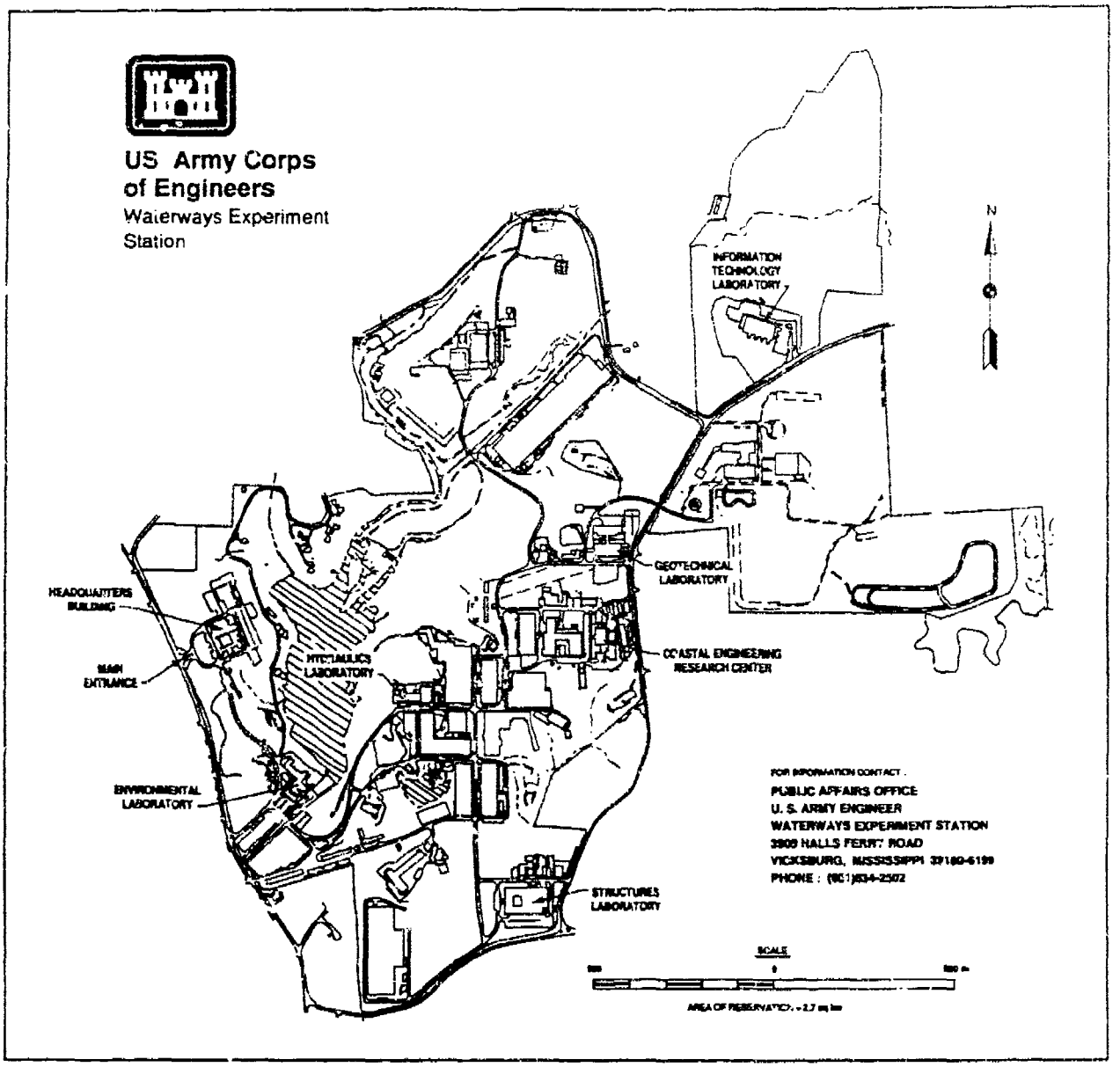

Waterways Experiment Station Cataloging-In-Publication Data

Webster, Steve L.

Force projection site evaluation using the electric cone penetrometer (ECP) and the dynamic cone penetrometer (DCP) / by Steve L. Webster, Randall W. Brown, Jonathan R. Porter ; prepared for U.S. Air Force, Headquarters, Air Force Civil Engineering Support Agency.

172 p. : ill. ; 28 cm. — (Technical report ; GL-94-17)

Includes bibliographic references.

1. Pavements — Testing — Instruments. 2. Runways (Aeronautics) — Testing. 3. Penetrometer. I. Brown, Randall W. II. Porter, Jonathan R. III. United States. Army. Corps of Engineers. IV. U.S. Army Engineer Waterways Experiment Station. V. Air Force Civil Engineering Support Agency. VI. Title. VII. Series: Technical report (U.S. Army Engineer Waterways Experiment Station) ; GL-94-17.

TA7 W34 no.GL-94-17

Contents

List of Tables

Preface

The investigation described in this report was sponsored by the Headquarters, Air Force Civil Engineering Support Agency (HQ AFCESA), Tyndall AFB, FL. The work was conducted under Military Interdepartmental Purchase Request Numbers N 92-21 and N 93-9, Project "Force Projection Site Evaluation." Technical Monitors were CPT M. J. Coats and Mr. Jim Murfee, AFCESA/RACO, now Wright Laboratory, Flight Dynamics Directorate, Air Base Systems Branch, (WL/FIVCO), Tyndall AFB, FL.

The study was conducted in two phases. The first phase involved field tests conducted at Maxwell AFB, AL, during the period 6 to 10 July 1992 under the direction of MAJ R. W. Brown, PhD, Department of Civil Engineering, USAF Academy, CO, and Mr. J. R. Porter, Wright Laboratory, Tyndall AFB, FL. The second phase was conducted at the U.S. Army Engineer Waterways Experiment Station (WES) during the period March 1992 through July 1993 by the Pavement Systems Division (PSD), Geotechnical Laboratory (GL). Personnel of the PSD involved in this study were Messrs. S. L. Webster, T. P. Williams, J. S. Tingle, A. W. Brown, and Ms. R. L. Santoni. This report was prepared by Mr. Webster, MAJ Brown, PhD, and Mr. Porter.

Field tests using the Air Force Contingency Test Van were conducted at WES during October 1992 under supervision of CPT D. J. Christiansen, Pavement Evaluation Team Chief, HQ AFCESA, Tyndall AFB, FL. Mr. D. A. Timian, Applied Research Associates (ARA), South Royalton, VT. conducted the seismic cone penetration tests at WES. The seismic cone test results are not included in this report.

The study was conducted under the general supervision of Dr. W. F. Marcuson III, Director, GL, and under the direct supervision of Drs. G. M. Hammitt II, Chief, PSD, and A. J. Bush III, Chief, Criteria Development and Applications Branch, PSD.

At the time of publication of this report, Director of WES was Dr. Robert W. Whalin. Commander was COL Bruce K. Howard, EN.

1 Introduction

Background

World political and economic changes over the last decade have dictated the United States Air Force (USAF) alter its concept of operations from prepositioning forces to projecting forces into the needed area. This force projection concept generates a requirement for rapid, accurate assessment of an unfamiliar airfield's load-carrying capability with minimum logistical support. USAF development of Dynamic Cone Penetrometer (DCP) and Electric Cone Penetrometer (ECP) capabilities have aided in meeting this requirement.

Electric cone penetrometer. The AFCESA's Contingency Soils/Pavement Testing Van (Figure 1) is a rugged and C-130 transportable vehicle equipped to deploy to a remote site and perform ECP tests, CBR tests, pavement coring and strength tests, soil classification and other lab testing, and computer analysis necessary for contingency airfield evaluations. The ECP is a major part of the contingency van. The ECP test is conducted in accordance with ASTM D3441-86 (ASTM 1989) for Quasi-static Friction-cone Penetration Tests in Soil. It uses the standard 1.41 in. diameter cone with a 60 degree conical tip (Figure 2). It has a 5.27-in.-long friction sleeve (area = 23.2 sq in.) located just beyond the cone base. A 1.5 in. diameter expander is located 5.25 in. behind the top of the friction sleeve to push the hole open and reduce friction drag on the push tube. The ECP is pushed through pavement layers to any desired depth (usually 5 ft) at a standard rate of 0.8 in. per second. The depth of penetration is measured with a string potentiometer mounted inside the van. The contingency van has a ballast of 32,000 lbs and a 20-ton hydraulic press that normally pushes the ECP cone 5 ft into the pavement. Two load cells inside the ECP independently measure the loads against the cone tip and friction sleeve. The load cells send analog data to signal conditioners where it is amplified and filtered. The analog signals are then digitized at the normal rate of one sample per second. The digital data is then stored in computer memory for future processing.

In pavement evaluations, the ECP measures shear strengths of the various material layers and reports the results in terms of cone tip and sleeve friction resistance (psi) with depth. The ratio of sleeve friction resistance to cone resistance, called the friction ratio, has been used to help classify soil types. The ECP can also be used to measure the thicknesses of the various pavement layers, which is critical information in pavement evaluations.

Dynamic cone penetrometer. The DCP is a hand held device designed to penetrate soils to depths of 39 in. with a 0.79 in. diameter cone (Figure 3). The 60 degree cone is forced into the ground by raising and dropping a 17.6-lb hammer. The number of hammer drops and cone penetration are recorded for each test. Data on cone penetration per hammer blow is translated into a DCP index value (mm/blow). Individual DCP shear strength values are reported for each test depth resulting in a strength with depth profile for each test location.

Current ECP/DCP correlations with CBR. There are correlations for both devices which estimate the bearing capacity of the soil in terms of CBR. The CBR values are then used with nomographs to determine allowable passes of certain aircraft. The accuracy of current correlations is weak for both devices. The DCP/CBR correlation is based on work done by others supplemented by a growing data base being developed at the Waterways Experiment Station (WES), Vicksburg, MS. The most recent DCP/CBR correlation is reported by Webster, Grau, and Williams (1992). The correlation is CBR = $292/DCP^{1.12}$ where DCP is in terms of mm/blow. Current ECP/CBR correlations are based on very limited data which were summarized by Buncher and Christiansen (1992). The Correlation Factor (CF) is defined by: Tip Pressure (tons/sq ft) X CF = CBR. Their research indicated that separate correlation factors (based on tip pressure in tons/sq ft)were appropriate for each of three soil groups: 0.26 for fat clays, 0.13 for gravels, and 0.11 for sands and lean clays. To simplify the evaluation process, they recommended a correlation factor of 0.12 be used for all soils except fat clays. They also recognized that further research was needed to refine the correlations and also incorporate sleeve friction for classifying soils.

Purpose

The purpose of the research effort described in this report was to improve the accuracy of USAF force projection site (contingency airfield) evaluations. The purposes of this report are to (1) describe ECP/CBR tests conducted at Maxwell AFB, AL, (2) describe ECP/DCP/CBR tests conducted on field test sections at WES, (3) present correlations developed for DCP versus CBR and ECP versus CBR, and (4) offer ECP test procedures for pavement evaluation.

Scope

This report describes the ECP, CBR, and other related soil tests conducted at two field test sites at Maxwell AFB, AL during the period 6 to 10 July 1992. The report also describes ECP, Seismic ECP, DCP, CBR, and related soil tests conducted on four field test sections constructed and tested during the period July - November 1992 at WES. This report describes the data analysis conducted which included (1) ECP data interpretation schemes, (2) effect of overburden on test results, (3) soil classification from ECP data,

(4) ECP versus CBR correlations, and (5) DCP versus CBR correlations. The report also describes recommended ECP test procedures for pavement evaluation. In the conduct of this study, other data was collected but is not presented in this report. This data included (1) falling weight deflectometer, (2) nuclear density and moisture, (3) sand cone density and moisture, and (4) seismic ECP test results. This data was collected for other studies and future reference.

2 Description of Tests

Maxwell AFB Field Tests

Test plan

The objectives of the prototype testing at Maxwell AFB (MAFB) were to (1) determine any equipment or procedural problems which could be corrected prior to the WES field tests, (2) assess the viability of adding seismic testing to the ECP, (3) collect ECP data on actual airfield pavements, and (4) obtain data on the effect of overburden on ECP test results.

Equipment upgrade. Prior to the MAFB field tests, the following modifications were made to the contingency van to improve its effectiveness for performing pavement evaluations:

a. *Hardware.* Changes consisted of upgrading the signal amplifiers, which are part of the data acquisition system. The upgrade to current state-of-the-art circuitry allowed increases in signal gain and an increase in the number of filtering options available, while reducing extraneous noise. After the system was debugged, the new amplifiers proved to be significantly quieter, yet more flexible, than the older amplifiers.

b. *Software.* The data acquisition software, which was written by Applied Research Associates, Inc. (ARA) in the ASYST data acquisition programming language, was upgraded to the newest version available from ARA. The benefits of this upgrade include more powerful oversampling routines to eliminate spikes and erroneous data points, and increased control of the data acquisition system (software selectable gains, sampling rates, filtering options, etc.). The combination of the new signal amplifiers and the new software produced a data acquisition system superior to its predecessor, resulting in better quality data that is easier to interpret.

c. *Seismic capacity.* The capability to perform seismic cone penetration tests was added to the contingency van. The data acquisition software upgrade mentioned previously included the modules necessary for seismic testing. In addition, three velocity seismometers were installed in the cone to be used as the receivers for the tests. Two seismic (shear

wave) sources were provided for further testing. The simpler one consists of a large wooden block with a data acquisition trigger attached. To provide the surcharge weight necessary for good energy transfer, the block is placed under one of the van's jacks before leveling. The block is struck with a sledge hammer to generate a shear wave. The second source is based on a prototype developed at the University of Florida (UF). A horizontally acting pneumatic hammer is connected to a movable mass in a steel box. The hammer can be fired in both directions to produce polarized shear waves. A special jacking plate was machined to mount the UF hammer to the contingency van. The air is supplied by the brake compressor on the van, and the hammer is fired by electric solenoid valves which draw power from the van's generator or inverter. Two base plates for the UF source can be used: one was developed for use in soils, the other for use on asphalt. Details of the development and operation of the UF source are reported by Bates (1992) and Maxwell (1990).

Description of tests conducted

Figure 4 shows the location of two test pits selected on abandoned portions of the airfield at MAFB. Original construction of the airfield at these locations is estimated to have occurred at least 50 years ago. The pavement at these test sites was last evaluated by the Air Force in 1980. The pavement at each test pit location was similar, consisting of an asphalt overlay on an asphalt macadam layer, a sand asphalt layer (pit 1 only), a river-run gravel base course, and a clay or silt subgrade. A typical plan view of the test pits is shown in Figure 5. Each test pit was approximately 3.5 ft wide by 17.5 ft long. The asphalt concrete, asphalt macadam, and sand asphalt (pit 1) layers were excavated from each pit prior to testing. ECP tests were also run thru the asphalt surface at an offset of 12 ft from the pit. Figures 6 and 7 show profiles of test pits 1 and 2 including the tests conducted. ECP, CBR, nuclear density and moisture content, oven moisture, and soil classification tests were performed.

Test sequence. The testing sequence began with a series of six ECP tests on an undisturbed pavement section, in a line parallel to the test pit. Concurrently, the asphalt and macadam layers of the test pit were removed. A series of six ECPs were then performed in the test pit, with the base course and subgrade as the only resisting layers. Following completion of the ECPs in the test pit, CBR series were performed on the surface of the base course in the test pit. One series (varying depth) of nuclear density/moisture content tests was performed on the base course material. During removal of the base course layer in the test pit, bag samples for material classification and moisture content samples were collected. Once the surface of the subgrade material was exposed, CBR series and nuclear density/moisture content tests were performed on the subgrade. Bag samples and moisture content samples of the subgrade material were collected prior to backfilling of the test pit.

ECP tests. The cone penetration tests were performed using AFCESA/DMP's contingency van. The penetrometer probe has a standard 1.41 in. diameter, 60° conical tip, and a 1.41-in. diameter by 5.27-in. long friction sleeve. The cone penetrometer was manufactured by Applied Research Associates (ARA). Data acquisition on the contingency van is handled by a 386 personal computer running proprietary software written by ARA in the ASYST Data Acquisition Programming Language. To achieve the goals of the tests at MAFB, it was sufficient to penetrate about 6 ft during each cone penetration test. For ECPs performed in the test pits, the surface of the asphalt was used as the datum so that tests in the pit and tests outside of the pit could be directly compared. It should be noted that the overburden stress at a given depth was different in the two series of ECP tests.

CBR tests. The CBR tests were performed in accordance with MIL-STD-621A (Department of Defense 1968). The contingency van provided the reaction weight for the CBR tests.

Nuclear density/moisture tests. The nuclear density and moisture content tests were performed on the base course and subgrade material of each test pit. The density tests were performed at 2-, 4-, 6-, 8-, 10-, and 12-in. depths in each material.

Laboratory tests. One moisture content sample of each material in both test pits was collected for comparison with the results of the nuclear moisture content tests. Bag samples of the materials were returned to the soils lab at AFCESA. Grain size distributions and Atterberg limits were determined for each material to allow classification by the Unified Soil Classification System (USCS) (WES 1960). Results of the laboratory tests are included in Appendix A.

WES Test Sections

Layout

A layout of the four WES test sections is shown in Figure 8. The test sections were constructed under shelter in WES Hangar No. 4. Each test section was 12 ft wide and varied in length from 30-144 ft. A description of the design, plan and profile, materials, and construction of each test section follows.

Test Section 1 (weak soil wedge)

Design. Test Section 1 contained a weak soil wedge and was designed to determine the capability of the ECP and DCP to detect and measure the strength and location of a thin weak soil layer. The ECP tests were conducted at two penetration rates to determine the effects of penetration rate on

detecting a thin weak soil layer. The standard penetration rate of 0.8 in./sec and a slower penetration rate of 0.2 in./sec were used.

Plan and profile. A plan and profile of test Section 1 (weak soil wedge) is shown in Figure 9. The test section consisted of a weak soil wedge of lean clay (CL), having a CBR < 10, sandwiched between two firm layers of clayey sand (SC), having a CBR > 10. The weak soil wedge varied in thickness from 0- to 24-in. ECP tests were conducted at 3-ft intervals along the 12-ft-wide by 30-ft-long test section. The ECP tests included 7 tests at the standard penetration rate of 0.8 in./sec, 7 tests at a penetration rate of 0.2 in./sec, and 4 seismic tests located as shown in Figure 8. In addition, DCP tests were conducted between the standard and slow-rate ECP tests. Two CBR pits were dug in test Section 1.

Materials. The properties of the clayey sand (SC) and lean clay (CL) are shown in Appendix A. The lean clay had a liquid limit (LL) of 39 and a plasticity index (PI) of 15 and was obtained from a site on the WES reservation. The clayey sand (SC) had a LL of 25 and PI of 11 and was purchased locally from Runyon Construction Co. It had a maximum aggregate size of 3/4 in. with 20 percent passing the No. 200 sieve.

Construction. A trench 48 inches deep was dug in the natural soil floor of Hangar No. 4. The bottom of the trench was compacted to CBR > 10 using a self-propelled smooth drum vibratory compactor. Two 6-in.-thick layers of clayey sand were installed in the bottom of the trench. The clayey sand was installed at a water content of 11 percent and was compacted using the smooth drum vibratory compactor and a self-propelled 36,000-lb rubber-tired roller. The CBR of the clayey sand was not measured but was well in excess of 10 CBR. Next, a wooden frame in the shape of the wedge was constructed on the firm clayey sand layer. The frame had support runners along the edges of the trench which allowed workers to screed the top of the weak soil layer to produce a smooth surface. The weak soil layer was then installed in 6-in.-thick horizontal lifts and compacted with a large plate compactor. The lean clay soil had been processed to a water content of 22-25 percent in order to obtain a CBR of < 10. Sheet 6-mil polyethylene was used to encapsulate the weak soil wedge and prevent the soil layer from drying during testing. The cover layer of firm clayey sand was then installed in 6-in.-thick horizontal lifts and compacted using the plate compactor. The final surface of the test section was compacted using the self-propelled smooth drum vibratory compactor. Care had to be taken to not over-compact the surface and damage the weak soil wedge. The test section was constructed in July 1992 and covered with membrane to prevent drying until testing in October 1992.

Test Section 2 (stepped base)

Design. Test Section 2 was designed to determine the capability of the ECP and DCP to measure the strengths and thicknesses of pavement base layers ranging from 6 to 18 in. thick. Half of the test section was surfaced

with 4 in. of asphalt concrete in order to test the effect of overburden on the ECP tests. The standard penetration rate of 0.8 in./sec was used for the ECP tests.

Plan and profile. A plan and profile of test Section 2 (stepped base) is shown in Figure 10. Item 1 contained a 6-in.-thick base course. Item 2 had an 12-in.-thick base course and item 3 had an 18-in.-thick base course. The East half of each test item was surfaced with 4-in. of asphaltic concrete. ECP and seismic tests were conducted at the locations indicated.

Materials. The properties of the crushed limestone base (SW-SM) and lean clay (CL) are shown in Appendix A. The lean clay was the same as that used in test Section 1. The crushed limestone was a well graded base course material and had a maximum aggregate size of 1 in. with 10 percent passing the No. 200 sieve. The fines were non-plastic and it was obtained from an existing WES stockpile. The asphalt concrete was a standard Mississippi DOT surface mix design and was purchased locally from APAC-Mississippi, Inc. The maximum aggregate size was 1/2 in. and the minimum Marshall Stability was 1,500 lbs.

Construction. A trench 48 in. deep was dug in the natural soil floor of Hangar No. 4. The bottom of the trench was compacted using a self-propelled smooth drum vibratory compactor. Two 4-in.-thick layers of clayey sand were placed and compacted in the bottom of the trench to produce a firm foundation for the pavement layers. The lean clay (CL) soil was installed and compacted in 6-in.-thick lifts at a water content of 16 to 17 percent (optimum water content was 15 percent). The soil was compacted using the smooth drum vibratory compactor and the self-propelled 36,000-lb rubber-tired roller. Sheet 6-mil polyethylene was used to encapsulate the CL soil layer and protect it from drying during the conduct of tests. The crushed limestone base was installed in 6-in.-thick lifts at a water content of 3 to 4 percent (near optimum) and compacted to maximum density possible using the smooth drum vibratory compactor and self-propelled rubber-tired roller. The 4-in.-thick layer of asphalt concrete was installed on the East half of the test section. It was installed in two lifts. Each lift was compacted first with 4 passes of a small vibratory plate compactor followed with 4 passes of a large vibratory plate compactor.

Test Sections 3 and 4

Design. These test sections were designed to improve the current data base relating ECP, DCP, and CBR. They were also designed to provide ECP data for studying the influence of a lack of confinement effects (no pavement overburden) at the top of the surface layer which would occur when evaluating unsurfaced airfields. Other design consideration were to determine the capability of ECP and DCP to measure soil layer thicknesses and measure strength changes between firm-over-weak and weak-over-firm pavement layers. Figure 11 shows a design matrix for variables tested. The design included seven soil types which covered the range of soils usually found in

airfield pavements. Each soil was tested in a wet (of optimum) and dry (of optimum) moisture condition. Test Section 3 was designed with a lean clay (CL) subgrade compacted at a water content to yield a CBR < 10 to represent a weak subgrade. Test Section 4 was designed with a clayey sand (SC) subgrade compacted at a water content designed to produce a firm subgrade having a CBR > 10. The wet CL surface soil over CL subgrade and dry SC surface over SC subgrade were eliminated from the matrix to eliminate redundant testing. Also, the dry Yuma sand (SP) was not tested since it could not be compacted sufficiently to prevent deep rutting under aircraft loads.

Plan and profile. Figures 12 and 13 show the plan and profile for test Sections 3 and 4. Each item had a surface dimension of 12 ft by 12 ft to allow adequate area for ECP, DCP, and CBR testing. Each soil layer was 2 ft thick. A 2-in.-thick limestone cap was installed over the SP and SM soils in order to help stabilize the surface of these items during testing.

Materials. The properties of the sandy gravel (GP), crushed limestone (SW-SM), clayey sand (SC), Yuma sand (SP), silty sand (SM), fat clay (CH), and lean clay (CL) are shown in Appendix A. The SW-SM, CL, and SC soils were the same as those used in test Sections 1 and 2. The GP soil was a pit run material having a 2-in. maximum aggregate size with 2.5 percent passing the No. 200 sieve. It was non plastic and purchased locally from Runyon Construction Co. The SP soil originally came from Yuma Arizona and was taken from a WES stockpile. The SM soil was manufactured at WES using a blend of Yuma sand and WES silt.

Construction. Two trenches 48 in. deep and 144 ft long were dug in the natural soil floor of Hangar No. 4. The bottom of the trenches was compacted using a self-propelled smooth drum vibratory compactor.

a. Bottom layer. The bottom and sides of the trenches were lined with polyethylene membrane and the bottom layer materials were placed in 6-in. lifts. Each lift of the CL soil in test Section 3 was compacted with 4 coverages of the big plate compactor. The CL had a water content of 20 to 22 percent resulting in a CBR < 5 which was too weak to compact with either the smooth drum vibratory compactor or self-propelled 36,000-lb rubber-tired roller. Each lift of the SC soil in test Section 4 was compacted with 4 to 6 coverages of both the smooth drum vibratory compactor and the self-propelled rubber-tired roller.

b. Surface layer. A layer of polyethylene membrane was used to separate the surface layer and bottom layer. The membrane served as a moisture barrier and as marker for accurately measuring the thickness of soil layers. The surface layer materials were installed in 6-in. lifts. Temporary forms constructed out of 2x6-in. lumber were used to separate the various surface layer materials during soil installation. Once a lift of soil was installed, the temporary forms were removed and all the soils in the lift were compacted as a single lift of soil. Each lift of soil in test Section 3 was compacted using 4 coverages of the big plate compactor. Each lift of soil in test Section 4 was compacted using 4-6

coverages with the smooth drum vibratory compactor. The rubber-tired roller was not used because it would have rutted several of the soils. During compaction with the smooth drum vibratory compactor, sheets of polyethylene were placed over soils that tended to stick to the drum and contaminate neighboring items. This procedure worked well and prevented contamination of test item soils. After the final soil lifts were completed, a 2-in.-thick layer of crushed limestone was placed and compacted over the SP and SM soil items in order to protect them and prevent them from rutting during testing.

Description of tests conducted

Test layout. Figure 14 shows a test layout for typical test items for test Sections 2, 3, and 4. The testing sequence was ECP seismic (at selected locations in test Section 1, Figure 9, and test Section 2, Figure 10), ECP at 0.8 in./sec at test locations E1-E8, ECP at 0.2 in./sec at test locations E9-E11, DCP tests at test locations D1-D4, followed by CBR pits with CBR tests at test locations C1-C6. Panels of 2-ft by 12-ft airfield landing mat were placed as shown in Figure 14 to support the test van tires without significantly changing the soil test properties. A test nomenclature was developed for describing each test performed. For example, W3I12E4 described WES test Section 3, test item 12, ECP test location 4. Figure 15 shows a typical test item profile for test Sections 2, 3, and 4. ECP penetrations were made to depths of 5 ft. CBR tests were conducted at 0-, 6-, 12-, 24-, and 36-in. depths in each test item. DCP tests were conducted to depths of 36 in.

ECP tests. The ECP tests were performed using the same procedures used during the MAFB tests. The standard ECP tests were conducted at two penetration rates (0.8 and 0.2 in./sec) in order to determine the effects of penetration rate on ECP-measured soil strengths and capability of detecting soil layer interfaces. For all ECP tests, an initial zero-depth reading was established by pushing the penetrometer cone into the soil layer until the base of the cone was flush with the surface of the soil.

DCP tests. The DCP tests were conducted according the procedure described by Webster, Grau, and Williams (1992). The DCP had a 60° conical cone with a base diameter of 0.79 in. The test procedure involved raising and dropping an 17.6-lb hammer a distance of 22.6 in. onto an anvil which drove the penetrometer rod and cone into the soil. Depth of cone penetration measurements were recorded approximately every inch or whenever any noticeable increase in the penetration rate occurred. The number of hammer blows between penetration measurements was also recorded. A DCP strength index in terms of penetration per hammer blow was calculated for each measurement interval. The DCP index was then correlated with field CBR values. In all cases, the DCP test was run from the original test item surface.

CBR tests. The CBR tests were performed in accordance with MIL-STD-621-A. The tests were conducted by technician and labor support with 20-30 years experience with CBR tests. All CBR proving rings used were

calibrated prior to and after CBR testing. All proving rings remained in calibration throughout testing. The CBR tests were conducted using the WES field CBR truck loaded with lead blocks for a reaction weight. Water content samples for oven drying were taken immediately after CBR tests were completed.

Nuclear density/moisture tests. The nuclear density and moisture content tests were performed in each CBR test pit. Four one-minute direct transmission density tests (6-in. depth) were performed at two locations along with each CBR test series. The nuclear tests were run prior to CBR tests with the source access hole located out of the zone of influence of the CBR tests. Useful data comparing the nuclear water content versus oven water content measurements was obtained at each depth in the CBR pits. The pit side wall influence on nuclear readings was determined for each material type and water content range tested. In a related study, separate nuclear density/moisture tests were conducted on the surface layer of each test item at a location outside the CBR pit area. These tests included 6-in.-depth direct transmission and surface backscatter density, nuclear moisture, sand cone density, and oven water content tests. Although none of this data is included in this report, it is available from Steve Webster, telephone No. 601-634-2282, WES.

Falling weight deflectometer. Nondestructive tests were performed on the surface of each test item in test Sections 2, 3, and 4 with the Dynatest model 8000 falling weight deflectometer (FWD). The FWD is an impact load device that applies a single-impulse transient load of approximately 25-30 millisecond duration. With this trailer-mounted device, a dynamic force is applied to the pavement surface by dropping a weight onto a set of rubber cushions which results in an impulse loading on an underlying circular plate 17.7 in. in diameter in contact with the pavement. The applied force and the pavement velocities are respectively measured with load cells and velocity transducers. Deflections are determined by integrating the velocity-time signatures. The drop height of the weights can be as high as 15.7 in. to produce a force up to approximately 25,000 lb. The system is controlled with a micro computer which also records the output data. Velocities were measured and deflections computed at the center of the load plate and at distances of 12, 24, 36, 48, 60 and 72 in. from the center of the plate in order to obtain deflection basin measurements. Although these data are not included in this report, they are available from Steve Webster, telephone No. 601-634-2282, WES.

3 Data Analysis

ECP Data Interpretation Schemes for Number and Thicknesses of Soil Layers

Data reduction

For data analysis, all ECP raw data files were first run through the contingency van's MKPLT software program with results saved as *.PLT files. Data from the *.PLT files were then brought into Microsoft Excel spreadsheets and plots of tip pressure (psi) and friction ratio (percent) versus depth (in.) for each ECP test were made as shown by the example in Figure 16. Plots this size allowed data reduction to the nearest 1/2 in. of depth when determining depths to soil layer interfaces.

Establishing number of soil layers in pavement structure

Figure 17 shows how both the friction ratio (FR) and tip pressure (TP) plots verses depth are used to find the number of soil layer types and their general depth locations within the pavement structure. This is done by looking at the FR curve and drawing (or visualizing) a vertical line thorough each zone where the FR values remain about the same or cycle back and forth through the same range. For example the FR curve in Figure 17 shows 3 soil types and their general depth ranges. The same procedure is followed for the TP curve which shows the same 3 soil layers in Figure 17. The TP curve generally takes several inches of depth to transition from a strong soil layer to a weaker soil layer. Also, when no pavement overburden is available, the TP curve generally takes several inches of depth to transition into the top soil layer and accurately measure its penetration resistance. Many of the ECP penetration test results were not as easy to understand as the example shown in Figure 17.

Strong to weak layer interfaces

When a strong soil overlies a weaker soil, the depth to the interface of the two soils is determined using the FR curve. For example, in Figure 18, the TP curve indicated that the stronger soil layer 1 overlies a weaker soil layer 2.

The interface depth between the two soil layers is determined by finding the point F1 where the friction ratio curve starts changing from soil 1 to soil 2 and adding 2 in. (an empirical adjustment based on distance to the sleeve's midpoint). In Figure 18, the point F1 occurs at a depth of 25.0 in. plus 2.0 in. yields an interface layer depth of 27.0 in. The actual interface depth for this test was 28.0 in.

Attempts at locating the interface depth using the TP curve were not as successful as those using the FR curve. This was mainly due to the transition zone encountered in the bottom portion of the strong surface layer and the additional penetration required to transition into the weaker soil. No reasonable procedure was found that would adequately locate the interface depth using the TP curve for the strong over weak soil condition.

Weak to strong layer interfaces

Weak to strong layer interfaces are determined using both the FR and TP curves. For example, in Figure 18, the TP curve indicates a weak soil 2 over a stronger soil 3. The interface depth is determined using the FR scheme described above. For example, point F2 plus 2.0 in. equals 50.5 in. for the interface depth. The interface depth is then also determined using the TP curve. Point T2 is located where the tip pressure curve starts a rapid increase in strength as it moves toward the higher strength soil. The point T2 plus 1.0 in. (an empirical adjustment based on distance between the cone's tip and base) determines the depth to the soil layer interface. In Figure 18, T2 is located at 48.5 in. plus 1.0 in. equals 49.5 in. for the layer interface. The soil layer interface is then determined as the average between the FR and TP schemes (50.0 in.). Actual interface was 49.5 in. for this test.

In order to test the accuracy of the FR plus 2.0 in. scheme and TP plus 1.0 in. scheme, 3 technicians independently determined the soil layer interface depths for all the test items using the two schemes. For the FR scheme, the results yielded an average error of 0.2 in. between the actual depth and the determined depth. The standard deviation was 1.6 in. and sample size was 271. For the TP scheme, the average error was -0.1 in. between the actual depth and the determined depth. The standard deviation was 1.2 in. and sample size was 178. In a few of the tests, neither the FR or TP scheme were able to determine soil layer changes or interface depths.

Transition layer strengths using ECP

The ECP tip pressure curve shows that strength changes do not occur discretely at layer interfaces when transitioning from a strong soil to a weaker soil. For example, Figure 19 shows a transition zone in soil 1 beginning at a depth of 15 in. with a tip pressure of 3,350 psi and entering soil 2 with a tip pressure of 850 psi. This would yield an average tip pressure of 2,100 psi for the transition layer. This supports the use of transition layer strengths for

evaluations. One contributing cause for this occurrence is the inability to compact a strong layer in the region adjacent to a weak layer.

Capability of ECP to locate weak soil layers

The weak soil wedge in WES test Section 1 varied in thickness ranging up to 24 in. Using the FR and TP schemes described above, the ECP was able to locate and measure the thickness of the weak soil layer with reasonable accuracy (individual tests missed the soil layer depth by as much as 3-in.; however, the average of several tests located the soil layer depth within 1-in.) at all locations tested. Appendix D shows the ECP data plots for test Section 1 for the .8 in./sec penetration rate. The ECP data plots for the .2 in./sec penetration rate were harder to interpretate and not quite as accurate as the .8 in./sec penetration rate.

Capability of ECP to measure thin base courses

WES test Section 2 contained test items with base courses 6.0, 12.0, and 18.0 in. thick. The ECP tests were run in both the unsurfaced (no pavement overburden) and the surfaced (4-in. AC pavement overburden) portions of each test item. Figures E1-E6 show the ECP tip pressure and friction ratio plots for these tests. The ECP was not able to measure the strength or thickness of the thin 6-in.-thick base in item W211 in either the unsurfaced or surfaced portions. The ECP was able to measure the thickness and strength of the 12.0 in. and 18.0 in. base layers in both the unsurfaced and surfaced portions of the items.

Effect of ECP Penetration Rate on Test Results

ECP penetration tests were conducted at two rates on WES test Sections 1, 3, and 4. The objective of these tests was to determine if a slower penetration rate would be more accurate in locating the depths of soil layer interfaces and also to measure the effects of penetration rate on tip pressure and friction ratio for various soil types. An analysis of test results by three independent technicians revealed that the slower penetration rate did not improve the accuracy in locating depths to soil layer interfaces. Test results showed the .8 in./sec test rate was slightly more accurate than the slower .2 in./sec rate. Table 1 summarizes the test results comparing the penetration rate effects on tip pressure and friction ratio. The data is grouped by soil type and shows an average difference of plus or minus 10 percent or less for each soil type. The average penetration rate effect on tip pressure for all soils combined was zero. The average penetration rate effect on friction ratio for all soils combined was minus 11 percent. The slower penetration rate affected the friction ratio most with the SM and SP soils. Based on the analysis of test data, the .8 in./sec penetration rate should be used as the standard penetration rate for all ECP tests.

Table 1
Effect of ECP Penetration Rate

ECP Penetration Rate = .8 in./sec				ECP Penetration Rate = .2 in./sec				Rate Effect on Tip Pressure			Rate Effect on Friction Ratio		
Test Item	Soil Type	Friction Ratio Percent	Tip Pressure psi	Test Item	Soil Type	Friction Ratio Percent	Tip Pressure psi	TIP .8-.2 psi	Difference Percent	Average Difference	FR .8-.2 Percent	Difference Percent	Average Difference Percent
W3106E07	CH	7.7	200	W3I06E11	CH	6.4	200	0	0		1.3	17	
W3107E07	CH	8.6	420	W3I07E11	CH	6.7	575	-155	-37		1.9	22	
W3107E08	CH	8.7	450	W3I07E11	CH	6.7	300	150	33		2.0	23	
W4107E07	CH	6.0	200	W4I07E11	CH	5.8	175	25	13		0.2	3	
W4107E08	CH	6.0	240	W4I08E11	CH	6.4	360	-125	-50	-10	-0.4	-7	12
W4108E07	CH	8.0	450										
W4108E08	CH	7.8	400										
W1IXE01	CL	4.0	450	W1IXE10	CL	3.2	250	200	44		0.8	20	
W1IXE03	CL	3.0	450	W1IXE12	CL	2.4	325	125	28		0.6	20	
W1IXE04	CL	2.3	400	W1IXE13	CL	2.0	350	50	13		0.3	13	
W1IXE05	CL	3.0	350	W1IXE14	CL	2.2	325	25	7		0.8	27	
W1IXE06	CL	2.8	250	W1IXE16	CL	2.4	350	-100	-40		0.4	13	
W1IXE07	CL	2.8	450	W1IXE18	CL	1.5	500	-50	-11		1.3	45	
W2I1E07	CL	2.5	1,100										
W2I2E07	CL	2.6	1,050										
W2I2E08	CL	2.6	1,050										
W2I3E07	CL	2.6	920										

(Sheet 1 of 7)

Table 1 (Continued)

ECP Penetration Rate = .8 in./sec				ECP Penetration Rate = .2 in./sec				Rate Effect on Tip Pressure			Rate Effect on Friction Ratio		
Test Item	Soil Type	Friction Ratio Percent	Tip Pressure psi	Test Item	Soil Type	Friction Ratio Percent	Tip Pressure psi	TIP .6-.2 psi	Difference Percent	Average Difference	FR .8-.2 Percent	Difference Percent	Average Difference Percent
W3I01E07	CL	2.9	375	W3I01E11	CL	2.4	425	-50	-13		0.5	17	
W3I01E08	CL	2.2	410										
W3I02E07	CL	2.0	500	W3I02311	CL	1.8	56C	-60	-12		0.1	5	
W3I02E08	CL	2.1	375										
W3I03E07	CL	1.9	440	W3I03E11	CL	1.6	475	-35	-8		0.3	16	
W3I03E08	CL	2.2	375										
W3I04E07	CL	1.9	575	W3I04E11	CL	3.2	575	0	0		-1.3	-68	
W3I04E08	CL	2.0	550										
W3I05E07	CL	1.7	450	W3I05E11	CL	3.0	650	-200	-44		-1.3	-76	
W3I05E08	CL	1.8	475										
W3I06E07	CL	1.8	550	W3I06E11	CL	3.0	600	-50	-9		-1.2	-67	
W3I06E08	CL	1.8	450										
W3I07E07	CL	3.0	380	W3I07E11	CL	1.8	400	-20	-5		1.2	40	
W3I07E08	CL	1.6	420										
W3I08E07	CL	3.3	825	W3I08E11	CL	3.7	750	75	9		-0.4	-12	
W3I08E07	CL	1.8	575	W3I08E11	CL	3.4	550	25	4		-1.6	-89	
W3I08E08	CL	3.4	725										
W3I08E08	CL	1.8	500	W3I08E11	CL	2.7	550	-50	-10		-0.9	-50	

(Sheet 2 of 7)

Table 1 (Continued)

ECP Penetration Rate = .8 in./sec				ECP Penetration Rate = .2 in./sec				Rate Effect on Tip Pressure			Rate Effect on Friction Ratio		
Test Item	Soil Type	Friction Ratio Percent	Tip Pressure psi	Test Item	Soil Type	Friction Ratio Percent	Tip Pressure psi	TIP .8-.2 psi	Difference Percent	Average Difference	FR .8-.2 Percent	Difference Percent	Average Difference Percent
W3I09E07	CL	1.8	550	W3I09E11	CL	2.8	500	50	9		-1.0	-56	
W3I09E08	CL	2.0	500										
W3I10E07	CL	1.7	625	W3I10E11	CL	2.3	575	50	8		-0.6	-35	
W3I10E08	CL	2.0	625	W3I10E11	CL	2.6	475	150	24		-0.6	-30	
W3I11E07	CL	2.8	275										
W3I11E08	CL	3.2	550	W3I11E11	CL	2.4	700	-150	-27		0.8	25	
W3I12E07	CL	3.0	275	W3I12E11	CL	2.4	550	-275	-100		0.6	20	
W3I12E08	CL	2.7	350										
W4I06E07	CL	2.6	1,150	W4I06E11	CL	4.0	950	200	17		-1.4	-54	
W4I06E08	CL	2.7	1,150										
W4I09E07	CL	3.7	1,300	W4I09E11	CL	3.8	1,200	100	8	-5	-0.1	-3	-13
W4I09E08	CL	3.2	1,275										
W3I01E07	GP	0.9	2,050	W3I01E11	GP	1.0	1,900	150	7		-0.1	-11	
W3I01E08	GP	1.0	2,025										
W3I12E07	GP	0 9	1,725	W3I12E11	GP	0.9	2,000	-275	-16		0.0	0	
W3I12E08	GP	1.1	1,850										
W4I01E07	GP	1.1	2,700	W4I01E11	GP	0.8	2,300	400	15		0.3	27	
W4I01E08	GP	0.8	2,850										

(Sheet 3 of 7)

Table 1 (Continued)

ECP Penetration Rate = .8 in./sec				ECP Penetration Rate = .2 in./sec				Rate Effect on Tip Pressure			Rate Effect on Friction Ratio		
Test Item	Soil Type	Friction Ratio Percent	Tip Pressure psi	Test Item	Soil Type	Friction Ratio Percent	Tip Pressure psi	TIP .8-.2 psi	Difference Percent	Average Difference	FR .8-.2 Percent	Difference Percent	Average Difference Percent
W4I12E07	GP	0.9	3,750	W4I12E11	GF	0.9	2,775	975	26	8	0.0	0	4
W4I12E08	GP	0.9	3,575										
W1LXE01	SC	1.9	825	W1IXE10	SC	0.8	400	425	52		1.1	58	
W1IXE01	SC	1.6	1,440	W1IXE10	SC	1.4	1,550	-110	-8		0.2	13	
W1IXE03	SC	1.3	860	W1IXE12	SC	1.6	700	160	19		-0.4	-28	
W1IXE03	SC	1.9	1,450	W1IXE12	SC	1.7	1,650	-200	-14		0.2	11	
W1IXE04	SC	1.0	770	W1IXE13	SC	1.0	800	-30	-4		0.0	0	
W1IXE04	SC	2.0	1,450	W1IXE13	SC	2.0	1,775	-325	-22		0.0	0	
W1IXE05	SC	1.4	950	W1IXE14	SC	0.9	850	100	11		0.5	36	
W1IXE05	SC	2.2	1,400	W1IXE14	SC	2.2	1,900	-500	-36		0.0	0	
W1IXE06	SC	1.3	900	W1IXE16	SC	1.3	1,200	-300	-33		-0.1	-4	
W1IXE06	SC	2.0	1,450	W1IXE16	SC	2.1	1,900	-450	-31		-0.1	-5	
W1IXE07	SC	1.1	950										
W1IXE07	SC	2.4	1,450										
W1IXE09	SC	1.1	1,000	W1IXE18	SC	1.2	1,125	-125	-13		-0.1	-9	
W1IXE09	SC	1.7	1,700	W1IXE18	SC	1.8	2,050	-350	-21		-0.1	-6	
WEI3E07	SC	1.2	780	W3I03E11	SC	1.1	540	240	31		0.1	8	
W3I03E08	SC	1.2	710										

(Sheet 4 of 7)

Table 1 (Continued)

ECP Penetration Rate = .8 in./sec				ECP Penetration Rate = .2 in./sec				Rate Effect on Tip Pressure			Rate Effect on Friction Ratio		
Test Item	Soil Type	Friction Ratio Percent	Tip Pressure psi	Test Item	Soil Type	Friction Ratio Percent	Tip Pressure psi	TIP .8-.2 psi	Difference Percent	Average Difference	FR .8-.2 Percent	Difference Percent	Average Difference Percent
W3I10E07	SC	1.7	1,800	W3I10E11	SC	1.6	1,550	250	14		0.1	6	
W3I10E08	SC	1.7	1,775										
W4I01E07	SC	3.2	1,550	W4I01E11	SC	2.5	1,400	150	10		0.7	22	
W4I01E08	SC	3.0	1,525										
W4I02E07	SC	2.3	1,600	W4I02E11	SC	2.7	1,600	0	0		-0.4	-17	
W4I02E08	SC	2.5	1,650										
W4I03E07	SC	1.4	1,025	W4I03E11	SC	2.2	1,300	-275	-27		-0.8	-57	
W4I03E07	SC	2.7	1,450	W4I03E11	SC	3.0	1,700	-250	-17		-0.3	-11	
W4I03E08	SC	1.8	1,100										
W4I03E08	SC	2.2	1,575										
W4I04E07	SC	2.9	1,650	W4I04E11	SC	2.4	1,800	-150	-9		0.5	17	
W4I04E08	SC	2.7	1,650										
W4I05E07	SC	2.4	1,675	W4I05E11	SC	2.8	1,625	50	3		-0.4	-17	
W4I05E08	SC	2.4	1,675										
W4I06E07	SC	2.3	1,700	W4I06E11	SC	3.0	1,475	225	13		-0.7	-30	
W4I06E08	SC	2.3	1,700										
W4I07E07	SC	2.4	1,550	W4I07E11	SC	2.4	1,625	-75	-5		0.0	0	
W4I07E08	SC	2.2	1,675										

(Sheet 5 of 7)

Table 1 (Continued)

ECP Penetration Rate = .8 in./sec				ECP Penetration Rate = .2 in./sec				Rate Effect on Tip Pressure			Rate Effect on Friction Ratio		
Test Item	Soil Type	Friction Ratio Percent	Tip Pressure psi	Test Item	Soil Type	Friction Ratio Percent	Tip Pressure psi	TIP .8-.2 psi	Difference Percent	Average Difference	FR .8-.2 Percent	Difference Percent	Average Difference Percent
W4I08E07	SC	2.4	1,575	W4I08E11	SC	2.3	1,500	75	5		0.1	4	
W4I08E08	SC	2.2	1,625										
W4I09E07	SC	3.0	1,625	W4I09E11	SC	2.6	1,540	85	5		0.4	13	
W4I09E08	SC	2.6	1,700										
W4I10E07	SC	2.4	1,750	W4I10E11	SC	2.6	1,725	25	1		-0.2	-8	
W4I10E08	SC	2.7	1,825										
W4I11E07	SC	2.6	2,200	W4I11E11	SC	2.8	1,800	400	18		-0.2	-8	
W4I11E08	SC	2.2	2,200	W4I11E11	SC	2.6	2,100	100	5		-0.4	-18	
W4I12E07	SC	2.8	1,900	W4I12E11	SC	2.4	1,900	0	0	-2	0.4	14	1
W4I12E08	SC	2.5	1,875										
W3I05E07	SM	1.4	900	W3I05E11	SM	1.8	850	50	6		-0.4	-29	
W3I05E08	SM	1.4	1,050										
W3I09E07	SM	1.6	950	W3I09E11	SM	1.7	950	0	0		-0.1	-6	
W3I09E08	SM	1.6	1,000										
W4I05E07	SM	1.4	1,275	W4I05E11	SM	2.0	1,175	100	8		-0.6	-43	
W4I05E08	SM	1.4	1,175										
W4I10E07	SM	1.7	1,550	W44I10E11	SM	2.2	1,400	150	10	6	-0.5	-29	-26
W4I10E08	SM	1.6	1,625										

(Sheet 6 of 7)

Table 1 (Continued)

ECP Penetration Rate = .8 in./sec				ECP Penetration Rate = .2 in./sec				Rate Effect on Tip Pressure			Rate Effect on Friction Ratio		
Test Item	Soil Type	Friction Ratio Percent	Tip Pressure psi	Test Item	Soil Type	Friction Ratio Percent	Tip Pressure psi	TIP .8-.2 psi	Difference Percent	Average Difference	FR .8-.2 Percent	Difference Percent	Average Difference Percent
W3I04E07	SP	0.7	1,250	W3I04E11	SP	0.9	1,400	-150	-12		-0.2	-29	
W3I04E08	SP	0.8	1,275										
W4I04E07	SP	0.4	1,025	W4I04E11	SP	0.8	1,050	-25	-2	-7	-0.4	-100	-64
W4I04E08	SP	0.5	1,100										
W2I2E07	SW-SM	0.7	1,600										
W2I2E08	SW-SM	0.8	2,230										
W2I3E07	SW-SM	0.7	2,600										
W3I02E07	SW-SM	0.6	3,300	W3I02E11	SW-SM	0.6	3,400	-100	-3		0.0	0	
W3I02E08	SW-SM	0.7	3,240										
W3I11E07	SW-SM	0.9	1,750										
W3I11E08	SW-SM	0.8	3,350	W3I11E11	SW-SM	0.6	3,150	200	6		0.2	25	
W4I02E07	SW-SM	0.6	6,000	W4I02E11	SW-SM	0.7	4,400	1,600	27		-0.1	-17	
W4I02E08	SW-SM	0.8	6,200										
W4I11E07	SW-SM	0.8	6,250	W4I11E11	SW-SM	0.8	5,550	700	11	10	0.0	0	2
W4I11E08	SW-SM	0.8	7,200										
						Total Difference		200		0	0.5		11

(Sheet 7 of 7)

Effect of Overburden on ECP Test Results

Measured surface soil layer strengths (with and without overburden). Table 2 shows the effect on tip pressure and friction ratio of ECP tests run through the pavement overburden and with the overburden removed. As mentioned above, the 6-in.-thick base (SM-SW) in test item W2I1 was too thin to detect with the ECP either with or without the overburden.

Table 2
ECP Measured Surface Soil Layer Strengths (With and Without Overburden)

Test Location	Soil Type	Without Overburden		With Overburden	
		Tip Pressure psi	Friction Ratio Percent	Tip Pressure psi	Friction Ratio Percent
MAFB Pit 1	SC	985	0.8	1,620	0.6
MAFB Pit 1	GC	508	0.8	1,350	0.7
W2I2	SW-SM	1,700	0.8	2,950	0.7
W2I3	SW-SM	2,600	0.7	3,300	0.7

Figure 20 shows the effect of a 4-in. AC overburden on the tip pressure in the SW-SM base layer for test item W2I2. Tests E02 and E03 were made without the AC overburden. Tests E06 and E07 were made through the AC overburden. The resulting tip pressure for the SW-SM base layer was 1,700 psi without overburden and 2,950 psi with the AC overburden. Additional examples showing the confinement effects of overburden material are shown in Appendix B for the MABF test data and in Appendix E for the WES test Section 2 data. The confinement effects of overburden material are significant on tip pressure but not on friction ratio.

The CBR correlations developed in this report are based on the no overburden condition which would be encountered when evaluating unsurfaced contingency airfields. ECP tests through AC pavement overburdens will yield higher CBR values in the material directly under the AC pavement layer when using these correlations. This is especially true when the material under the AC pavement is coarse grained. One would guess less of an effect in cohesive soils, although, this study did not address such a situation. More tests and analysis are needed in order to fully understand the effects of overburden on ECP tests. The tests should include various thicknesses of AC overburden, soil type under the overburden, the effects of running ECP tests through a 4-in. core hole, a 6-in. core hole, and no pavement overburden at all. The overburden tests conducted at MAFB and WES were insufficient to fully understand and interpret ECP test results through pavement layers.

Based on the MAFB and WES tests (Appendices B and E), the depth of influence of the AC overburdens on the ECP test ranged up to 14 in. into the material under the overburden.

Depth required to measure surface layer strength (no overburden). For unsurfaced contingency airfields (with no pavement overburden), the lack of confinement at the top of the surface layer affects ECP measurements. As mentioned above, this effect was very evident in all the MAFB and WES tests conducted. Depending on soil type, the cone tip pressure recorded a low value at zero depth and gradually built up to a maximum value at some depth into the soil layer. The penetration depth required for measuring the actual strength of the surface soil layer is shown in Table 3 for the various soil types tested.

Table 3
ECP Depth Required to Measure Surface Layer Strength (No Overburden)

Test Location	Soil Type	Average Penetration Depth Required, in.
WES	CH	1
MAFB	CC	4
WES	CL	5
WES	SC	5
MAFB	SC	6
WES	SW-SM	10
WES	SM	11
WES	GP	13
WES	SP	18

Test results showed that the penetration depth required to measure the surface layer strength is related to the gradation and plasticity characteristics of the materials. The ECP can measure strengths of relatively thin surface layers of fine-grained plastic materials but requires thicker surface layers for the non-plastic coarser-grained materials.

Soil Classification from ECP Data

ECP data can be analyzed to provide an index of soil classification. A great deal of research has been conducted on this subject resulting in several soil classification charts using ECP data. An ECP soil classification system (Robertson et al. 1986) was selected for use with the MAFB and WES test

data. Figure 21 shows a plot of the data in terms of friction ratio versus tip pressure with the Robertson classification chart overlay. Also on Figure 21 is the Robertson et al. description of the different soil zones and this report's authors' interpretation of the soil zones according to the Unified Soil Classified System (USCS). All ECP data shown was run at the standard penetration rate of 0.8 in./sec and were taken at depths of 0 to 60 in.

In general, all the test data plotted very well within the proper classification zones using either the Robertson zone description or the USCS. The SW-SM, GP, SC (MAFB), and SP soils all charted in zones 8, 9, and 10. All of the SC (WES), SM, and GC soils except 5 samples charted in zone 7. The CL, ML, and MH soils all charted in zones 4, 5, and 6. The CH soil charted in zone 3. The only troublesome soil encountered was the CL soil which ranged over 3 zones and displayed an inconsistent relationship between tip pressure and friction ratio.

Analysis of the soil classification data showed the ECP to be a very useful tool in classifying soils (when direct sampling is not possible) for pavement evaluation purposes. The soils can be grouped into different zones for ECP correlations with CBR.

ECP Versus CBR Correlations

Interpretation of ECP data plots. A summary of CBR data for the WES test sections is presented in Table 4. The CBR values listed represent the average of three or more CBR tests performed at each test depth listed. As in accordance with MIL-STD-621A, if the results of the three tests in any group did not show reasonable agreement, additional tests were performed and the average was used as the CBR for that location.

In order to develop correlations between ECP and CBR, some interpretation of ECP data plots was necessary. For analysis purposes, all ECP data was plotted in the forms as shown in Appendices C, D, E, and F. Only selected plots are presented in the Appendices. A complete set of the ECP plots used in the CBR correlations is available from WES. In the WES tests, up to four tip pressure or friction ratio curves were presented on each plot for each test item. Interpretation of the ECP data plots typically used the average values of the four curves per plot.

Tip pressure versus CBR. Figure 22 shows a plot of the four tip pressure curves for the ECP tests conducted around the CBR pit for test item W4108 (ECP tests E02, E03, E06, and E07). For data interpretation, a horizontal line was drawn at the top and bottom of the SC soil layer using actual field measured depths. A vertical line was then drawn through the CH and SC soil layers representing the average tip pressures for each soil. Zone of influence transitioning into and out of each soil layer were not considered for the purposes of developing the ECP/CBR correlations. Also, for the CH soil, the

Table 4
Summary of CBR/Moisture Data WES Test Sections, Oct-Nov 1992

Depth, in.	W1I1(5,14) Avg. CBR	W1I1(5,14) Avg. M Percent	Depth, in.	W1I(4,13) Avg. CBR	W1I(4,13) Avg. M Percent	Depth, in.	W2I1 Avg. CBR	W2I1 Avg. M Percent	W2I2 Avg. CBR	W2I2 Avg. M Percent	W2I3 Avg. CBR	W2I3 Avg. M Percent
0	21.0	10.3	0.0	22.0	11.3	0.0	51.0	2.7	61.0	3.0	66.0	3.3
6	8.2	11.2	6.0	9.0	10.4	6.0	18.0	15.4	30.0	3.2	35.0	4.1
12	14.0	11.6	12.0	8.2	10.6	12.0	18.0	16.3	16.0	16.3	29.0	4.4
25	2.8	24.5	24.0	4.9	22.3	18.0			15.0	16.5	18.0	17.5
30	2.4	21.8	27.0	3.6	22.1	30.0					18.0	16.1

Depth, in.	W3I1 Avg. CBR	W3I1 Avg. M Percent	W3I2 Avg. CBR	W3I2 Avg. M Percent	W3I3 Avg. CBR	W3I3 Avg. M Percent	W3I4 Avg. CBR	W3I4 Avg. M Percent	W3I5 Avg. CBR	W3I5 Avg. M Percent	W3I6 Avg. CBR	W3I6 Avg. M Percent
0	33.0	6.6	77.0	2.8	14.0	11.0	21.0	6.3	19.0	11.5	8.0	33.5
6	22.0	5.7	38.0	3.1	19.0	10.9	20.0	7.8	20.0	12.8	11.0	30.3
12	30.0	5.8	41.0	3.5	4.0	11.2	17.0	10.2	13.0	14.5	7.0	34.6
24	2.1	21.9	2.4	22.1	2.4	22.2	3.5	21.4	2.7	21.5	3.3	22.3
36	2.1	21.3	2.8	21.2	2.5	21.4	3.1	20.7	3.1	20.8	3.4	21.5

Depth, in.	W3I7 Avg. CBR	W3I7 Avg. M Percent	W3I8 Avg. CBR	W3I8 Avg. M Percent	W3I9 Avg. CBR	W3I9 Avg. M Percent	W3I10 Avg. CBR	W3I10 Avg. M Percent	W3I11 Avg. CBR	W3I11 Avg. M Percent	W3I12 Avg. CBR	W3I12 Avg. M Percent
0	10.0	20.2	17.0	8.7	16.0	5.4	34.0	6.0	24.0	1.5	22.0	2.8
6	11.0	24.4	15.0	9.4	16.0	8.0	35.0	6.9	21.0	1.9	27.0	3.9

(Continued)

Table 4 (Concluded)

Depth, in.	W3I7		W3I8		W3I9		W3I10		W3I11		W3I12	
	Avg. CBR	Avg. M Percent	Avg. CBR	Avg. M Percent	Avg. CBR	Avg. M Percent	Avg. CBR	Avg. M Percent	Avg. CBR	Avg. M Percent	Avg. CBR	Avg. M Percent
12	7.8	21.1	6.6	12.2	16.0	8.3	19.0	8.7	26.0	1.9	50.0	5.0
24	2.8	22.8	3.2	20.7	2.4	22.4	3.1	20.7	2.7	20.6	1.2	22.5
36	1.0	22.2	2.6	20.3	1.9	20.3	2.5	20.8	3.4	19.5	2.3	20.2
Depth, in.	W4I1		W4I2		W4I3		W4I4		W4I5		W4I6	
	Avg. CBR	Avg. M Percent	Avg. CBR	Avg. M Percent	Avg. CBR	Avg. M Percent	Avg. CBR	Avg. M Percent	Avg. CBR	Avg. M Percent	Avg. CBR	Avg. M Percent
0	17.0	6.8	67.0	4.0	17.0	8.9	5.8	4.9	22.0	12.2	11.0	17.7
6	17.0	10.0	46.0	3.6	16.0	11.9	12.0	6.3	16.0	12.5	26.0	16.3
12	24.0	7.9	98.0	3.9	25.0	10.6	10.0	7.2	24.0	13.8	23.0	16.9
24	30.0	10.9	21.0	12.0	28.0	11.1	26.0	11.1	27.0	11.3	26.0	11.3
36	27.0	11.0	21.0	11.1	27.0	10.6	23.0	11.1	23.0	11.2	27.0	11.0
Depth, in.	W4I7		W4I8		W4I9		W4I10		W4I11		W4I12	
	Avg. CBR	Avg. M Percent	Avg. CBR	Avg. M Percent	Avg. CBR	Avg. M Percent	Avg. CBR	Avg. M Percent	Avg. CBR	Avg. M Percent	Avg. CBR	Avg. M Percent
0	5.0	34.1	13.0	21.8	22.0	8.3	8.4	5.3	53.0	1.6	23.0	3.6
6	7.4	35.2	14.0	25.4	29.0	10.2	21.0	7.3	120.0	2.9	23.0	5.0
12	8.8	35.0	25.0	20.7	20.0	12.5	20.0	8.1	145.0	2.4	22.0	4.2
24	23.0	11.1	32.0	10.6	30.0	11.4	28.0	11.1	34.0	11.0	23.0	12.2
36	24.0	11.0	33.0	10.6	27.0	10.7	28.0	11.1	25.0	10.5	27.0	10.8

E07 curve was ignored since it did not agree with the other three curves which showed close agreement. Average CBR values were shown on the plot for each depth for which they were available. A representative tip pressure and CBR value was then assigned to each soil layer using judgement in selecting the appropriate average CBR value. In Figure 22, the average CBR value for the 0-in., 6-in., and 12-in. depths was used to obtain a 17 CBR and 450 psi tip pressure for the CH layer. For the SC soil, an average 33 CBR and 1575 psi tip pressure was interpreted. In some test items, two sets of tip pressure versus CBR could be interpreted within a given soil layer.

Friction ratio. Figure 23 shows a plot of the corresponding four friction ratio curves for test item W4108. Again, ignoring the transition zones, vertical lines were drawn through the average friction ratio curves for each soil. In this case, the E06 curve was ignored for the CH soil since it did not agree with the other three curves. Some soils such as the CH material tended to have a wide, fluctuating range in friction ratio values. The average friction ratio was 8.0 percent for the CH material and 2.4 percent for the SC material.

Summary of tip pressure, friction ratio and CBR correlation data. In general, the data interpretation for representative values for tip pressure, friction ratio, and CBR was not as simple as shown in the above examples. A significant amount of judgment had to be used in many instances. Table 5 summarizes the test data used in developing the ECP/CBR correlations.

ECP versus CBR correlations. Eleven different soils representing ten different USCS classifications were tested. A total of 135 data samples were included in the regression analysis. Statistical Analysis System "SAS" and Statgraphics (Version 6) computer software programs were used in the analysis.

a. *One group regression analysis.* An initial regression was made using all 135 data samples in the data set. Some transformations in the dependent (CBR) and independent (TP, FR) variables were made to determine what kind of relationships existed. The common transformations to the CBR, TP, and FR variables were the inverse, polynomial (2, 2, 3 degree), square root, and logarithmical. For the TP and FR variables the product and division between the two variables were also included in the regression analysis. The regression analysis included the method of selecting the variables such as forward, backward, and stepwise. These methods were used to determine which of the variables had the most influence on the model. Results of the analysis showed that the simple equation CBR = 0.078969 x FR + 0.211765 x TP, with an R^2 = 0.9146, was as good as more complex equations. In this regression analysis, equations without an intercept were better than those with an intercept. The equations developed correlated better with the actual data when CBRs were greater than 10. Below CBR 10 the data were scattered and inconsistent. Additional analysis was performed using two soil groups.

Table 5
Summary of Tip Pressure, Friction Ratio, and CBR Correlation Data
ECP Penetration Rate = 0.8 in./sec

Test Item	Soil Type	Friction Ratio Percent	Tip Pressure psi	CBR Percent
W3I06E07	CH	7.7	200	8.6
W3I07E07	CH	3.6	420	10.0
W3I07E08	CH	8.7	450	10.0
W3I07E08	CH	6.8	340	7.8
W4I07E07	CH	6.0	200	8.1
W4I07E08	CH	6.0	240	8.1
W4I08E07	CH	3.0	450	17.0
W4I08E08	CH	7.8	400	17.0
W1IXE01	CL	4.0	450	
W1IXE03	CL	3.0	450	
W1IXE04	CL	2.1	425	3.6
W1IXE05	CL	3.0	350	2.6
W1IXE06	CL	2.8	300	
W1IXE07	CL	2.6	450	
W2I1E07	CL	2.5	1,100	15.0
W2I2E07	CL	2.6	1,050	15.0
W2I2E08	CL	2.6	1,050	15.0
W2I3E07	CL	2.6	920	18.0
W3I01E07	CL	2.9	375	2.1
W3I01E08	CL	2.2	410	2.1
W3I02E07	CL	2.0	500	2.6
W3I02E08	CL	2.1	375	2.6
W3I03E07	CL	1.9	440	2.5
W3I03E08	CL	2.2	375	2.5
W3I04E07	CL	1.9	575	3.3
W3I04E08	CL	2.0	550	3.3
W3I05E07	CL	1.7	450	2.9
W3I05E08	CL	1.8	475	2.9
W3I06E07	CL	1.8	550	3.4
W3I06E08	CL	1.8	450	3.4
W3I07E07	CL	3.0	380	1.9
W3I07E08	CL	1.6	420	1.9
W3I08E07	CL	3.3	825	16.0
W3I08E07	CL	3.0	500	6.6
W3I08E07	CL	2.5	575	3.2
W3I08E07	CL	1.8	400	2.6
W3I08E08	CL	3.4	725	16.0

(Sheet 1 of 4)

Table 5 (Continued)

Test Item	Soil Type	Friction Ratio Percent	Tip Pressure psi	CBR Percent
W3I08E08	CL	1.8	500	2.9
W3I09E07	CL	1.8	550	2.2
W3I09E08	CL	2.0	500	2.4
W3I09E08	CL	2.5	325	1.9
W3I10E07	CL	1.7	625	3.1
W3I10E07	CL	2.5	475	2.5
W3I10E08	CL	2.0	625	3.1
W3I10E08	CL	2.5	425	2.5
W3I11E07	CL	2.8	275	2.7
W3I11E07	CL	2.0	450	3.4
W3I11E08	CL	3.2	550	3.0
W3I12E07	CL	3.0	275	1.2
W3I12E07	CL	2.0	425	2.3
W3I12E08	CL	2.7	350	1.2
W4I06E07	CL	2.6	1,150	24.0
W4I06E08	CL	2.7	1,150	24.0
W4I09E07	CL	3.7	1,300	24.0
W4I09E08	CL	3.2	1,275	24.0
MAX2I1&2	GC	0.7	560	16.0
MAX2I3&6	GC	0.9	520	14.0
MAX2I4&5	GC	0.9	445	11.0
W3I01E07	GP	0.9	2,050	28.0
W3I01E08	GP	1.0	2,025	28.0
W3I12E07	GP	0.9	1,725	38.0
W3I12E08	GP	1.1	1,850	38.0
W4I01E07	GP	1.1	2,700	24.0
W4I01E08	GP	0.8	2,850	24.0
W4I12E07	GP	0.9	3,750	23.0
W4I12E08	GP	0.9	3,575	23.0
MAX2I1&2	MH	2.9	270	5.0
MAX2I3&4	MH	3.3	235	2.5
MAX2I5&6	MH	3.0	205	3.6
MAX1I1&2	ML	2.5	260	6.0
MAX1I3&4	ML	1.7	235	6.7
MAX1I5&6	ML	3.1	250	7.0
MAX1I1&2	SC	0.8	810	19.0
MAX1I3&4	SC	0.8	855	21.0
MAX1I5&6	SC	0.9	1,290	28.0
W1IXE01	SC	1.9	825	

(Sheet 2 of 4)

Table 5 (Continued)

Test Item	Soil Type	Friction Ratio Percent	Tip Pressure psi	CBR Percent
W1IXE01	SC	1.7	1,450	
W1IXE03	SC	1.2	860	
W1IXE03	SC	1.9	1,490	
W1IXE04	SC	1.0	850	8.6
W1IXE04	SC	2.0	1,450	
W1IXE05	SC	1.4	950	11.0
W1IXE05	SC	2.2	1,400	
W1IXE06	SC	1.2	925	
W1IXE06	SC	2.0	1,450	
W1IXE07	SC	1.2	1,100	
W1IXE07	SC	2.5	1,450	
W1IXE09	SC	1.3	1,125	
W1IXE09	SC	1.6	1,450	
W3I03E07	SC	1.2	780	16.0
W3I03E08	SC	1.2	710	16.0
W3I10E07	SC	1.7	1,800	34.0
W3I10E07	SC	1.1	700	19.0
W3I10E08	SC	1.7	1,775	34.0
W3I10E08	SC	1.3	850	19.0
W4I01E07	SC	3.2	1,550	28.0
W4I01E08	SC	3.0	1,525	28.0
W4I02E07	SC	2.3	1,600	21.0
W4I02E08	SC	2.5	1,650	21.0
W4I03E07	SC	1.4	1,025	19.0
W4I03E07	SC	2.7	1,450	28.0
W4I03E08	SC	1.8	1,100	19.0
W4I03E08	SC	2.2	1,575	28.0
W4I04E07	SC	2.9	1,650	25.0
W4I04E08	SC	2.7	1,650	25.0
W4I05E07	SC	2.4	1,675	25.0
W4I05E08	SC	2.4	1,675	25.0
W4I06E07	SC	2.3	1,700	27.0
W4I06E08	SC	2.3	1,700	27.0
W4I07E07	SC	2.4	1,550	24.0
W4I07E08	SC	2.2	1,675	24.0
W4I08E07	SC	2.4	1,575	33.0
W4I08E08	SC	2.2	1,625	33.0
W4I09E07	SC	3.0	1,625	28.0
W4I09E08	SC	2.6	1,700	28.0

(Sheet 3 of 4)

Table 5 (Concluded)

Test Item	Soil Type	Friction Ratio Percent	Tip Pressure psi	CBR Percent
W4I10E07	SC	2.4	1,750	28.0
W4I10E08	SC	2.7	1,750	28.0
W4I11E07	SC	2.6	2,200	34.0
W4I11E07	SC	2.6	1,900	25.0
W4I11E08	SC	2.2	2,200	34.0
W4I11E08	SC	2.6	1,800	25.0
W4I12E07	SC	2.8	1,900	25.0
W4I12E08	SC	2.5	1,875	25.0
W3I05E07	SM	1.4	900	17.0
W3I05E08	SM	1.4	1,050	17.0
W3I09E07	SM	1.6	950	16.0
W3I09E08	SM	1.6	1,000	16.0
W4I05E07	SM	1.4	1,100	20.0
W4I05E08	SM	1.4	1,175	20.0
W4I10E07	SM	1.7	1,625	20.0
W4I10E08	SM	1.6	1,625	20.0
W3I04E07	SP	0.7	1,250	19.0
W3I04E08	SP	0.8	1,275	19.0
W4I04E07	SP	0.4	1,025	11.0
W4I04E08	SP	0.5	1,100	11.0
W2I2E07	SW-SM	0.7	1,600	30.0
W2I2E08	SW-SM	0.8	2,230	30.0
W2I3E07	SW-SM	0.7	2,600	35.0
W3I02E07	SW-SM	0.6	3,300	52.0
W3I02E08	SW-SM	0.7	3,240	52.0
W3I11E07	SW-SM	0.9	1,725	24.0
W3I11E08	SW-SM	0.8	3,350	24.0
W4I02E07	SW-SM	0.6	6,000	70.0
W4I02E08	SW-SM	0.8	6,200	70.0
W4I02E08	SW-SM	0.8	6,900	98.0
W4I11E07	SW-SM	0.8	6,250	120.0
W4I11E07	SW-SM	0.8	2,300	53.0
W4I11E07	SW-SM	0.8	6,800	145.0
W4I11E08	SW-SM	0.8	7,200	120.0
W4I11E08	SW-SM	0.8	1,800	53.0
W4I11E08	SW-SM	0.8	7,700	145.0

(Sheet 4 of 4)

b. *Two group regression analysis.* The data set was then divided into two groups: CBR < 10 and CBR > 10. The same regression analysis described above was applied in this analysis. Table 6 shows some of the equations developed for each CBR group. The square root of the CBR looked good as a transformation, and the use of the intercept in the equation give worse R^2 results in both groups. The selection of these equations was based on the R^2 values, residual plots, and observed versus predicted plots. A review of the normability and residuals plots revealed that the models overpredicted CBR (gave unconservative values) and were inconsistent when the CBR was less than 10.

Table 6
Regression Models for CBR < 10 and CBR > 10

Group	Model	R^2
CBR < 10	$CBR^{0.5} = 0.5106 \times FR^{0.5} + 0.2721 \times TP^{0.5}$	0.9107
	$CBR^{0.5} = 3.4599 + 1.4730 \times FR^{0.5} + 0.5619 \times TP^{0.5}$	0.7449
	$CBR^{0.5} = 0.2351 \times FR^{0.5} + 0.1515 \times TP^{0.5} + 0.0099 \times FR \times TP$	0.9560
CBR > 10	$CBR^{0.5} = 0.2993 \times FR^{0.5} + 0.4343 \times TP^{0.5}$	0.9781
	$CBR^{0.5} = 0.6387 - 0.0090 \times FR^{0.5} + 0.4128 \times TP^{0.5}$	0.7852
	$CBR^{0.5} = 0.3801 \times FR^{0.5} + 0.4439 \times TP^{0.5} - 0.00096 \times FR \times TP$	0.9780

c. *Four group regression analysis.* Based on the friction ratio versus tip pressure graph in Figure 21, it appeared that four correlations could be developed based on four soil groups that could be identified using the field ECP tip pressure and friction ratio data. The data set was divided in the four soil groups shown in Table 7 based on the soil classification zones shown in Figure 21. For each group fourteen equations were chosen from the regression analysis for further study. These models included the transformation variables discussed previously. Some erratic behavior was found in the group 2 data at low CBR values < 10.

Table 7
Four Soil Groups Used in Regression Analysis

Group	Soil Classification		Test Data Soil Type
	Soil Zones	Soil Types	
1	3	MH, CH, OH	CH
2	4, 5, 6	ML, CL, OL, MH	CL, MH (MAFB), ML (MAFB)
3	7	GC, SP, SM, SC	SC, SM, GC (MAFB)
4	8, 9, 10	GW, GP, GM, GC, SW, SP, SM, SC	GP, SP, SW-SM, SC (MAFB)

The simple equation CBR = C_1 x Friction + C_2 x TP gave a reasonable fit for groups 1, 3, and 4. More complicated equations did not significantly improve the results of the simple equations for these soil groups. The best equation for group 2 was CBR = e^(C_1 x FR + C_2 x TP). Table 8 shows the recommended ECP versus CBR correlations developed for the four soil groups.

Table 8
Recommended ECP versus CBR Correlations

Equation	Soil Group	C_1	C_2	R^2
CBR = C_1 x FR + C_2 x TP	1	0.5040	0.02075	0.9246
CBR = 2.7183^(C_1 x FR + C_2 x TP)	2	0.1180	0.00214	0.9206
CBR = C_1 x FR + C_2 x TP	3	2.1007	0.0131	0.9726
CBR = C_1 x FR + C_2 x TP	4	-3.2314	0.0160	0.9159

Plots of the predicted versus observed (from the test data) CBR and normal probability for the recommended ECP versus CBR correlations are presented in Appendix G. Data plotting below the 45° line in the predicted versus observed CBR plots are conservative and represent lower-than-actual CBR values. Group 1 only had 7 observations for each variable. More tests are needed in order to verify or modify the coefficients for the group 1 equation. The group 2 data was the most inconsistent and had the most data below 10 CBR. For the same value of CBR different values of tip pressure and friction ratio were obtained. The equation for group 2 will generally be conservative and predict lower than actual CBR values for CBR > 10. The equation for group 3 will generally yield slightly conservative CBR values. Seven data points in the group 4 data plotted a significant distance from the 45° line on the unconservative side. However, it was felt that some of the actual CBR values for this group may have been greater than those measured. Obtaining a smooth test surface for the CBR piston without disturbing the soil was difficult for some of the soils in this group. Any small disturbance of the soil surface would yield a lower-than-actual CBR.

Figures 24-27 present the recommended ECP versus CBR correlations in graphical form. In order to use these plots, the tip pressure and friction ratio test data is first compared with Figure 21 and Table 7 in order to determine the zone, then group of the soil layer tested. The appropriate ECP versus CBR correlation plot (Figures 24-27) is then entered using the tip pressure and friction ratio values and the rated CBR for the soil layer is determined.

DCP Data Analysis

Depth required for DCP to measure surface layer strength

As with the ECP test, the lack of confinement at the top of the surface layer affects the DCP measurements. The penetration depth required for measuring the actual strength of the surface soil layer with the DCP is shown in Table 9 for the various soil types tested.

Table 9
DCP Depth Required to Measure Surface Layer Strength (No Overburden)

Test Location	Soil Type	Average Penetration Depth Required, in.
WES	CH	1
WES	CL	3
WES	SC	4
WES	SW-SM	4
WES	SM	5
WES	GP	5
WES	SP	11

As with the ECP, test results showed that the DCP penetration depth required to measure the surface layer strength is related to the gradation and plasticity characteristics of the materials. The DCP can measure strengths of thin surface layers of fine-grained plastic materials but requires thicker surface layers for the non-plastic coarser-grained materials. The DCP requires less penetration depth than the ECP to measure the surface layer strength and should be the test device used when thin surface soil layers cannot be measured by the ECP.

Capability of DCP to locate weak soil layers

The weak soil wedge in WES test Section 1 varied in thickness ranging up to 24 in. The DCP accurately detected the weak soil layer at all 9 locations tested. In all locations, the DCP measured the transition zone a few inches above the top of the weak soil layer and then measured the depth to the bottom of the layer to within 1 in.

Capability of DCP to measure thin base courses (no overburden)

WES test Section 2 contained test items with base courses 6.0, 12.0, and 18.0 in. thick. The DCP tests were run in the unsurfaced (no pavement overburden) areas of each test item. The DCP was able to measure the strength and thickness of each base. The thicknesses were measured to within 1-in. using the average DCP data from four tests in each test item. The depth to the bottom of the base layer was determined using the midpoint of the transition zone between the base and subgrade. Using this procedure the DCP thickness of the 6 in. base in item W2I1 was measured to be 7 in., the 12 in. base in item W2I2 was measured to be 11.2 in., and the 18 in. base in item W2I3 was measured to be 18.25 in. The strength of each base was also able to be determined after the DCP cone had penetrated approximately 2.0 in. into the base in each item and overcame the effects of no confining overburden.

DCP versus CBR correlation

Interpretation of DCP data. In order to develop correlations between DCP and CBR, some interpretation of DCP data plots was necessary. For analysis purposes, all DCP data was plotted in the form as shown in Figure 28. Four DCP curves were presented on each plot for each test item. Interpretation of the DCP data plots generally used the average values of the four curves per plot. Transitions zones at the top of the surface layer and between the soil layers were not used in the CBR correlations. The analysis procedure involved matching the average CBR value for a particular soil depth with the average DCP index (mm/blow) for the soil zone extending 6 in. below the depth the CBR test. Some judgement had to be used in matching the CBR versus DCP index values. Table 10 shows the 102 data samples used in the DCP versus CBR analysis. A complete set of the DCP plots used in the CBR correlations is available from WES. DCP tests in the CH soil were sometimes affected by clay sticking to the penetration rod. This would tend to yield higher than actual CBR values. Past WES experience has indicated that cleaning and oiling the penetration rod helped in preventing the clay from sticking to the rod, however, it did not significantly improve the test results. DCP tests in highly plastic clays are generally accurate for depths to approximately 12 in.

Test DCP data versus current correlation. Figure 29 shows a plot of CBR versus DCP Index for all the test data along with the current WES correlation line (DCP in mm/blow). The data above CBR 10 matches the current correlation within reason. However, the CL data below CBR 10 and all of the CH data did not agree with the current correlation. For example, a DCP value of 70 mm/blow would indicate a CBR 2.5 using the current correlation. The actual field CBR for the CH soil sample was 5. The current correlation yields lower-than-actual CBR values for the CH soil and higher-than-actual CBR values for the CL soil. Therefore, new correlations were developed for the CH and CL soils. Regression analysis of the CH soil data resulted in the equation CBR = 1/(0.002871 x DCP) with an R^2 value of 0.9802 (DCP in

Table 10
Summary of DCP and CBR Correlation Data

Test Item	Soil Type	DCP mm/blow	CBR Percent	DCP in./blow	Test Item	Soil Type	DCP mm/blow	CBR Percent	DCP in./blow
W1I1D4	CL	40.0	4.9	1.57	W3I3	SC	40.0	4.0	1.57
W1I1D4	CL	44.0	3.6	1.73	W3L10	SC	7.6	35.0	0.30
W1I1D5	CL	40.0	2.6	1.57	W3I10	SC	15.0	19.0	0.59
W2I1	CL	16.0	18.0	0.63	W4I3	SC	11.0	17.0	0.43
W2I1	CL	13.0	18.0	0.51	W4I3	SC	10.0	16.0	0.39
W2I2	CL	12.5	16.0	0.49	W4I3	SC	9.0	25.0	0.35
W2I3	CL	13.5	18.0	0.53	W4I1	SC	7.0	30.0	0.28
W3I1	CL	35.0	2.1	1.38	W4I2	SC	8.5	21.0	0.33
W3I2	CL	50.0	2.4	1.97	W4I3	SC	8.3	28.0	0.33
W3I4	CL	30.0	3.5	1.18	W4I4	SC	8.0	26.0	0.31
W3I5	CL	33.0	2.7	1.30	W4I5	SC	9.0	27.0	0.35
W3I8	CL	30.0	3.2	1.18	W4I6	SC	9.0	26.0	0.35
W3I9	CL	30.0	2.4	1.18	W4I7	SC	9.0	23.0	0.35
W3I10	CL	24.0	3.1	0.94	W4I8	SC	9.0	32.0	0.35
W3I11	CL	20.0	2.7	0.79	W4I8	SC	7.5	33.0	0.30
W3I12	CL	32.0	1.8	1.26	W4I9	SC	7.3	30.0	0.29
W3I3	CL	32.0	2.4	1.26	W4I9	SC	8.0	27.0	0.31
W3I8	CL	12.0	15.0	0.47	W4I10	SC	7.5	28.0	0.30
W3I8	CL	27.0	6.6	1.06	W4I12	SC	6.5	23.0	0.26

(Sheet 1 of 3)

Table 10 (Continued)

Test Item	Soil Type	DCP mm/blow	CBR Percent	DCP in./blow	Test Item	Soil Type	DCP mm/blow	CBR Percent	DCP in./blow
W4I6	CL	14.0	11.0	0.55	W1I1D4	SC	16.0	13.0	0.63
W4I6	CL	11.0	26.0	0.43	W1I1D4	SC	22.0	8.2	0.87
W4I6	CL	11.0	23.0	0.43	W3I5	SM	13.0	20.0	0.51
W4I9	CL	9.3	22.0	0.37	W3I5	SM	11.0	13.0	0.43
W4I9	CL	8.0	29.0	0.31	W3I9	SM	17.0	16.0	0.67
W4I9	CL	8.5	20.0	0.33	W4I5	SM	16.0	22.0	0.63
W3I6	CH	45.0	8.0	1.77	W4I5	SM	12.0	16.0	0.47
W3I6	CH	41.0	11.0	1.61	W4I5	SM	11.0	24.0	0.43
W3I6	CH	48.0	7.0	1.89	W4I10	SM	20.0	8.4	0.79
W3I7	CH	20.0	10.0	0.79	W4I10	SM	10.5	21.0	0.41
W3I7	CH	28.0	11.0	1.10	W4I10	SM	8.8	20.0	0.35
W3I7	CH	41.0	7.8	1.61	W4I4	SP	50.0	5.8	1.97
W4I7	CH	70.0	5.0	2.76	W4I4	SP	20.0	12.0	0.79
W4I7	CH	48.0	7.4	1.89	W4I4	SP	12.0	10.0	0.47
W4I7	CH	45.0	8.8	1.77	W3I4	SP	17.0	20.0	0.67
W4I8	CH	23.0	13.0	0.91	W3I4	SP	11.0	17.0	0.43
W4I8	CH	23.0	14.0	0.91	W2I1	SW-SM	7.5	51.0	0.30
W3I1	GP	8.0	22.0	0.31	W2I2	SW-SM	5.0	61.0	0.20
W3I1	GP	6.1	30.0	0.24	W2I2	SW-SM	6.4	30.0	0.25

(Sheet 2 of 3)

Table 10 (Concluded)

Test Item	Soil Type	DCP mm/blow	CBR Percent	DCP in./blow	Test Item	Soil Type	DCP mm/blow	CBR Percent	DCP in./blow
W4I1	GP	17.0	20.0	0.67	W2I3	SW-SM	5.0	66.0	0.20
W4I1	GP	11.0	17.0	0.43	W2I3	SW-SM	4.0	35.0	0.16
W3I12	GP	10.0	22.0	0.39	W2I3	SW-SM	6.0	29.0	0.24
W3I12	GP	7.0	27.0	0.28	W3I2	SW-SM	3.8	77.0	0.15
W3I12	GP	6.2	50.0	0.24	W3I2	SW-SM	4.4	38.0	0.17
W4I1	GP	10.0	17.0	0.39	W3I2	SW-SM	4.0	41.0	0.16
W4I1	GP	8.0	24.0	0.31	W3I11	SW-SM	6.0	24.0	0.24
W4I12	GP	7.2	23.0	0.28	W4I2	SW-SM	4.0	67.0	0.16
W4I12	GP	6.0	23.0	0.24	W4I2	SW-SM	4.2	46.0	0.17
W4I12	GP	5.0	22.0	0.22	W4I2	SW-SM	2.0	98.0	0.08
W1I1D5	SC	12.0	14.0	0.47	W4I11	SW-SM	4.0	53.0	0.16
'3I3	SC	14.0	14.0	0.55	W4I11	SW-SM	1.0	120.0	0.04
W3I3	SC	20.0	19.0	0.79					

(Sheet 3 of 3)

mm/blow). Regression analysis of the CL soil data resulted in the equation CBR = $1/(0/017019 \times DCP)^2$ with an R^2 value of 0.9362 (DCP in mm/blow). The CL correlation should only be used for CBR values below 10. The CL data above 10 CBR fit the standard correlation best.

4 Conclusions and Recommendations

ECP Conclusions

The ECP is an effective device for locating the interface depths of the various soil layers in a pavement.

a. *Strong to weak soil layer interface.* The interface depth is best determined using the FR versus depth curve. The interface depth is determined by locating the depth where the FR curve starts changing from Soil 1 to Soil 2 and adding 2 in.

b. *Weak to strong soil layer interfaces.* This type interface is best determined using both the FR and TP versus depth curves. The interface depth is first determined using the FR scheme described above. It is then determined using the TP curve by locating the depth where the TP curve starts a rapid increase in strength as it moves toward the higher strength soil and adding 1 in. The average of the two depths is recorded as the interface depth.

The ECP device is an effective device for locating and measuring the strength of transition zones within a strong soil layer that overlies a weaker soil. The use of transition layer strengths for airfield evaluations is recommended.

An ECP test penetration rate of .8 in./sec should be adopted as the standard penetration rate for airfield evaluations. Test results at a slower penetration rate of .2 in./sec did not improve the accuracy in locating depths to soil layer interfaces. The slower penetration rate did not significantly affect the TP results but did affect the FR values for the SM and SP soils.

The effects of overburden (e.g. AC pavement layer) on ECP test results are significant. Increases in TP values of 100 percent or more were measured in base layers at MAFB. Overburden effects on FR values were not significant. Based on the MAFB and WES tests, the depth of influence of the AC overburdens on the ECP test ranged up to 14 in. into the material under the overburden. More tests and analysis are needed in order to fully understand

the effects of overburden on ECP tests. The ECP versus CBR correlations developed in this report are based on the no overburden condition which would be encountered when evaluating unsurfaced contingency airfields. ECP tests through AC pavement overburdens will yield higher CBR values in the material directly under the AC pavement layer when using these correlations.

ECP tests on surface layers with no pavement overburden require a certain penetration depth before the surface layer strength can be measured. The lack of confinement at the top of the surface layer affects the ECP test. The required surface layer penetration depth is related to the gradation and plasticity characteristics of the material. The ECP can measure strengths of relatively thin (6 in. or less) surface layers of fine-grained plastic materials but requires thicker (6 to 12 in.) surface layers for the non-plastic coarser-grained materials.

The ECP was not able to measure the strength or thickness of a thin (6-in.-thick) base layer when tested in an unsurfaced condition or through a 4-in.-thick AC overburden.

The ECP is a very useful tool in classifying soils (when direct sampling is not possible) for pavement evaluation purposes. Based on TP and FR values, the soils can be grouped into different zones (according to Robertson et al. 1986) for ECP correlations with CBR.

The Air Force Contingency Test Van with its ECP test capabilities offers a significant improvement to current test methods and procedures for evaluating pavements. The ECP test can measure the thicknesses and strengths of pavement layers, classify the materials in each layer sufficiently to use proper CBR strength correlation equations, and locate and provide strength measurements of transition zones within soil layers.

DCP Conclusions

As with the ECP test, the lack of confinement at the top of the surface layer affects the DCP measurements. The DCP requires less penetration depth than the ECP to measure the surface layer strength and should be the test device used when thin surface soil layers cannot be measured by the ECP.

The DCP accurately detected the thin weak soil wedge at all 9 locations tested. In all locations, the DCP measured the transition zone a few inches above the top of the weak soil layer and then measured the depth to the bottom of the layer to within 1 in.

The DCP was able to measure the strength and thickness of the thin 6-in.-thick base layer in test Section 2. This layer was too thin to measure using the ECP.

The DCP test data agreed within reason with the current DCP versus CBR correlation. However, none of the CL data below CBR 10 and none of the CH data agreed with the current correlation. Separate DCP versus CBR correlations are required for CH soils and CL soils below CBR 10.

Recommendations

Additional tests and analysis should be conducted in order to fully understand the effects of overburden on ECP tests. The tests should include various thicknesses of AC overburden, soil type under the overburden, the effects of running ECP tests through the pavement layer, a 4-in. core hole, a 6-in. core hole, and with no pavement overburden at all.

Data comparing field traffic performance versus ECP, DCP, and CBR needs to be developed. Relating ECP and DCP test results directly to traffic performance would eliminate the need for converting the data to CBR values before evaluating the pavement.

The data reduction software for the Contingency Van should be upgraded to classify the soil by zone (Robertson et al. 1986) and group (as listed in this report). The software could use the group number to key into the proper CBR correlation equation. The printer on the Contingency Van should be upgraded to a laser jet type and the output plots TP and FR versus depth should be scaled so soil layer interface depths could be estimated to the nearest in. (See example plot in Figure 16).

The following ECP test procedures for pavement evaluation are recommended.

a. *Zero-depth reading* For all ECP tests, an initial zero-depth reading should be established by pushing the penetrometer cone into the soil layer until the base of the cone is flush with the surface of the soil.

b. *ECP tests.* Run all ECP tests at the standard penetration rate of .8 in./sec. Run at least three tests for each pavement area being evaluated.

c. *Data reduction.* For data analysis, all ECP raw data files should be run through the contingency van's MKPLT software program with results saved as *.PLT files. Data from the *.PLT files should then be brought into a spreadsheet like Microsoft Excel and plots of tip pressure (psi) and friction ratio (percent) versus depth (in.) for each ECP test should be made as shown by the example in Figure 16. Plots this size allow data reduction to the nearest 1/2 in. of depth when determining depths to soil layer interfaces.

d. Number of soil layers. Use the TP and FR plots to determine the number and general locations of the various soil layers in the pavement structure. Use the procedure described in this report.

e. Interface depths. Determine the interface depth locations for each soil layer using the TP and FR schemes described in this report. Include the transition zone layers when penetrating from strong to weak soil layers.

f. TP and FR layer values. Determine the average TP and FR values for each soil layer. Ignore the erroneous TP values near the top of the surface layer (Use Table 3 as a guide). Also, do not consider erroneously high TP values located within the zone of influence (5 to 14 in. into the base material) of any pavement overburden.

g. Classify soil. Classify the soil layers by zone (Figure 21) and then by group (Table 7).

h. CBR rating. Determine the rated CBR of the soil layer by using the appropriate ECP versus CBR correlation in Table 8.

The DCP test procedures for pavement evaluations should be conducted according to the procedure described by Webster, Grau, and Williams (1992). The current DCP versus CBR correlation should be used for all soils except CL soils below CBR 10 and CH soils. The new correlations (Figure 29) for CL soils below CBR 10 and CH soils should be used.

The DCP requires less penetration depth than the ECP to measure the surface layer strength and should be the test device used when thin surface soil layers cannot be measured by the ECP.

References

American Society for Testing and Materials. (1989). "Standard test method for deep, quasi-static, cone and friction-cone penetration tests of soil," Designation: D 3441-86, Philadelphia, PA.

Bates, Z. C. (1992). "Development of correlations between shear moduli determined using the seismic ECP and standard penetration test data," University of Florida, Gainesville, FL.

Buncher, M. S., and Christiansen, D. J. (1992). "USAF's new contingency soils/pavement testing van," HQ Air Force Civil Engineering Support Agency, Tyndall AFB, FL.

Department of Defense. (1968). "Military standard test method for pavement subgrade, subbase, and base-course materials," MIL-STD-621A, Washington, DC.

Maxwell, K. H. (1990). "Seismic cone penetration testing in Florida soils," University of Florida, Gainesville, FL.

Robertson, P. K., Campanella, R. G., Gillespie, D., and Greig, J. (1986). "Use of piezometer cone data," Use of In Situ Tests in Geotechnical Engineering, ASCE Geotechnical Special Publication, pp. 1263-1280.

Webster, S. L., Grau, R. H., and Williams, T. P. (1992). "Description and application of dual mass dynamic cone penetrometer," Instruction Report GL-92-3, U.S. Army Waterways Experiment Station, Vicksburg, MS.

U.S. Army Waterways Experiment Station. (1960). "The Unified Soil Classification System," Technical Memorandum No. 3-357, Vicksburg, MS.

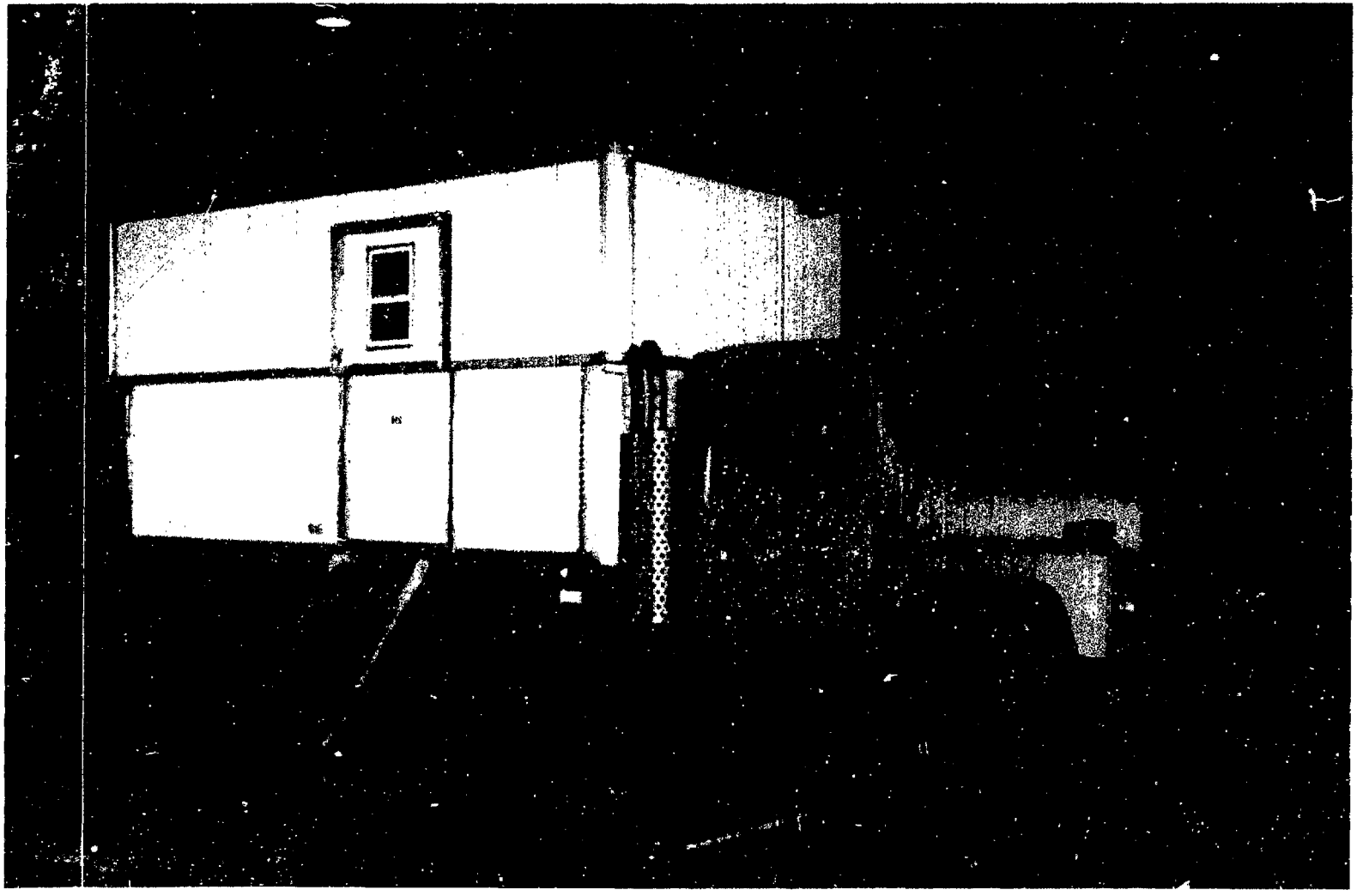

Figure 1. Contingency soils/pavement testing van

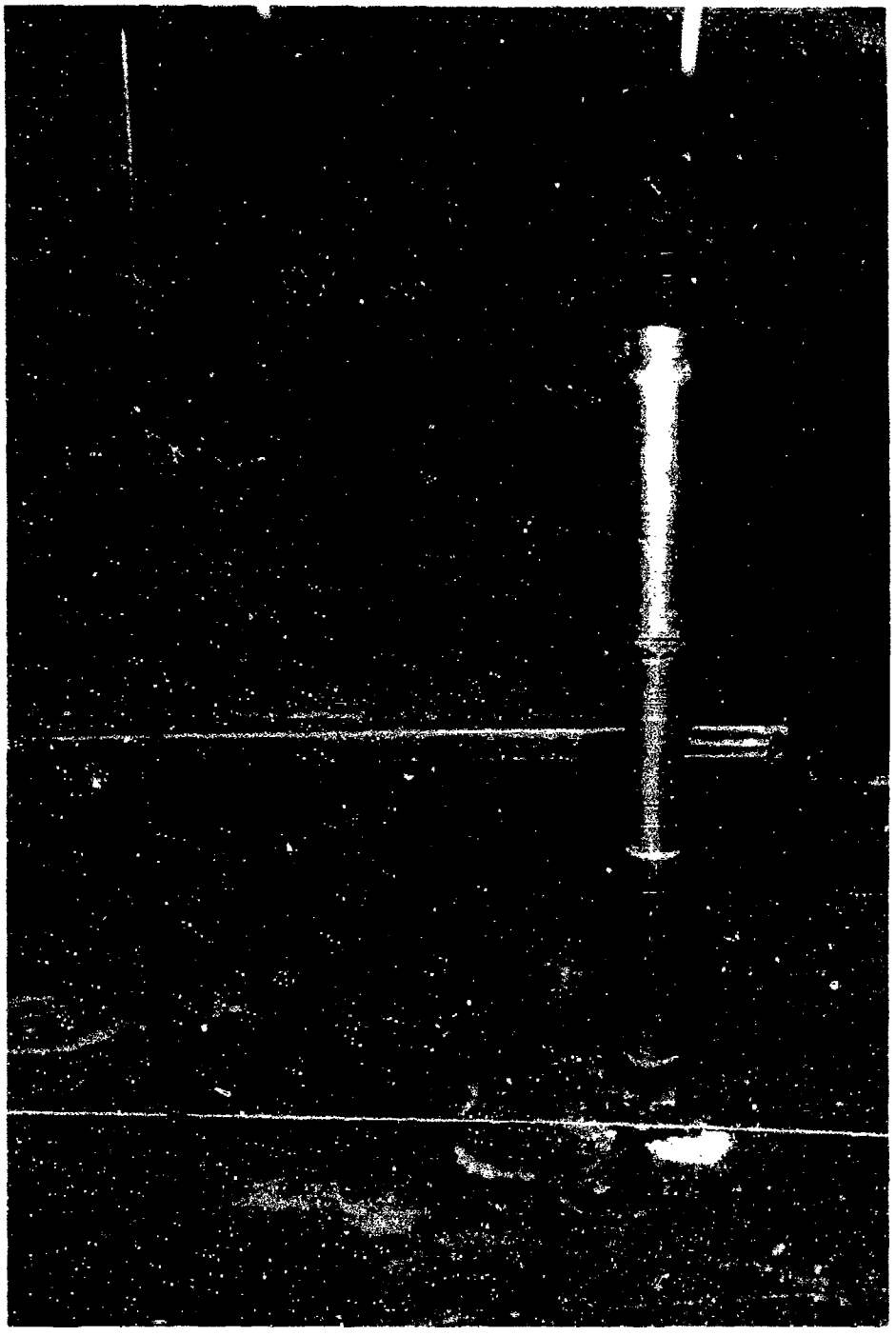

Figure 2. ECP test cone

Figure 3. Dynamic cone penetrometer

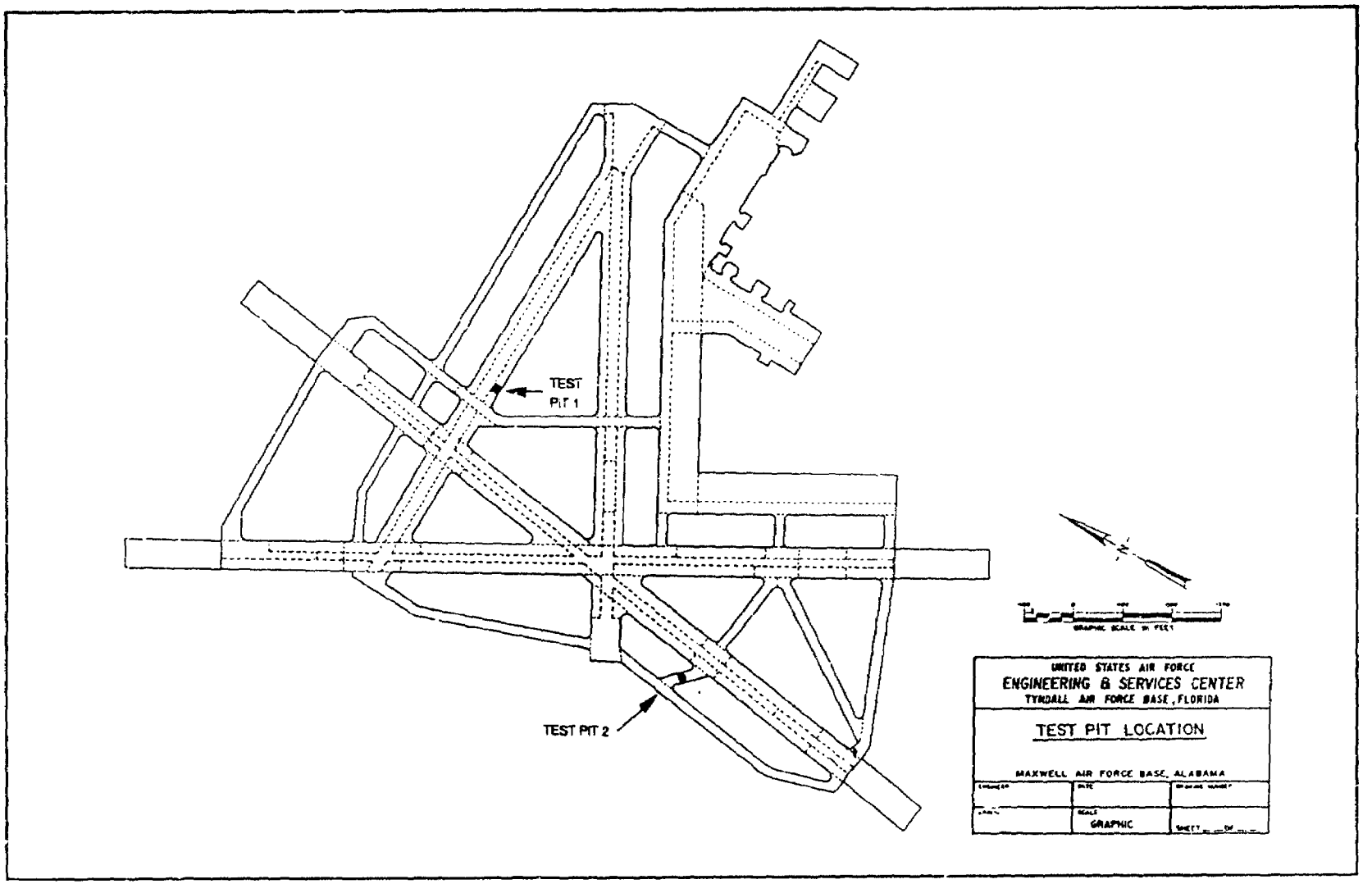

Figure 4. Maxwell AFB test pit locations

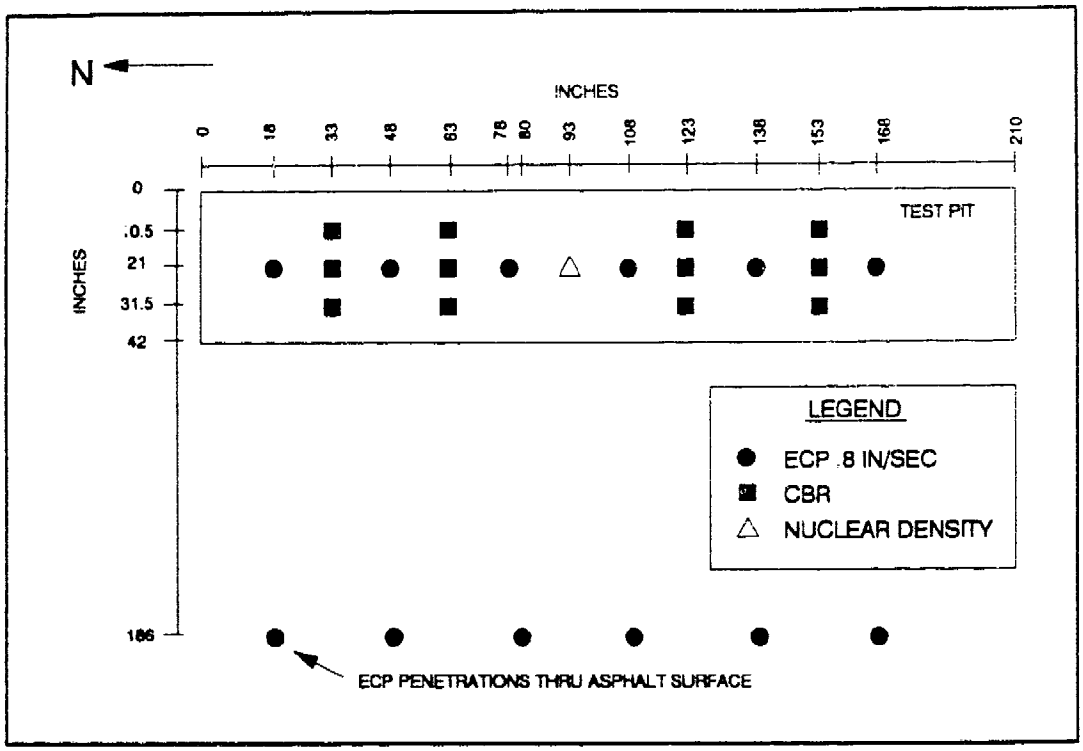

Figure 5. Typical plan view of test pits, Maxwell AFB, AL

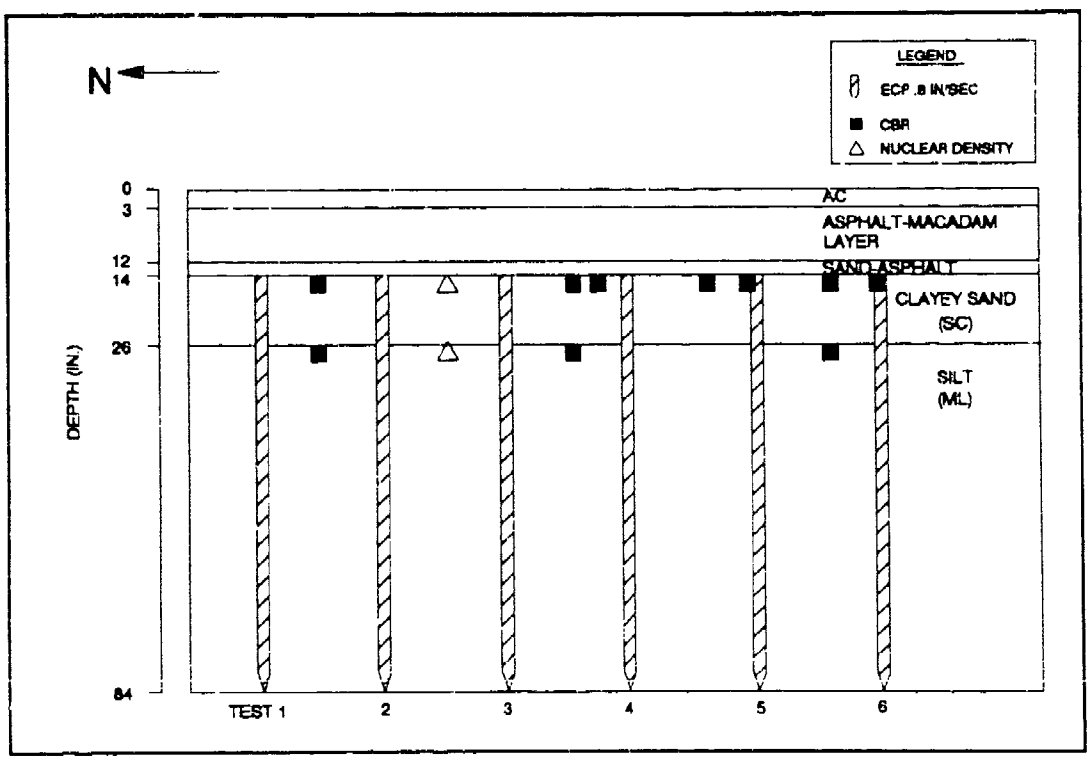

Figure 6. Profile of test pit 1, Maxwell AFB, AL

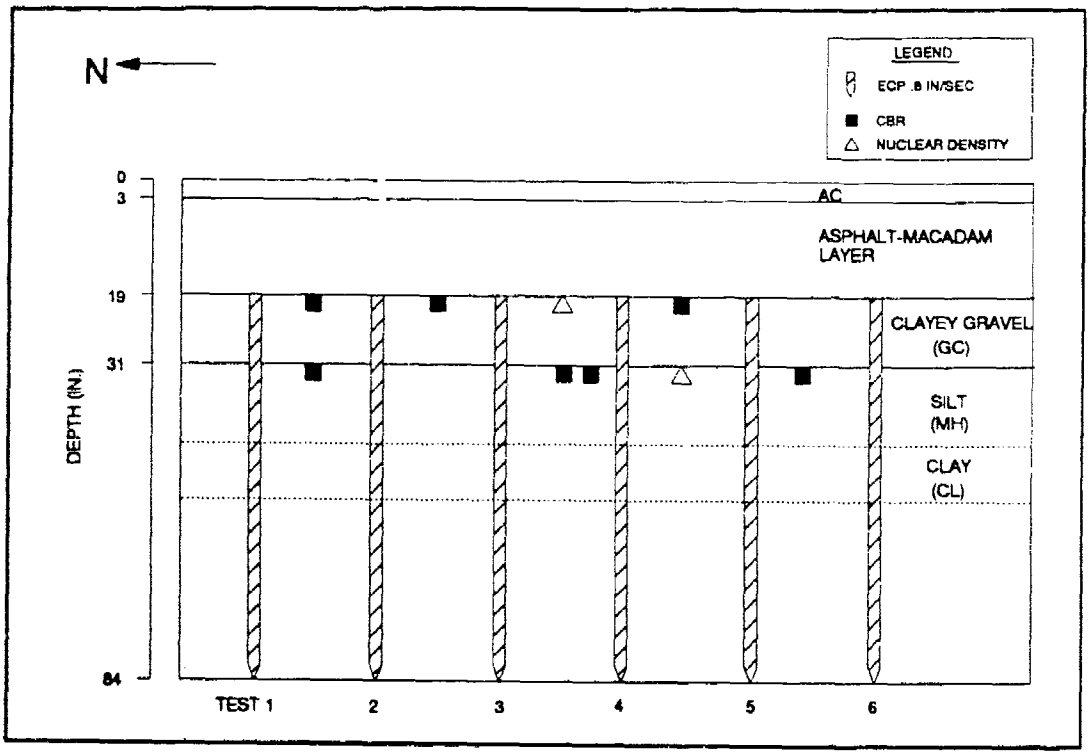

Figure 7. Profile of test pit 2, Maxwell AFB, AL

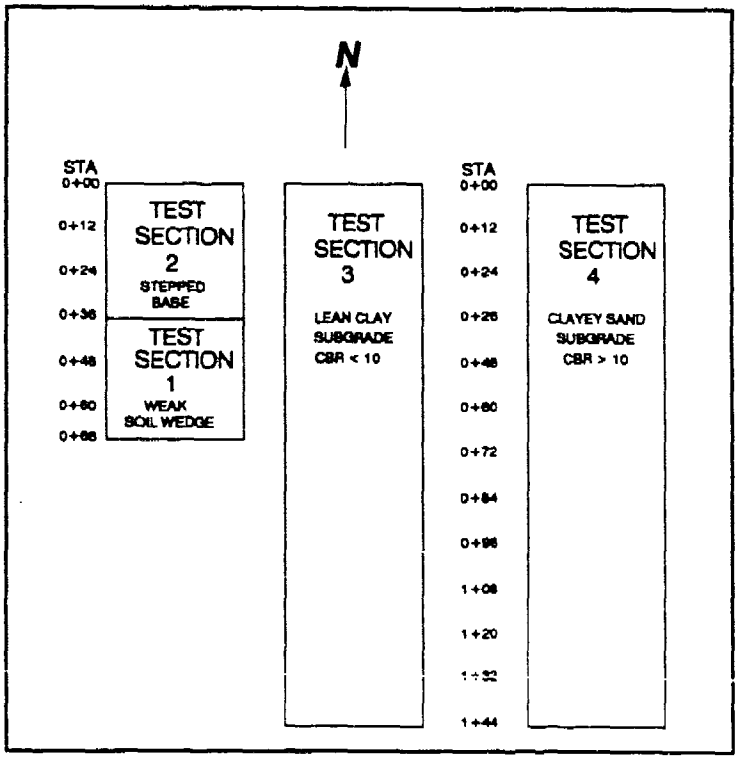

Figure 8. Layout of WES test sections

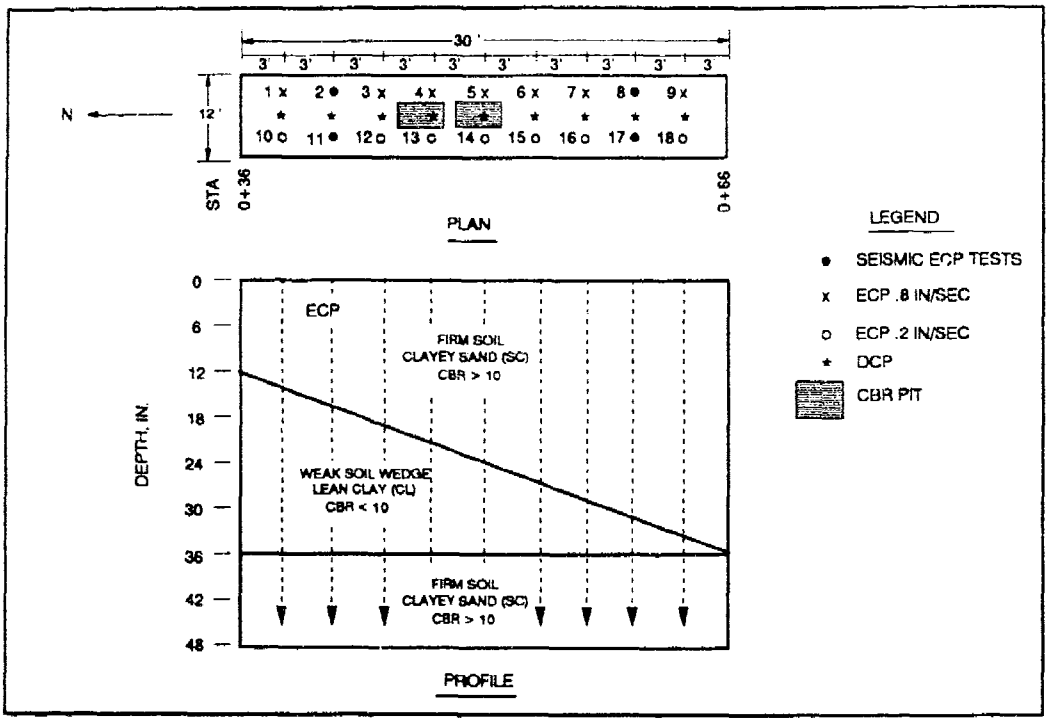

Figure 9. Plan and profile of test section 1 (soil wedge)

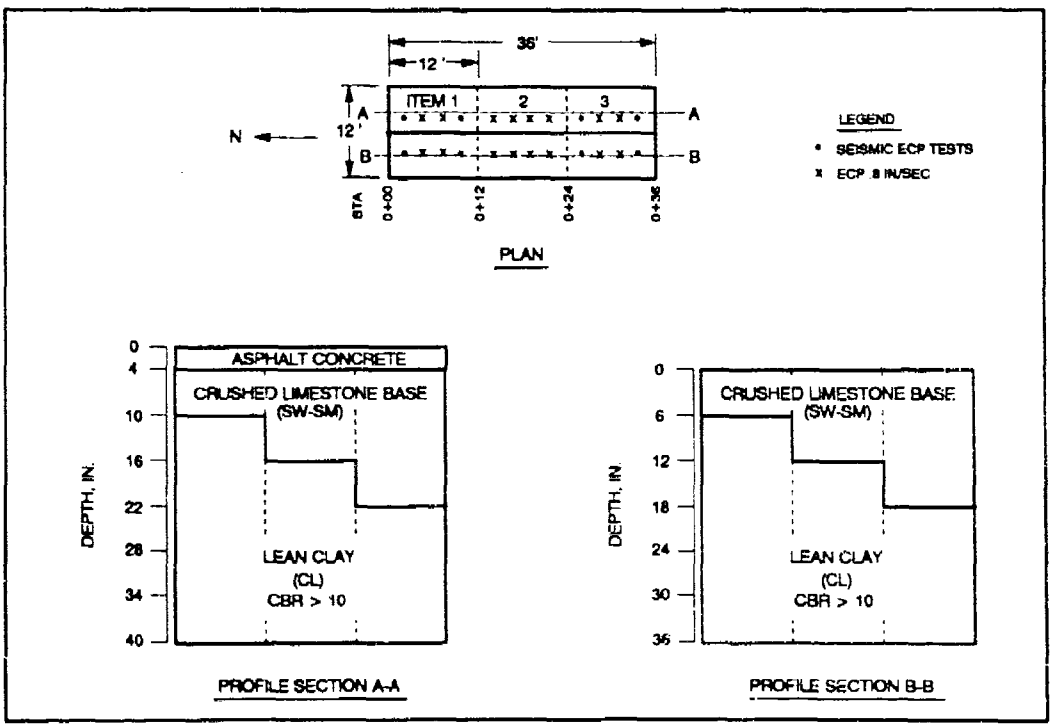

Figure 10. Plan and profile of test section 2 (stepped base)

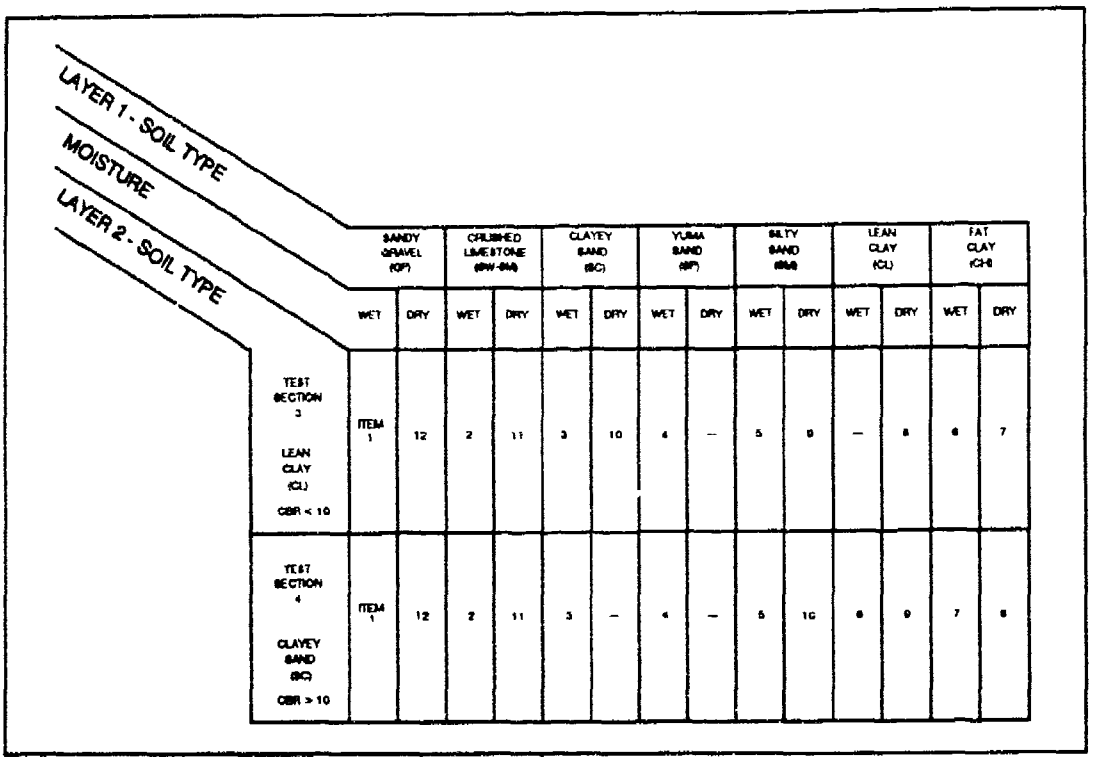

Figure 11. Experimental design for WES test sections 3 and 4

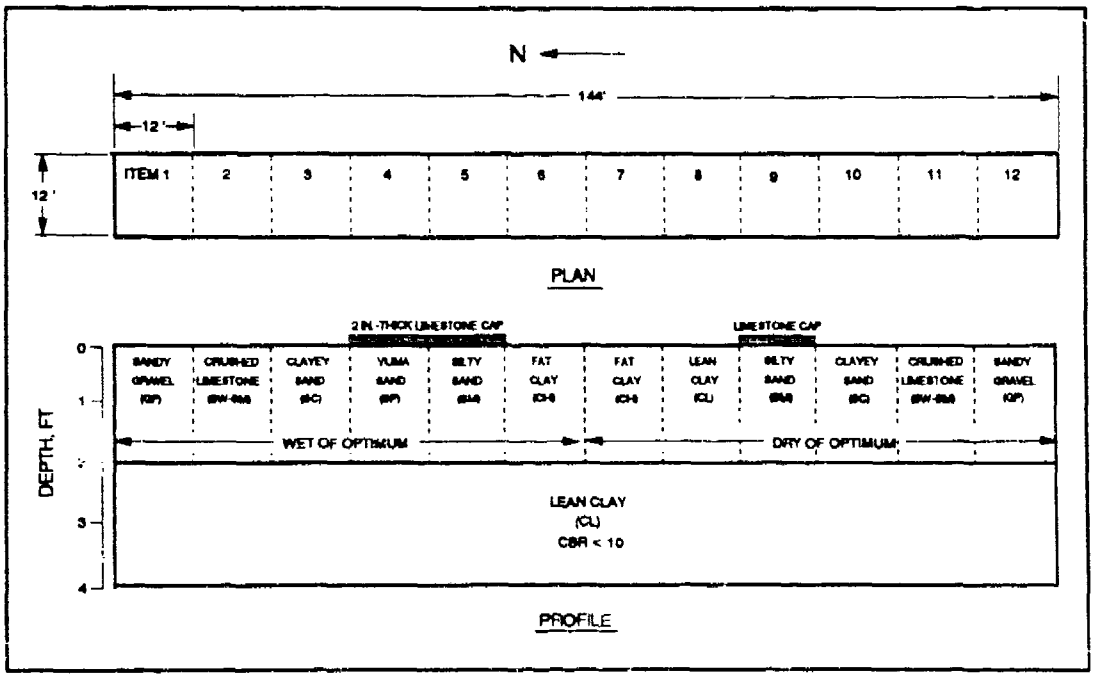

Figure 12. Plan and profile of test section 3

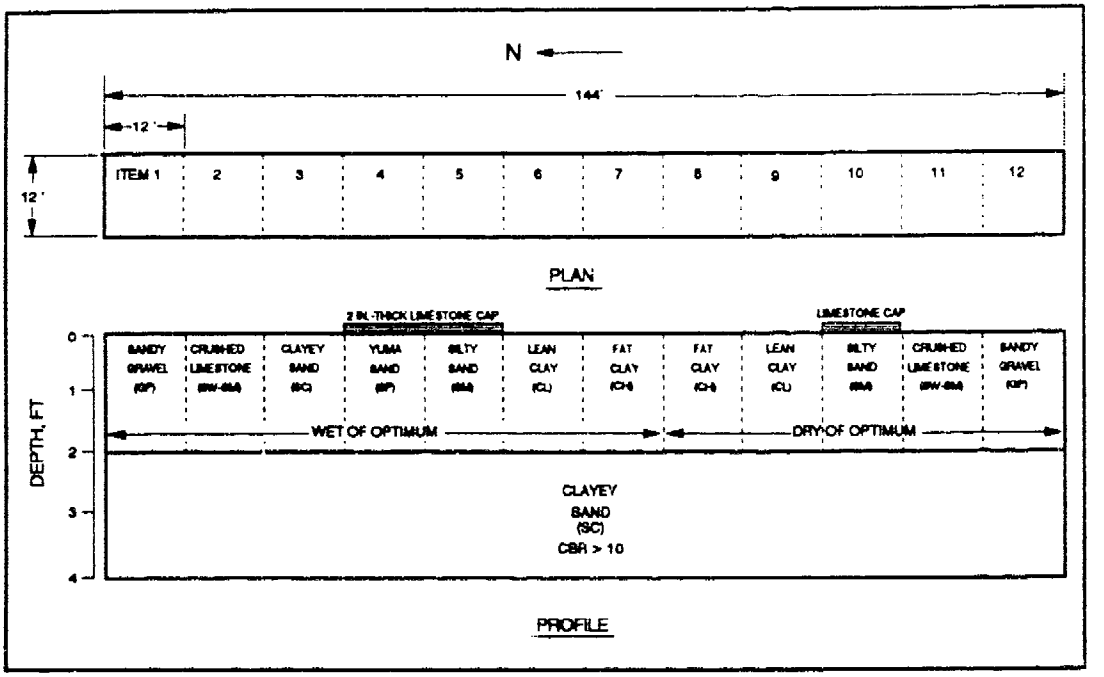

Figure 13. Plan and profile of test section 4

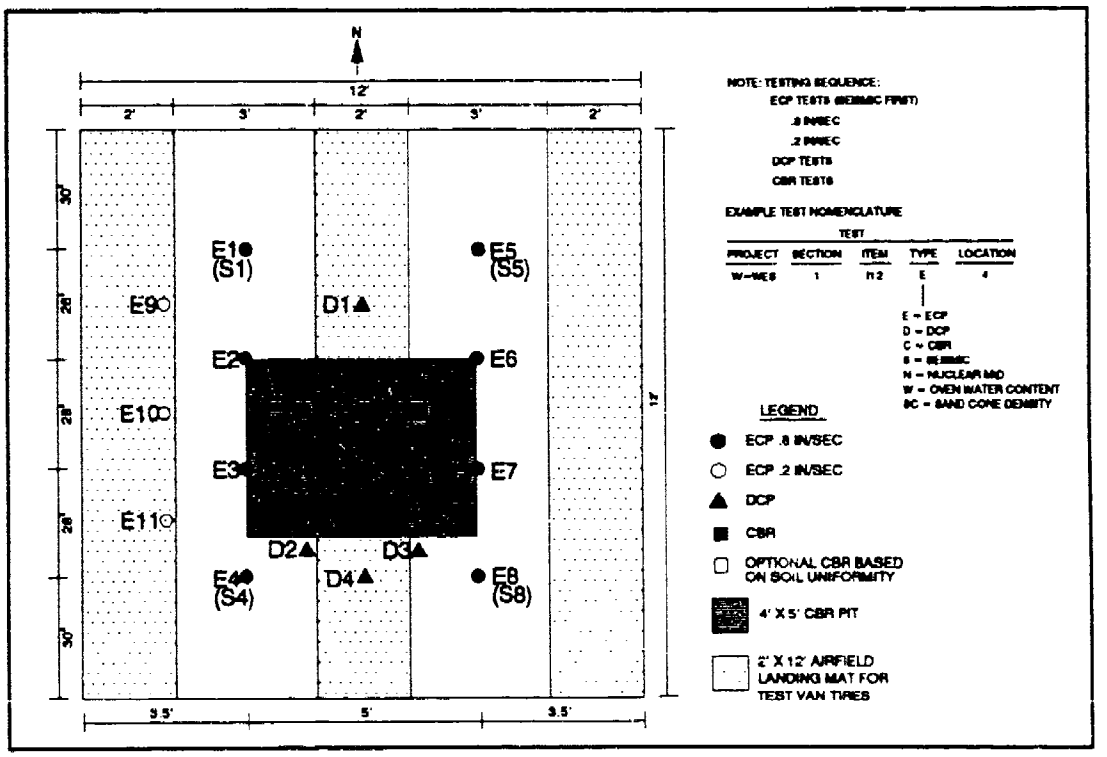

Figure 14. Test layout for typical test item for test sections 2, 3, and 4

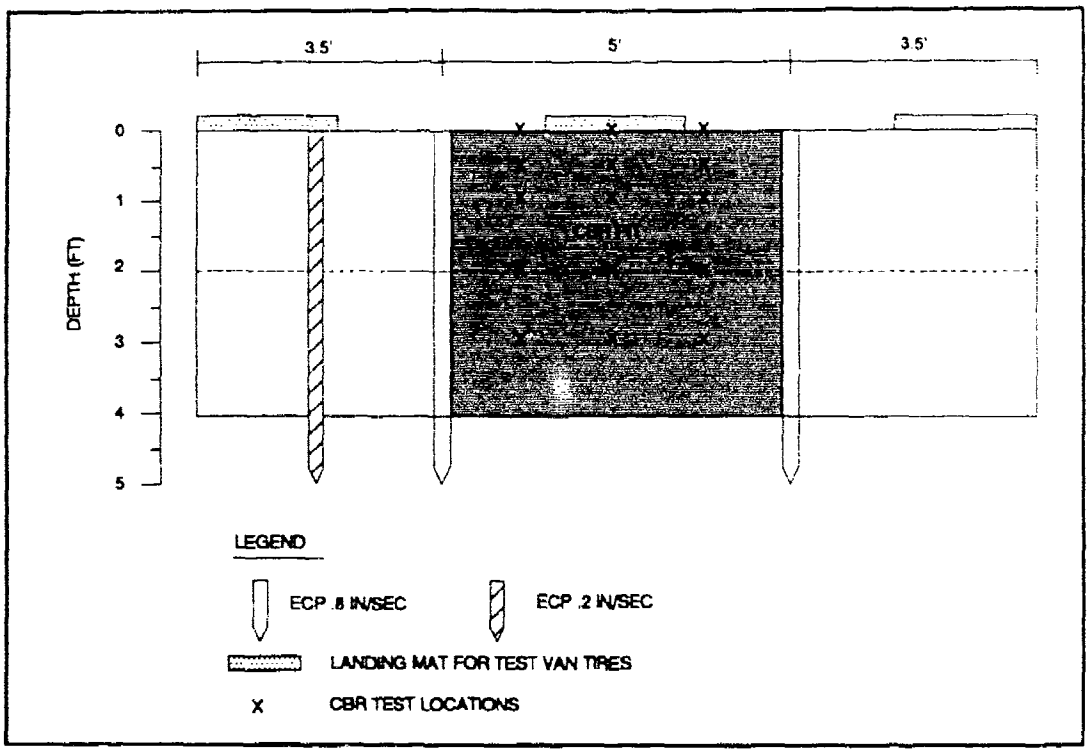

Figure 15. Typical test item profile for test sections 2, 3, and 4

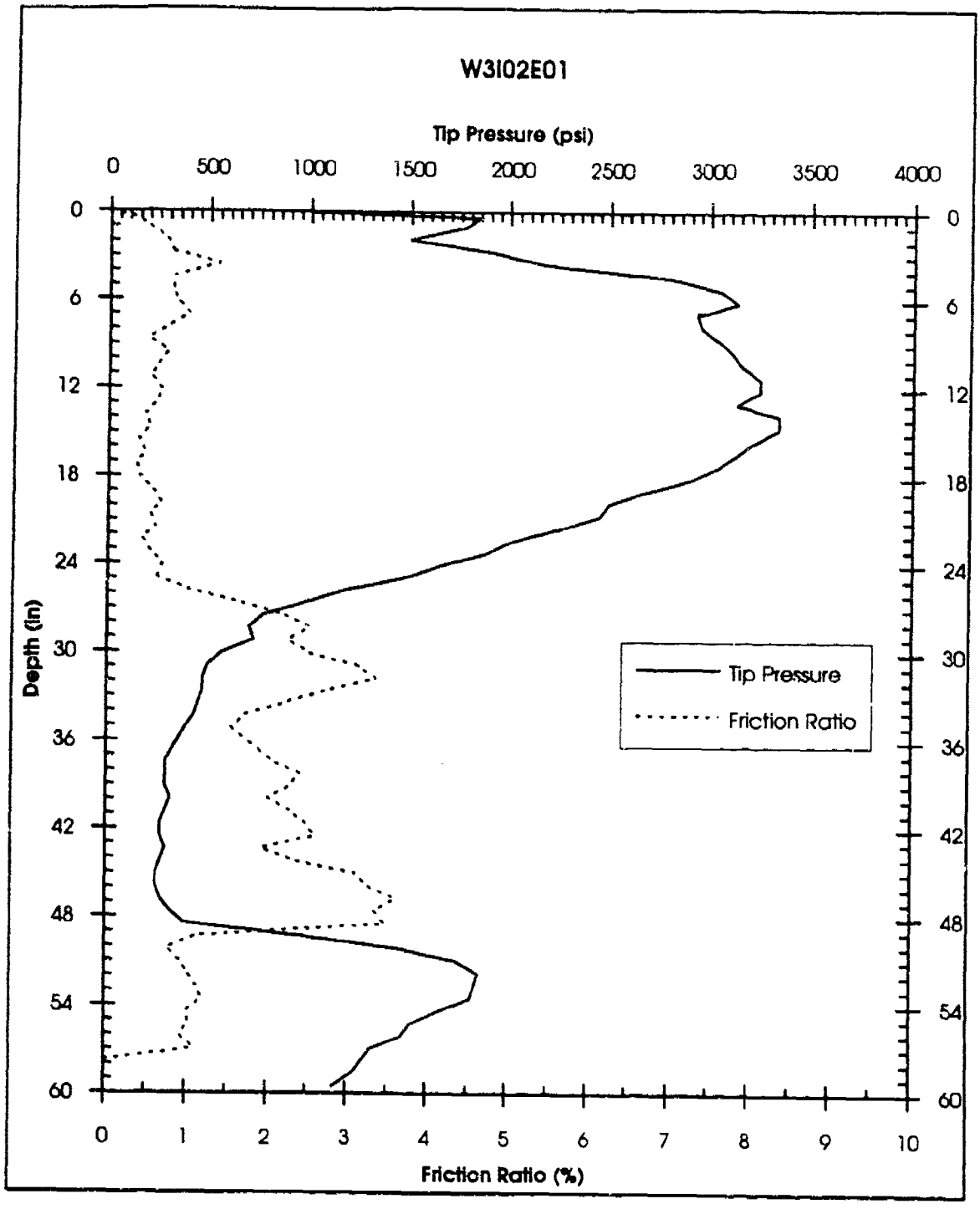

Figure 16. Example plot of ECP test data

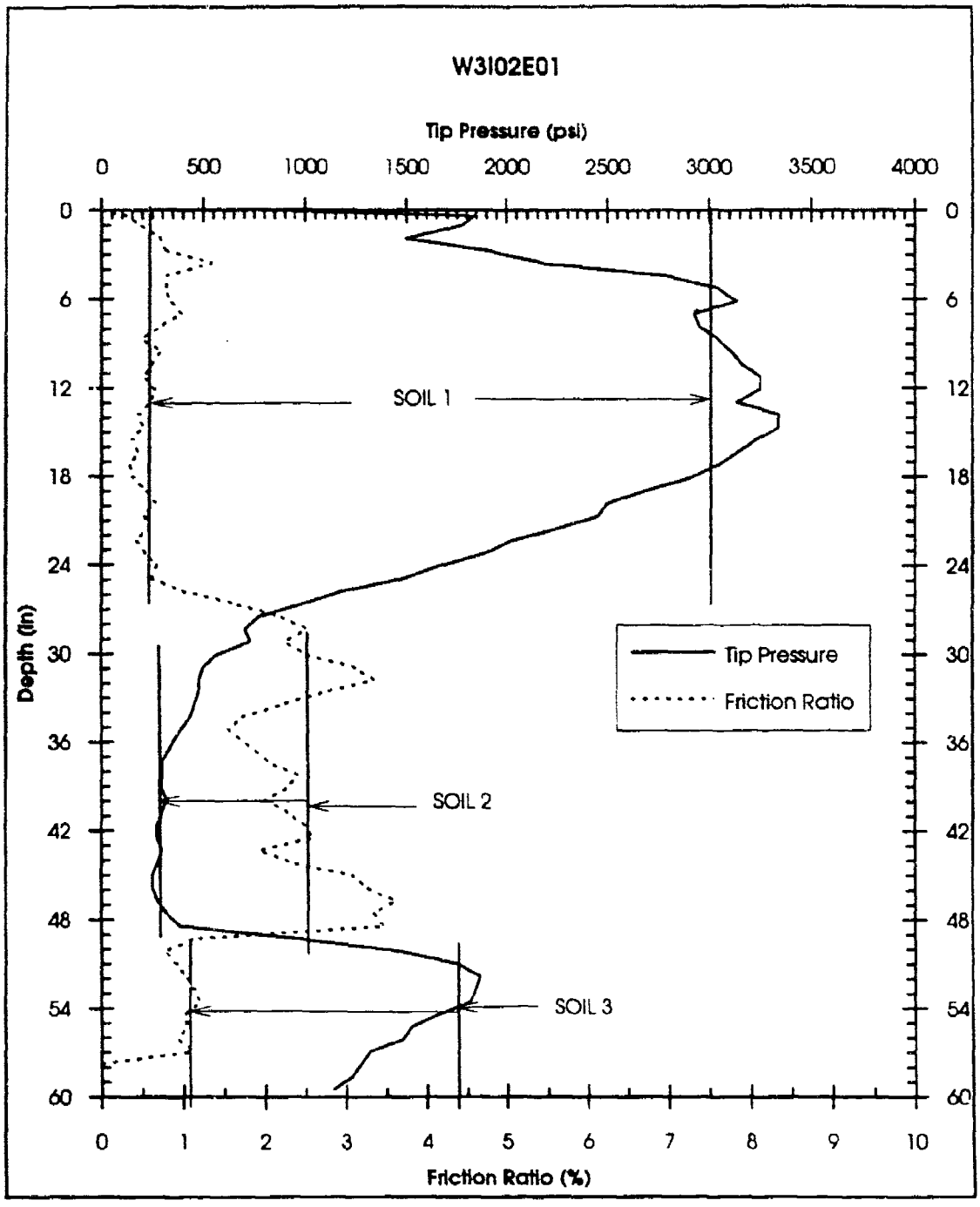

Figure 17. Using friction ratio and tip pressure plots to find soil layer type

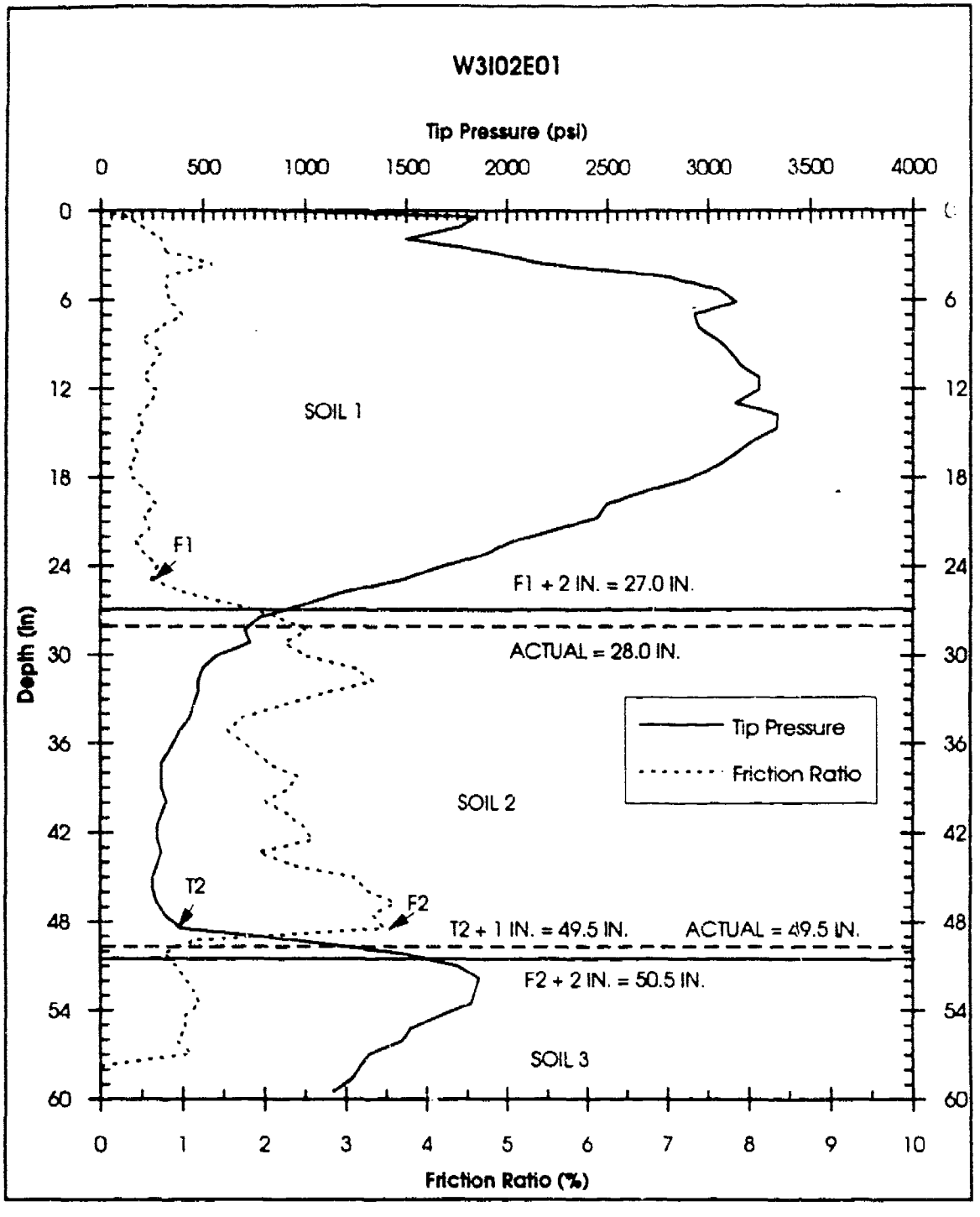

Figure 18. Using friction ratio and tip pressure plots to find soil layer interfaces

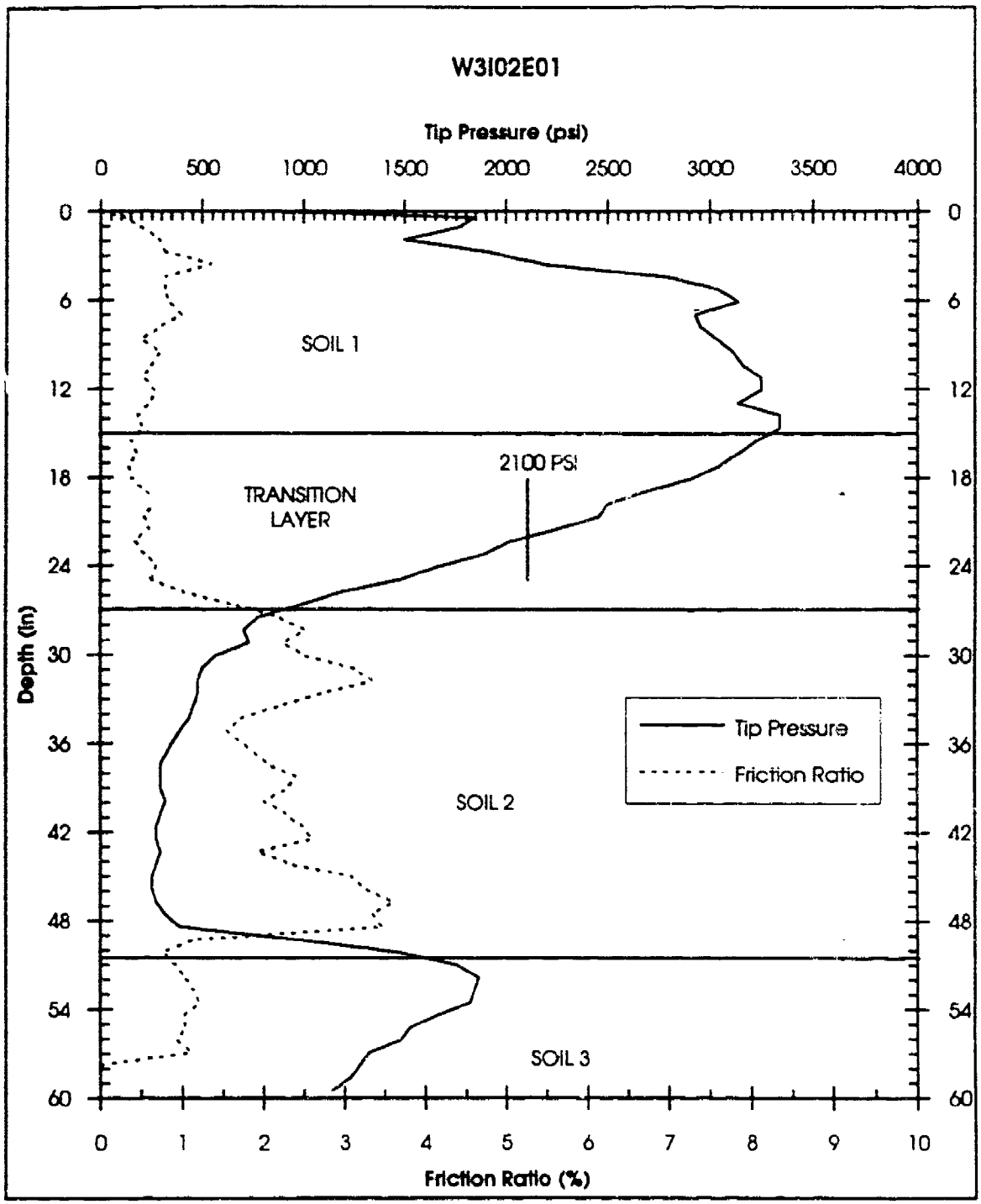

Figure 19. Using tip pressure curve to locate soil layer strength transition zone

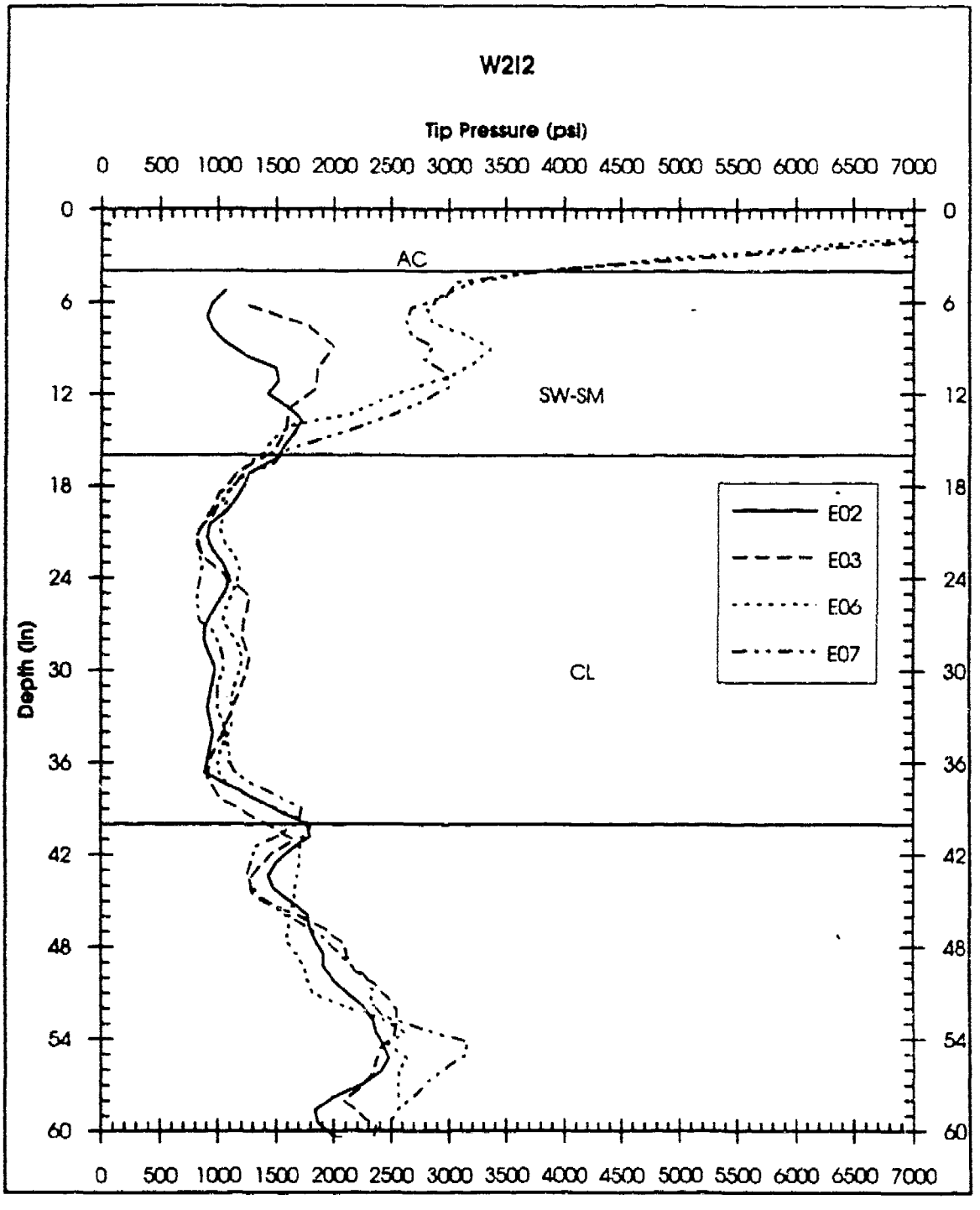

Figure 20. Effect of 4-in. AC overburden on tip pressure in test item W212

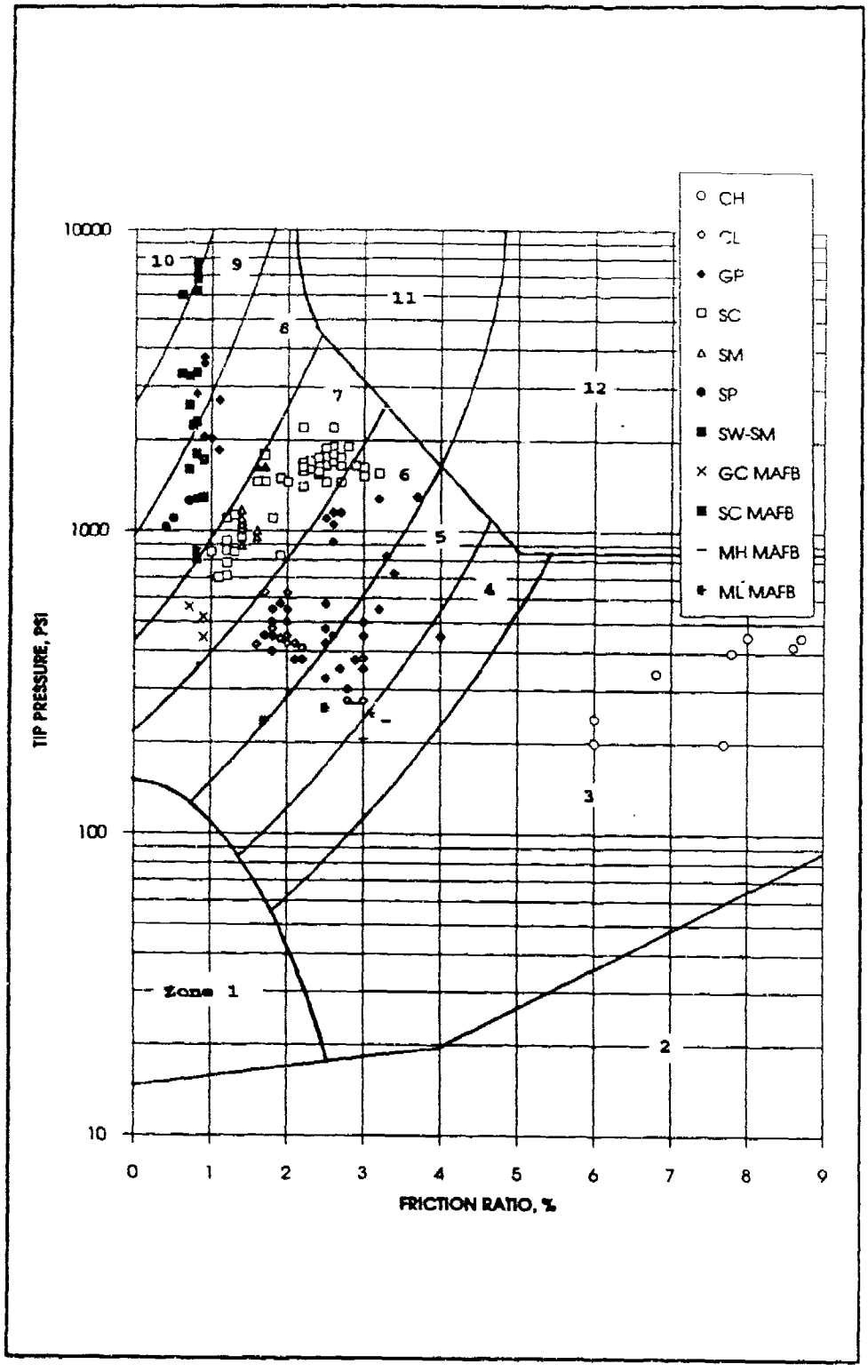

Figure 21. ECP test data overlay on Robertson et al. classification chart (Continued)

LEGEND FOR SOIL CLASSIFICATION SYSTEM BY ECP		
Zone	**Soil Behavior Type**	**USCS Group**
1	Sensitive Fine Grained	
2	Organic Material	OH
3	Clay	MH, CH, OH
4	Silty Clay to Clay	CL, OL, MH
5	Clayey Silt to Silty Clay	ML, CL, OL
6	Sandy Silt to Clayey Silt	ML, CL
7	Silty Sand to Sandy Silt	GC, SP, SM, SC
8	Sand to Silty Sand	GC, SW, SP, SM, SC
9	Sand	GP, GM, GC, SW
10	Gravelly Sand to Sand	GW, GP, GM
11	Very Stiff Fine Grained[1]	
12	Sand to Clayey Sand[1]	
[1] Overconsolidated or Cemented.		

Figure 21. (Concluded)

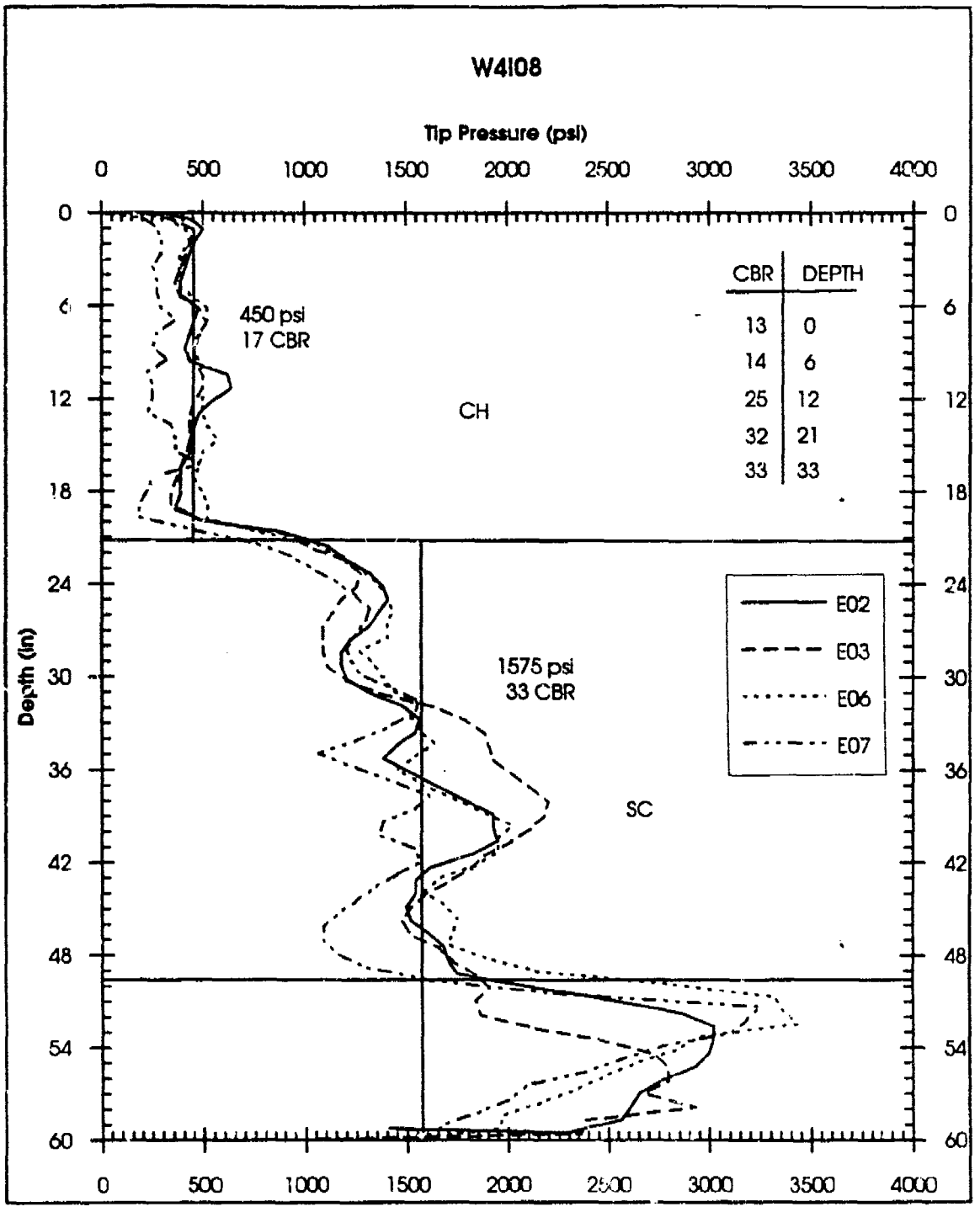

Figure 22. Typical plot of tip pressure curves used in ECP data interpretation

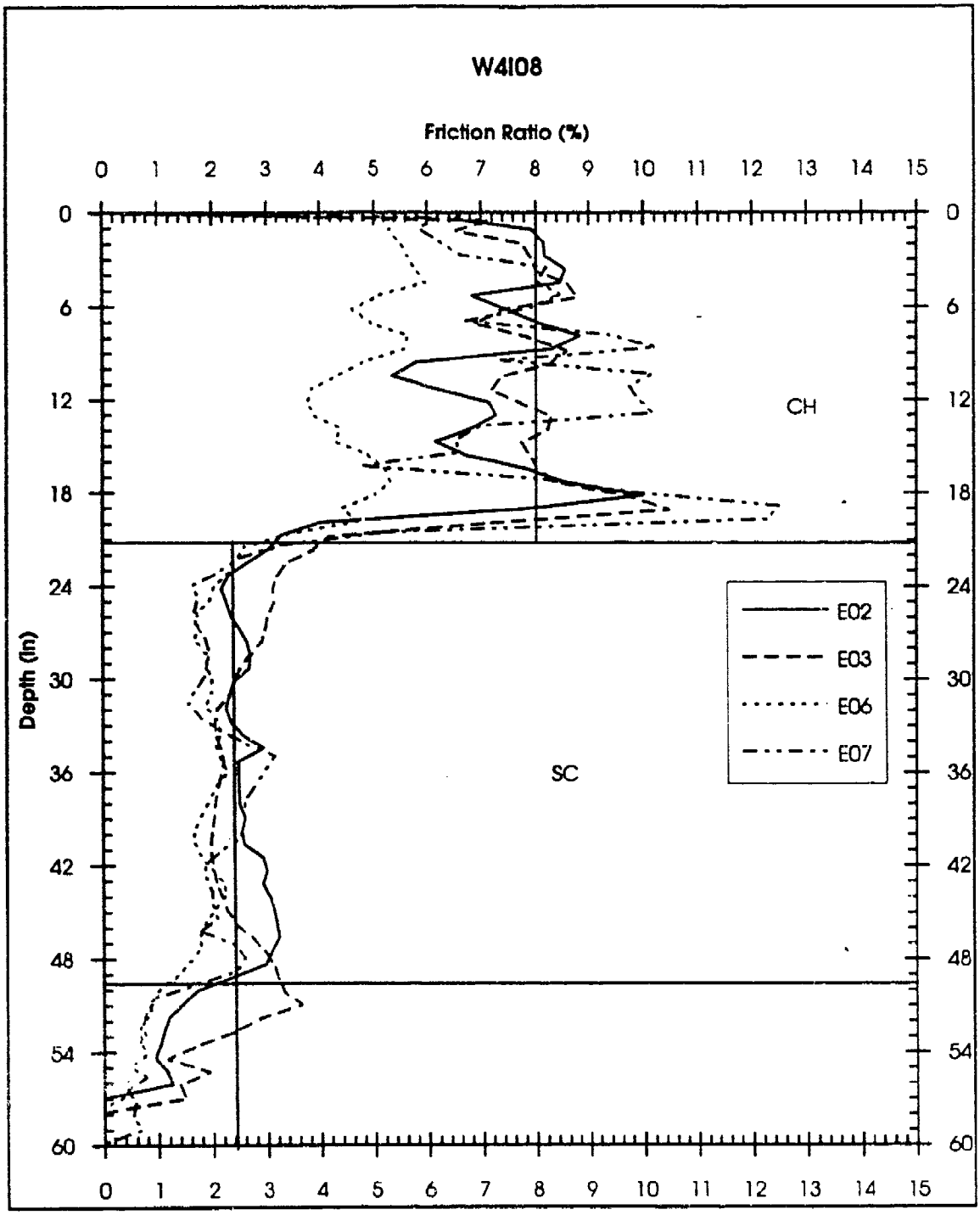

Figure 23. Typical plot of friction ratio curves used in ECP data interpretation

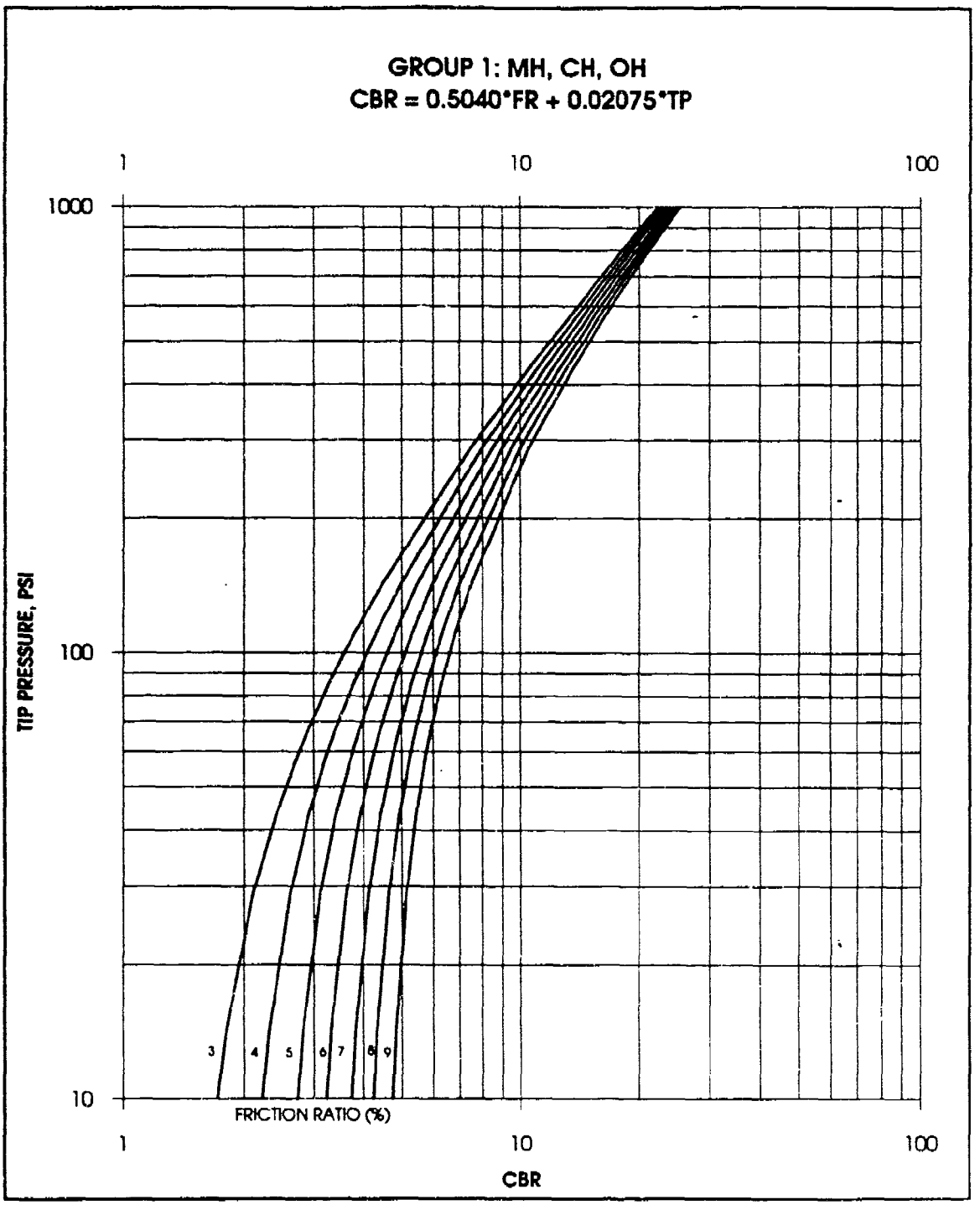

Figure 24. ECP versus CBR correlation for group 1 soils

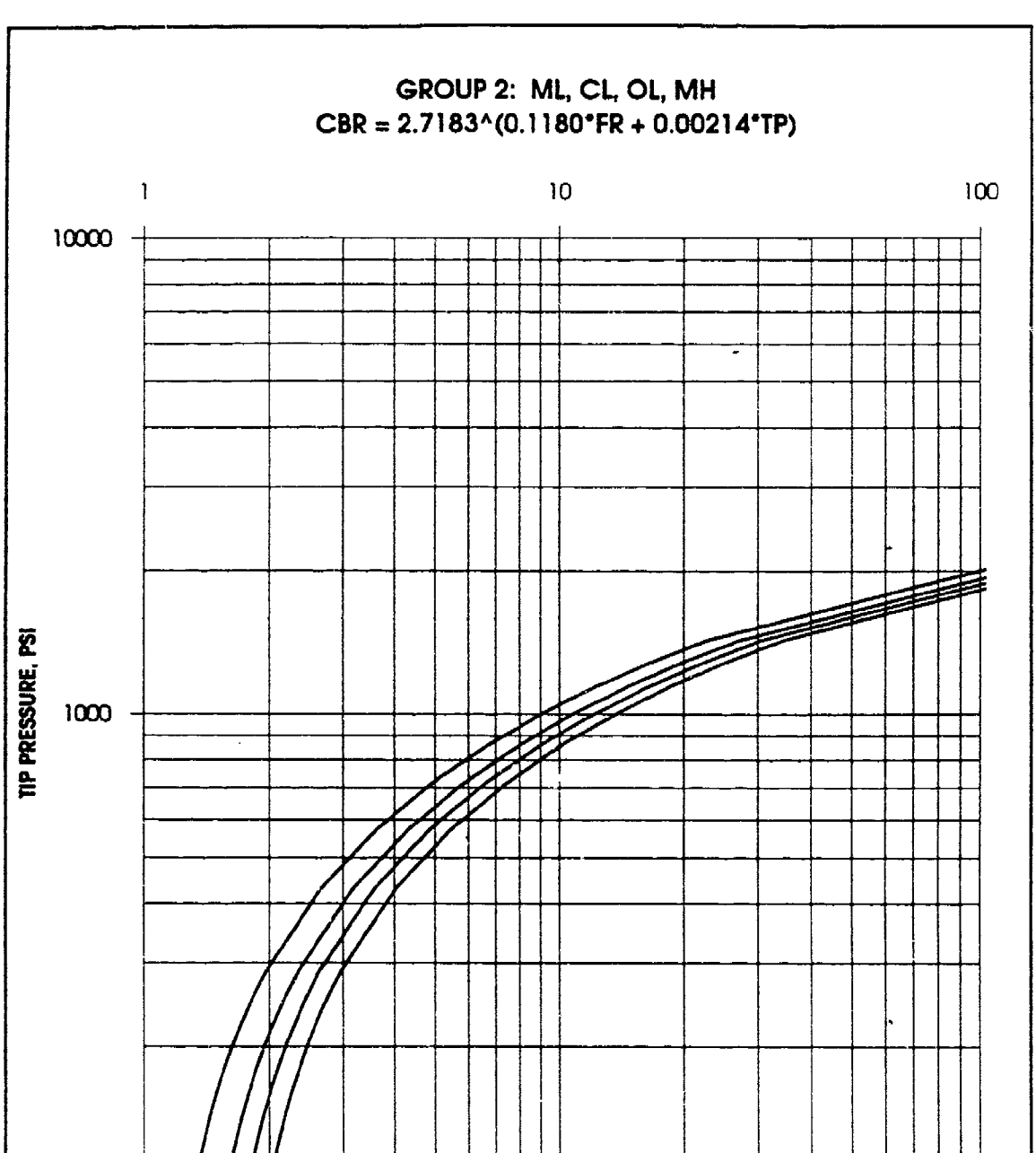

Figure 25. ECP versus CBR correlation for group 2 soils

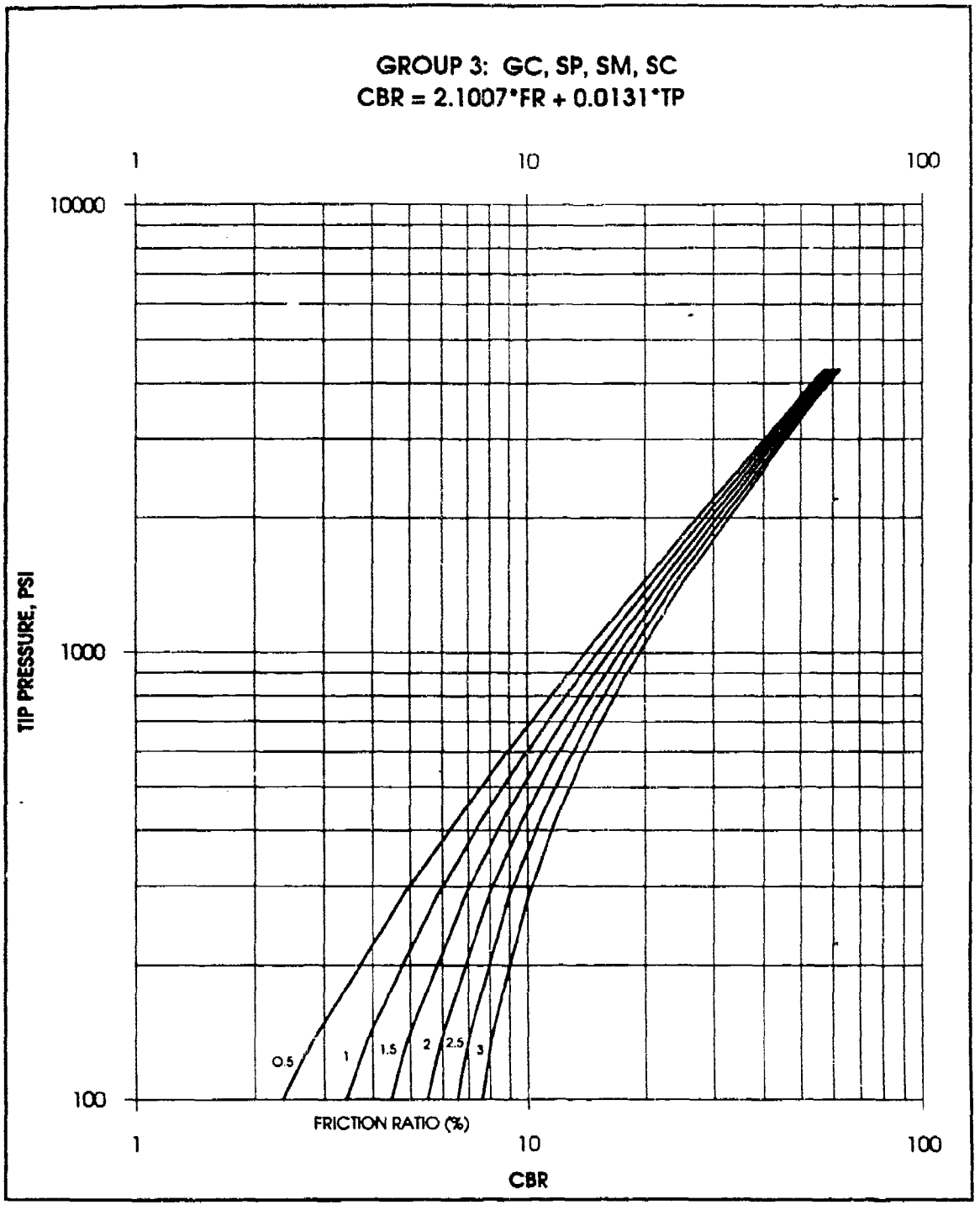

Figure 26. ECP versus CBR correlation for group 3 soils

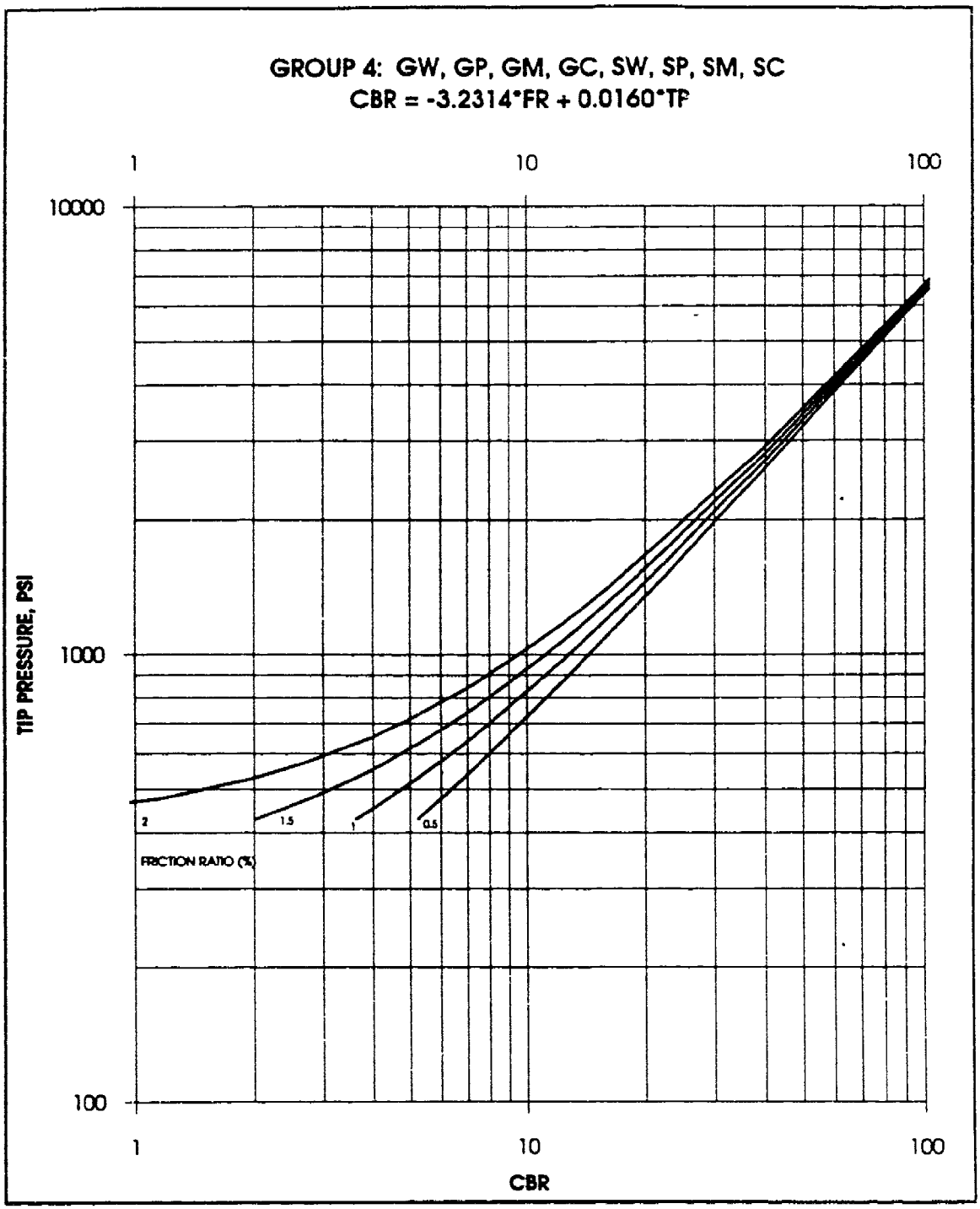

Figure 27. ECP versus CBR correlation for group 4 soils

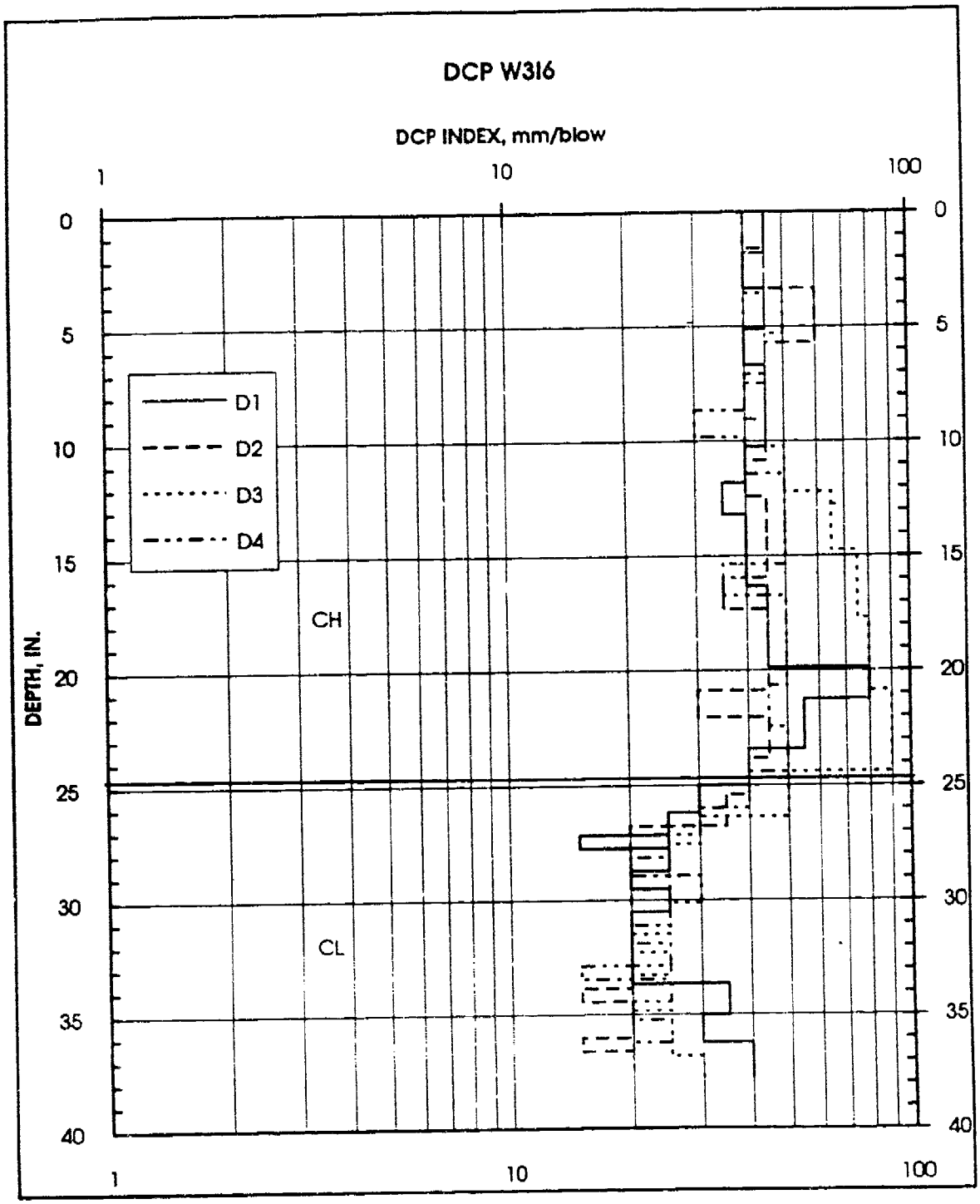

Figure 28. Typical DCP data plot used in data interpretation

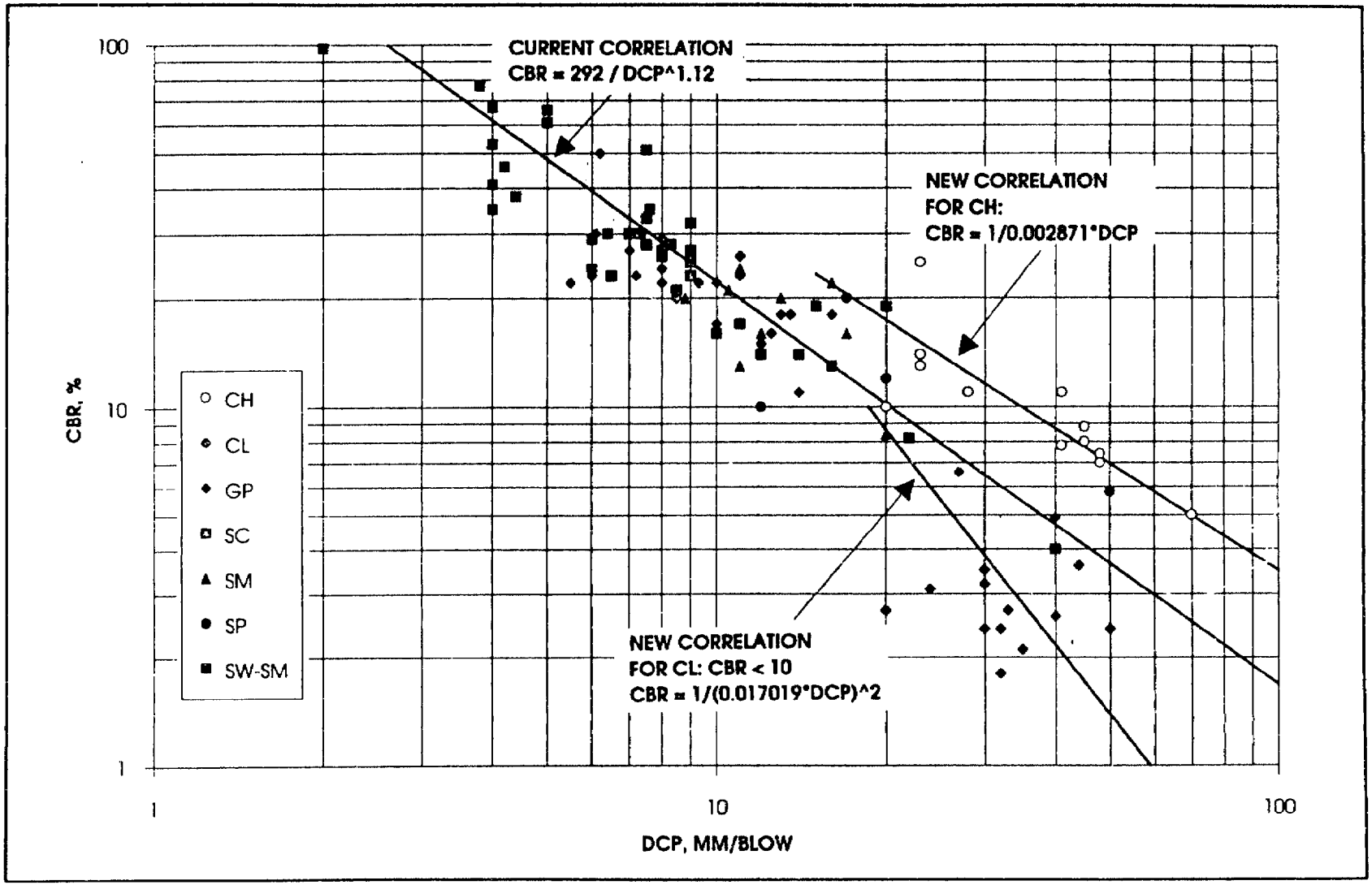

Figure 29. Plot of DCP and CBR test data versus current WES correlation

Appendix A
Soil Classification Data

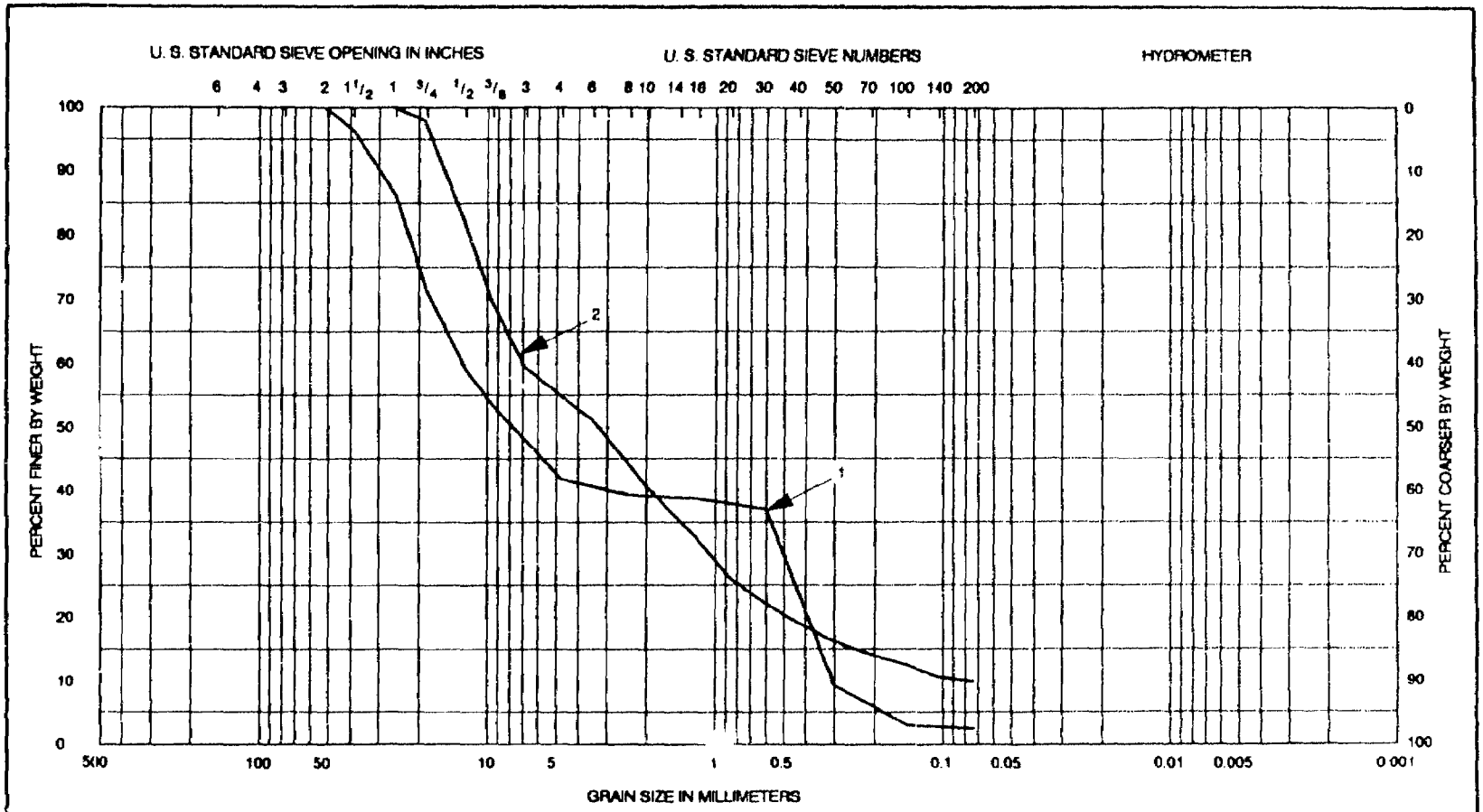

SAMPLE NO	MATERIAL	CLASSIFICATION	NAT W%	LL	PL	PI
1	PIT RUN	SANDY GRAVEL (GP)				NP
2		CRUSHED LIMESTONE (SW-SM)				NP

GRADATION CURVES

PROJECT	AIR FORCE FORCE PROJECTION SITE EVALUATION
SOURCE	VICKSBURG, MS WATERWAYS EXPERIMENT STATION
BORING NO.	
DATE	08 SEP 92

Figure A1. Classification data for WES GP and SW-SM soils

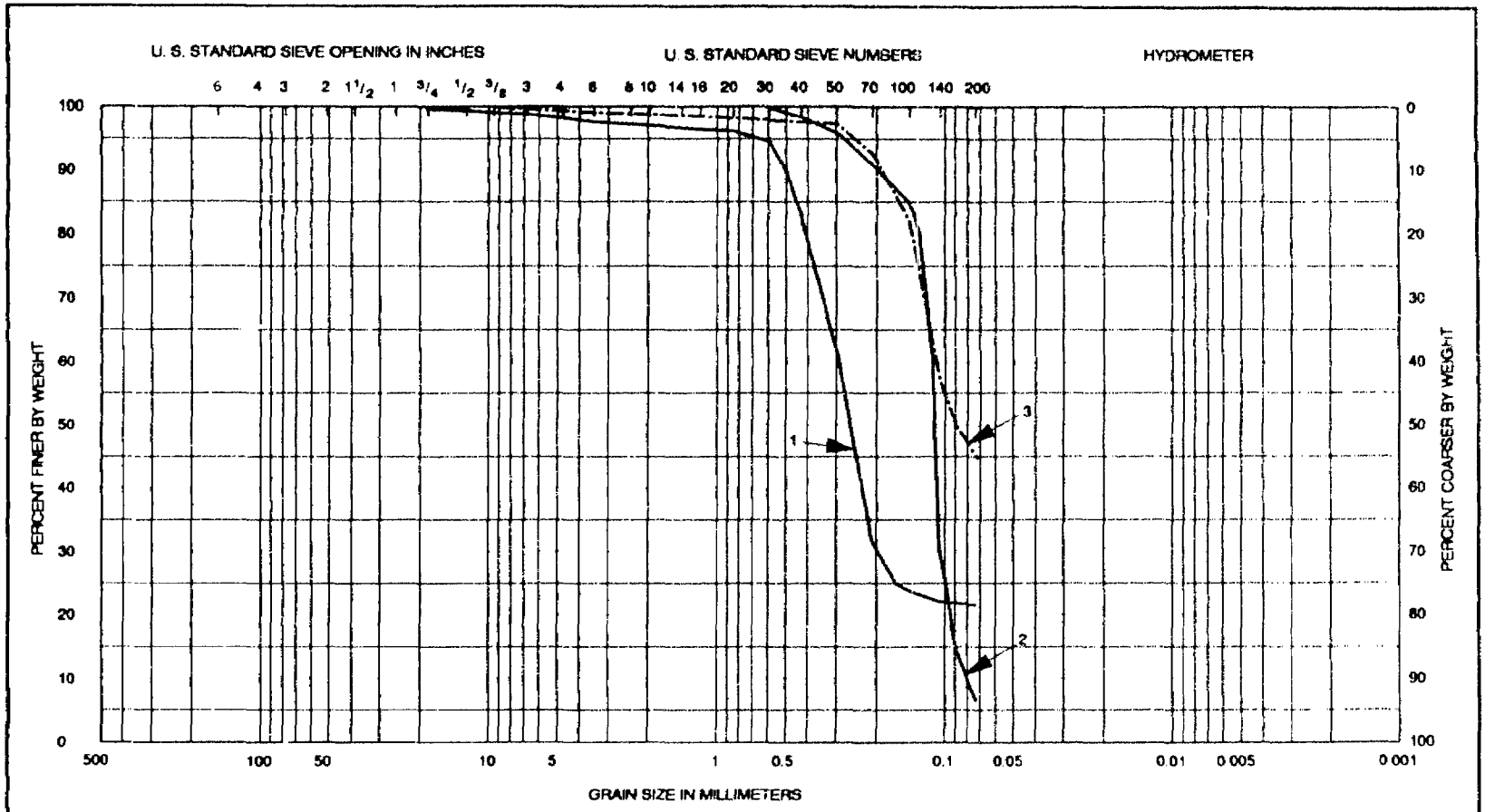

SAMPLE NO	MATERIAL	CLASSIFICATION	NAT W%	LL	PL	PI
1		CLAYEY SAND (SC)		25	14	11
2		YUMA SAND (SP)				NP
3		SILTY SAND (SM)				NP

GRADATION CURVES

PROJECT	AIR FORCE FORCE PROJECTION SITE EVALUATION
SOURCE	VICKSBURG, MS WATERWAYS EXPERIMENT STATION
BORING NO.	
DATE	08 SEP 92

Figure A2. Classification data for WES SC, SP and SM soils

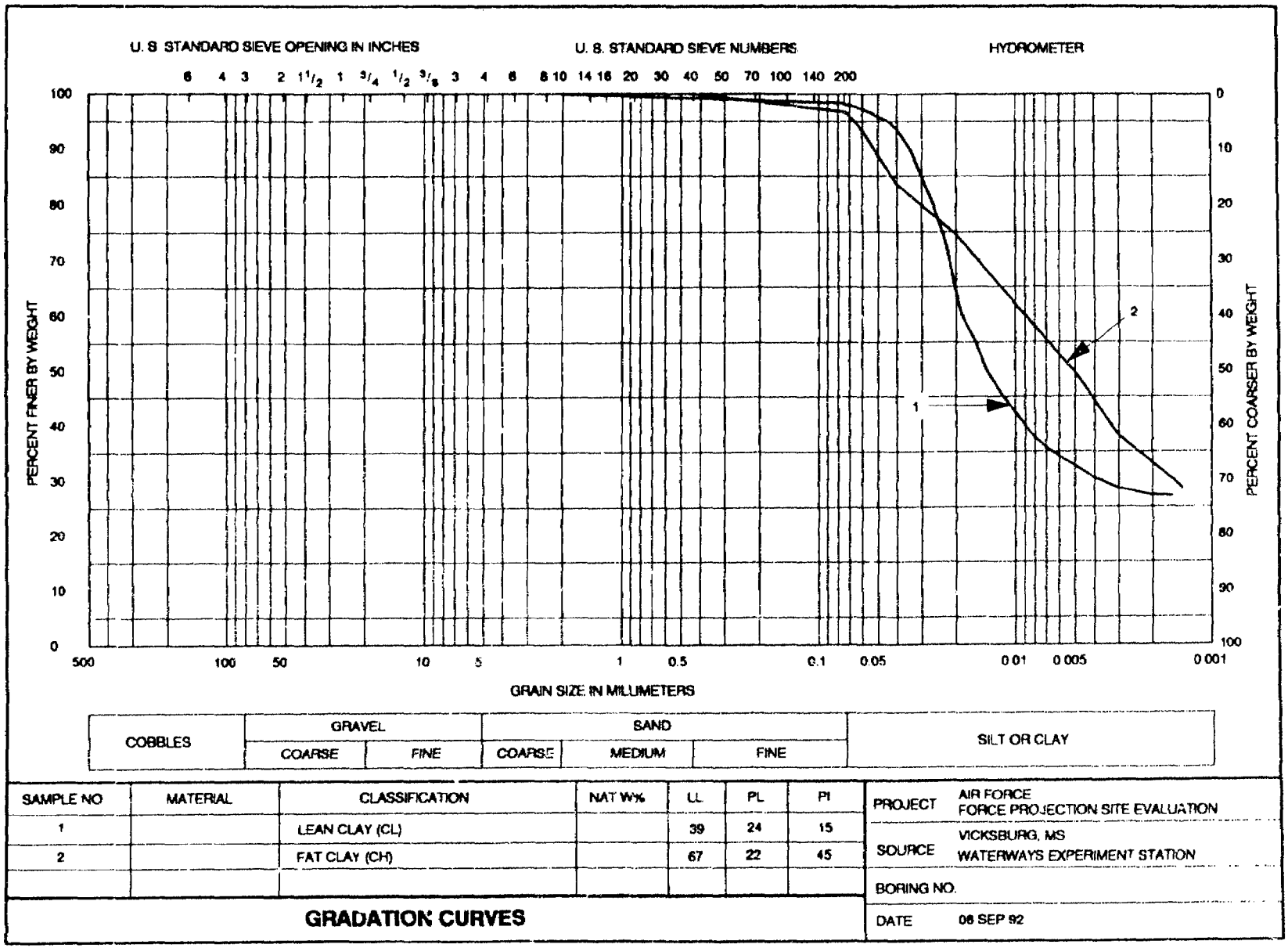

SAMPLE NO	MATERIAL	CLASSIFICATION	NAT W%	LL	PL	PI
1		LEAN CLAY (CL)		39	24	15
2		FAT CLAY (CH)		67	22	45

GRADATION CURVES

PROJECT	AIR FORCE FORCE PROJECTION SITE EVALUATION
SOURCE	VICKSBURG, MS WATERWAYS EXPERIMENT STATION
BORING NO.	
DATE	08 SEP 92

Figure A3. Classification data for WES CL and CH soils

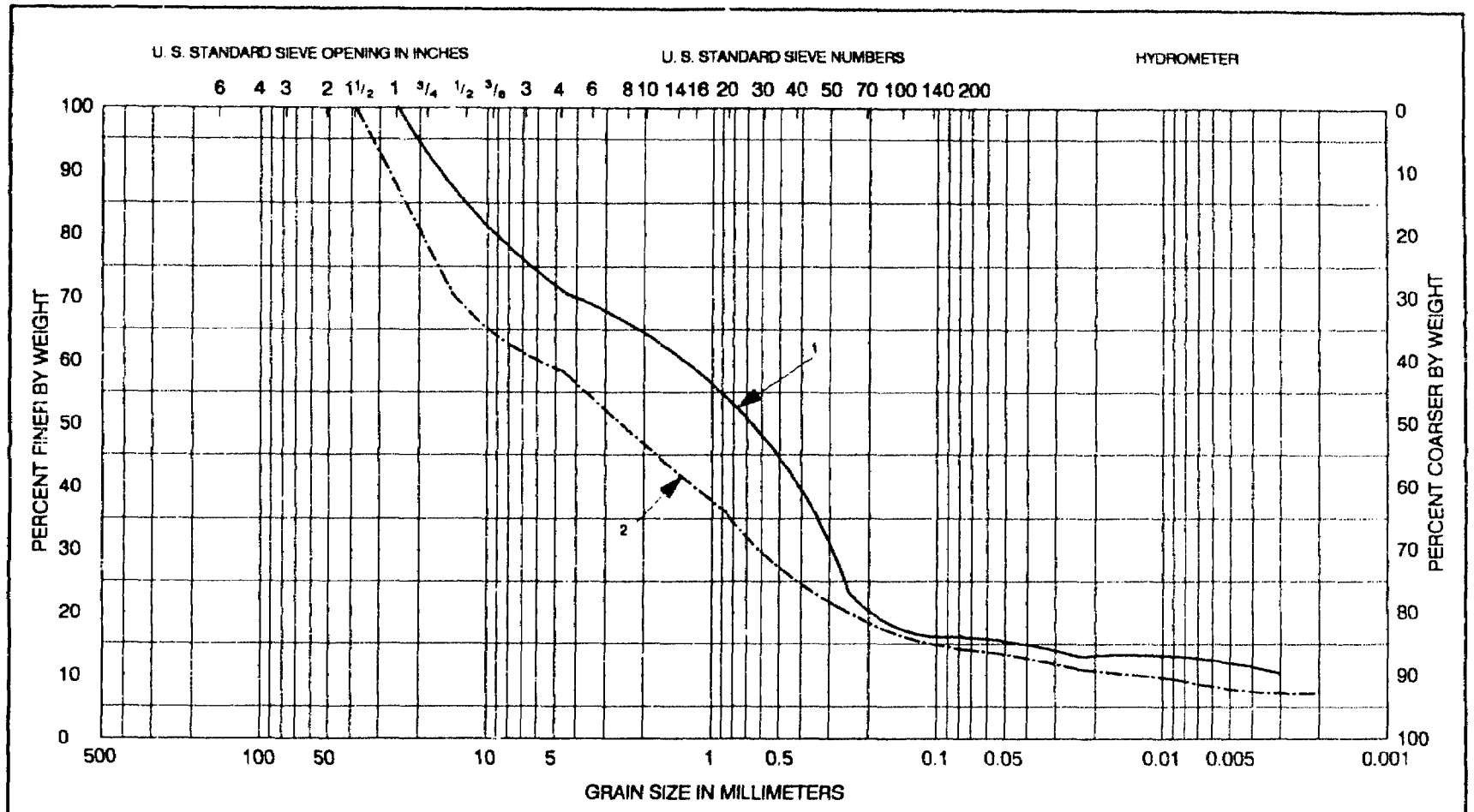

SAMPLE NO.	MATERIAL	CLASSIFICATION	NAT W%	LL	PL	PI
1		CLAYEY SAND (SC)	7.4	46.8	25.7	21.1
2		CLAYEY GRAVEL (GC)	9.1	38.0	19.0	19.0

GRADATION CURVES

PROJECT AIR FORCE FORCE PROJECTION SITE EVALUATION

SOURCE MAXWELL AFB, AL

BORING NO.

DATE AUG 92

Figure A4. Classification data for MAFB SC and GC soils

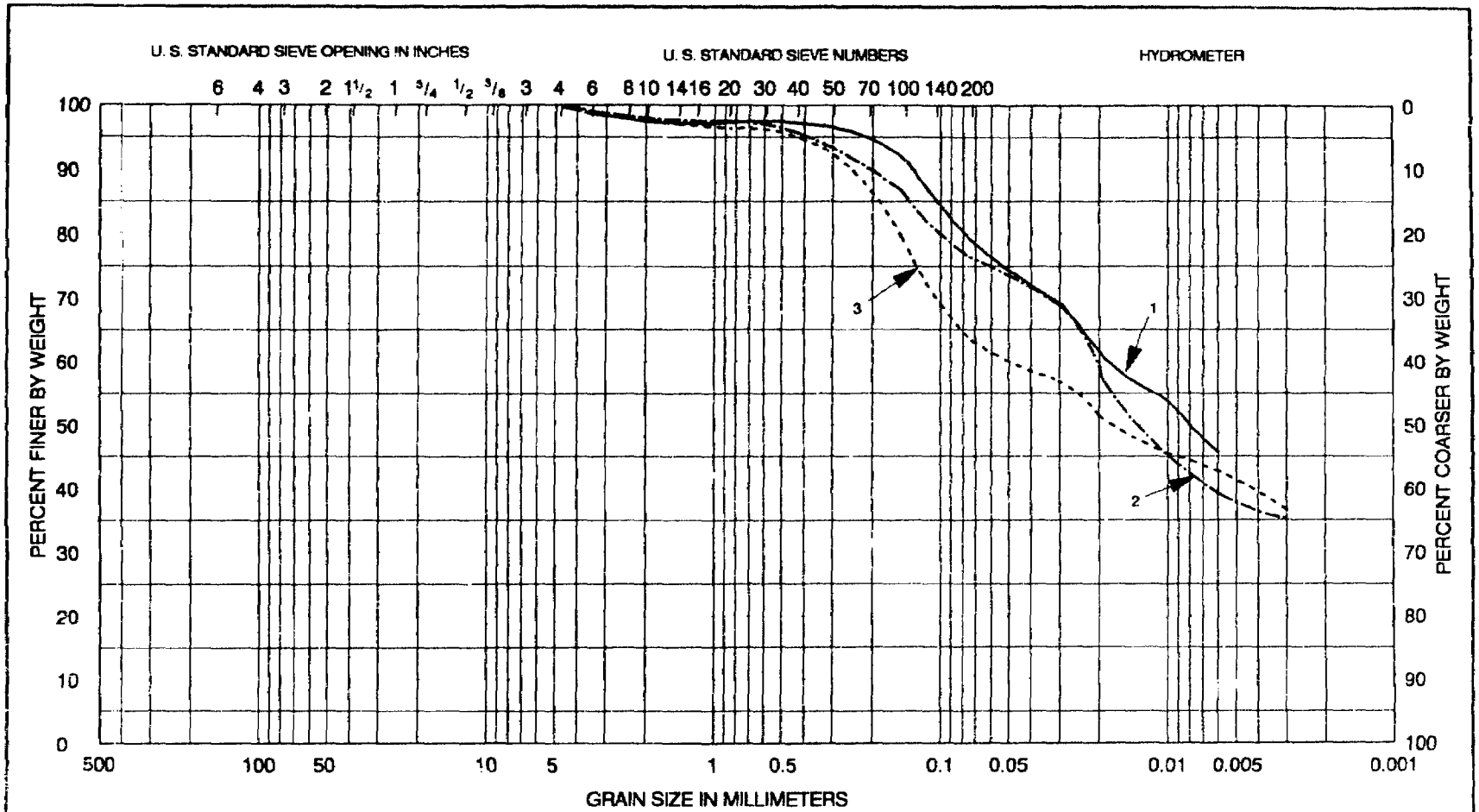

SAMPLE NO	MATERIAL	CLASSIFICATION	NAT W%	LL	PL	PI
1		SILT (MH)	25.7	51.0	31.7	19.3
2		LEAN CLAY (CL)	19.6	42.6	24.0	18.6
3		SILT (ML)	22.3	45.9	32.9	13.0

GRADATION CURVES

PROJECT AIR FORCE FORCE PROJECTION SITE EVALUATION

SOURCE MAXWELL AFB, AL

BORING NO.

DATE AUG 92

Figure A5. Classification data for MAFB MH, CL and ML soils

Appendix B
MAFB ECP Plots With and Without Overburden

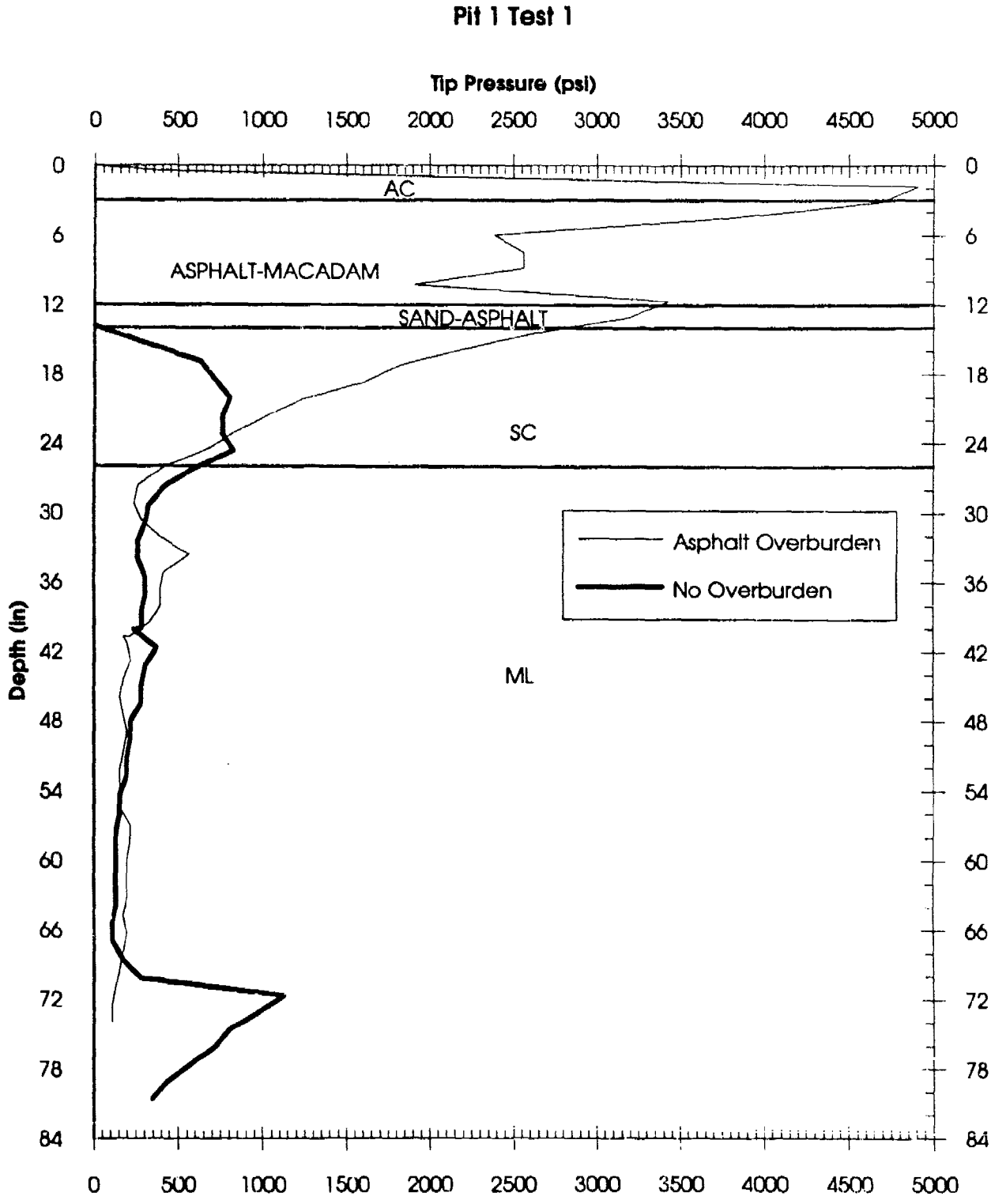

Figure B1. ECP TP versus depth for MAFB pit 1 test 1

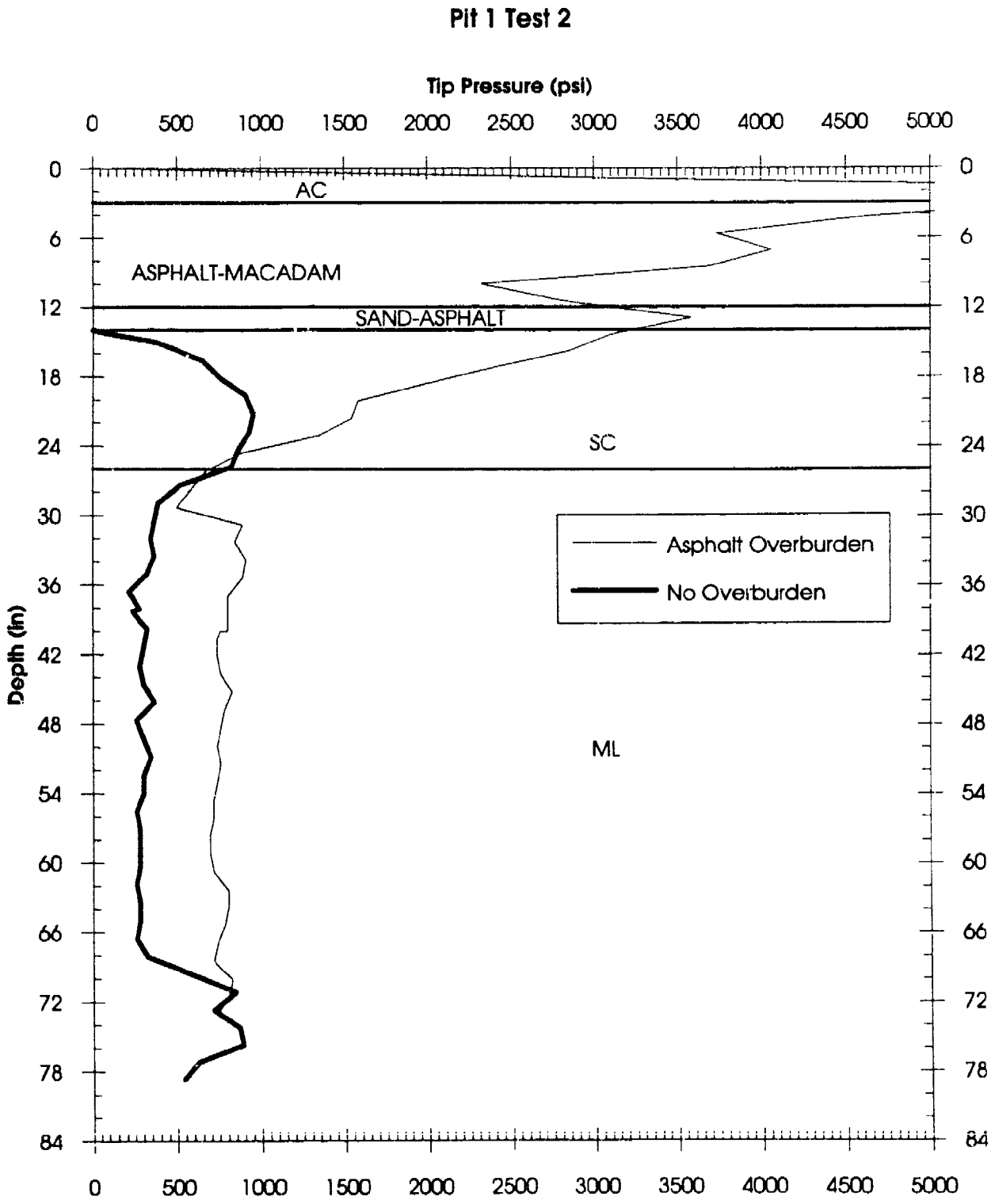

Figure B2. ECP TP versus depth for MAFB pit 1 test 2

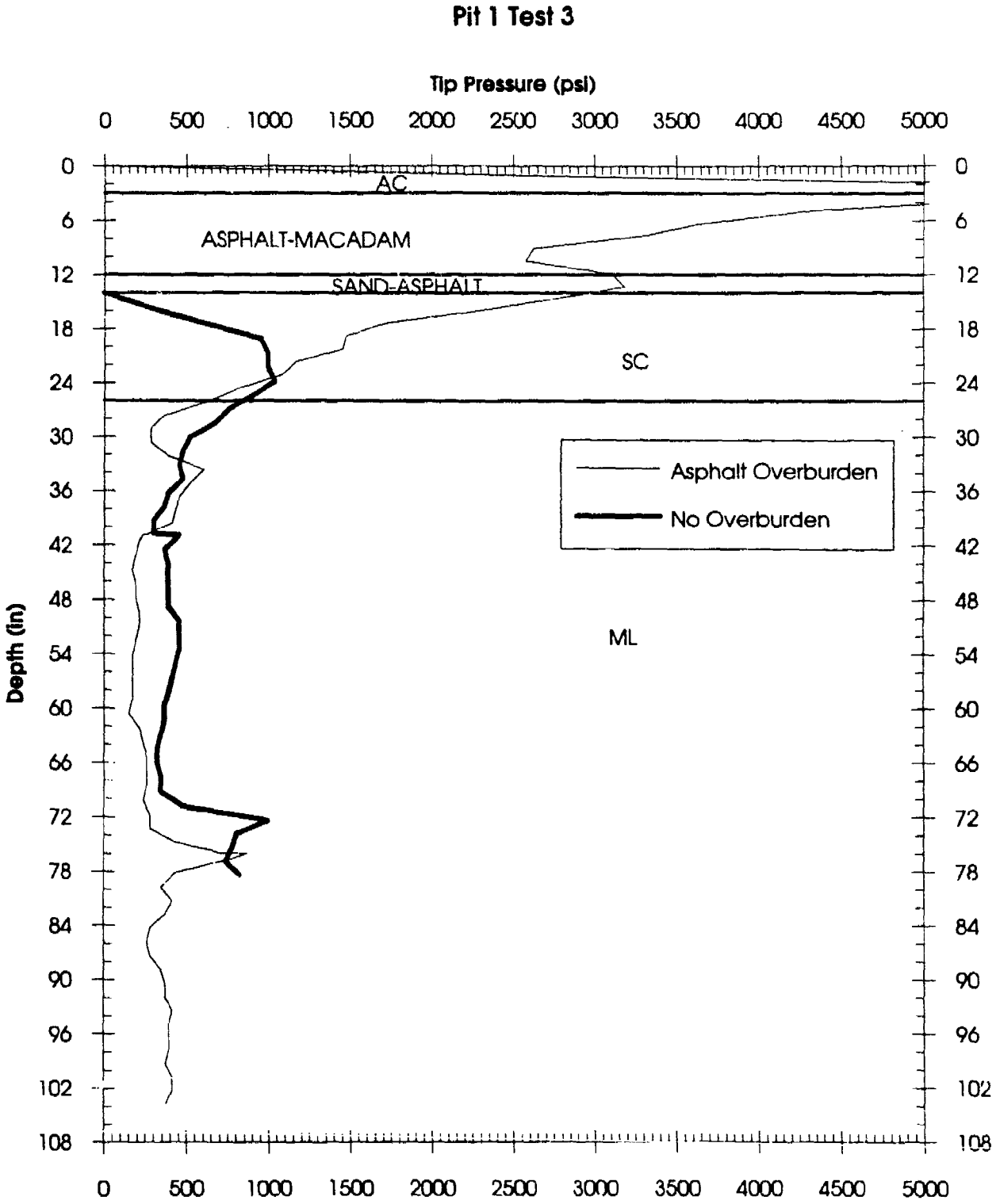

Figure B3. ECP TP versus depth for MAFB pit 1 test 3

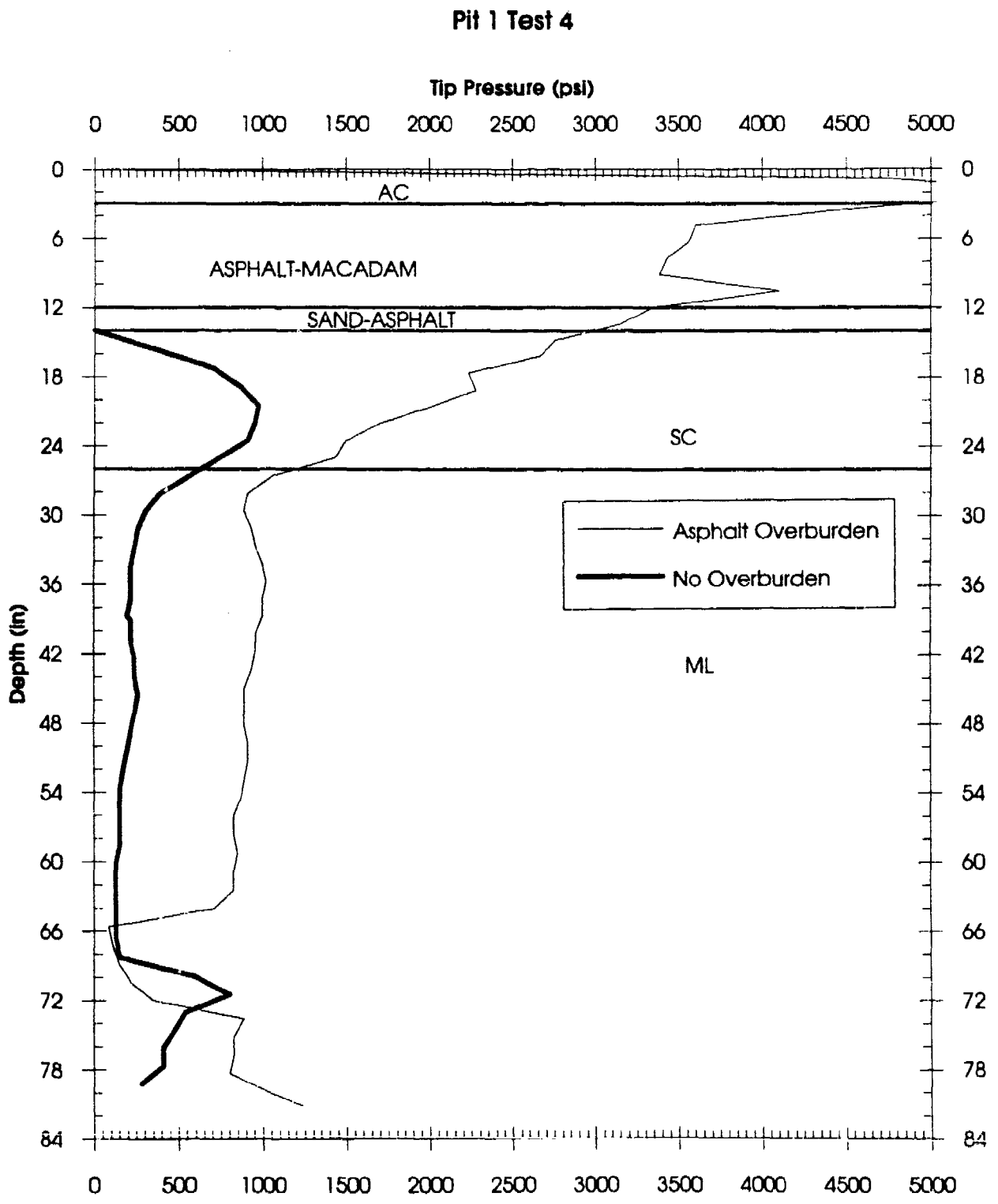

Figure B4. ECP TP versus depth for MAFB pit 1 test 4

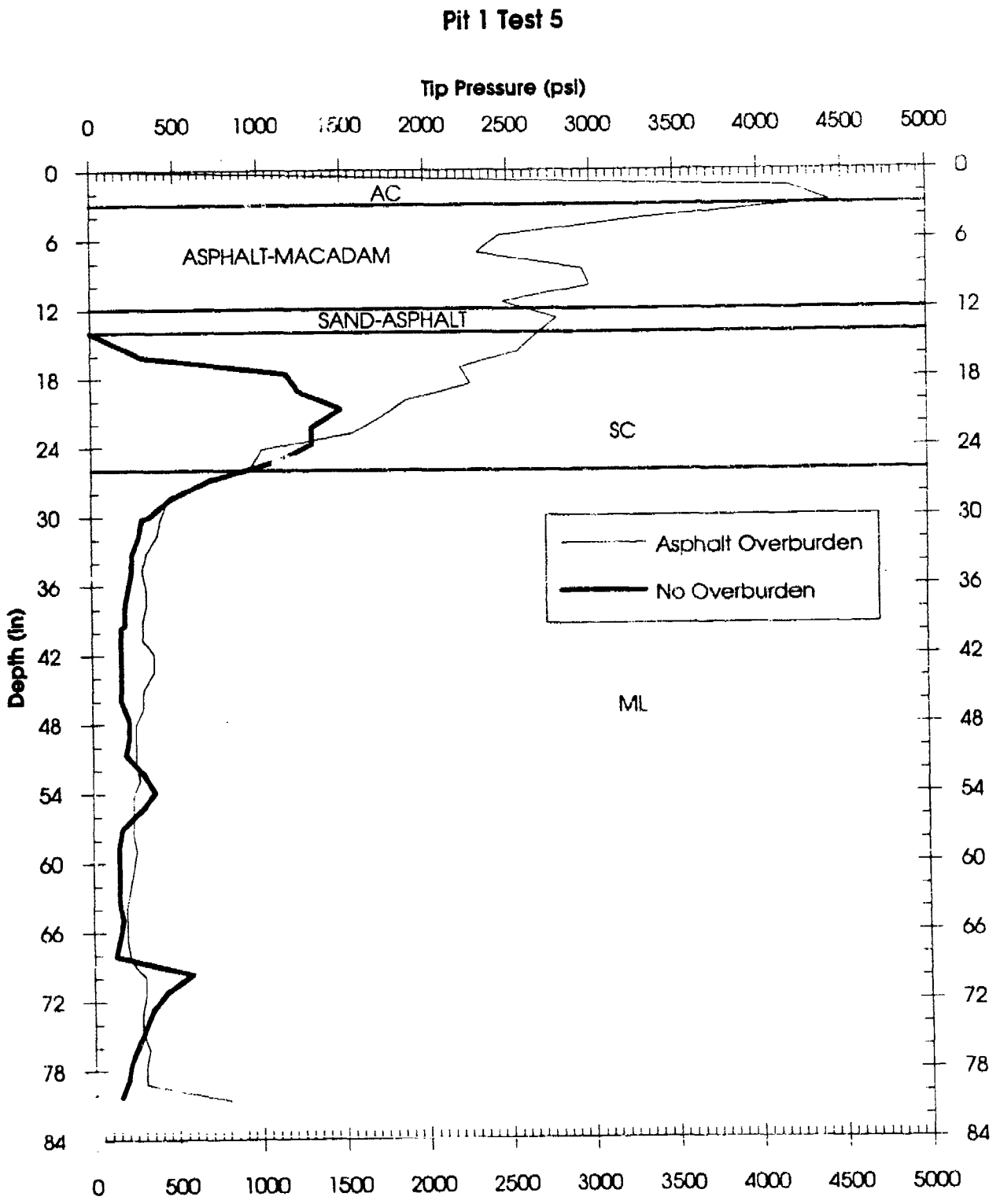

Figure B5. ECP TP versus depth for MAFB pit 1 test 5

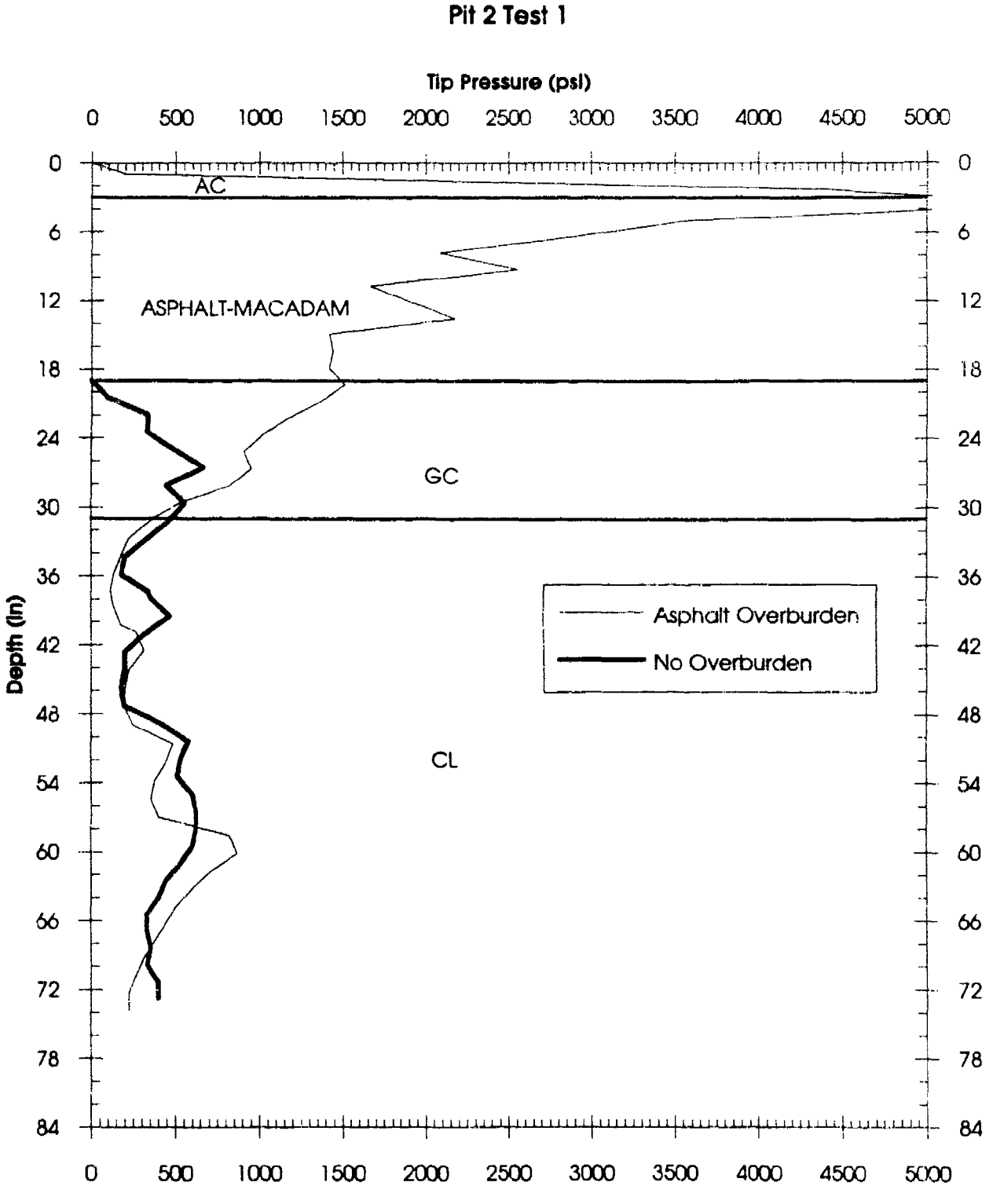

Figure B6. ECP TP versus depth for MAFB pit 2 test 1

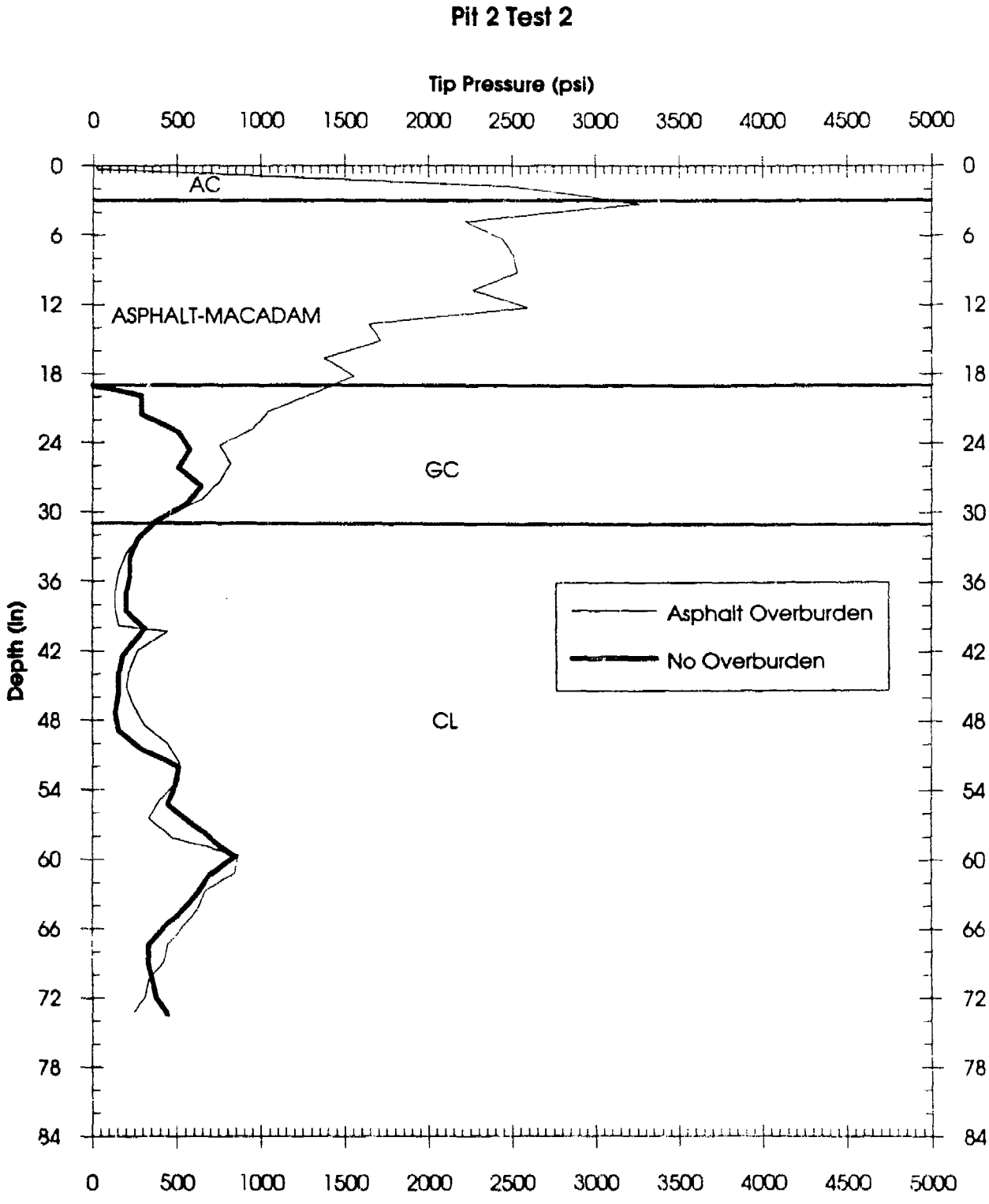

Figure B7. ECP TP versus depth for MAFB pit 2 test 2

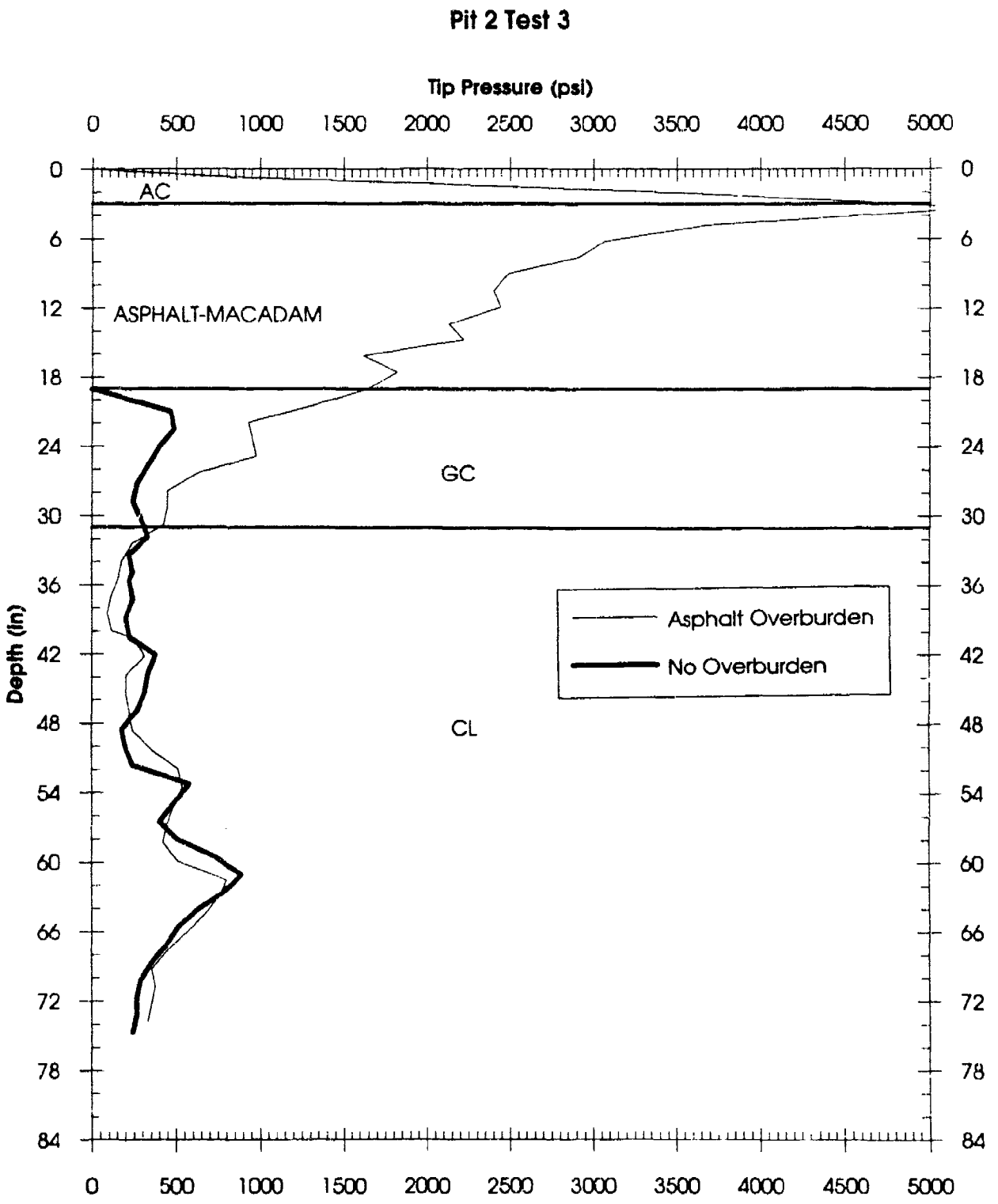

Figure B8. ECP TP versus depth for MAFB pit 2 test 3

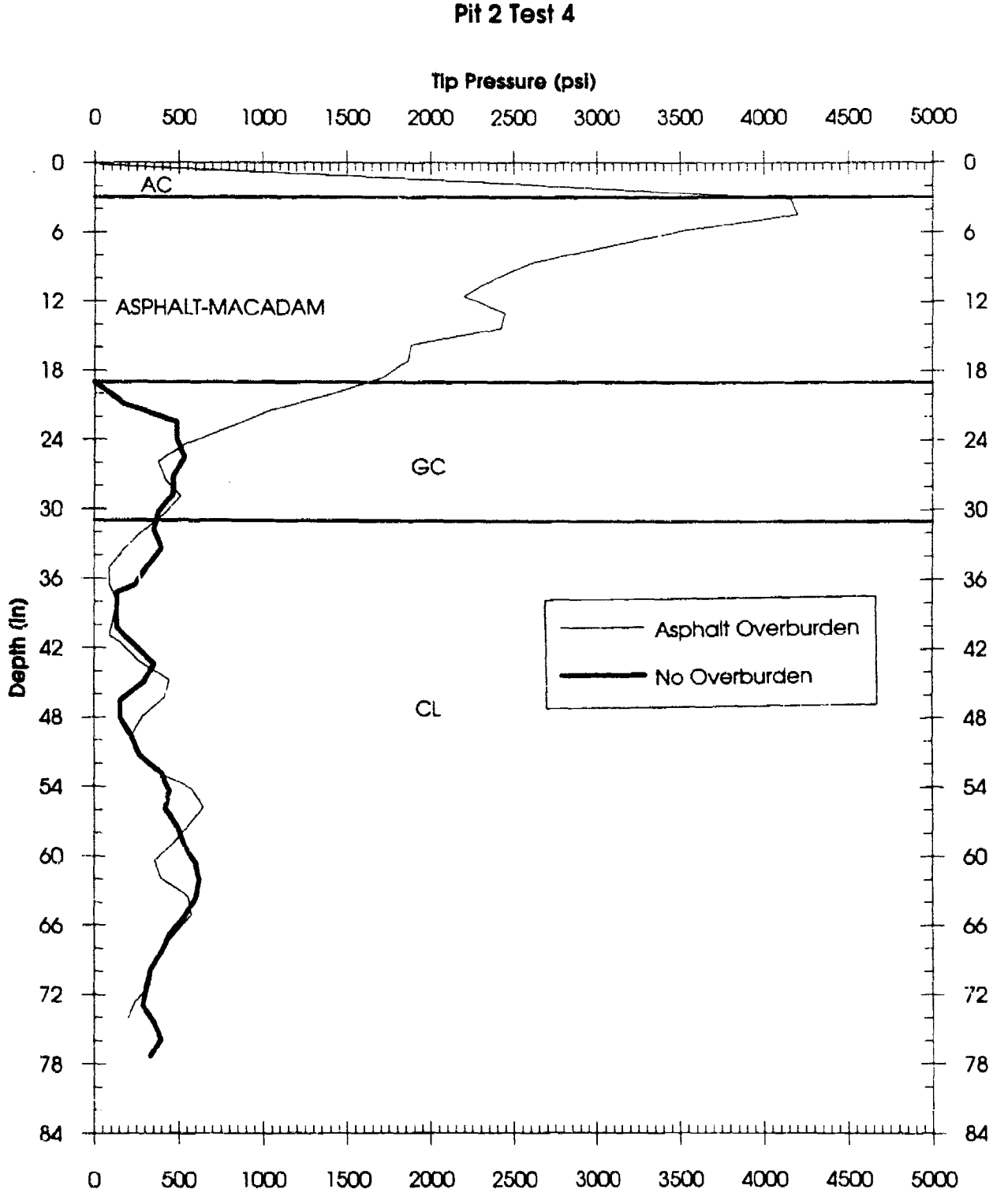

Figure B9. ECP TP versus depth for MAFB pit 2 test 4

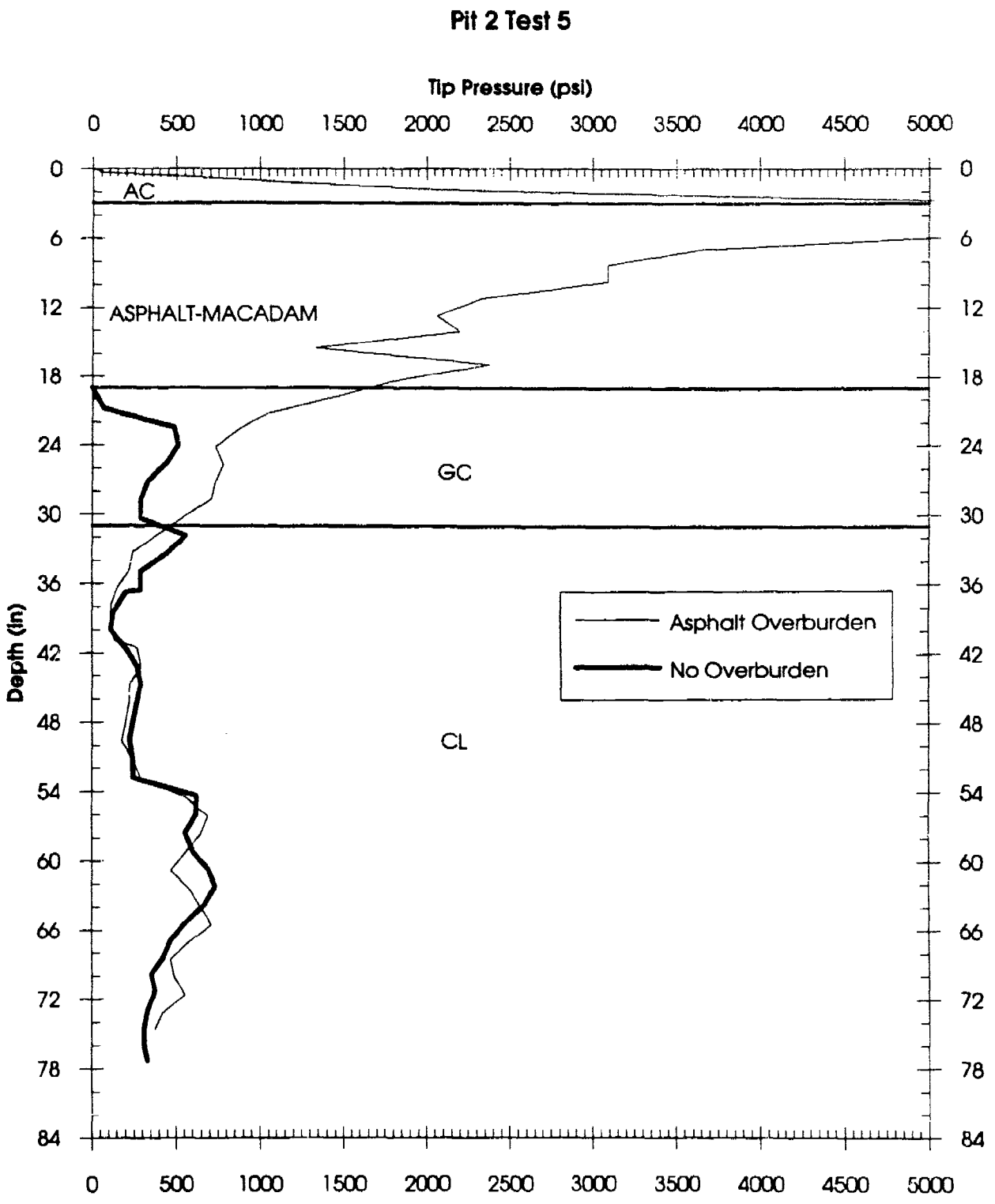

Figure B10. ECP TP versus depth for MAFB pit 2 test 5

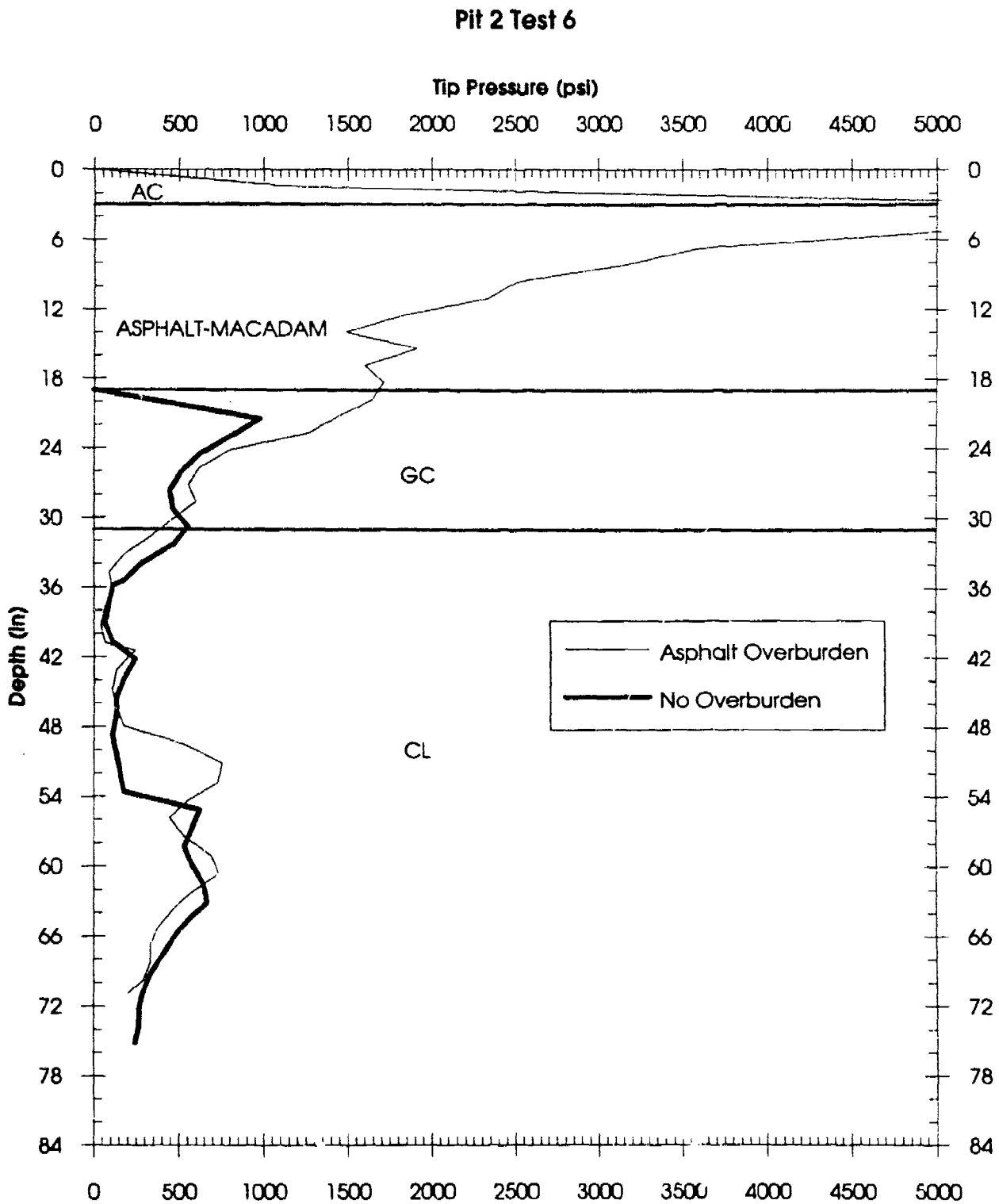

Figure B11. ECP TP versus depth for MAFB pit 2 test 6

Appendix C
Typical MAFB ECP Plots

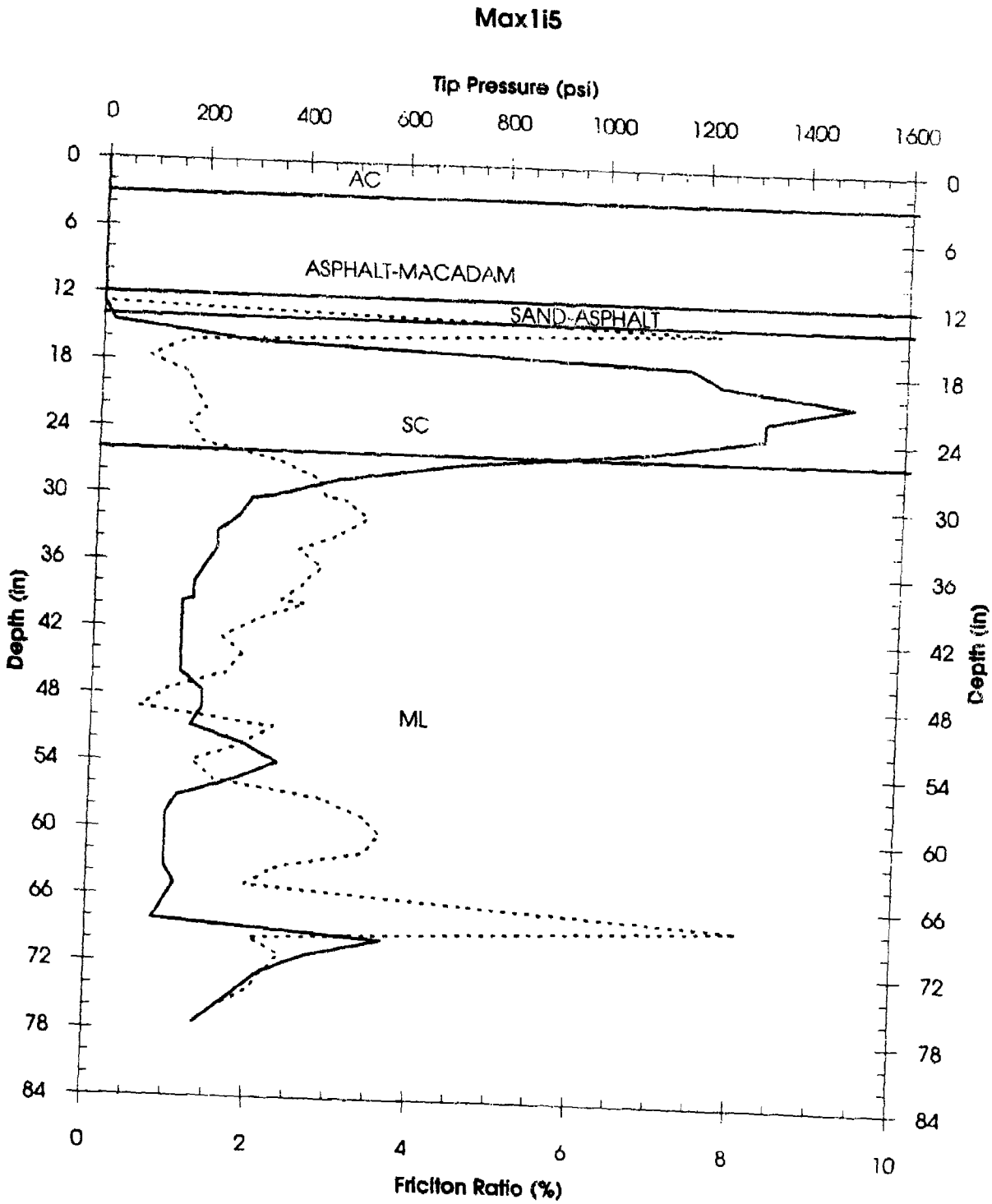

Figure C1. ECP TP and FR versus depth for MAFB 1I5

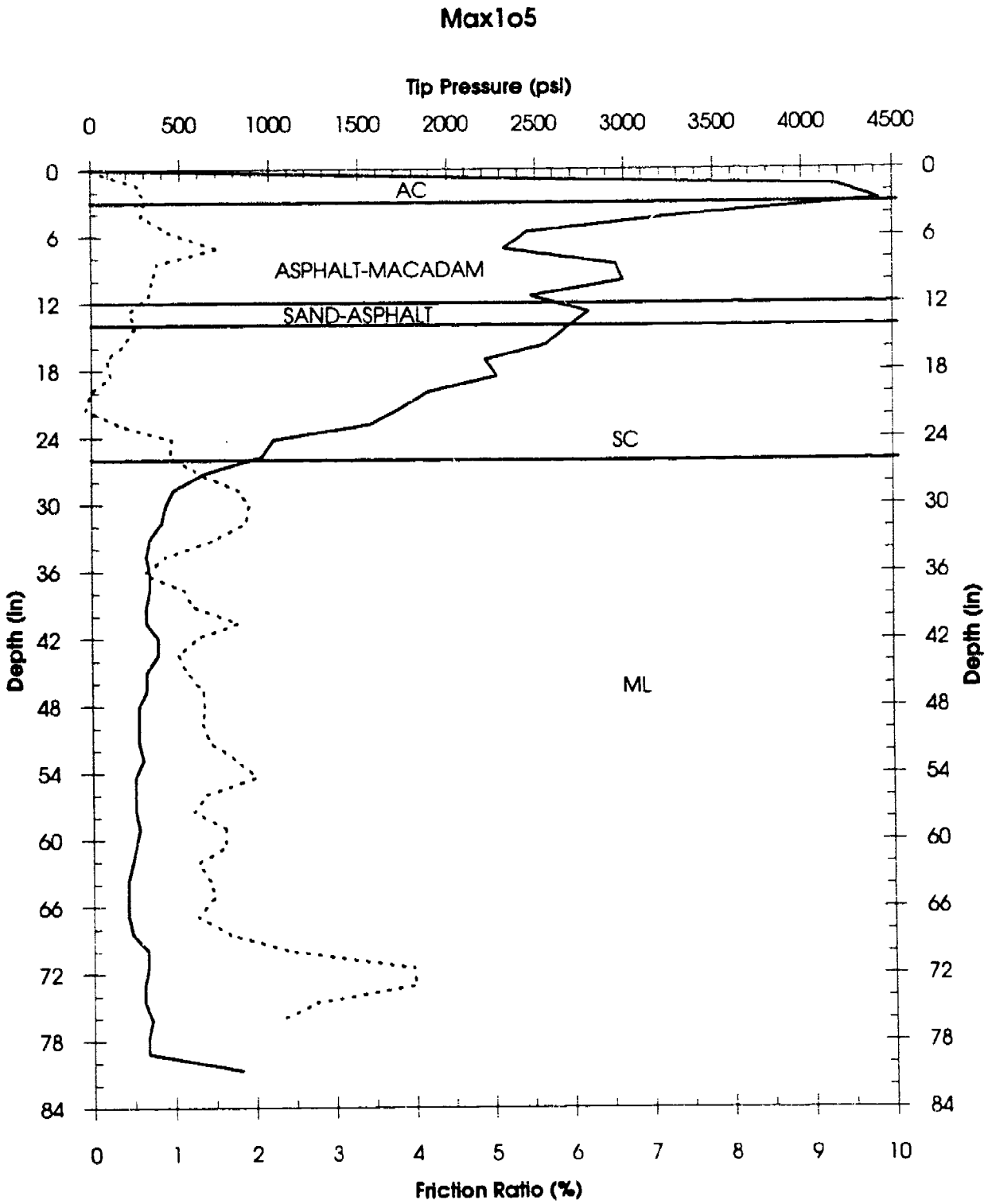

Figure C2. ECP TP and FR versus depth for MAFB1O5

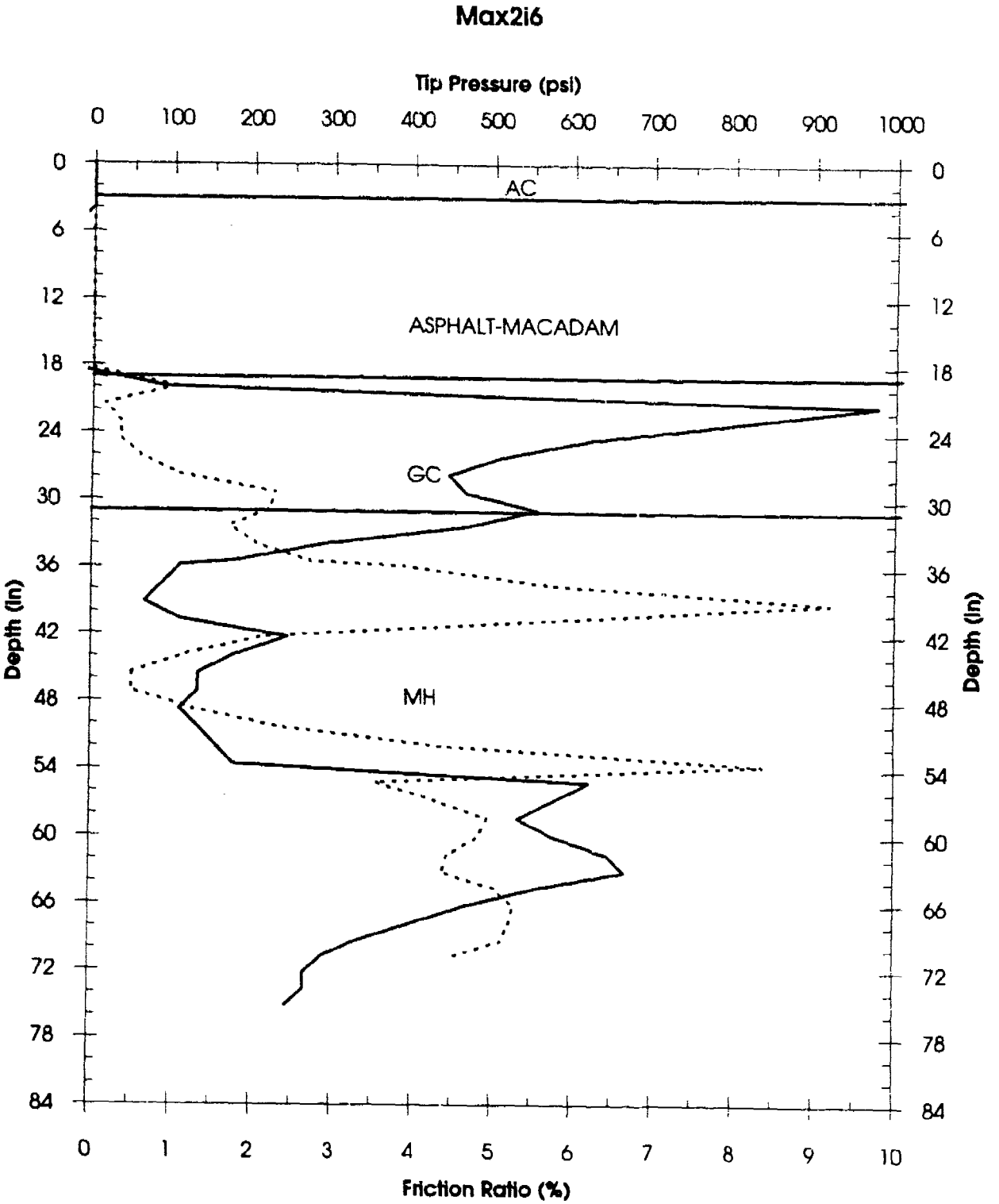

Figure C3. ECP TP and FR versus depth for MAFB2I6

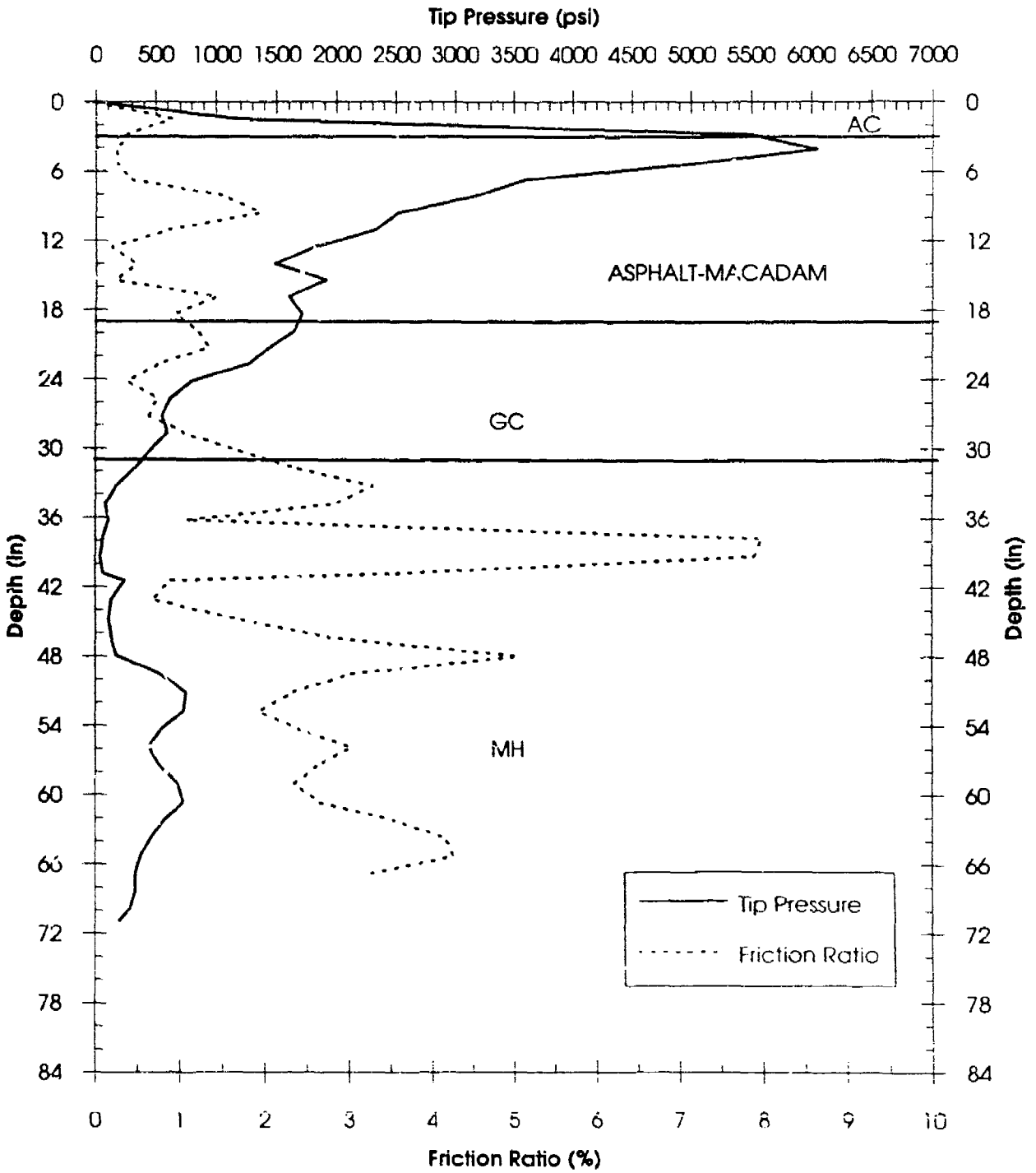

Figure C4. ECP TP and FR versus depth for MAFB2O6

Appendix D
WES ECP Plots, Test Section 1 (Soil Wedge), Penetration Rate = 0.8 in./sec

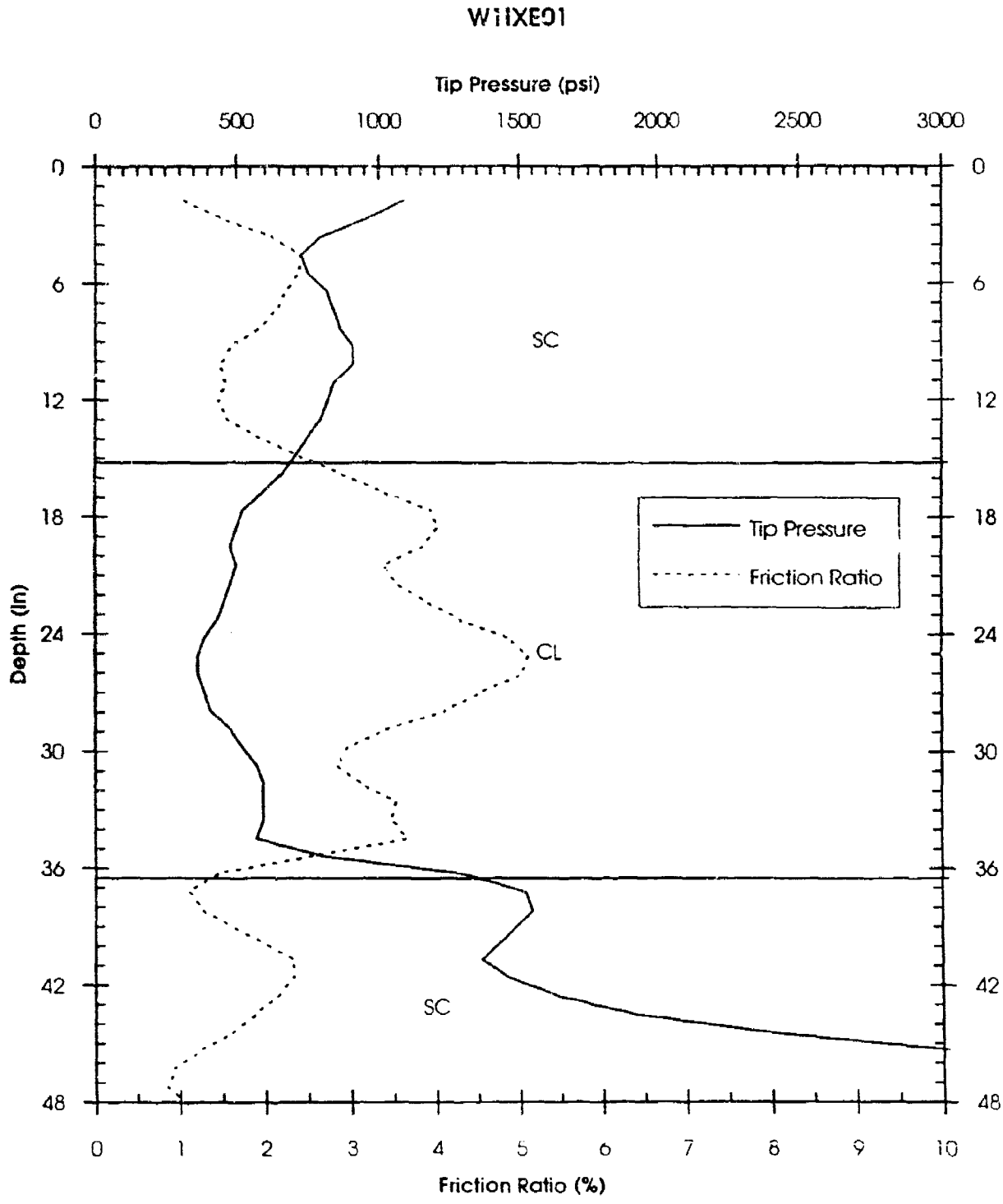

Figure D1. ECP TP and FR versus depth for W1IXE01

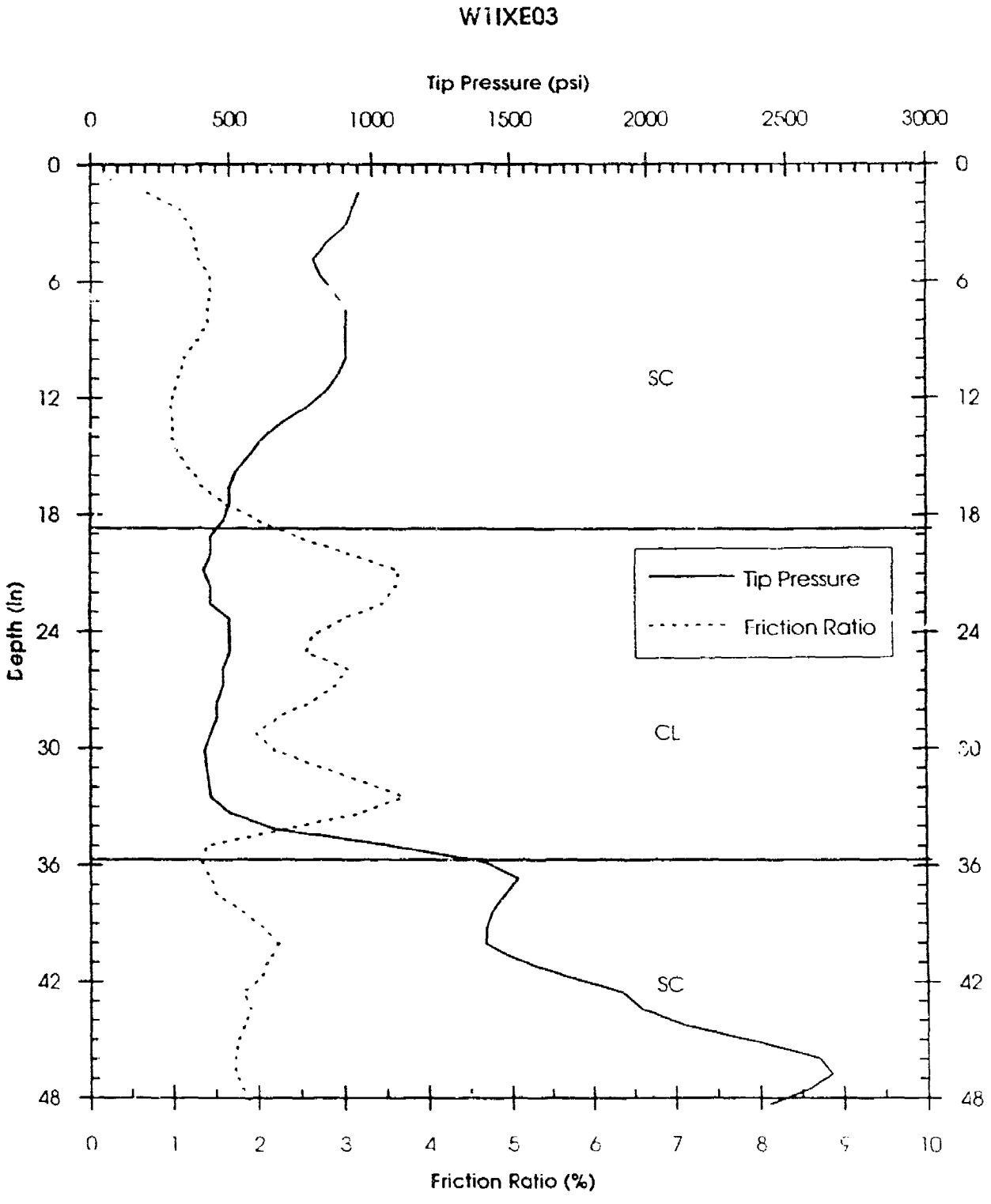

Figure D2. ECP TP and FR versus depth for W1IXE03

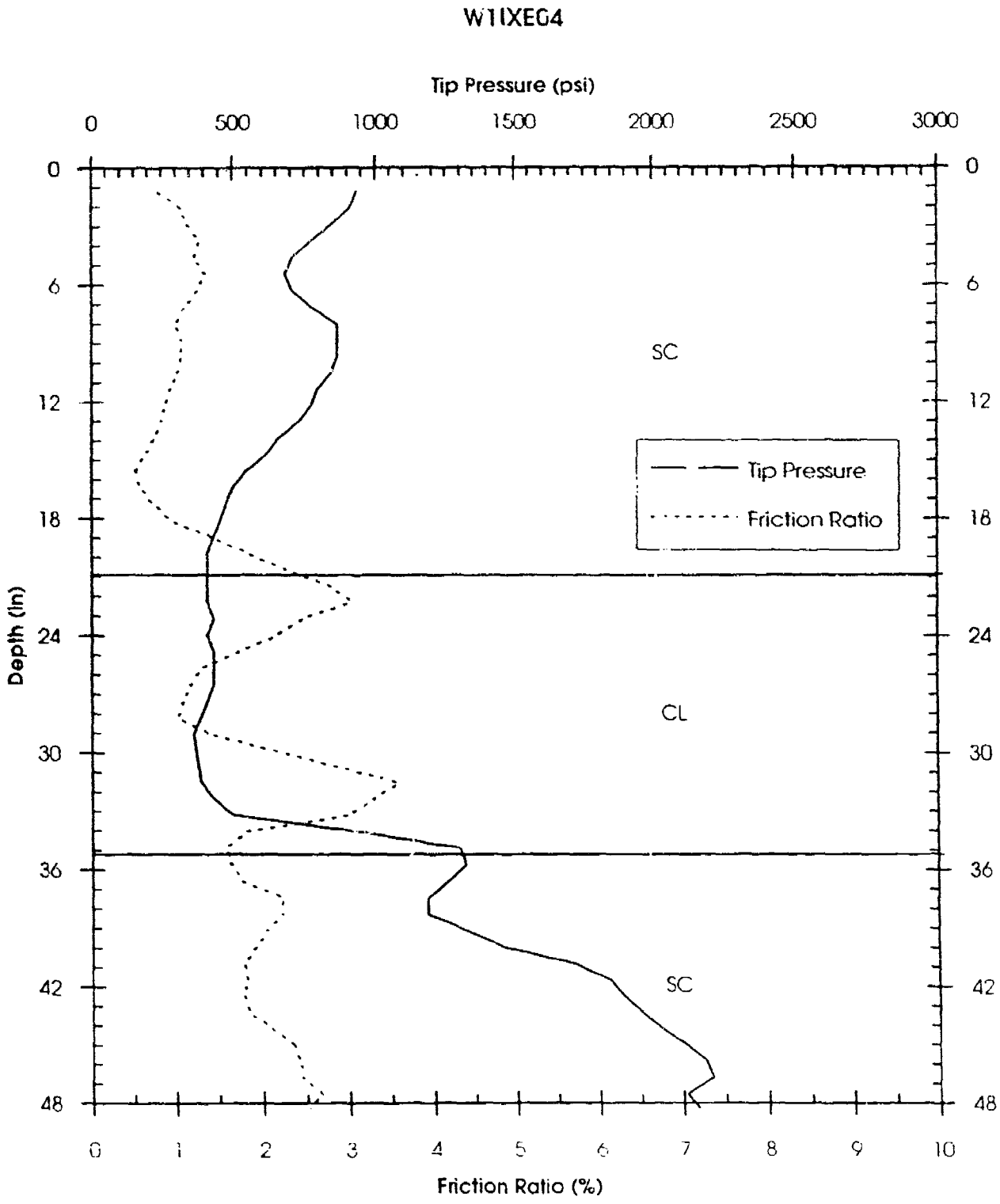

Figure D3. ECP TP and FR versus depth for W1IXE04

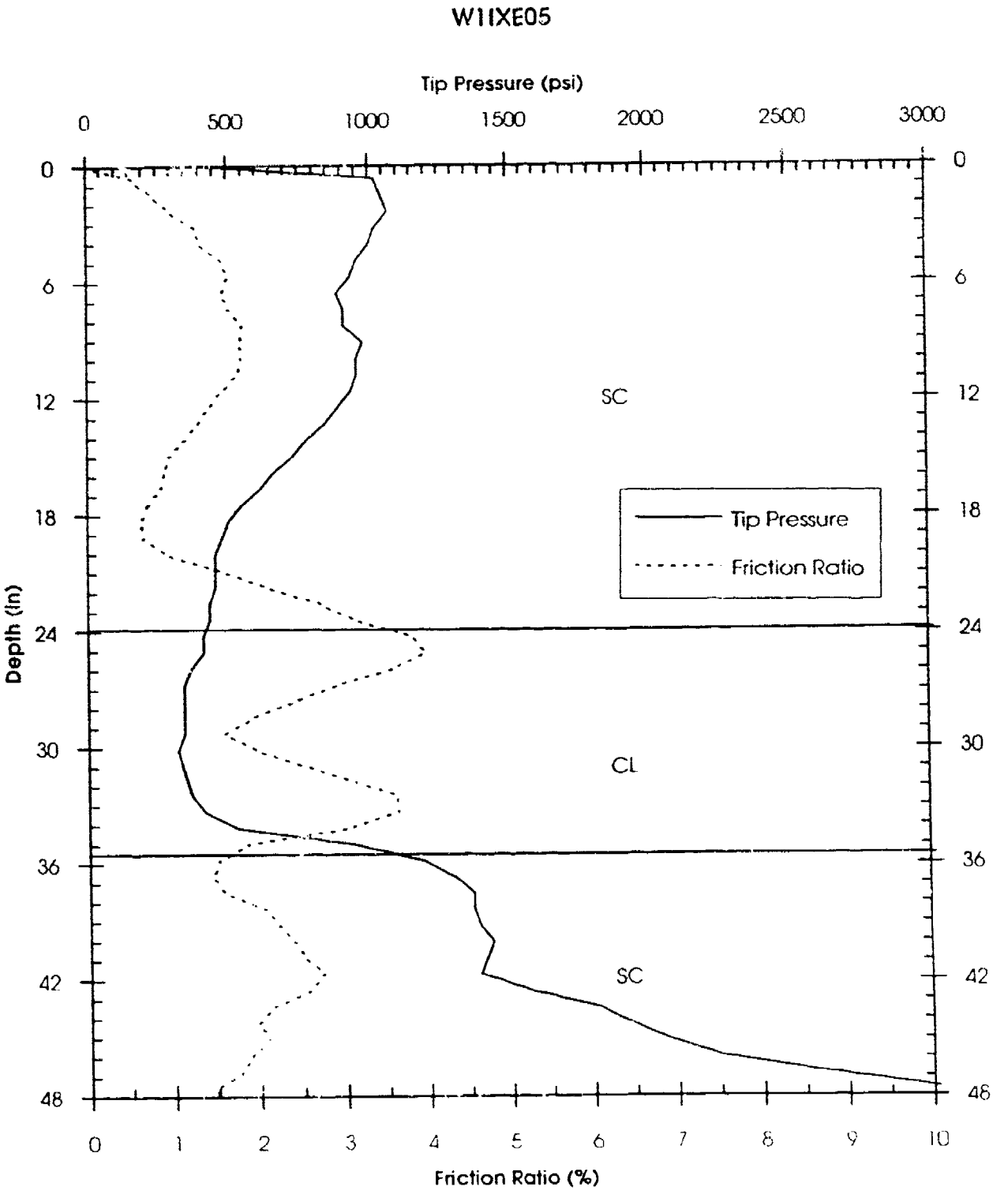

Figure D4. ECP TP and FR versus depth for W11XE05

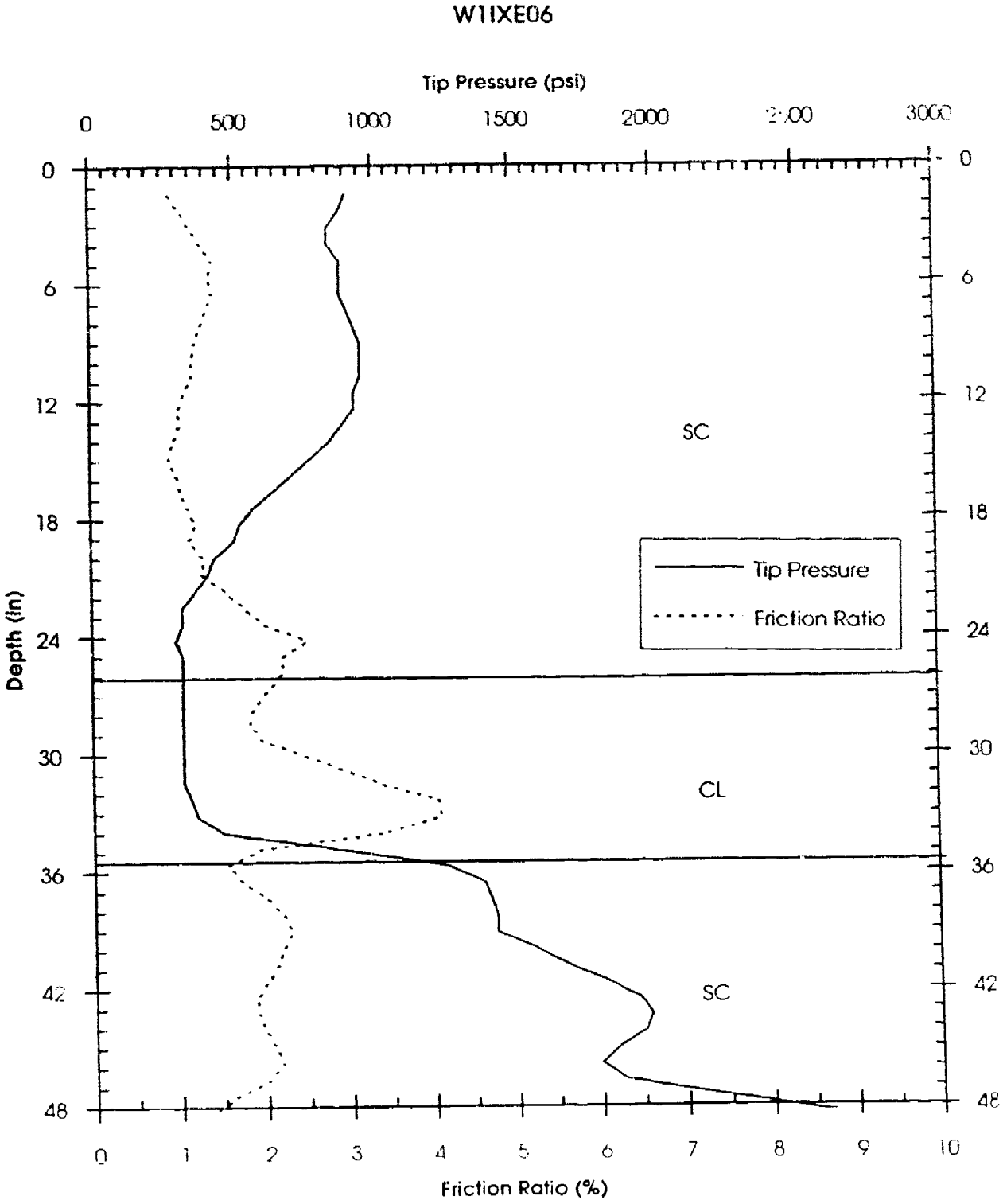

Figure D5. ECP TP and FR versus depth for W1IXE06

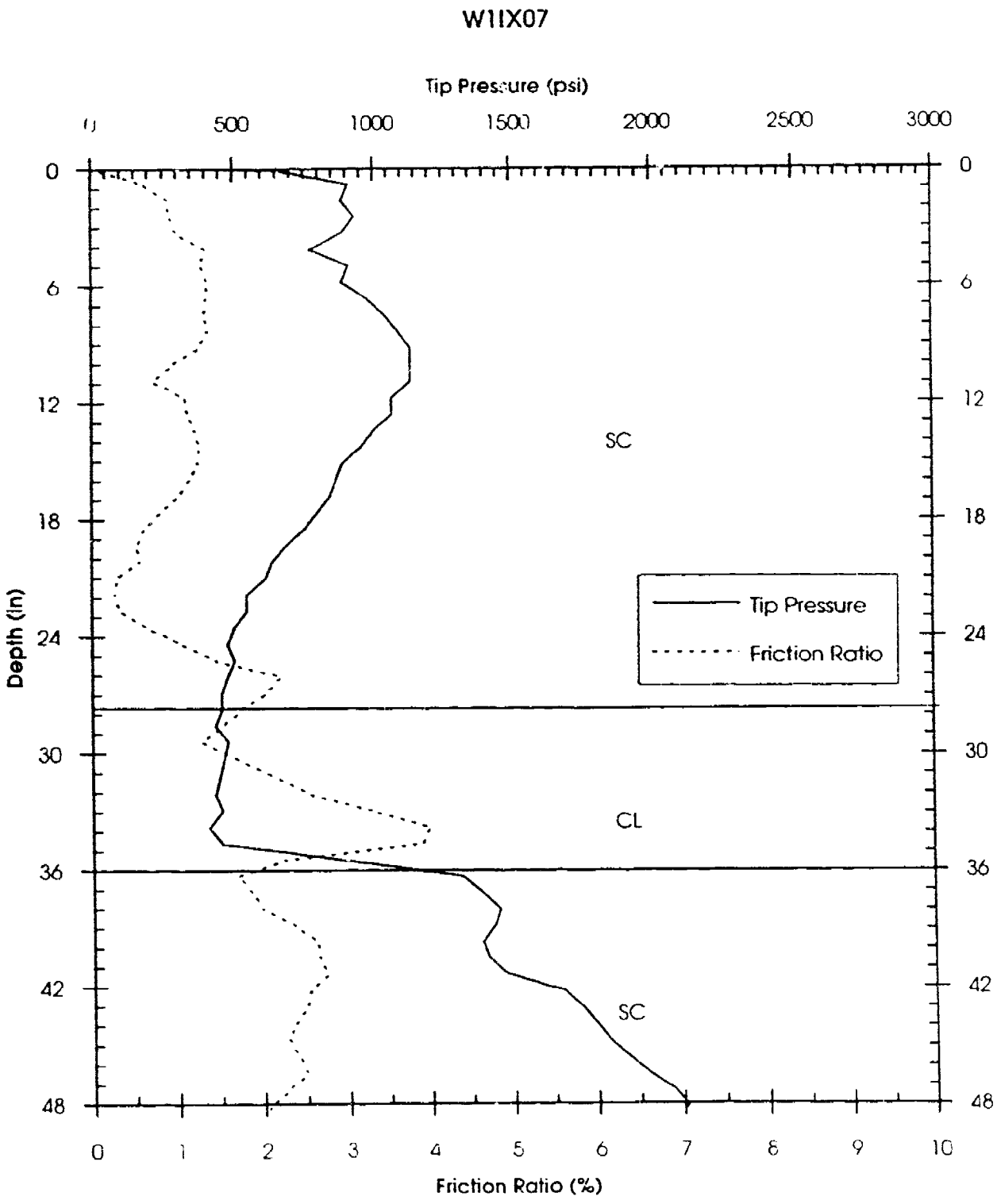

Figure D6. ECP TP and FR versus depth for W11XE07

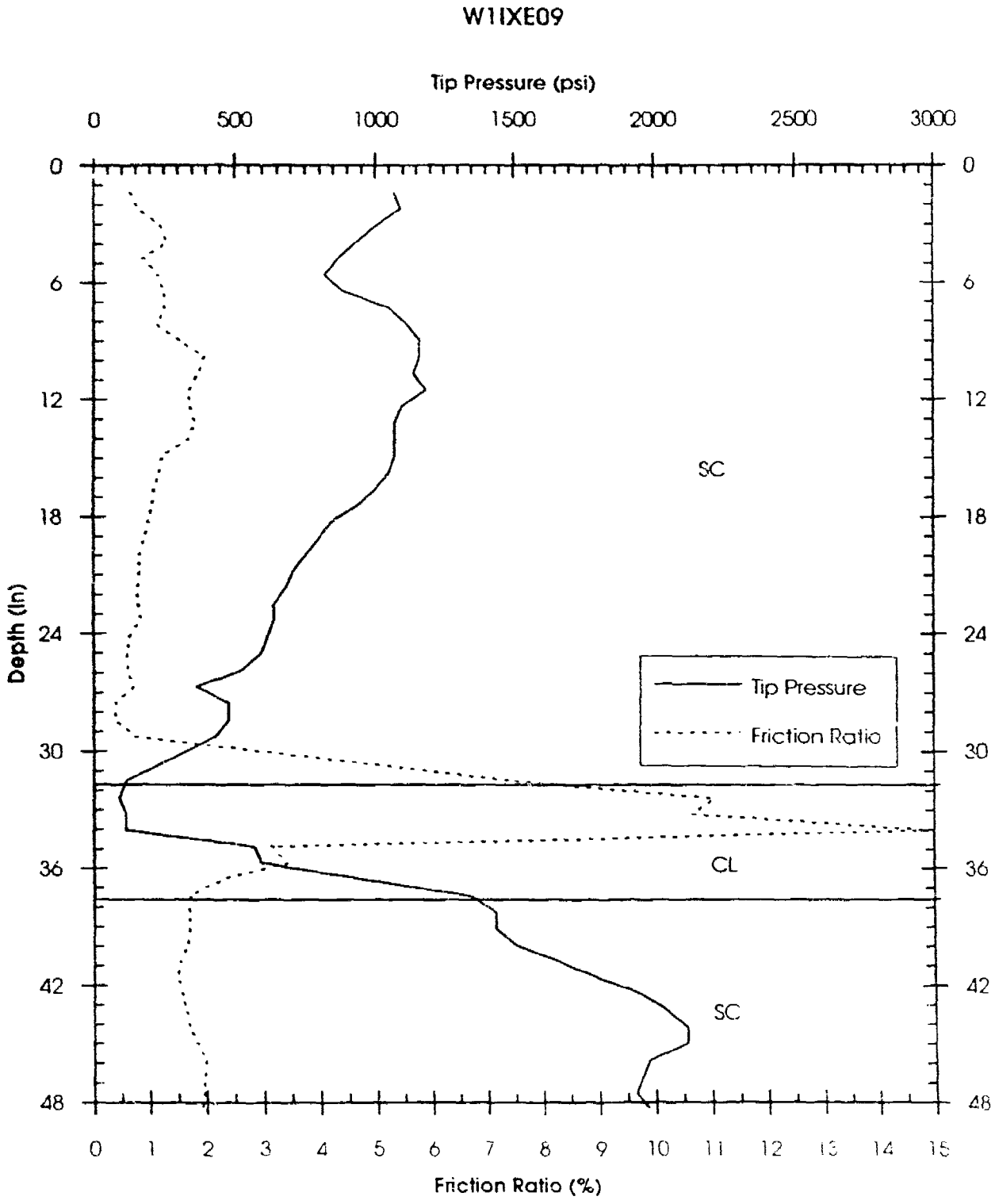

Figure D7 ECP TP and FR versus depth for W1IXE09

Appendix E
Typical WES ECP Plots, Test Section 2 (Stepped Base)

W211

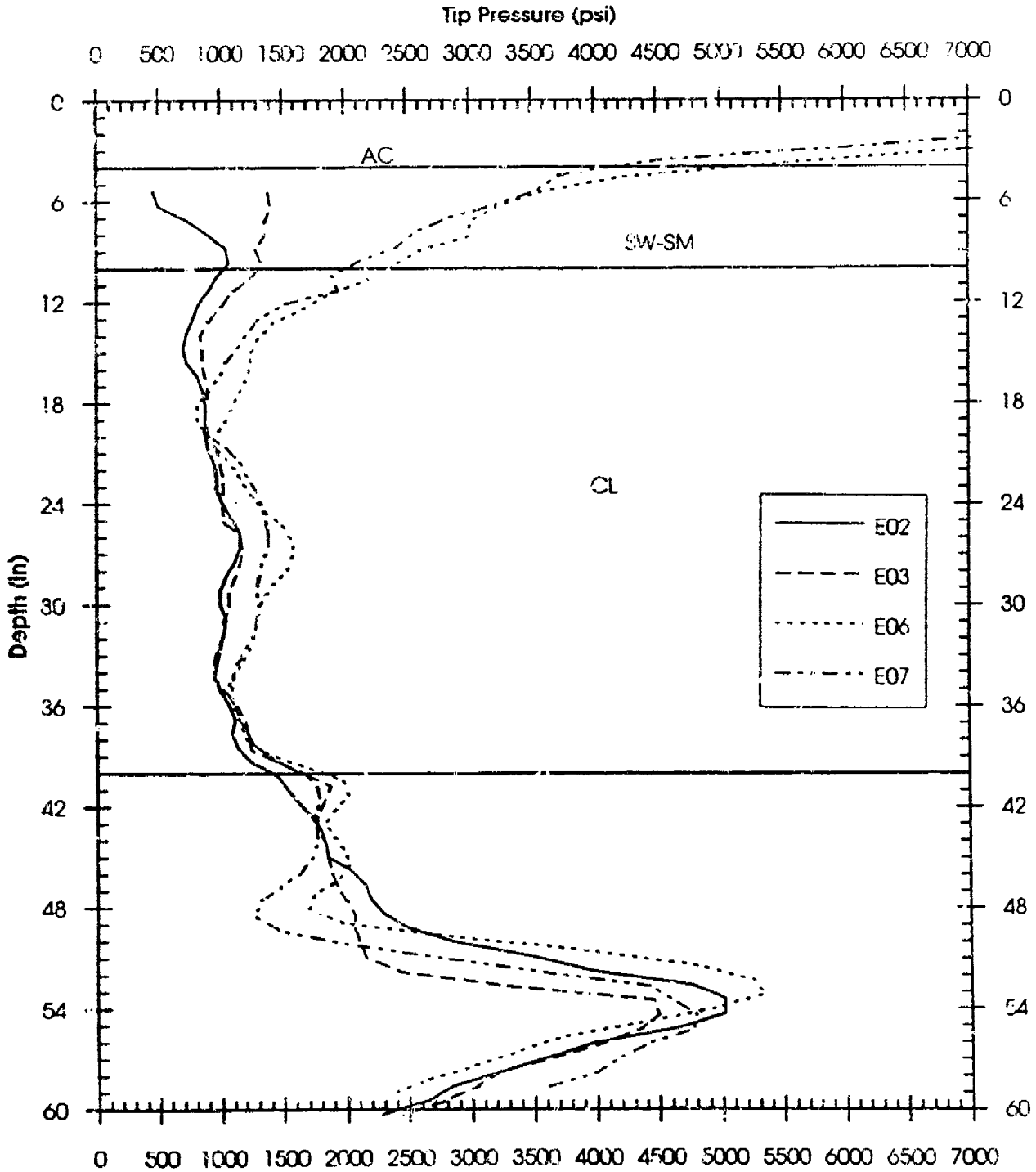

Figure E1. ECP TP versus depth for W2I01

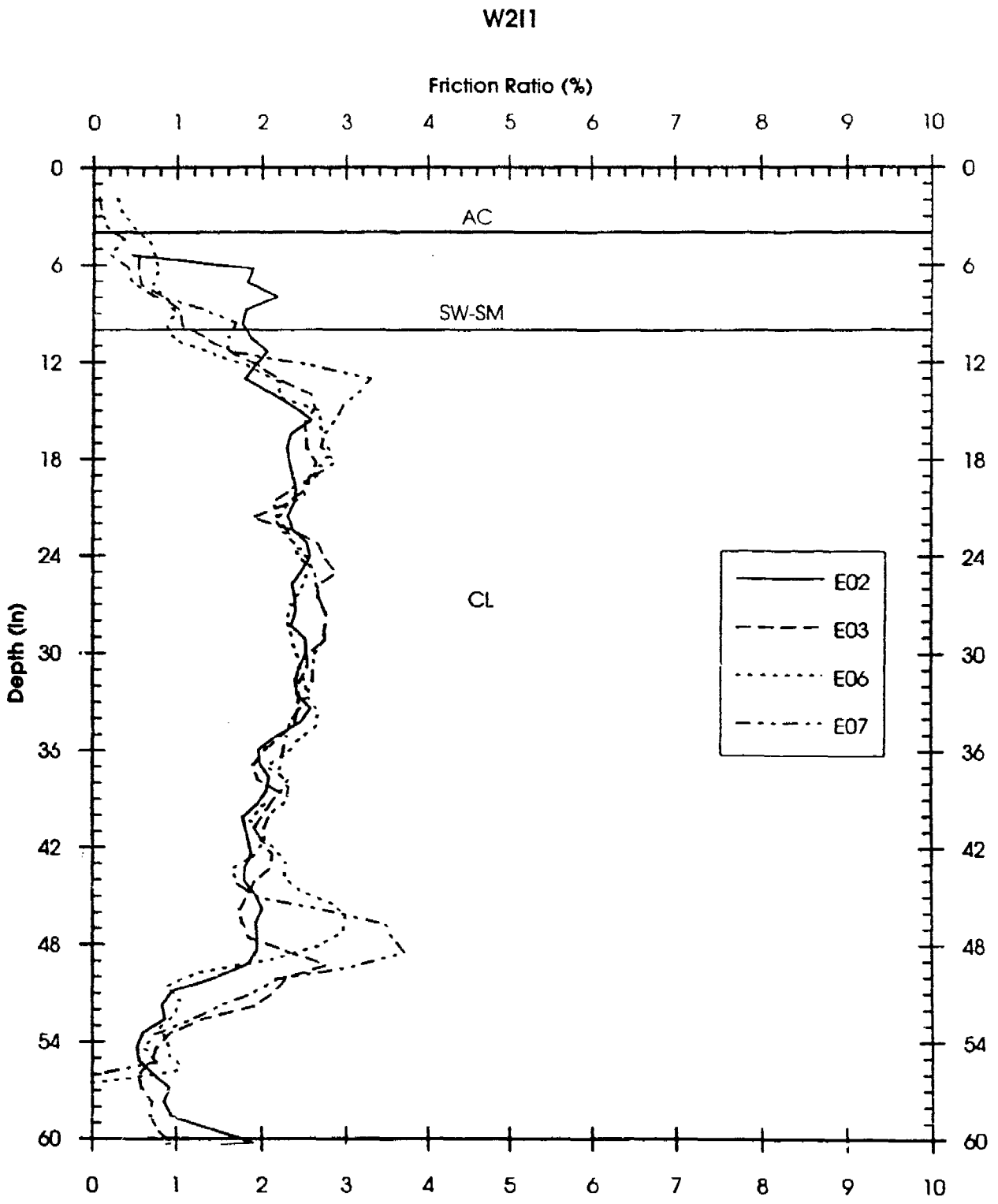

Figure E2. ECP FR versus depth for W2I01

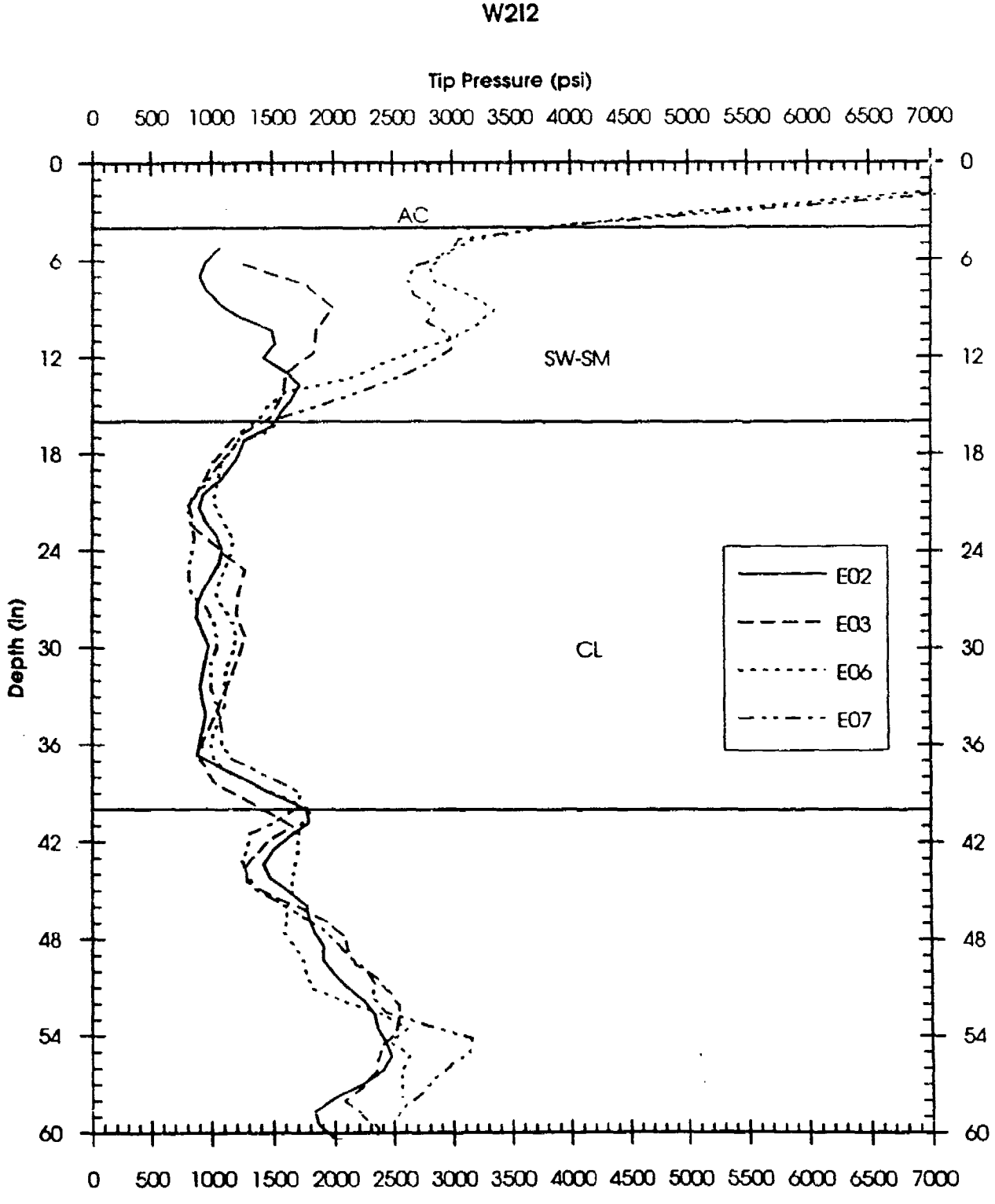

Figure E3. ECP TP versus depth for W2102

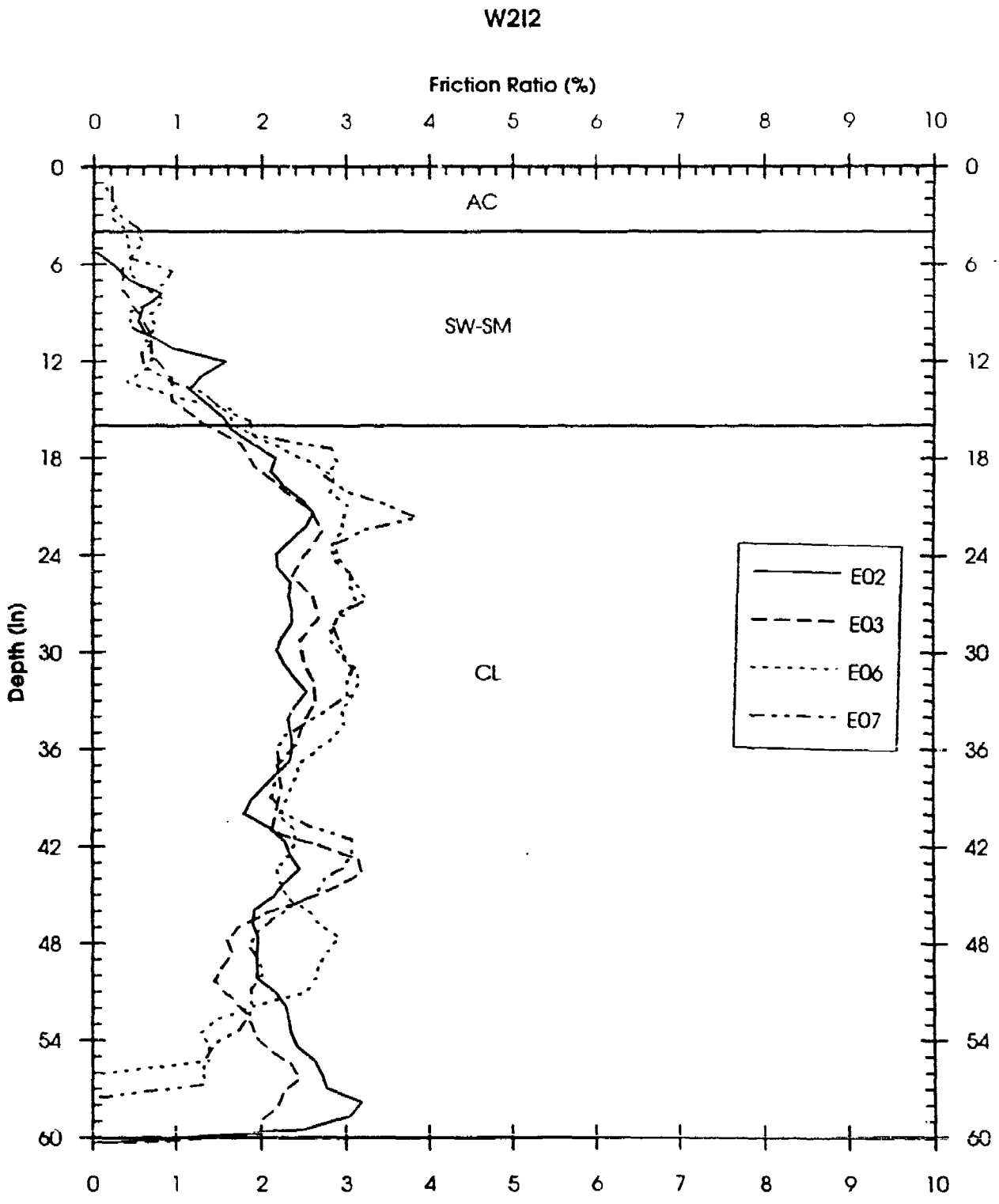

Figure E4. ECP FR versus depth for W2I02

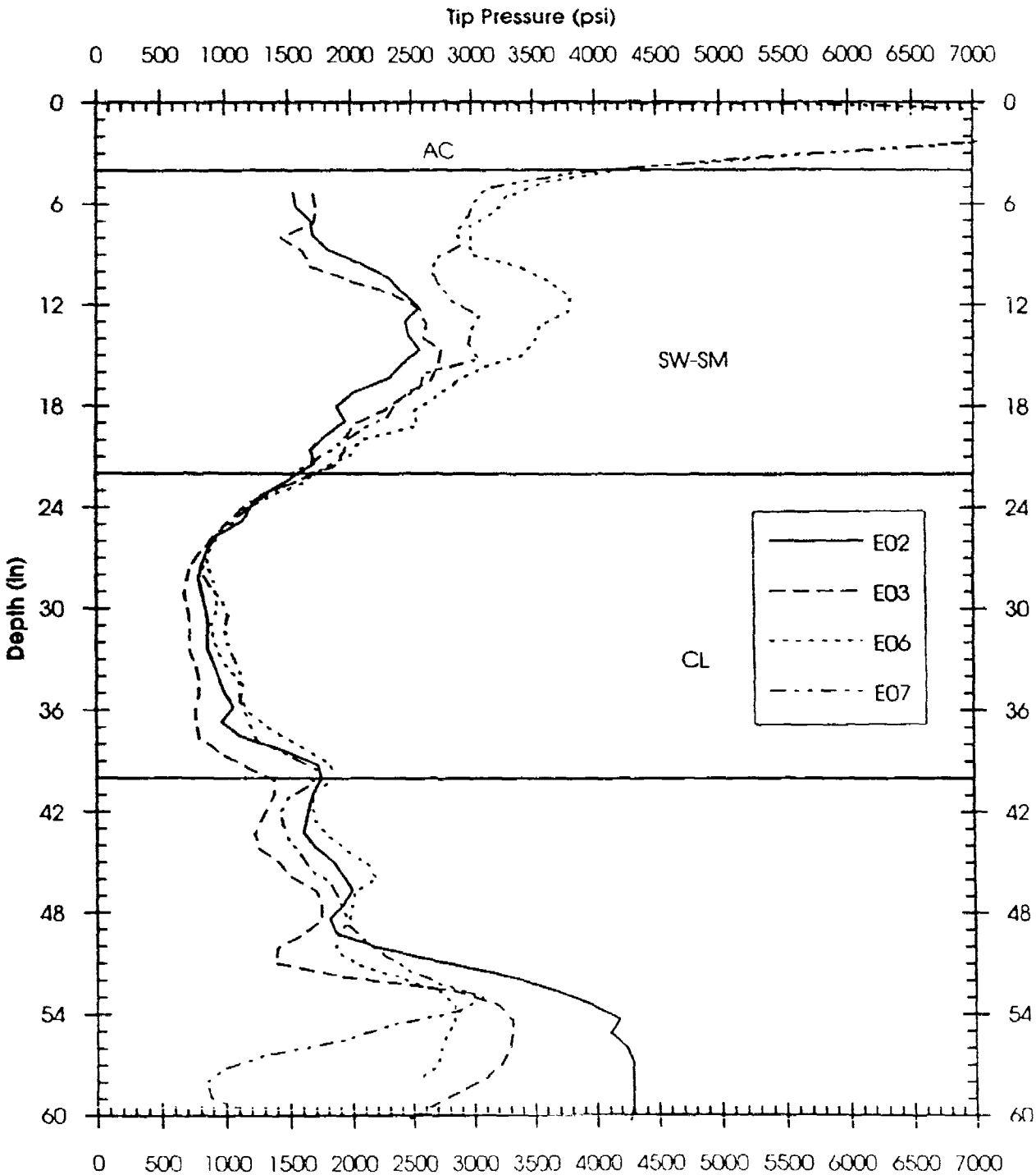

Figure E5. ECP TP versus depth for W2103

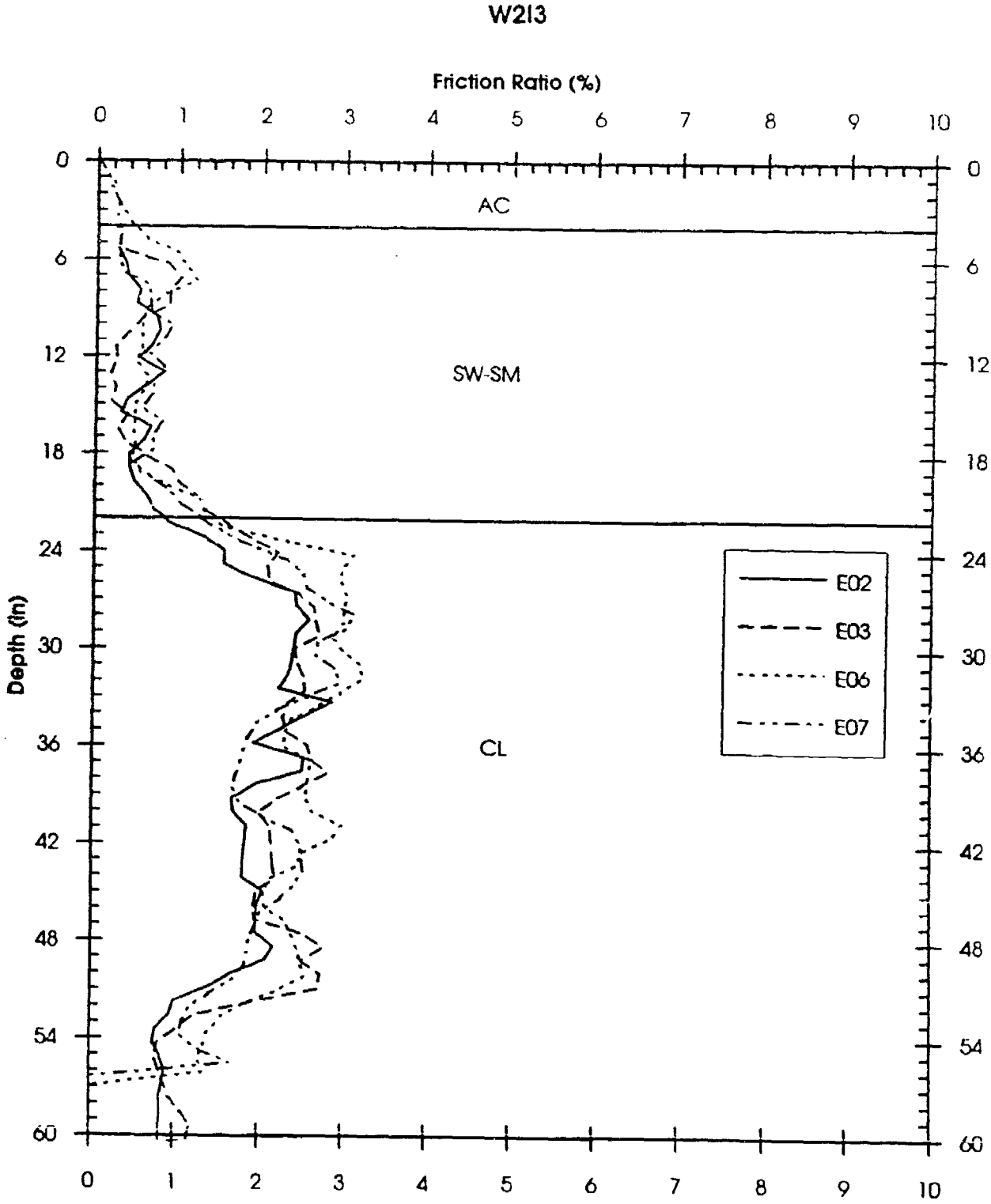

Figure E6. ECP FR versus depth for W2I03

Appendix F
Typical WES ECP Plots, Test Sections 3 and 4

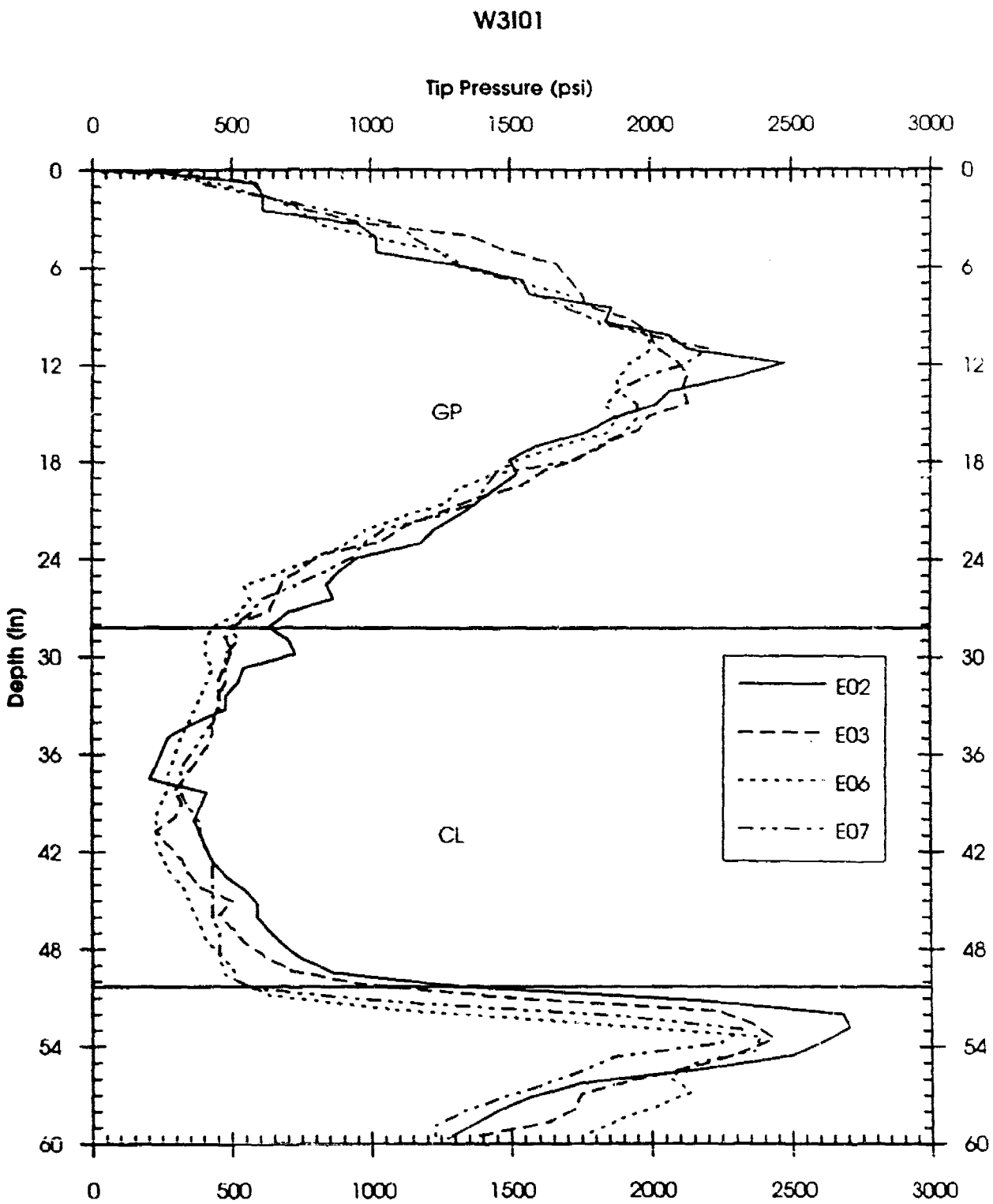

Figure F1. ECP TP versus depth for W3I01

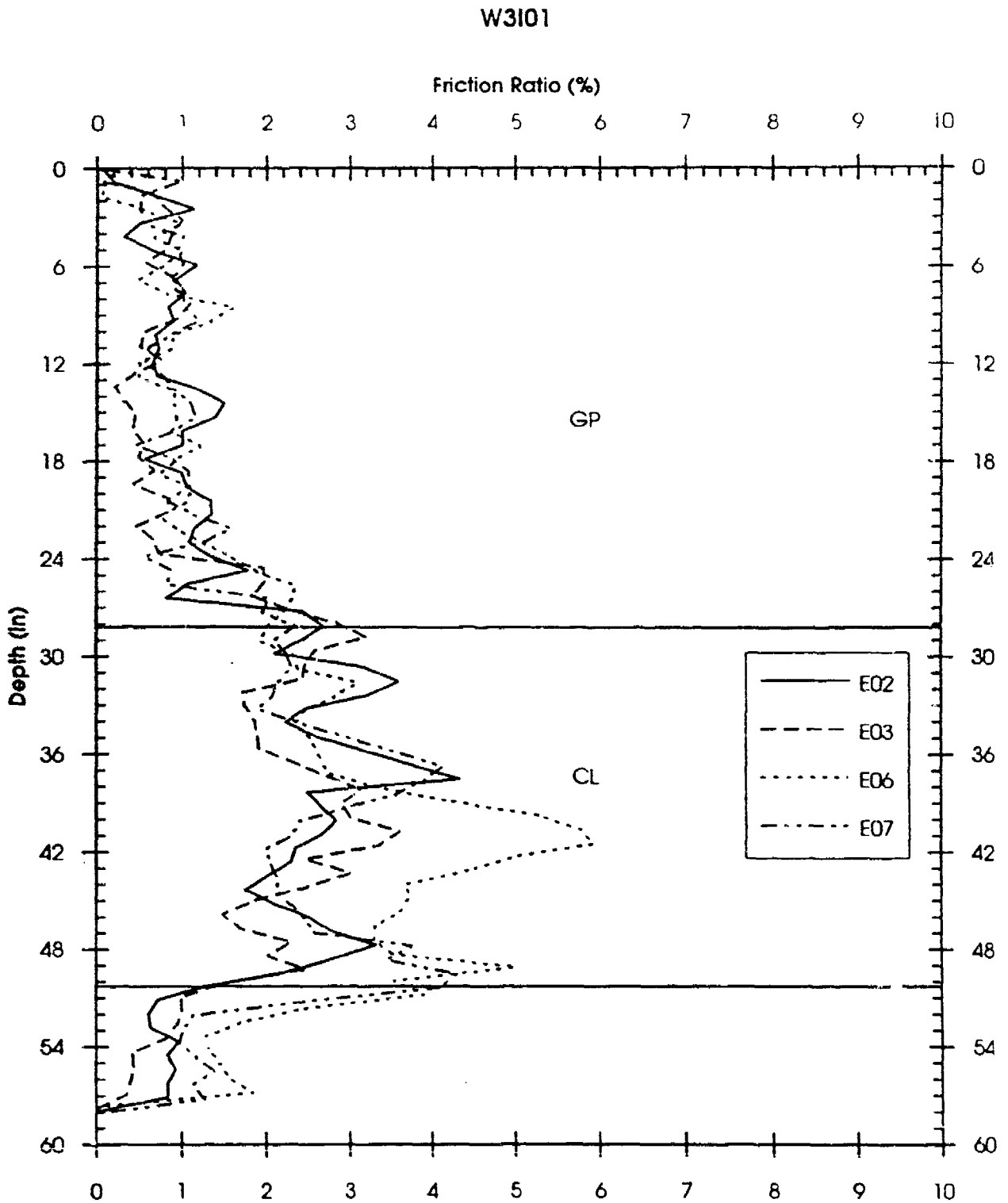

Figure F2. ECP FR versus depth for W3I01

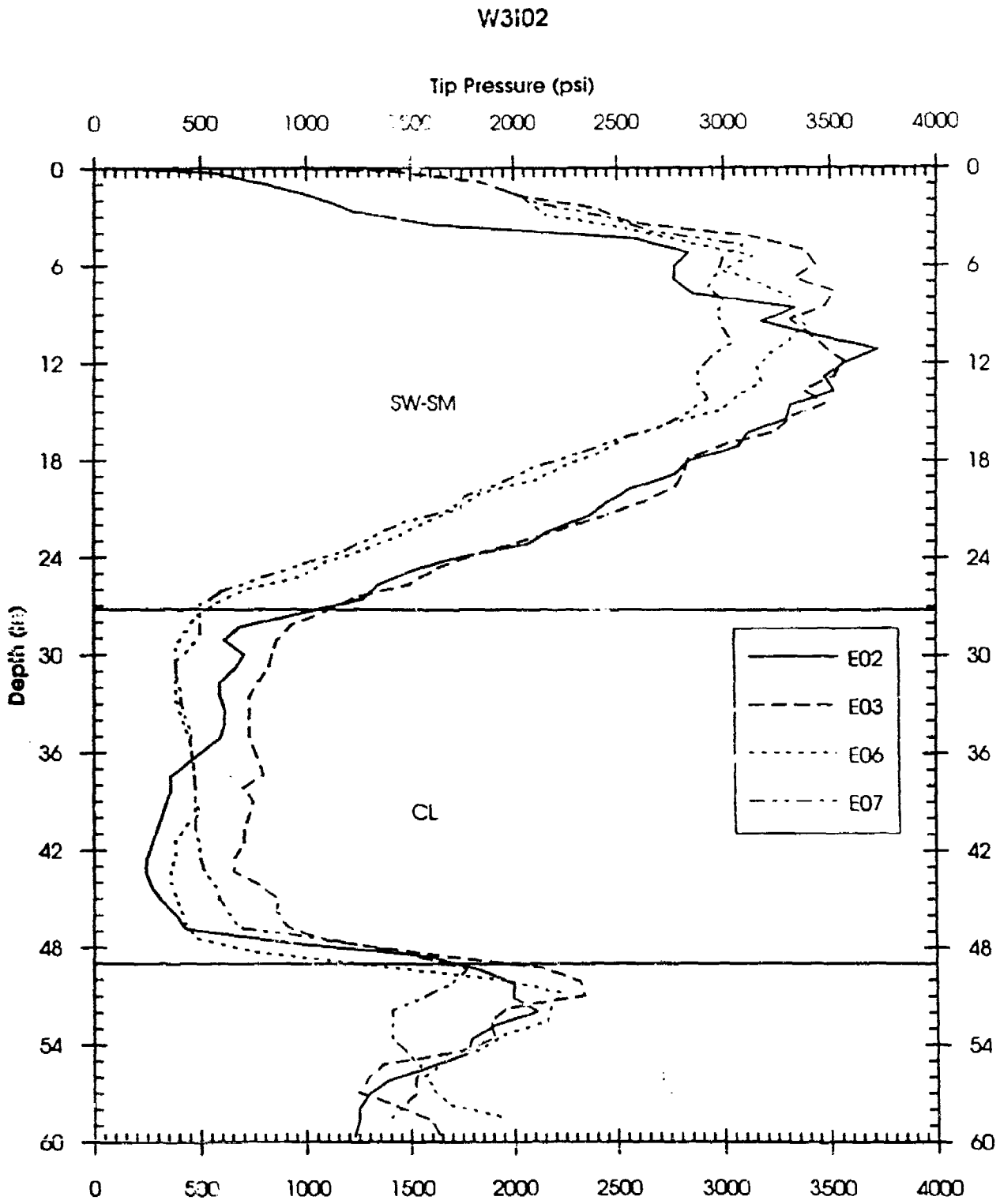

Figure F3. ECP TP versus depth for W3I02

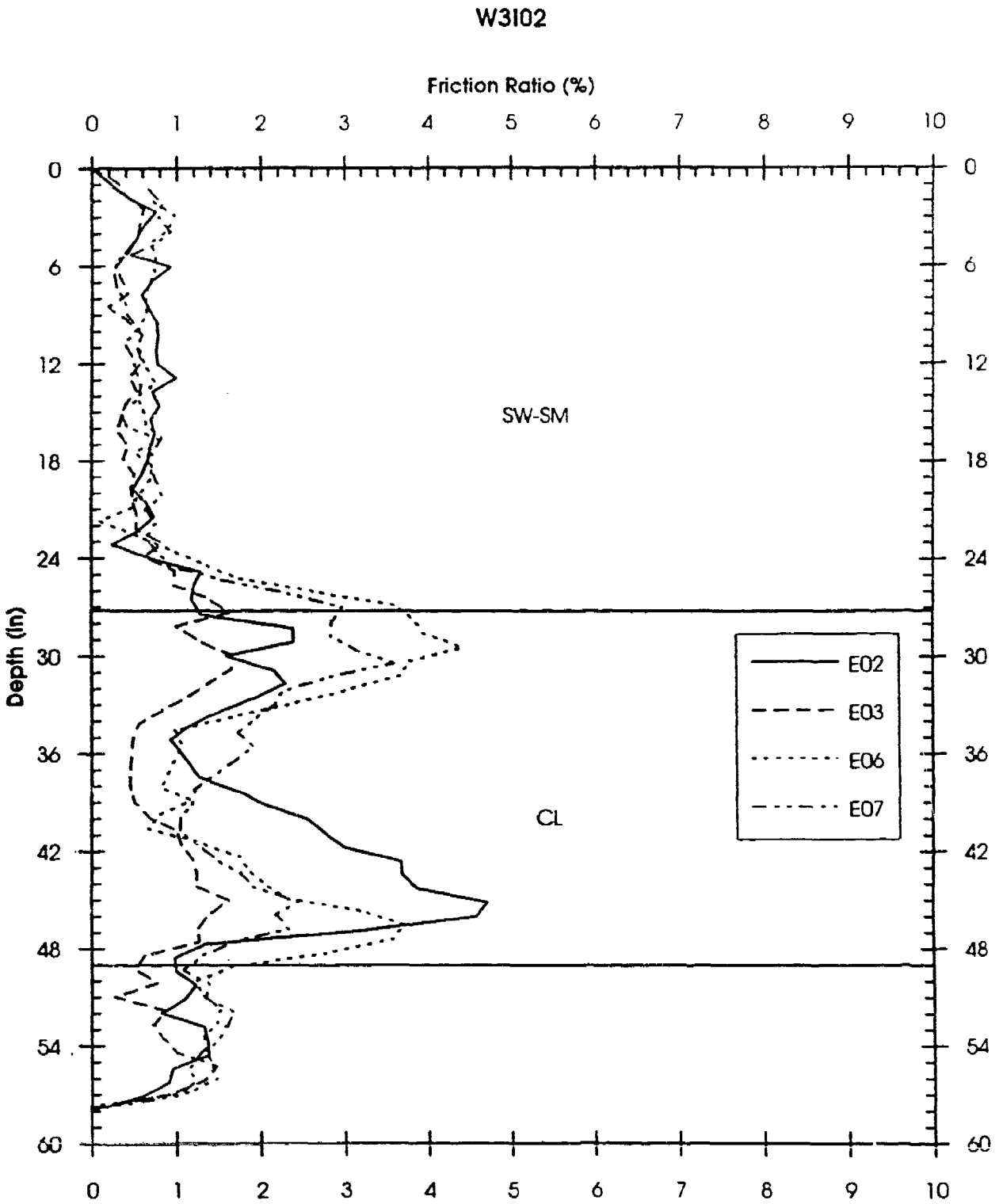

Figure F4. ECP FR versus depth for W3102

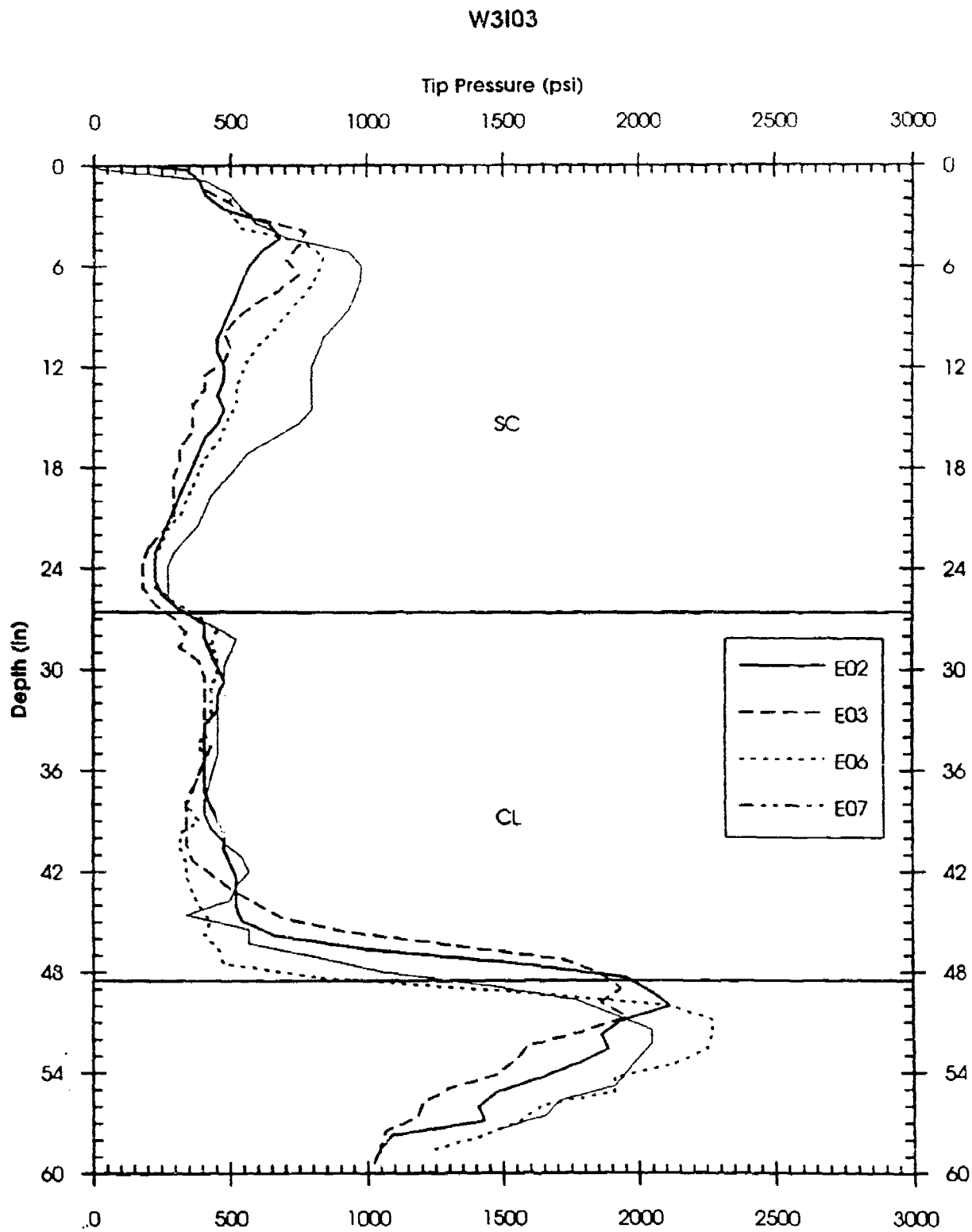

Figure F5. ECP TP versus depth for W3103

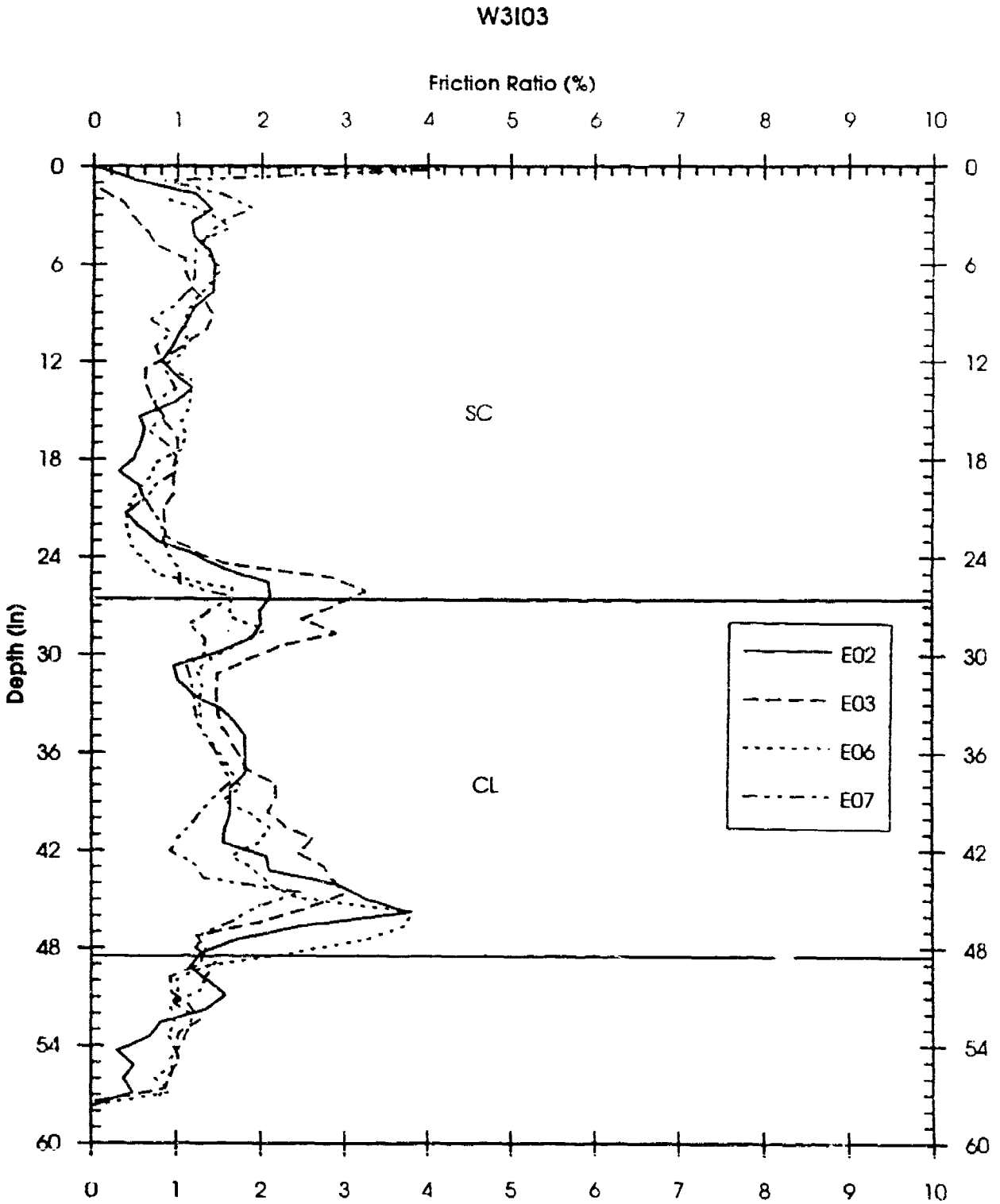

Figure F6. ECP FR versus depth for W3103

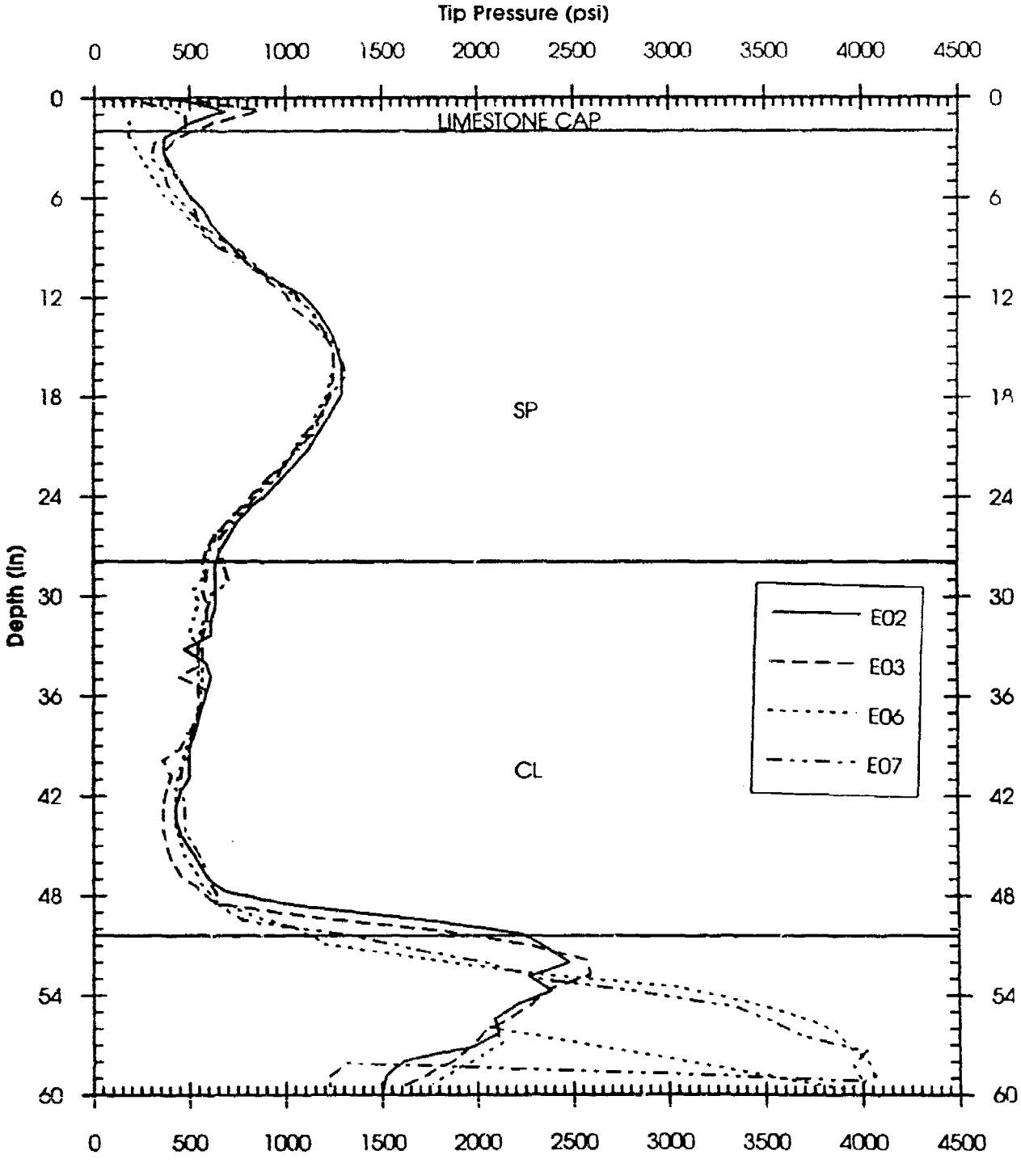

Figure F7. ECP TP versus depth for W3I04

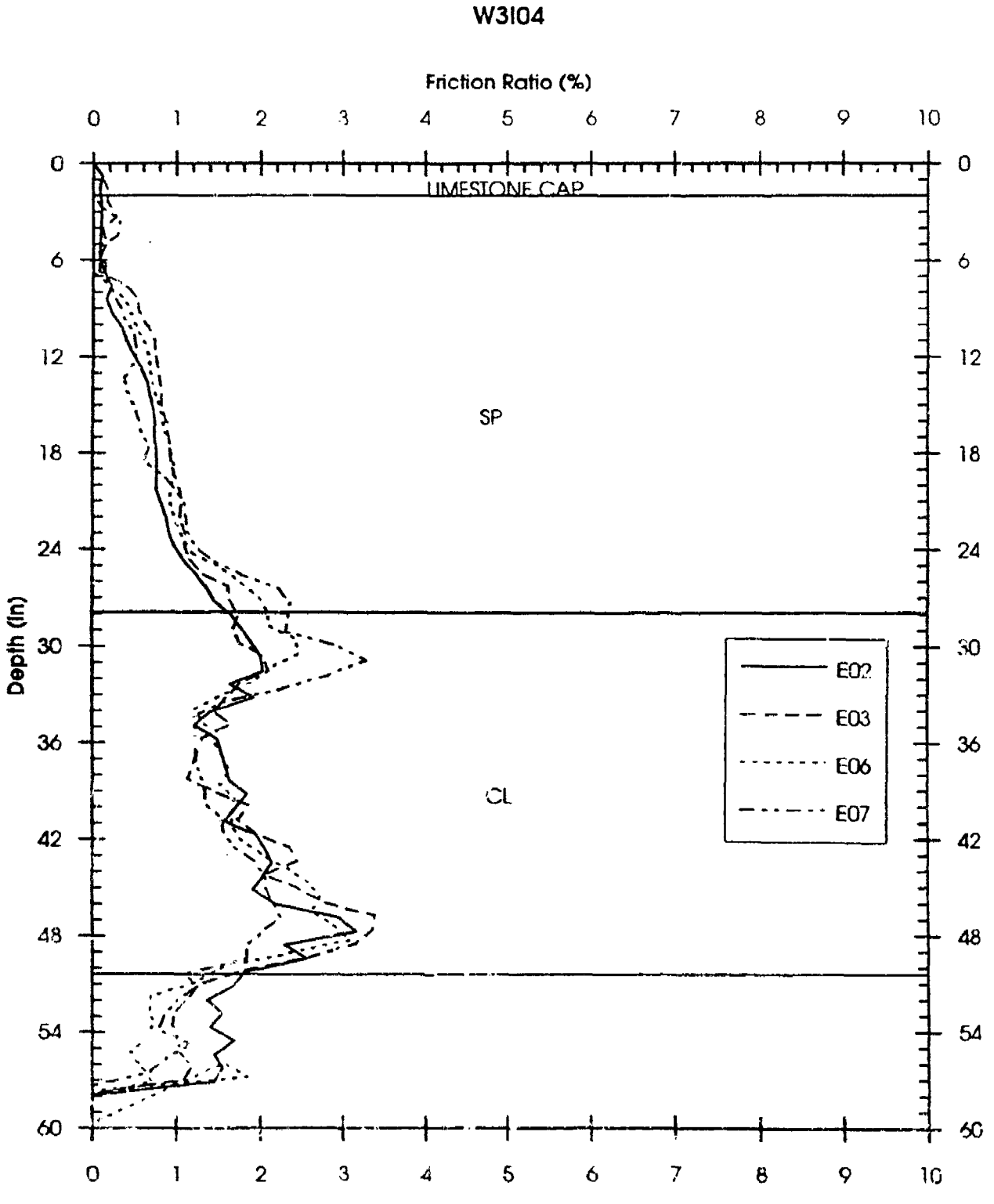

Figure F8. ECP FR versus depth for W3104

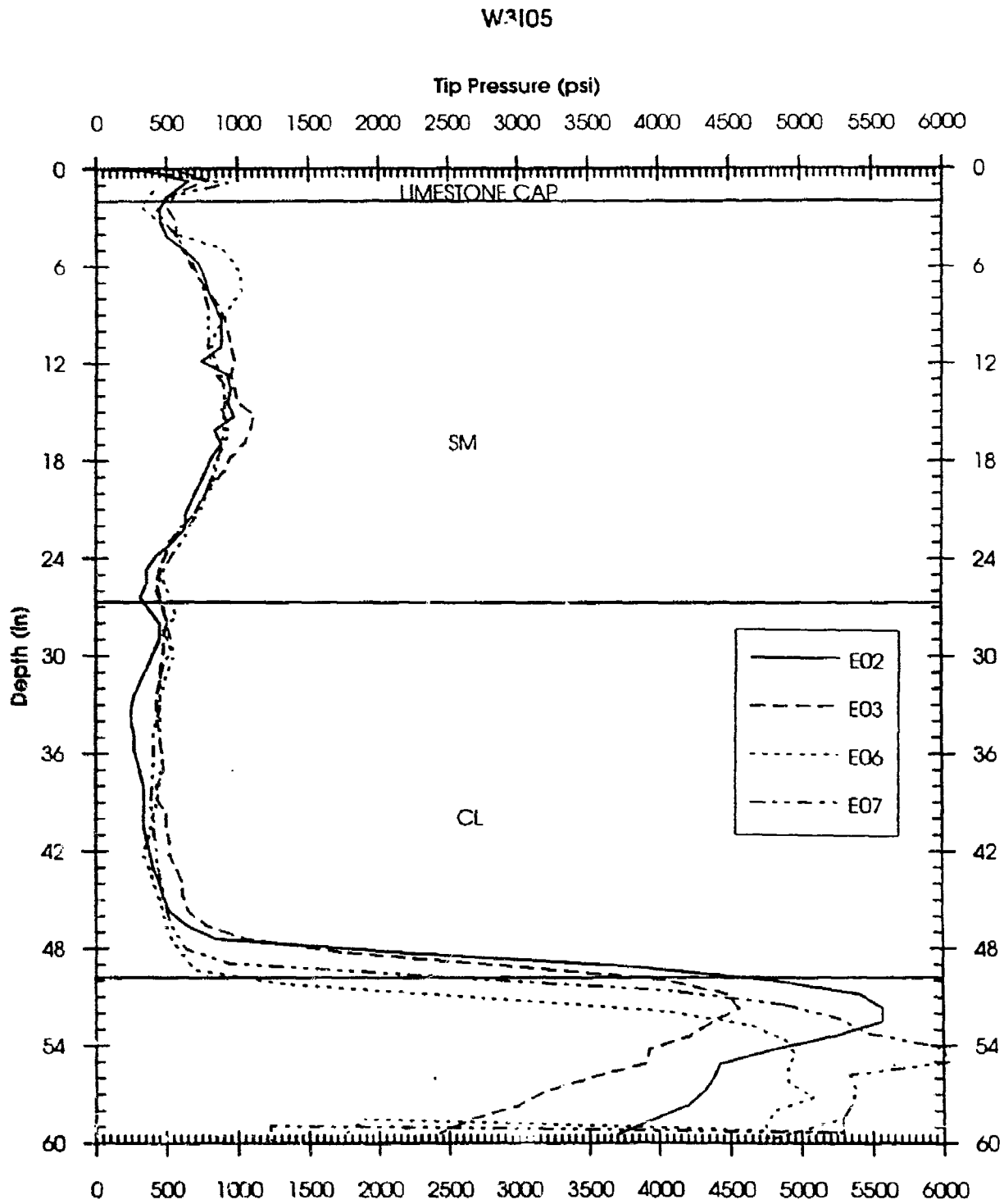

Figure F9. ECP TP versus depth for W3105

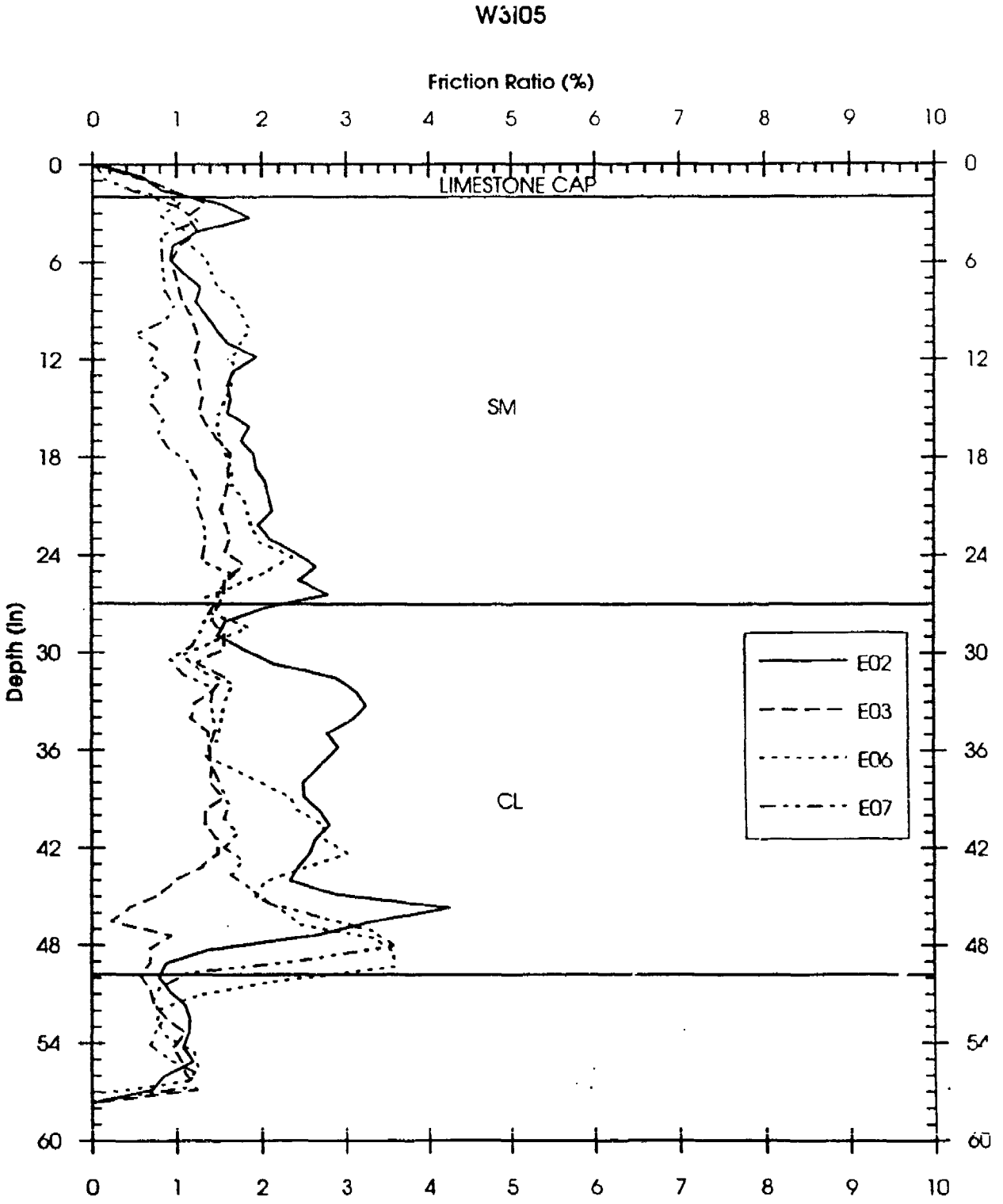

Figure F10. ECP FR versus depth for W3105

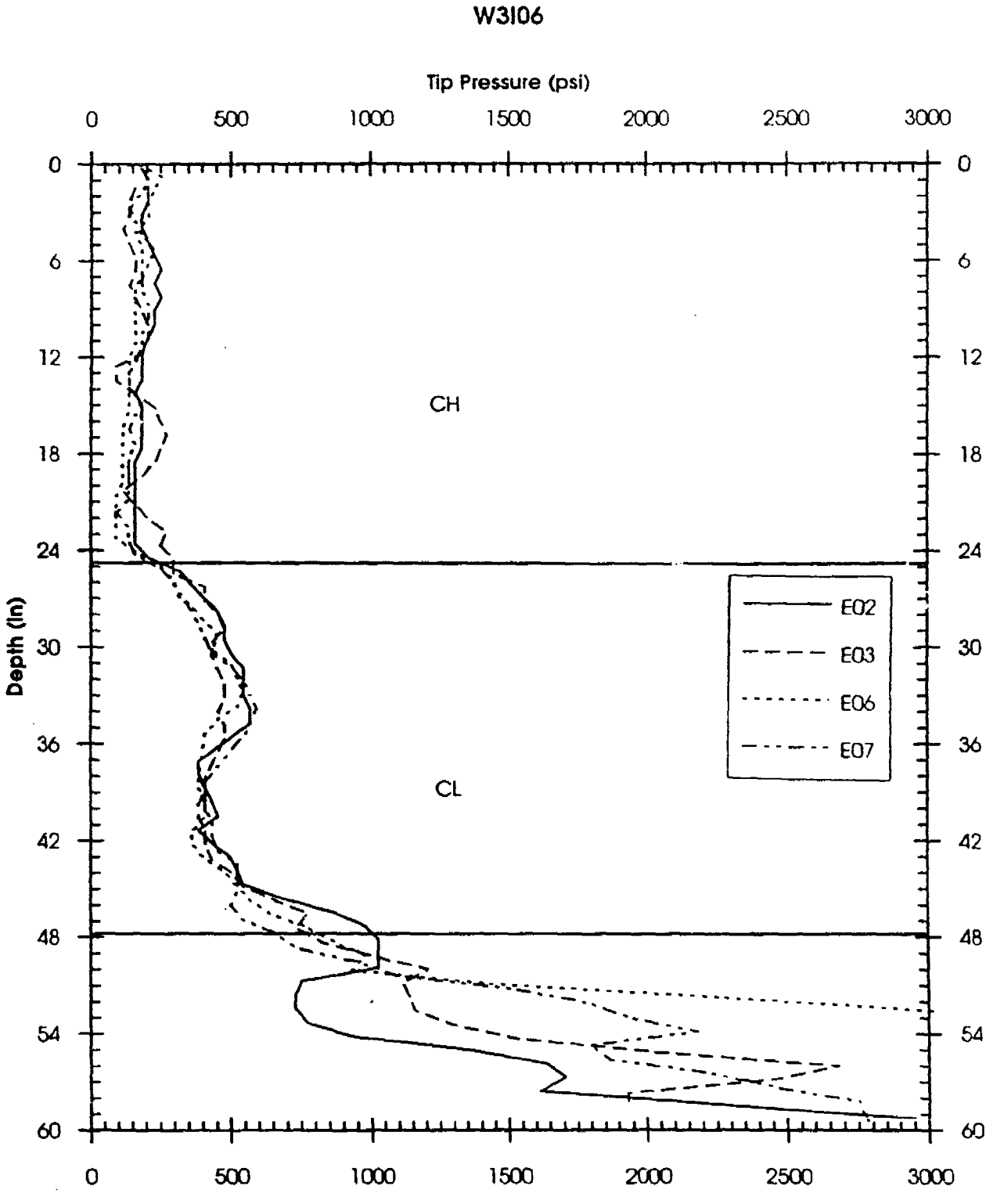

Figure F11. ECP TP versus depth for W3106

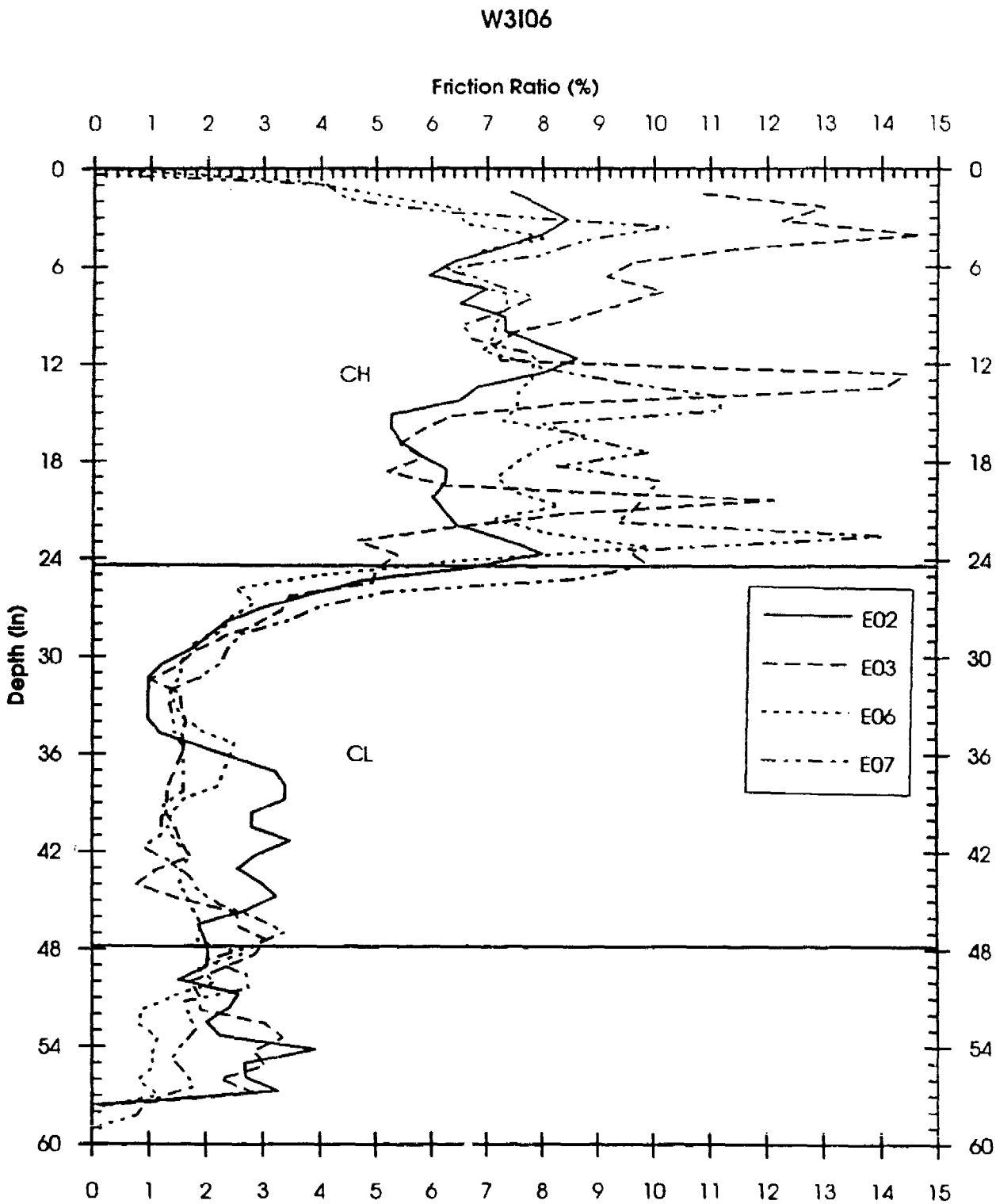

Figure F12. ECP FR versus depth for W3106

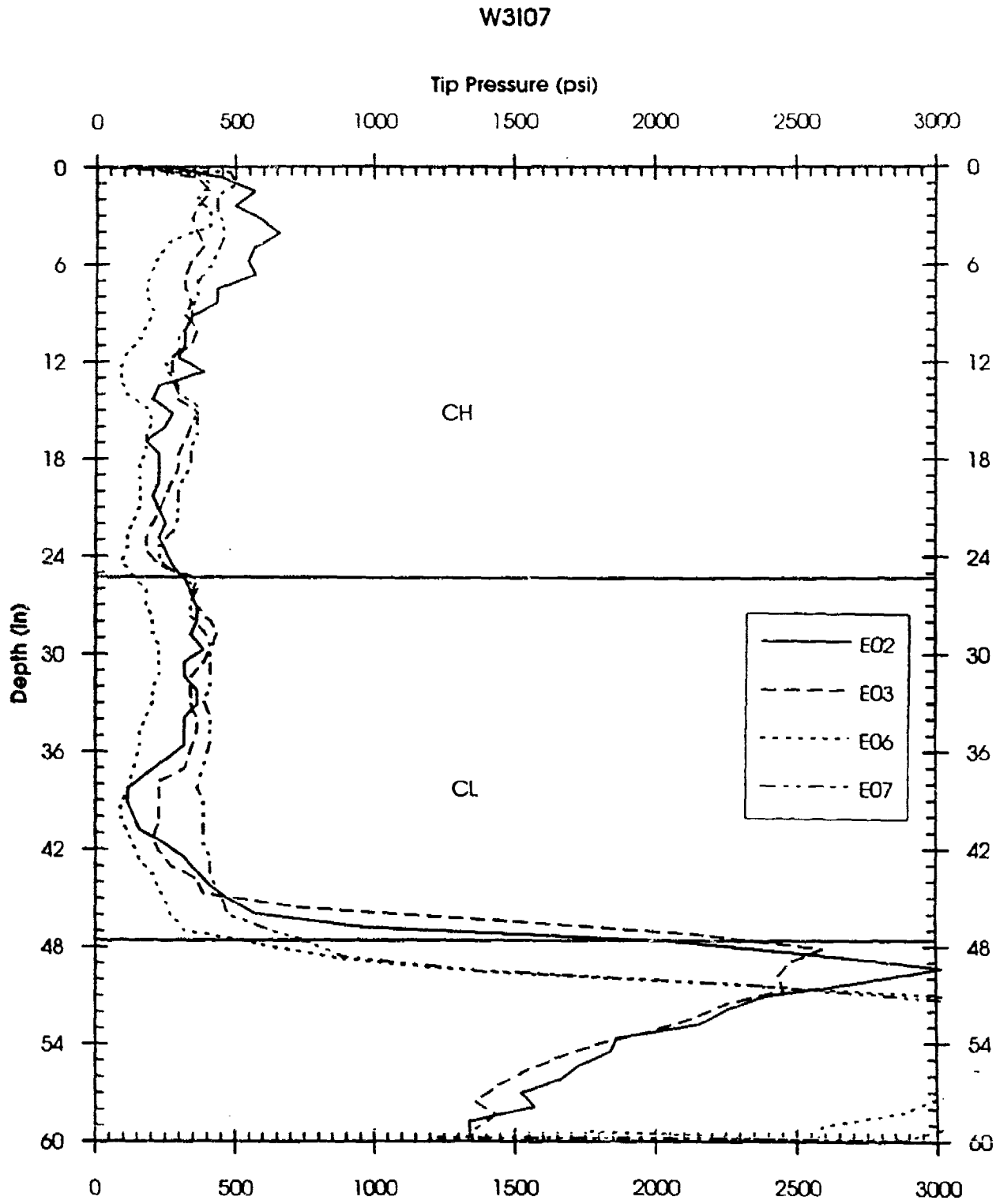

Figure F13. ECP TP versus depth for W3107

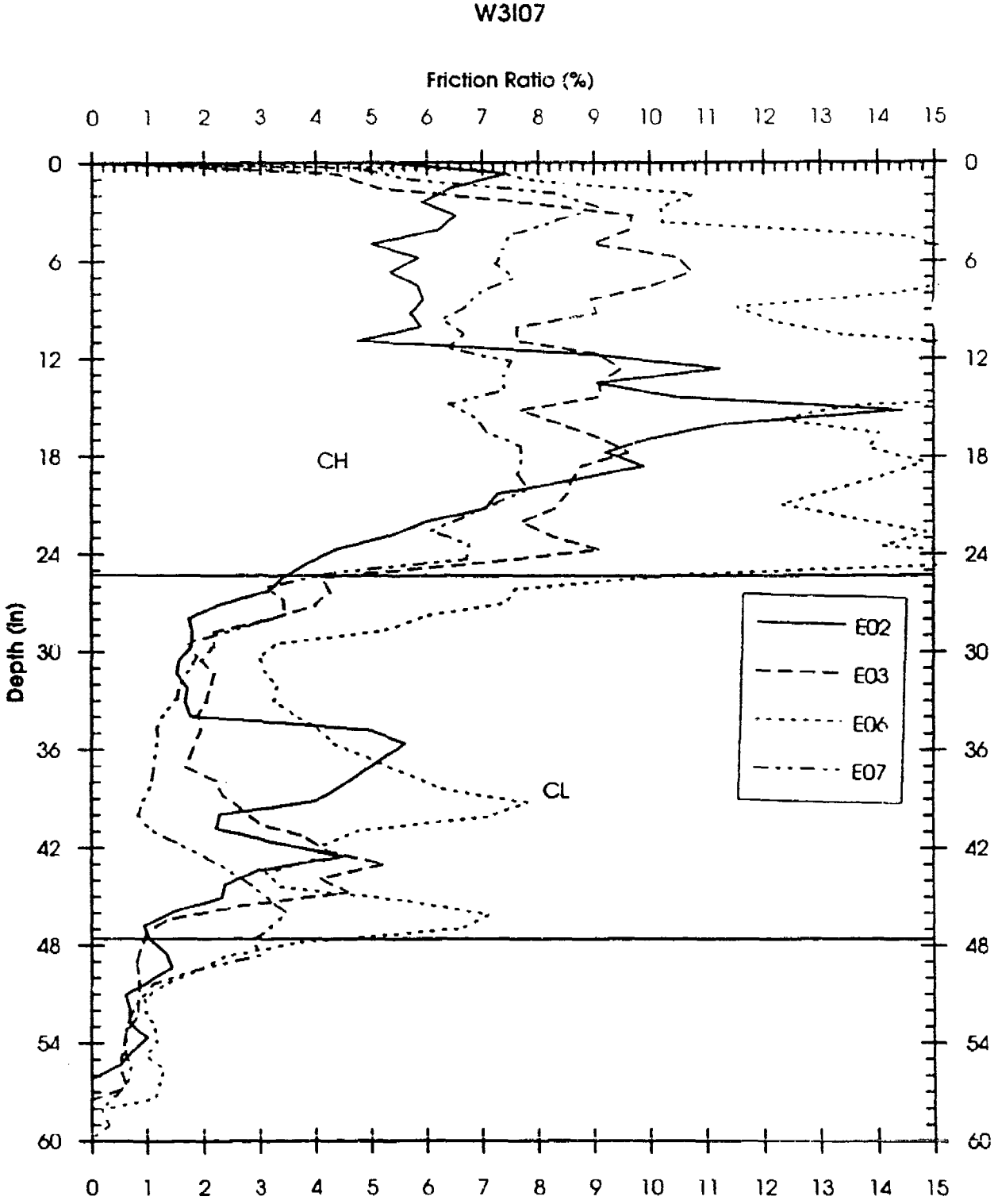

Figure F14. ECP FR versus depth for W3107

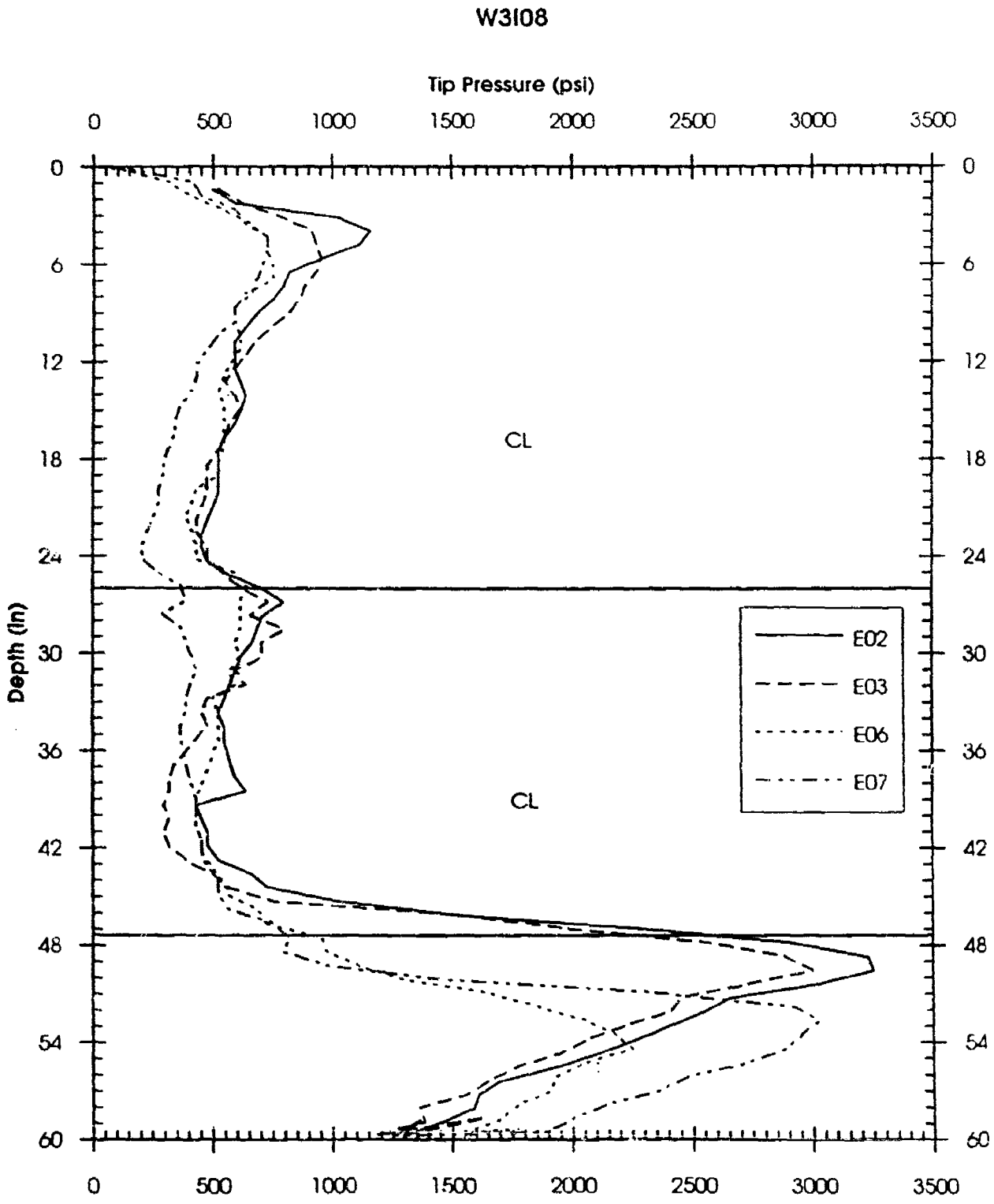

Figure F15. ECP TP versus depth for W3108

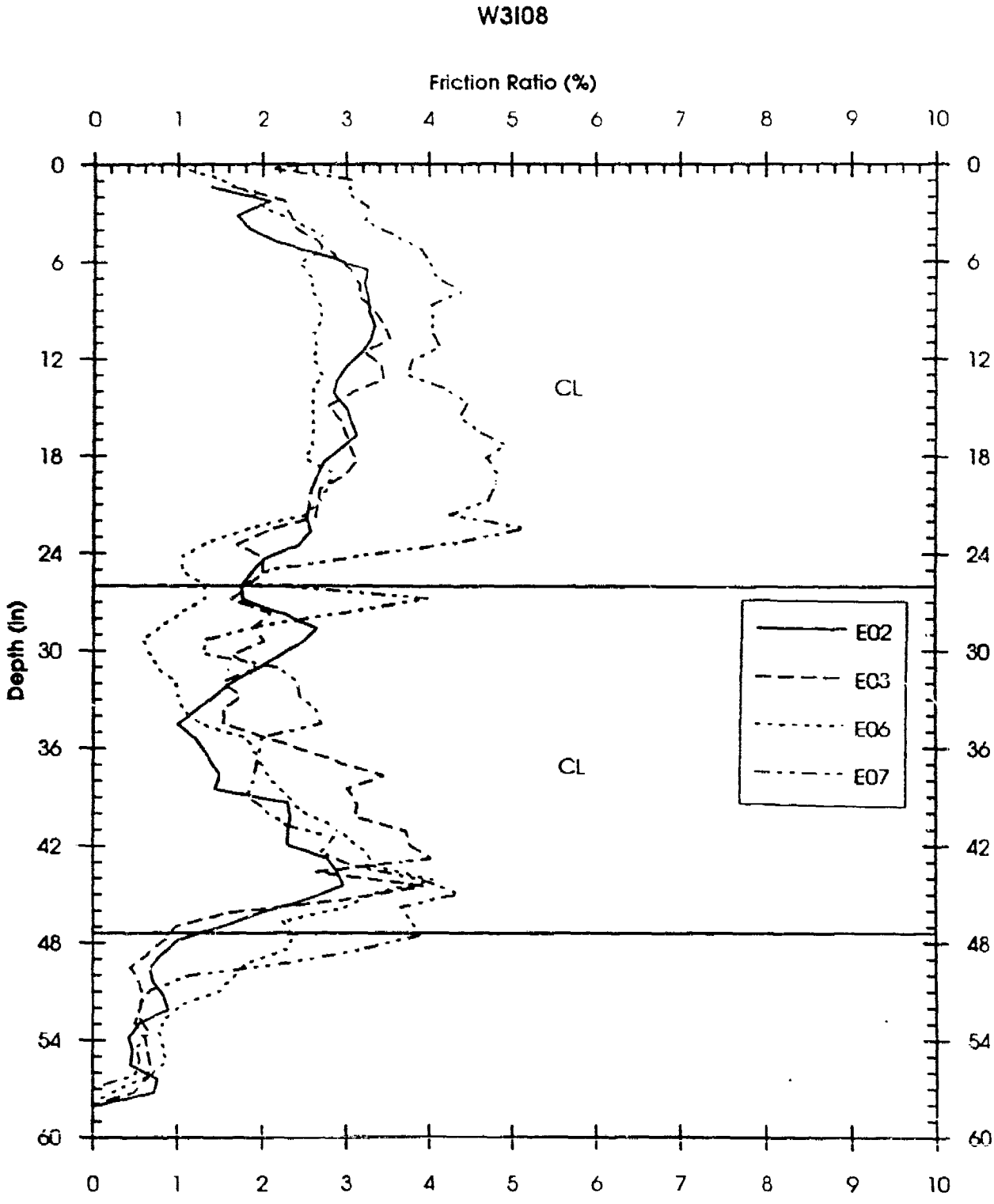

Figure F16. ECP FR versus depth for W3108

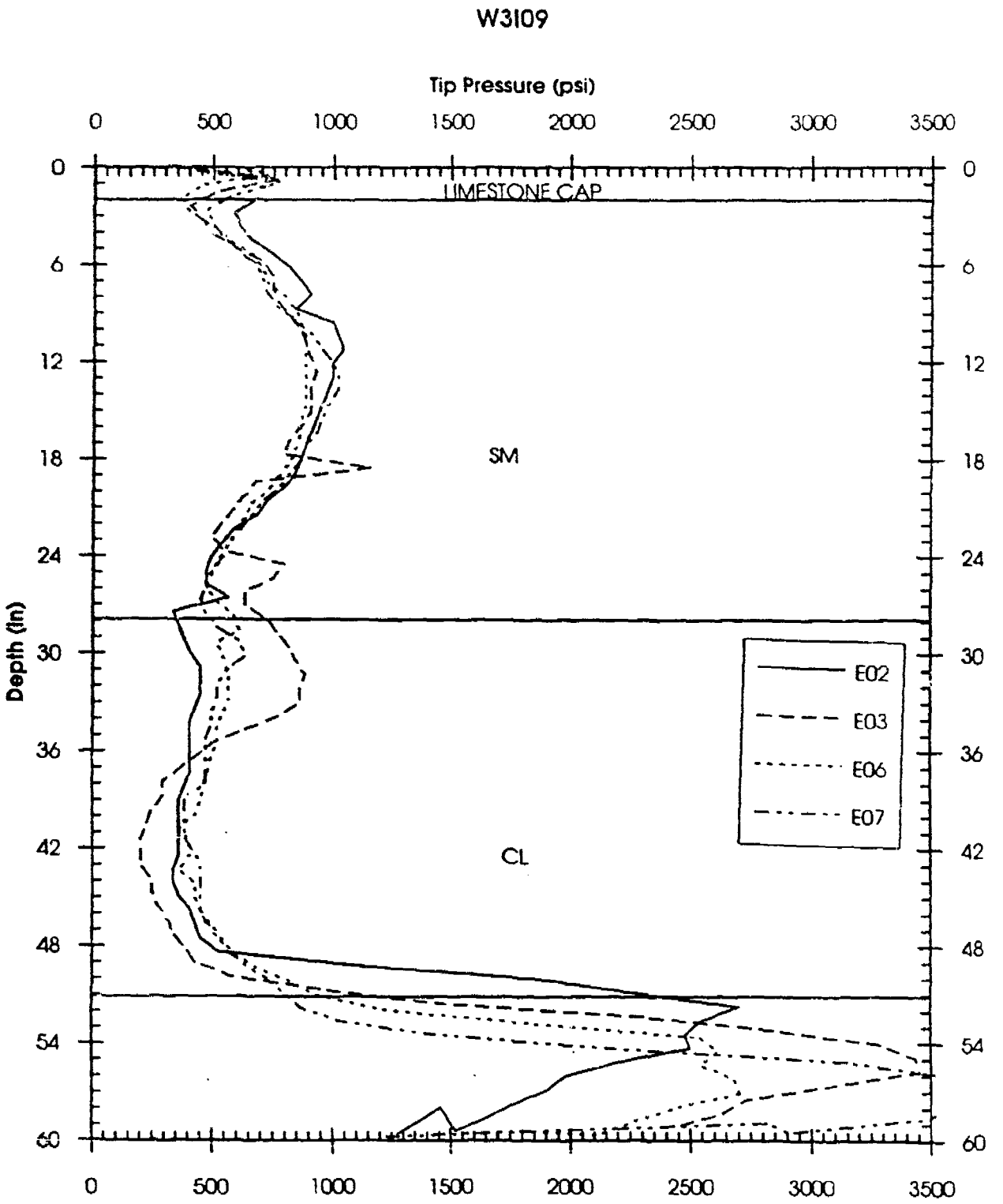

Figure F17. ECP TP versus depth for W3109

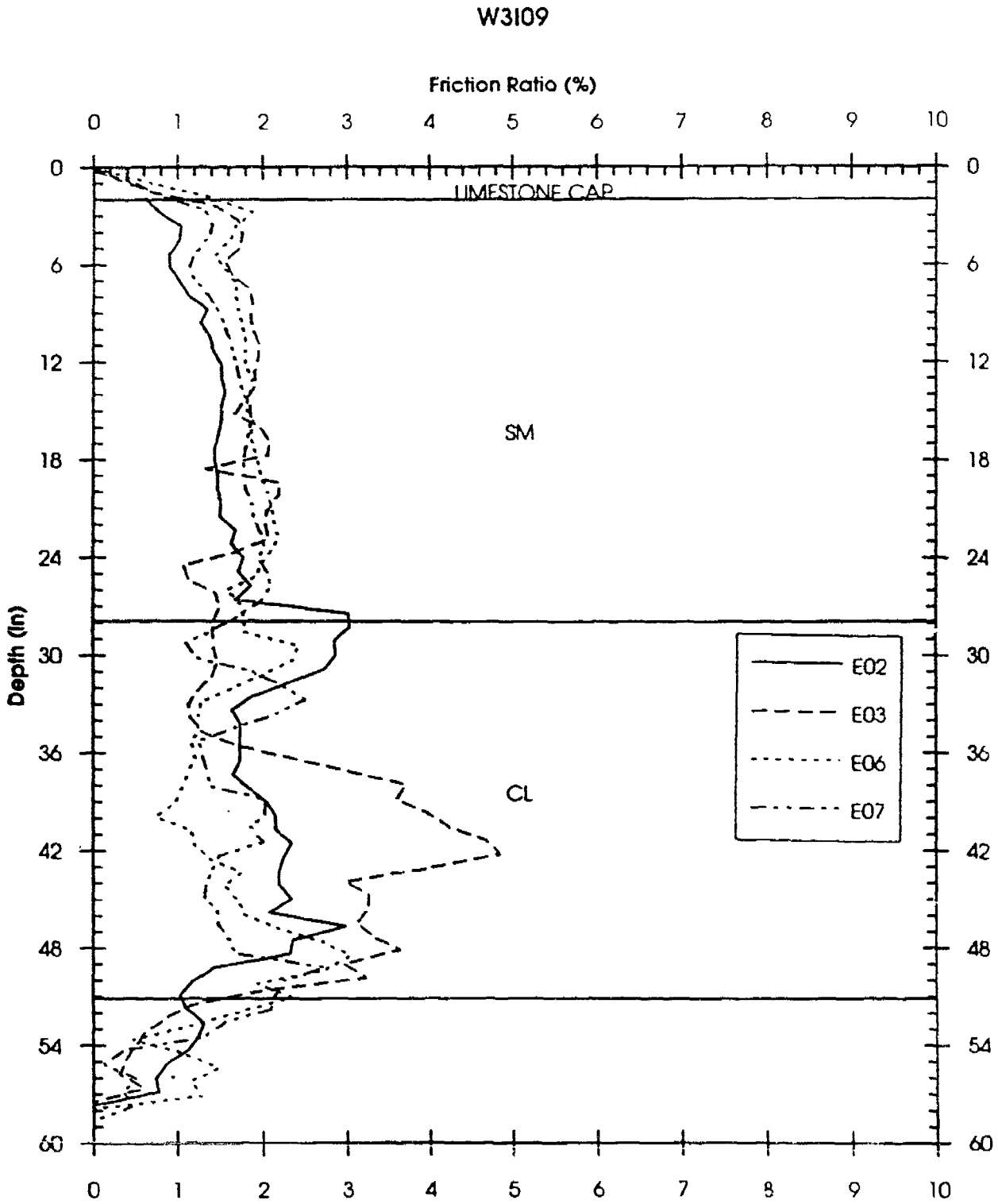

Figure F18. ECP FR versus depth for W3O9

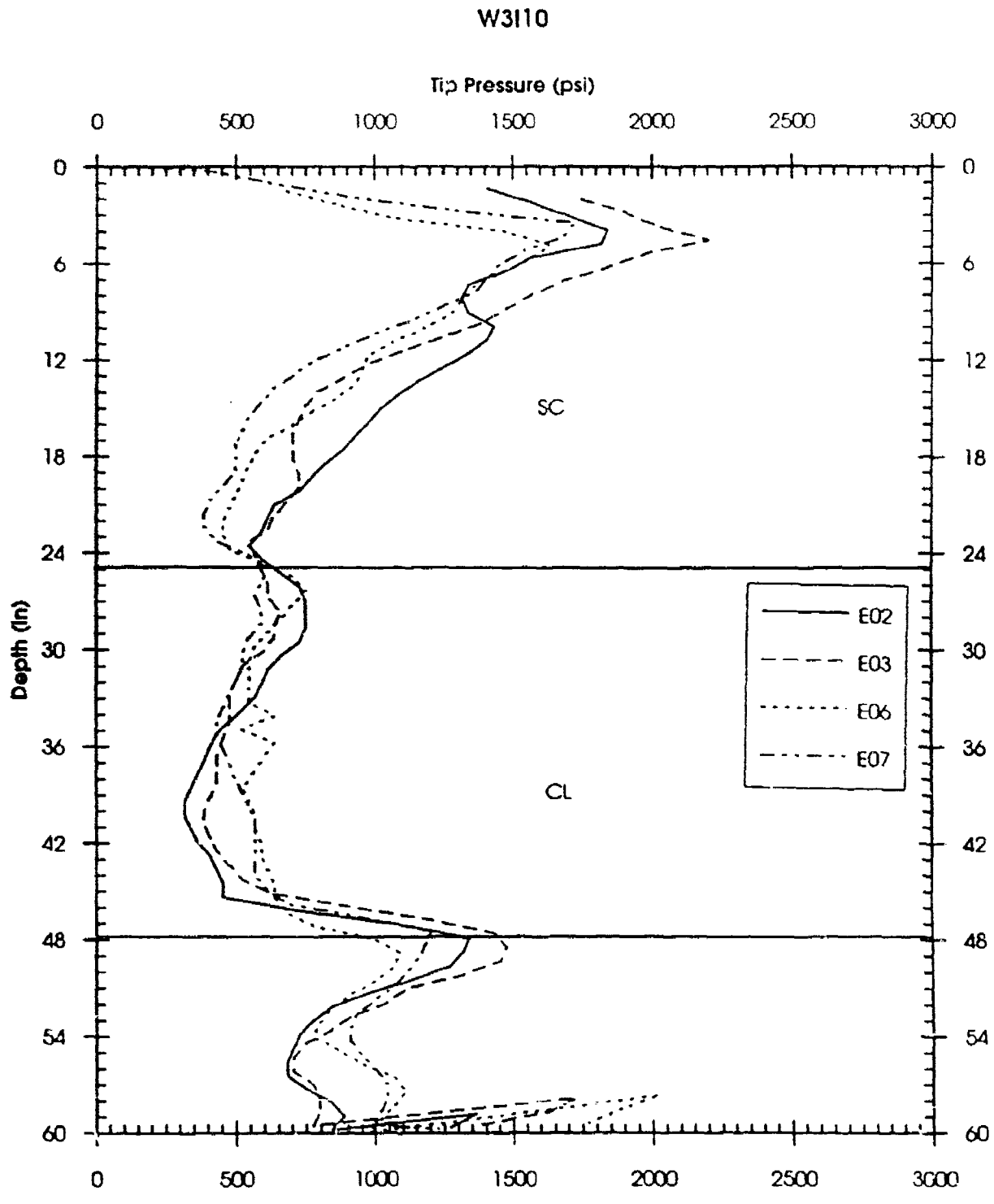

Figure F19. ECP TP versus depth for W3I10

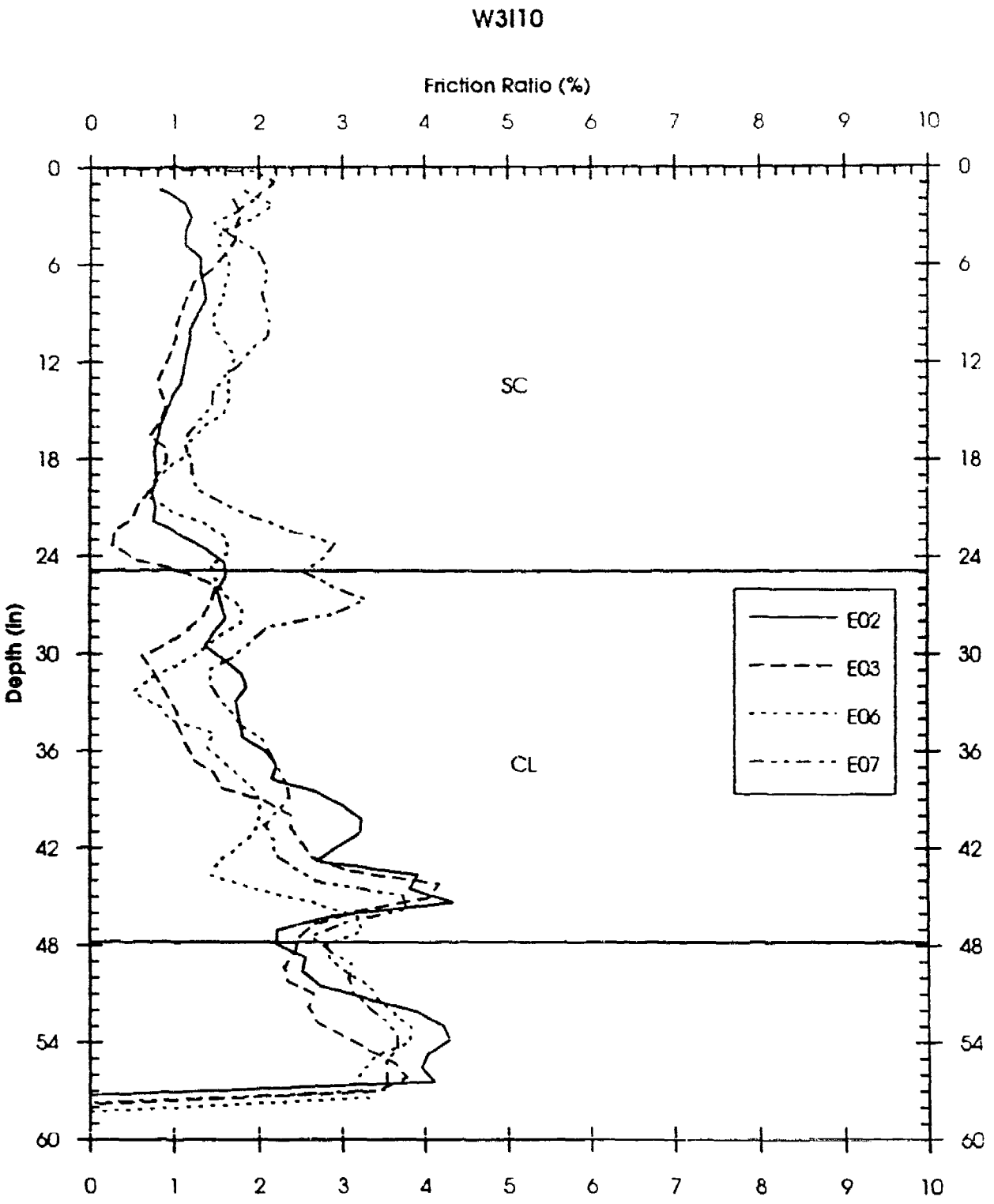

Figure F20. ECP FR versus depth for W3I10

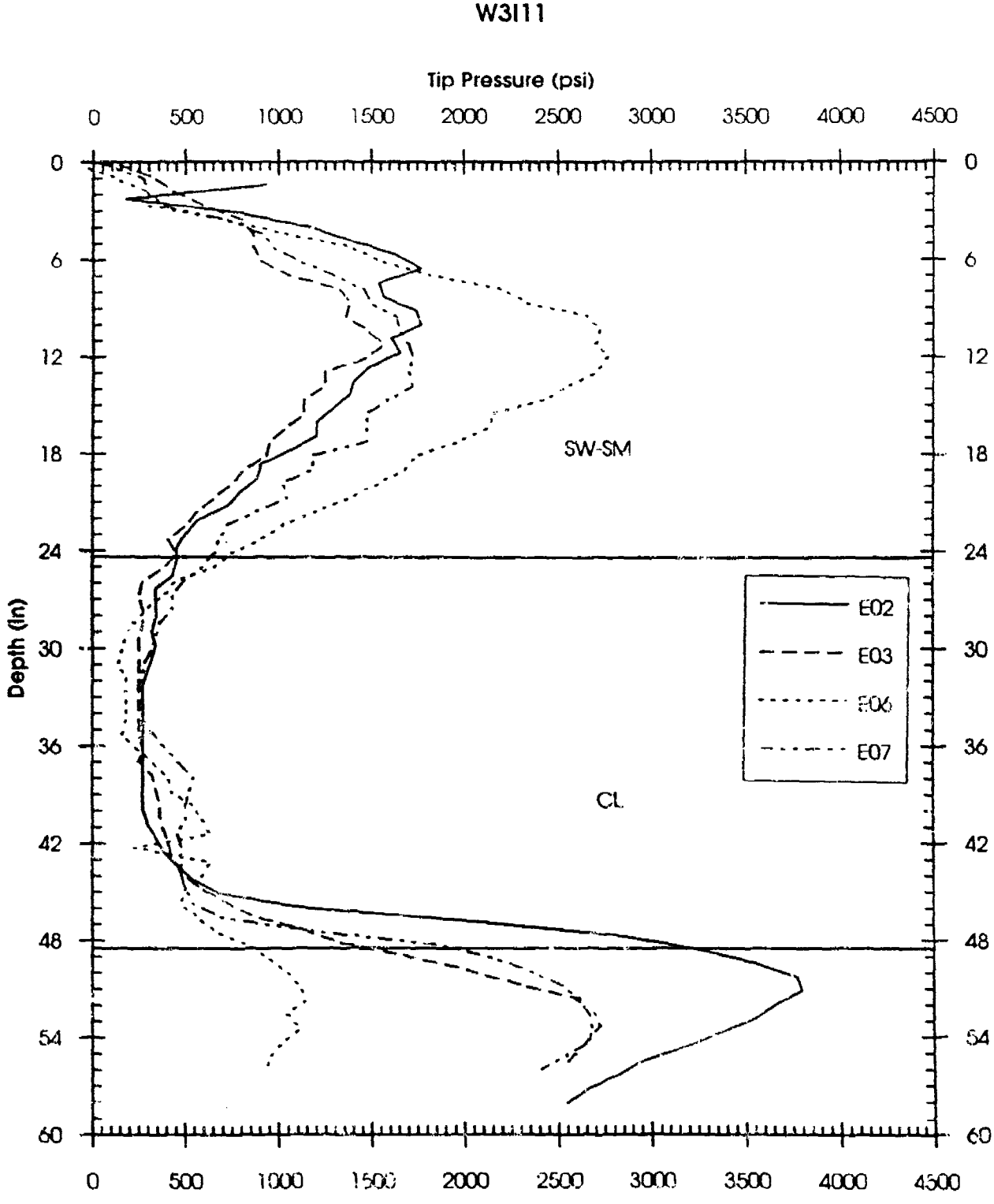

Figure F21. ECP TP versus depth for W3I11

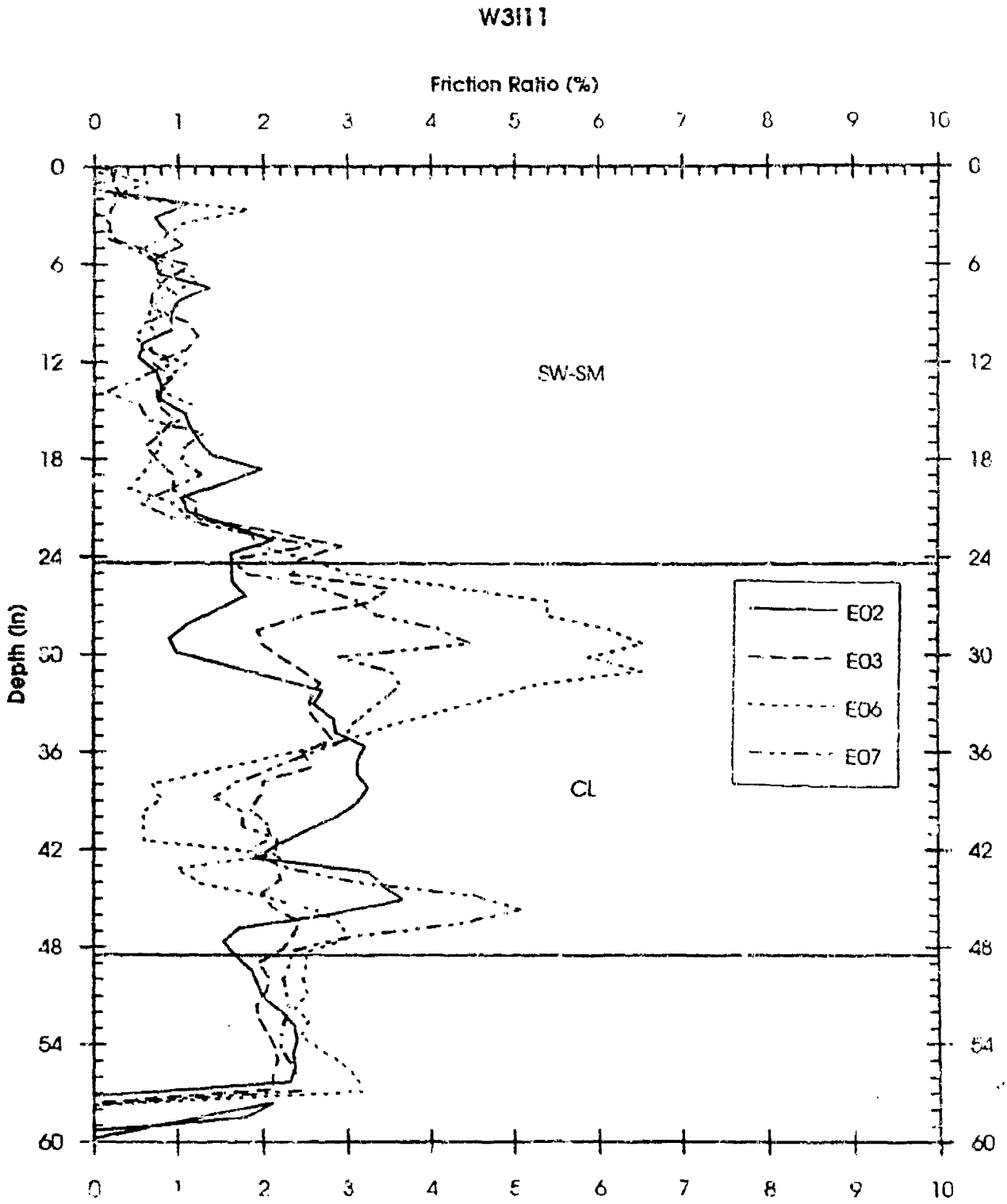

Figure F22. ECP FR versus depth for W3I11

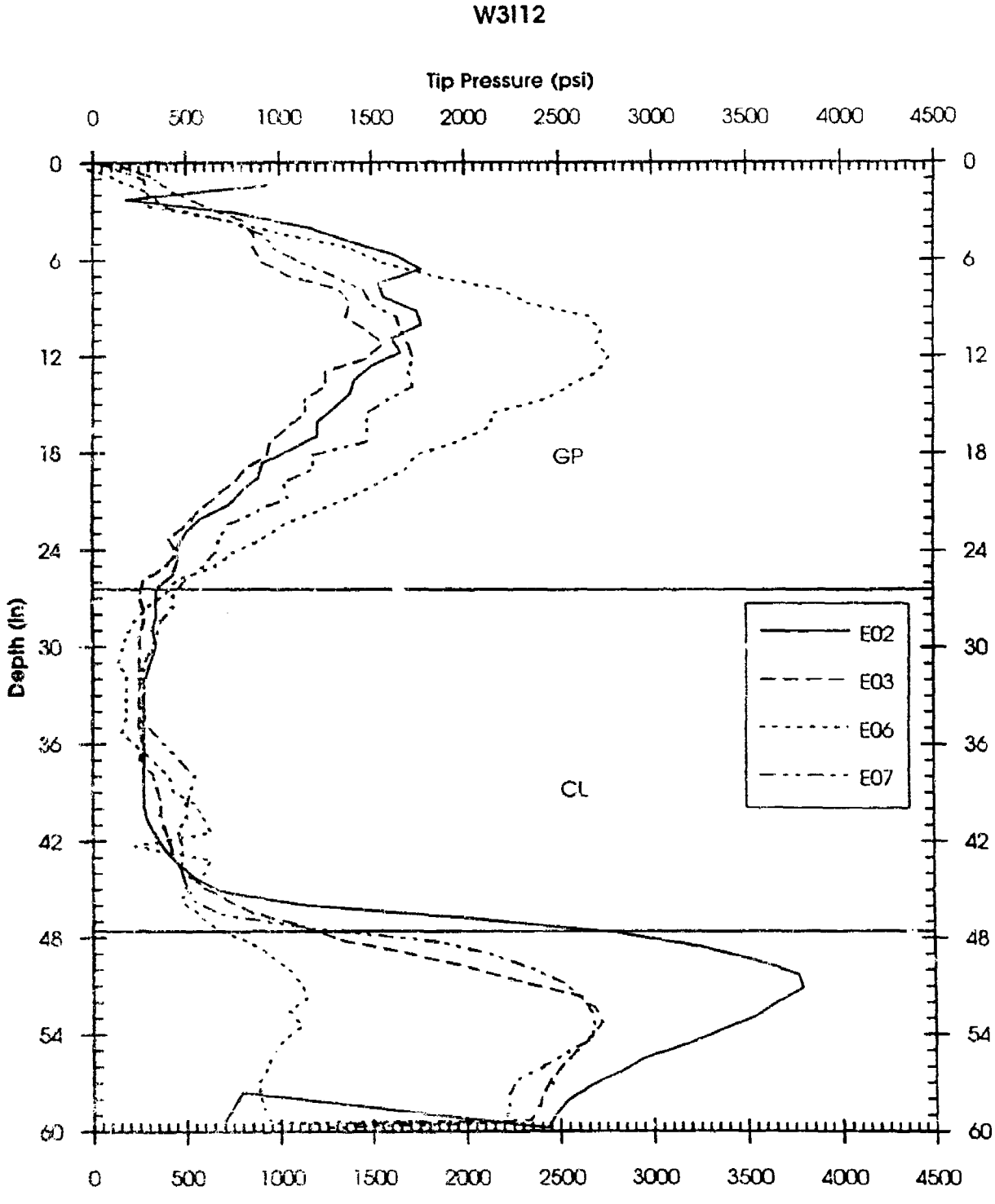

Figure F23. ECP TP versus depth for W3I12

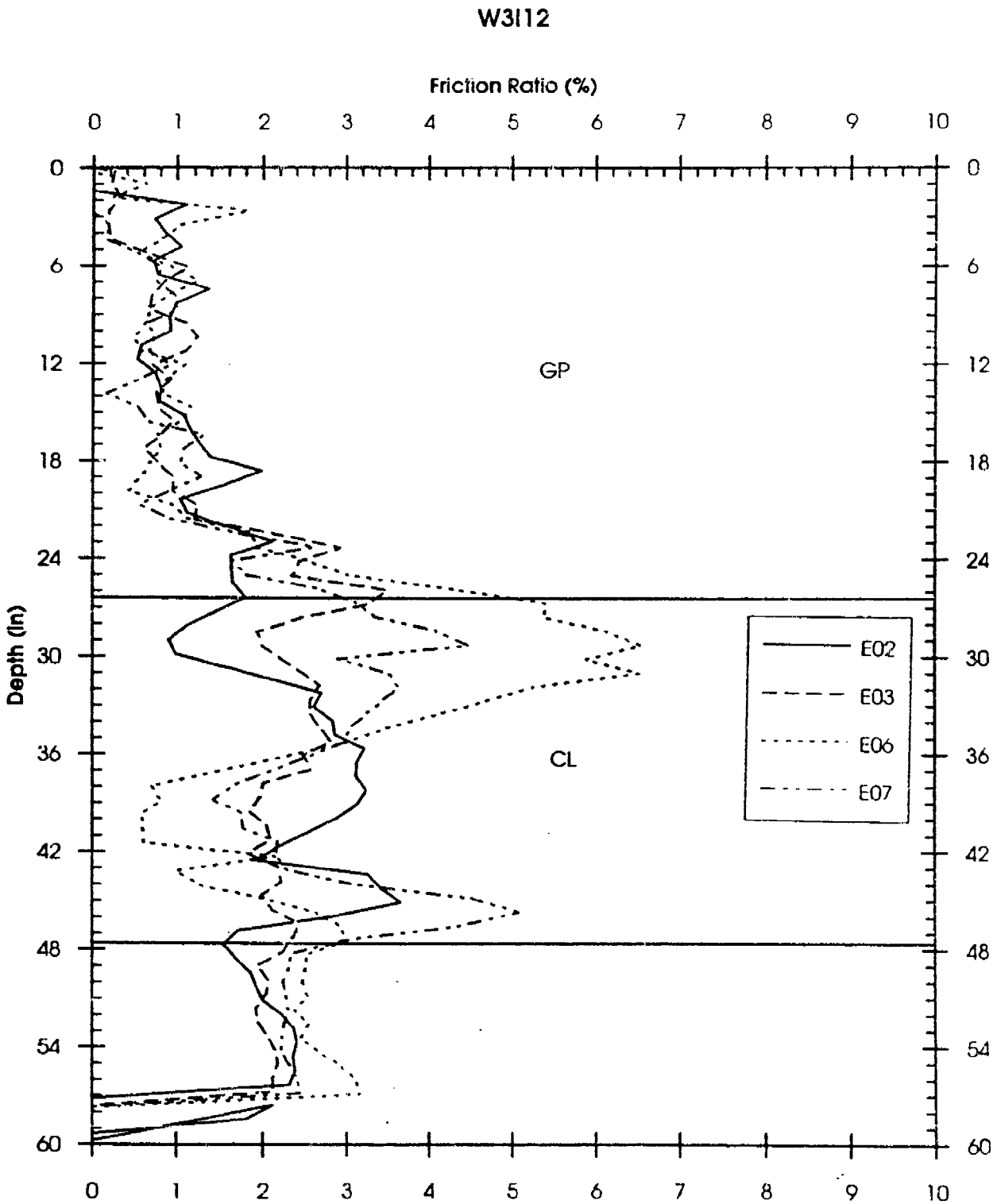

Figure F24. ECP FR versus depth for W3112

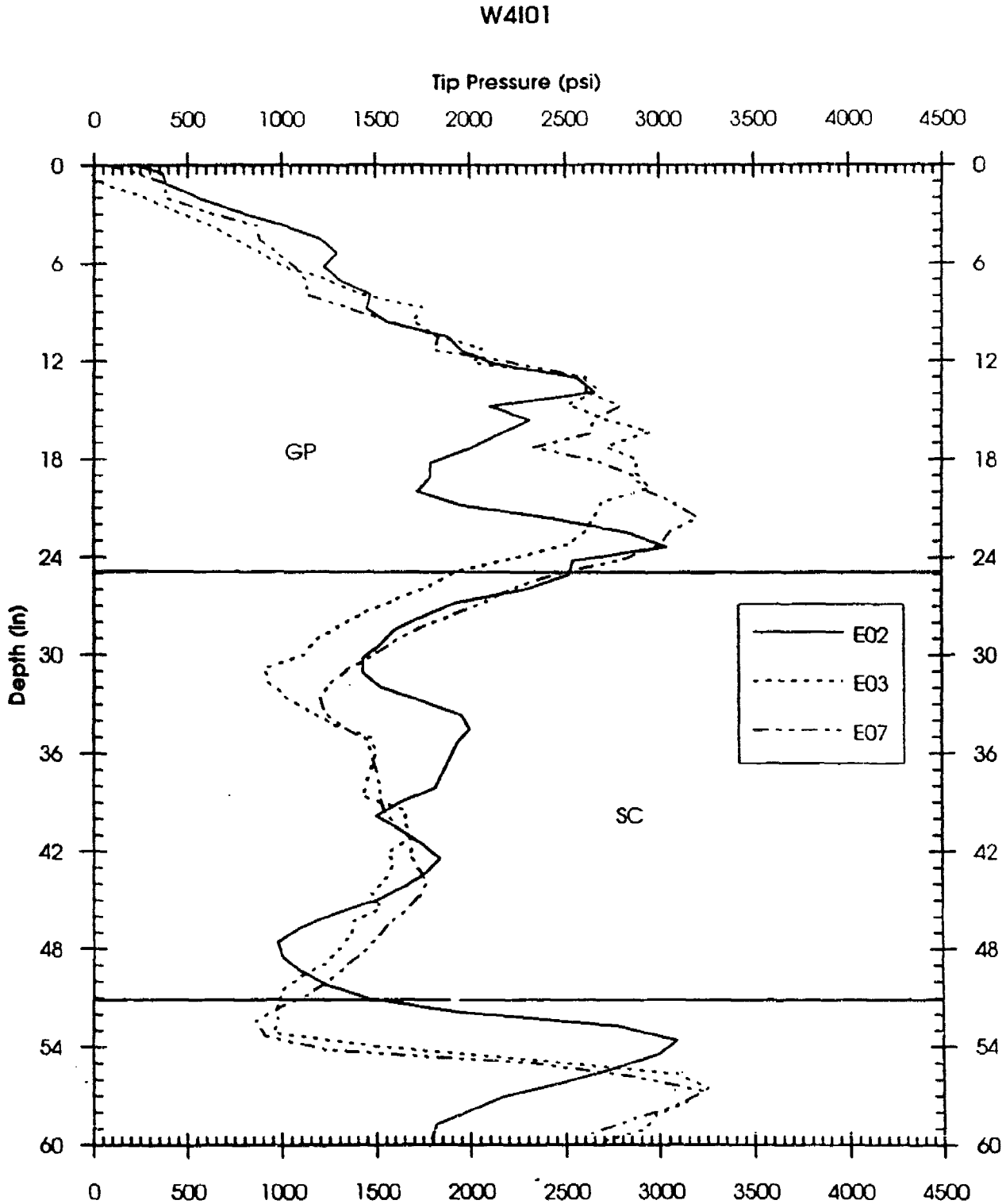

Figure F25. ECP TP versus depth for W4101

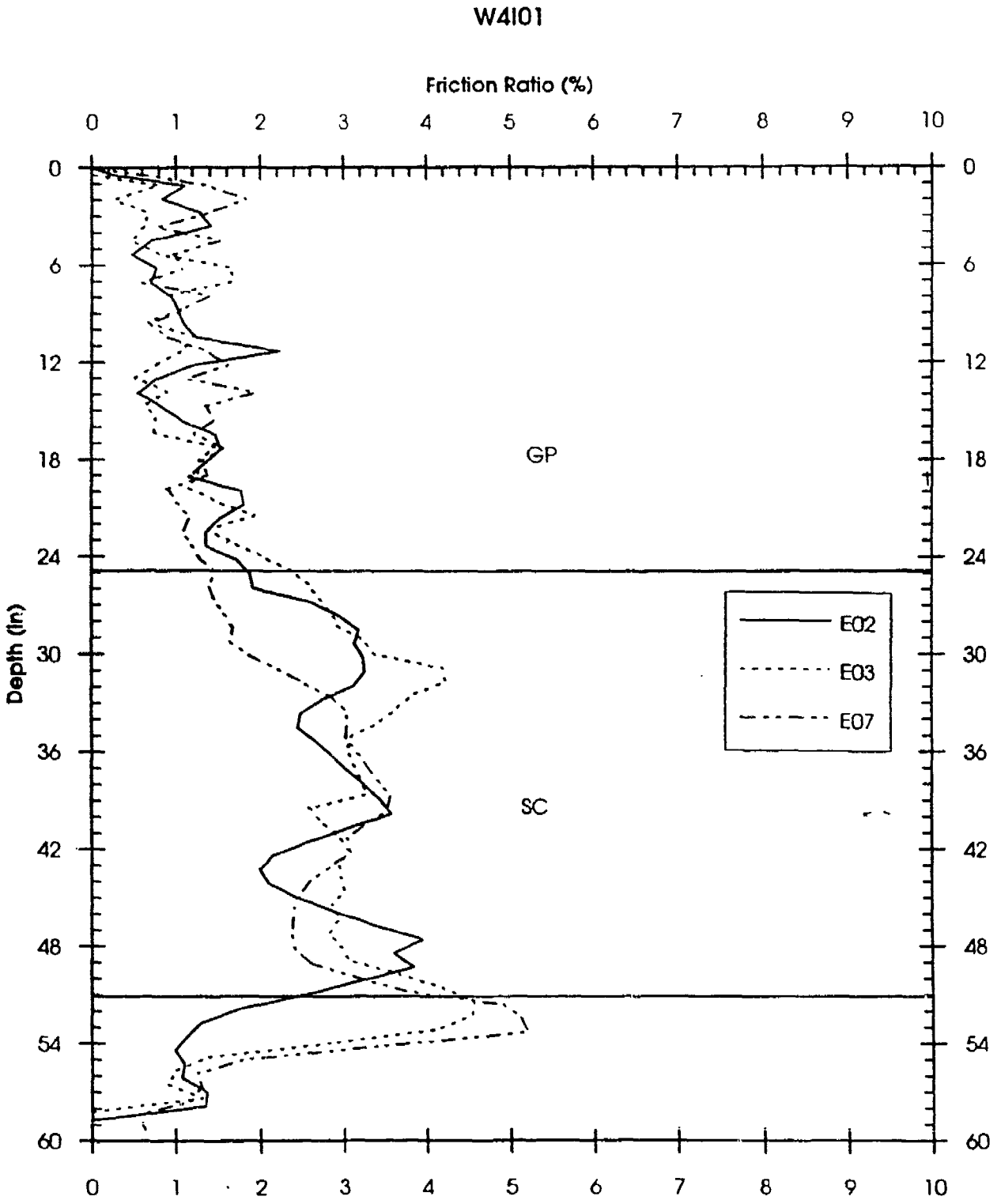

Figure F26. ECP FR versus depth for W4101

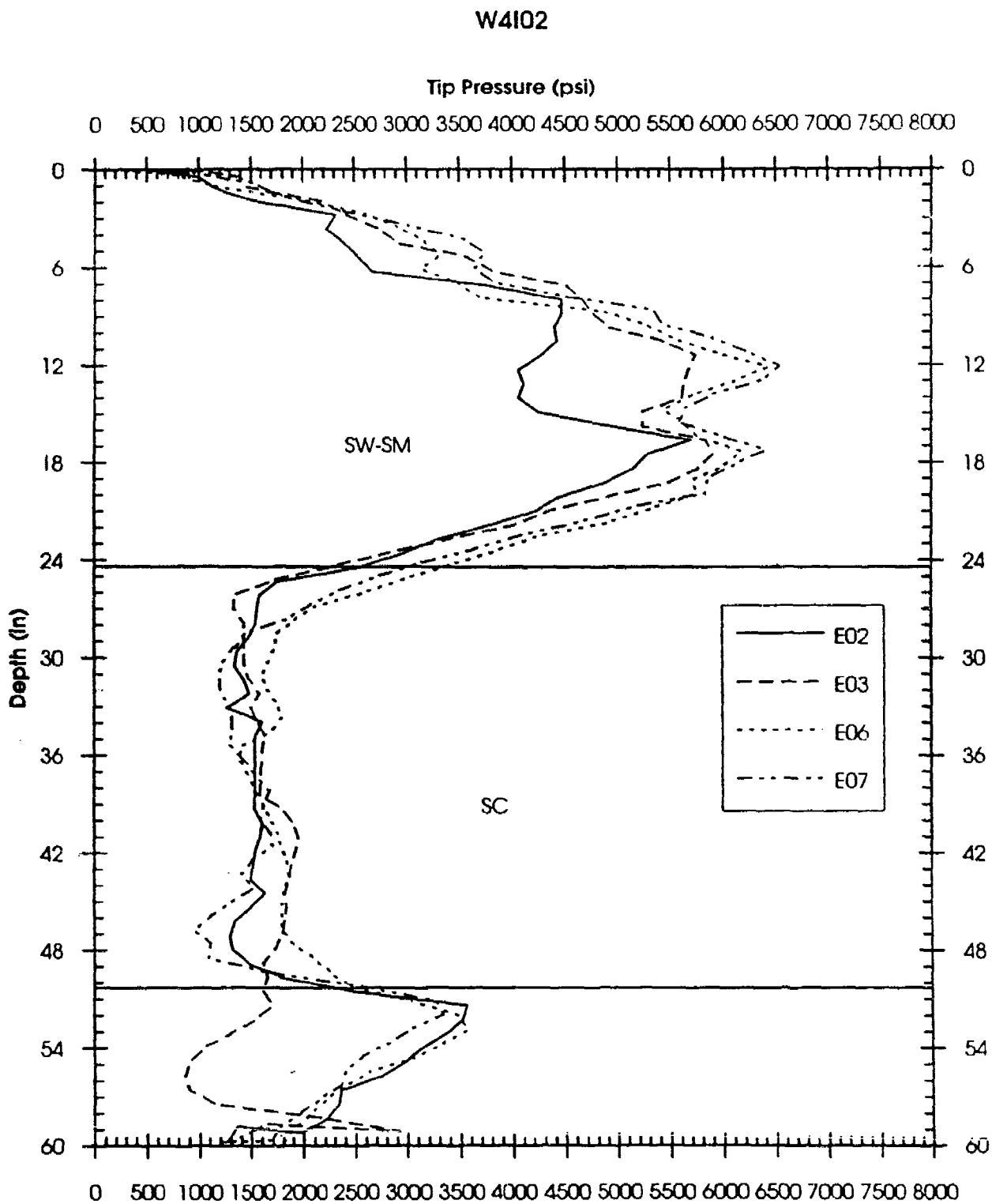

Figure F27. ECP TP versus depth for W4102

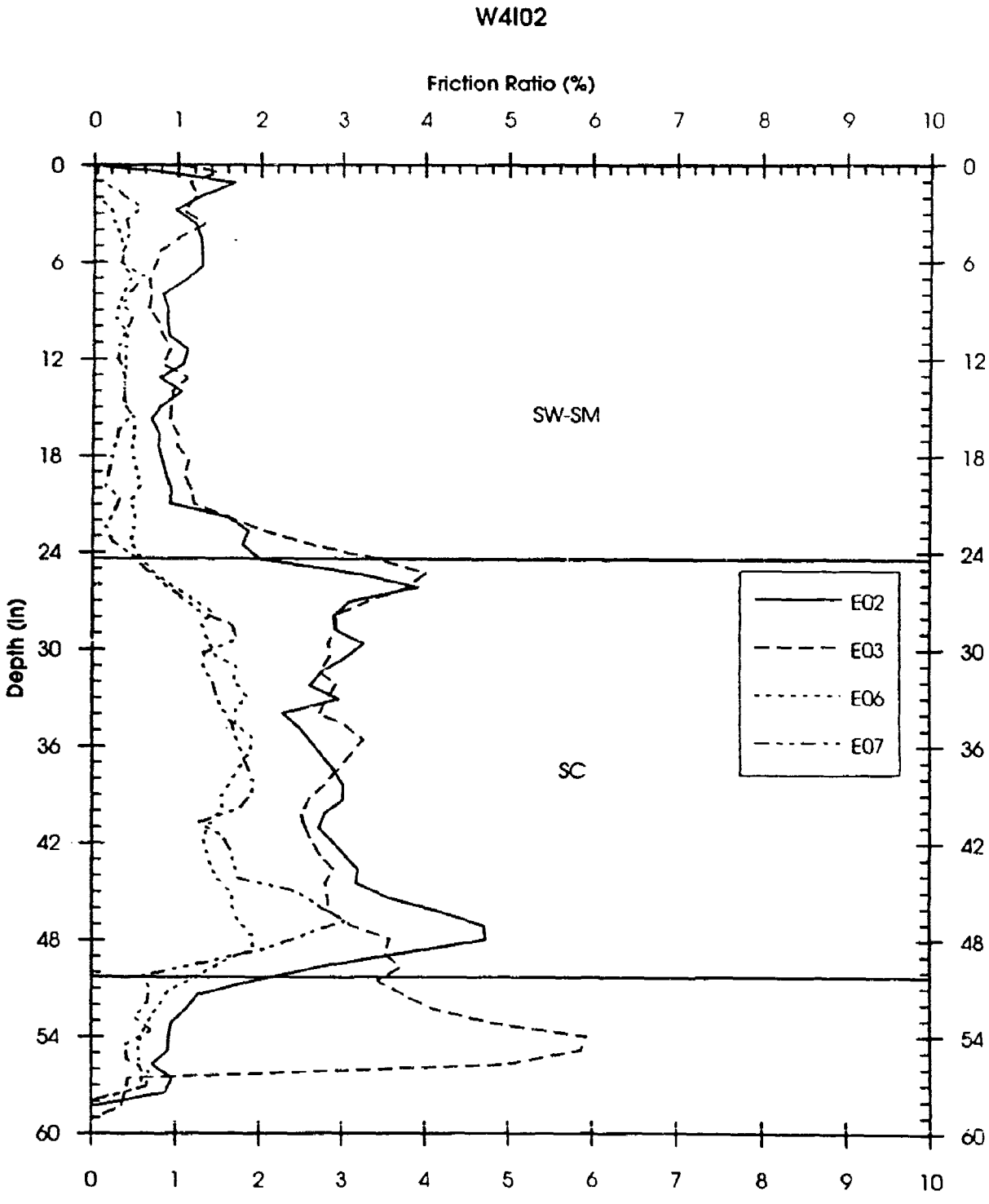

Figure F28. ECP FR versus depth for W4I02

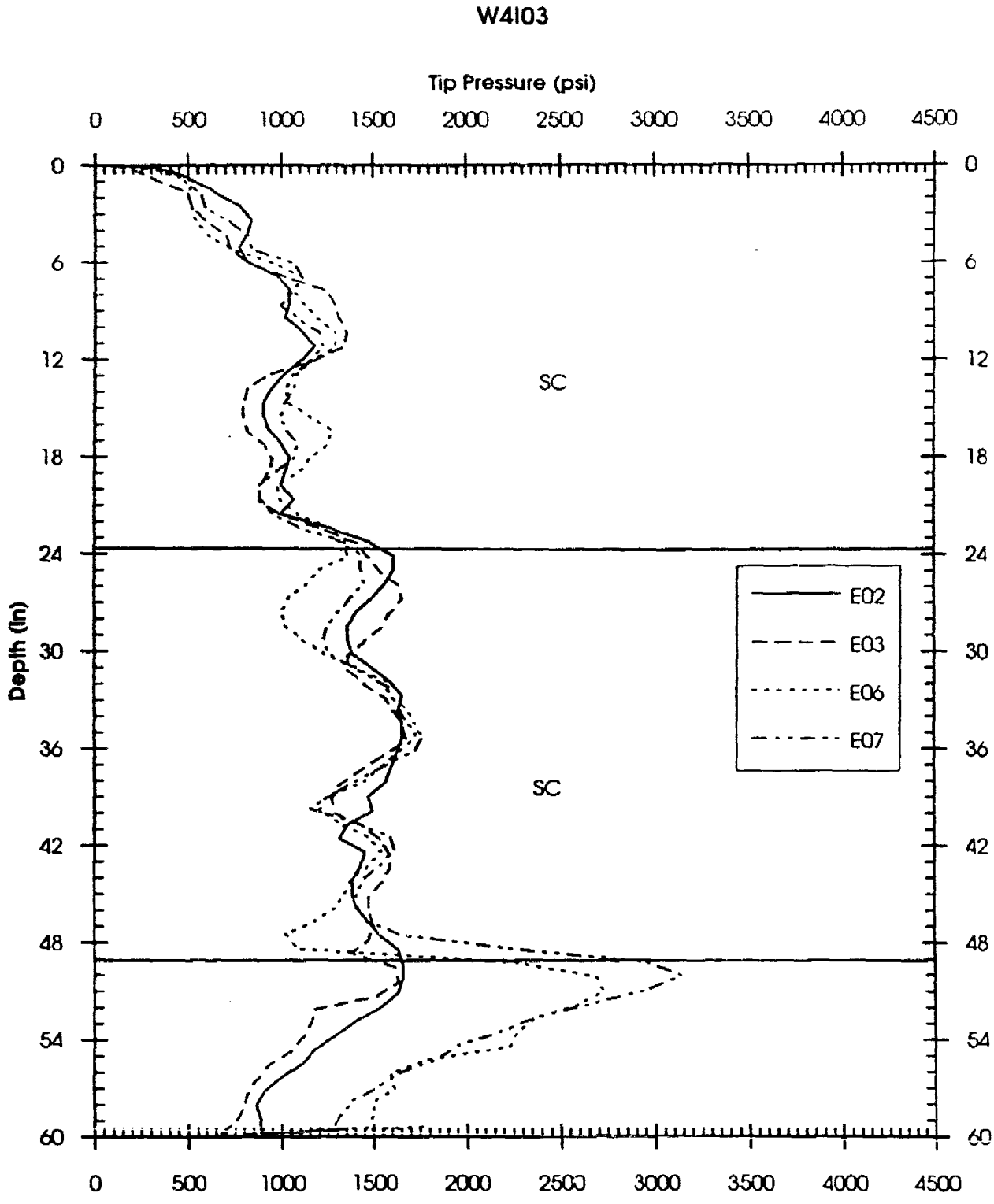

Figure F29. ECP TP versus depth for W4103

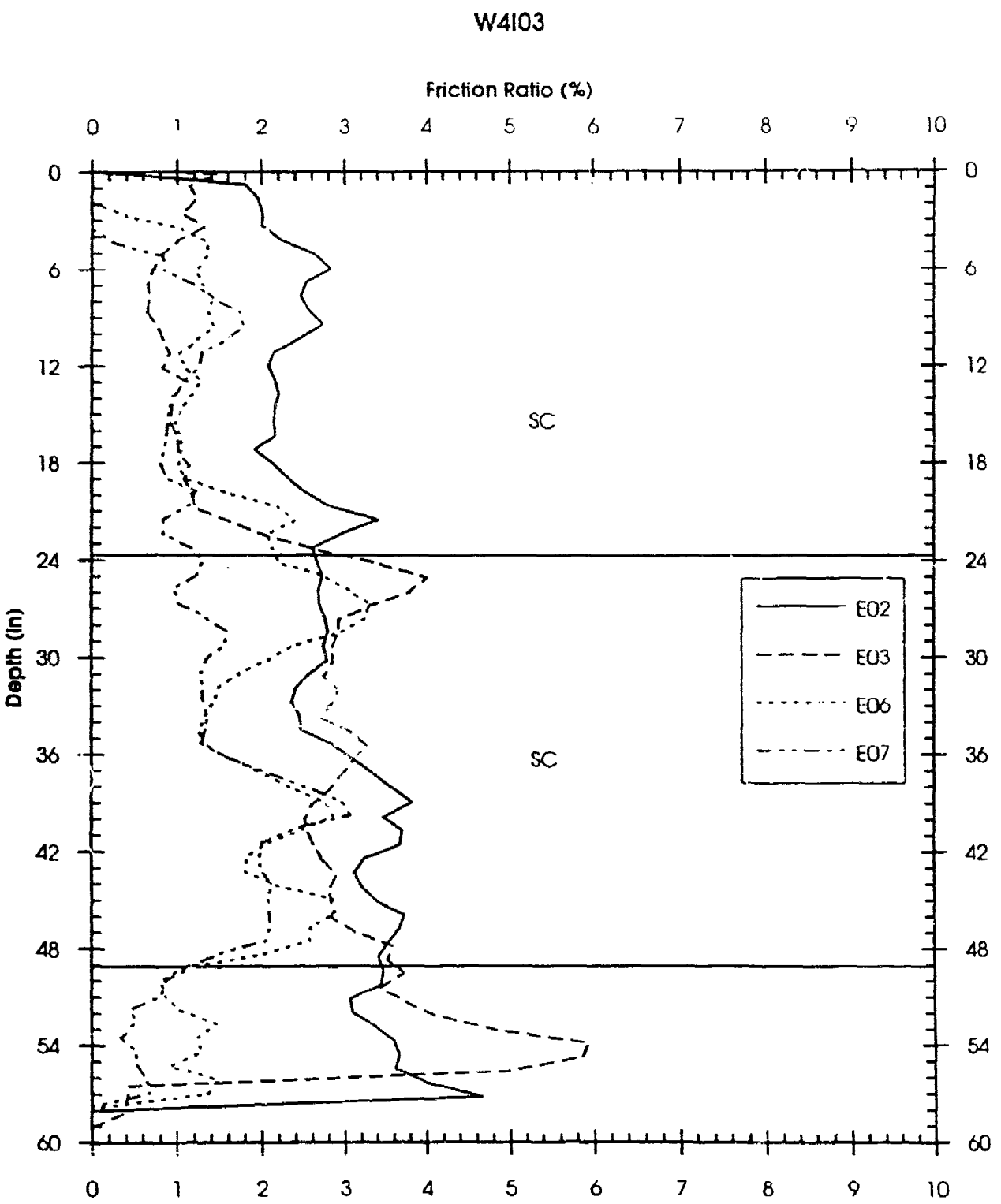

Figure F30. ECP FR versus depth for W4103

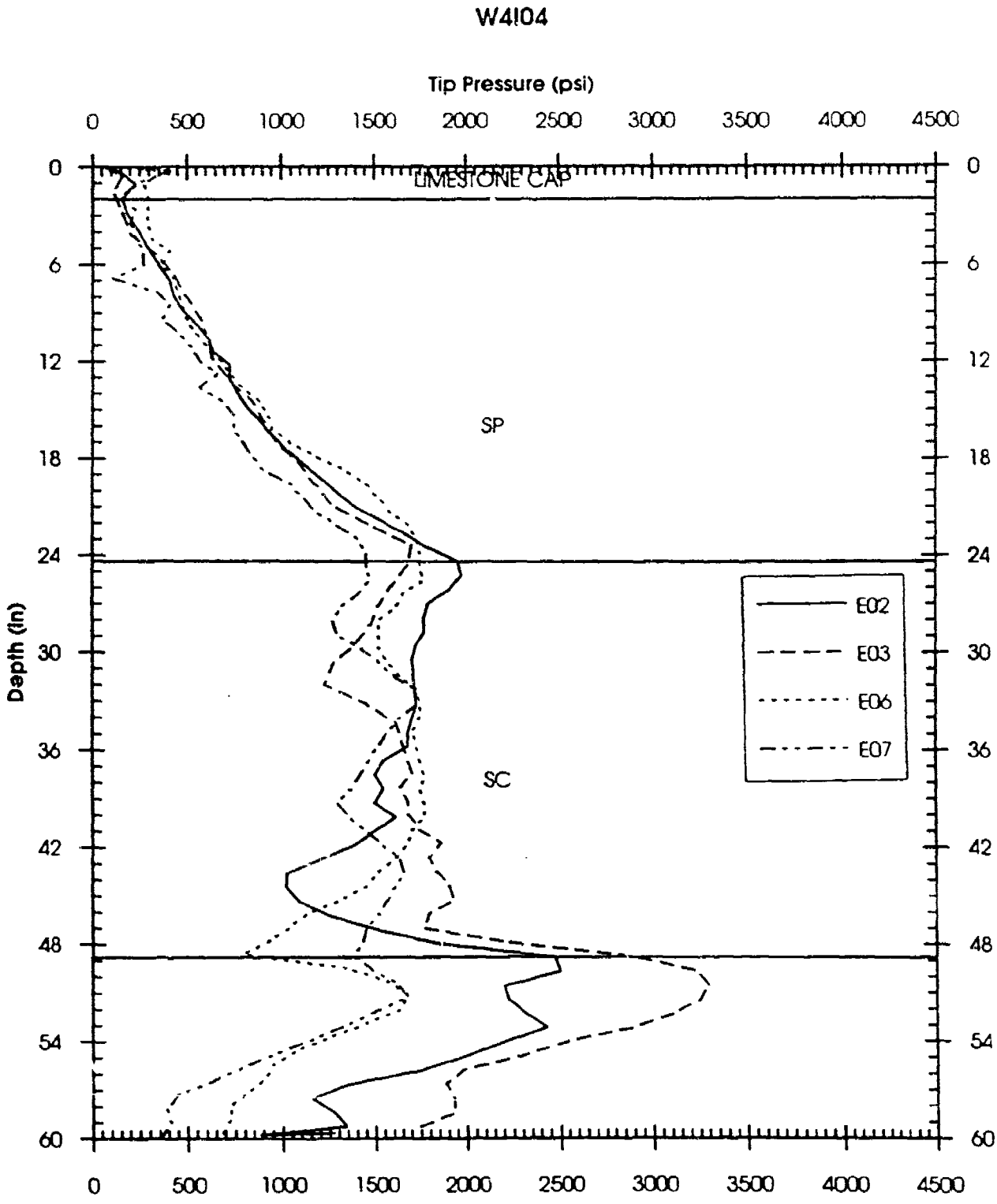

Figure F31. ECP TP versus depth for W4i04

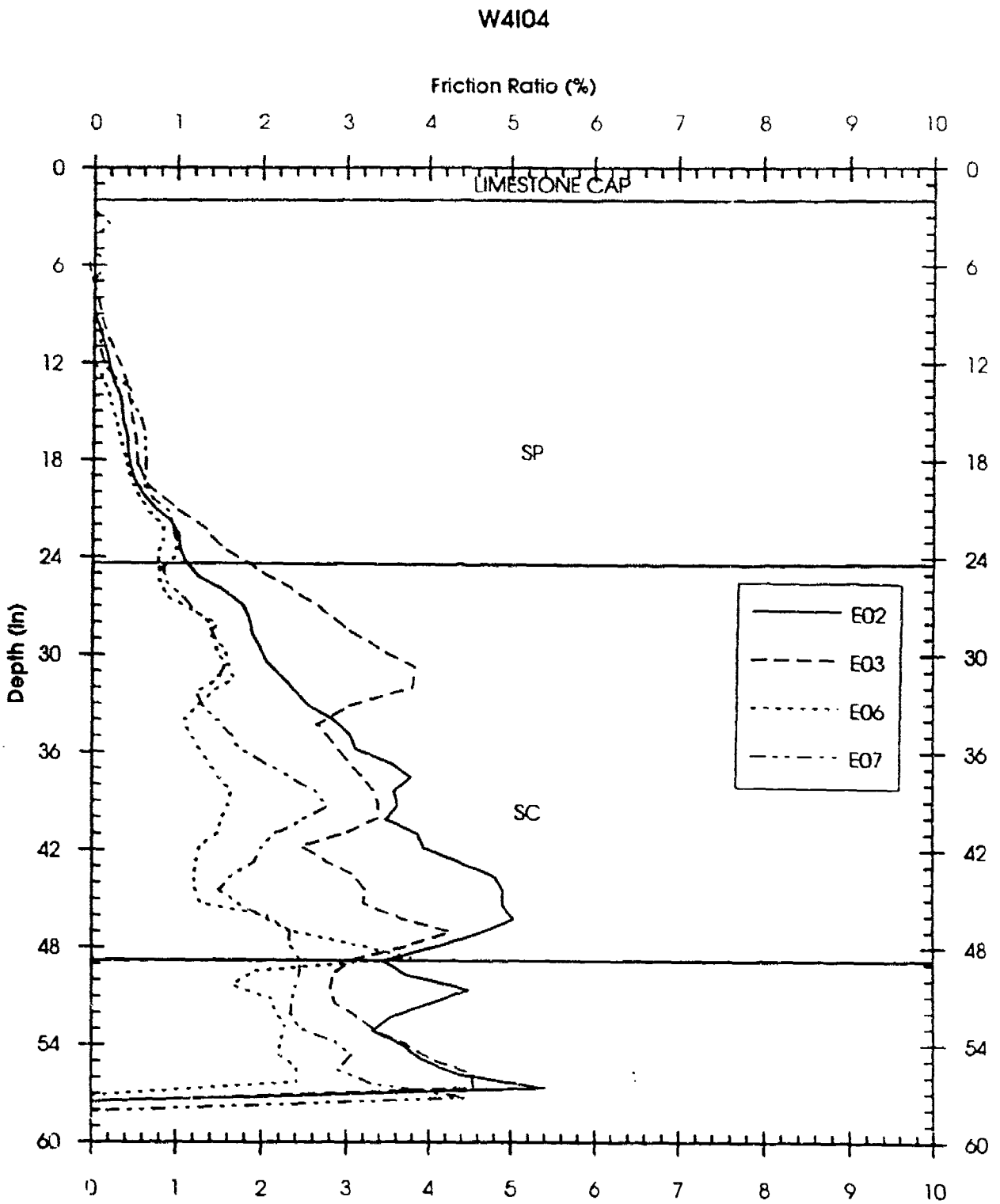

Figure F32. ECP FR versus depth for W4104

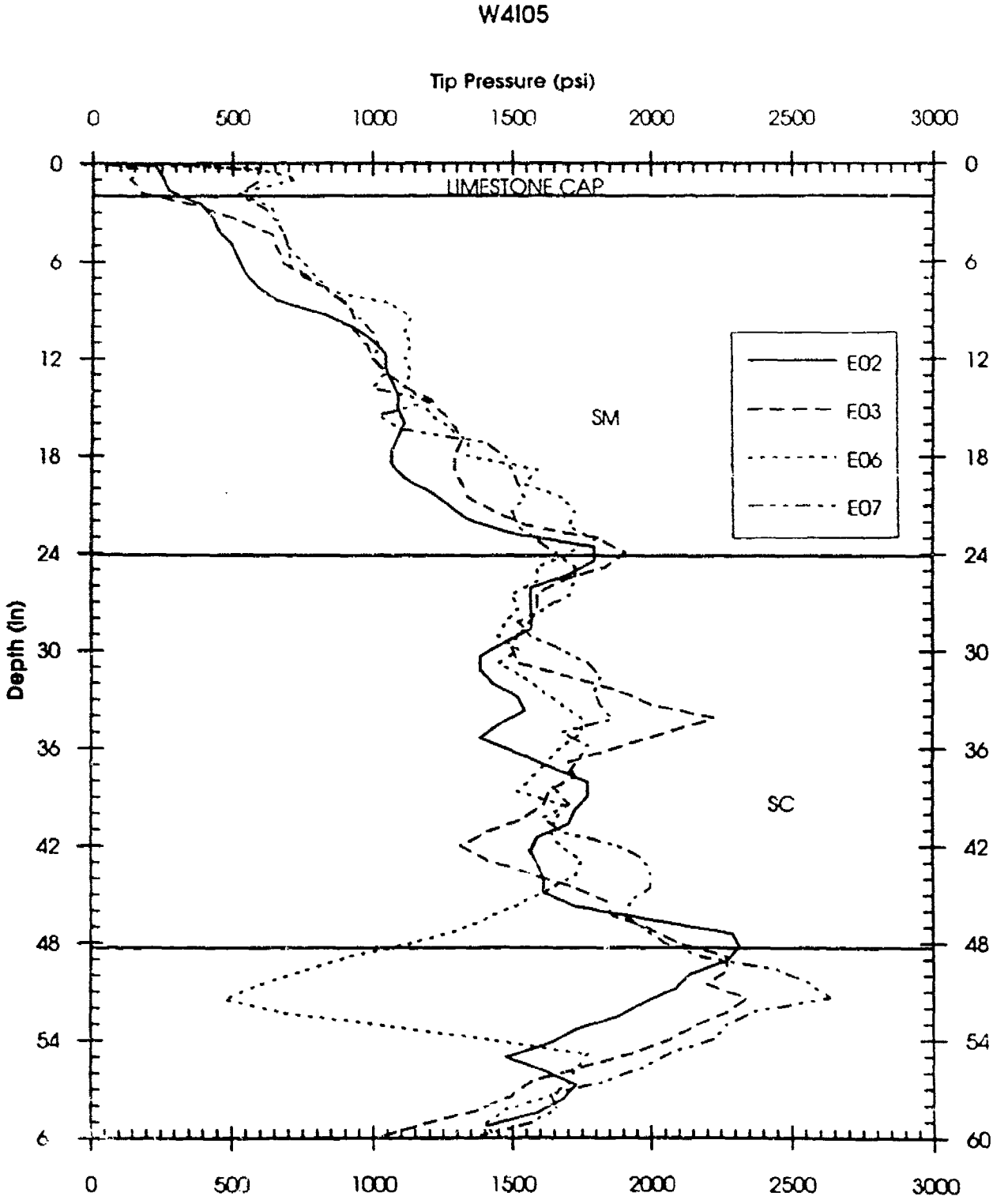

Figure F33. ECP TP versus depth for W4105

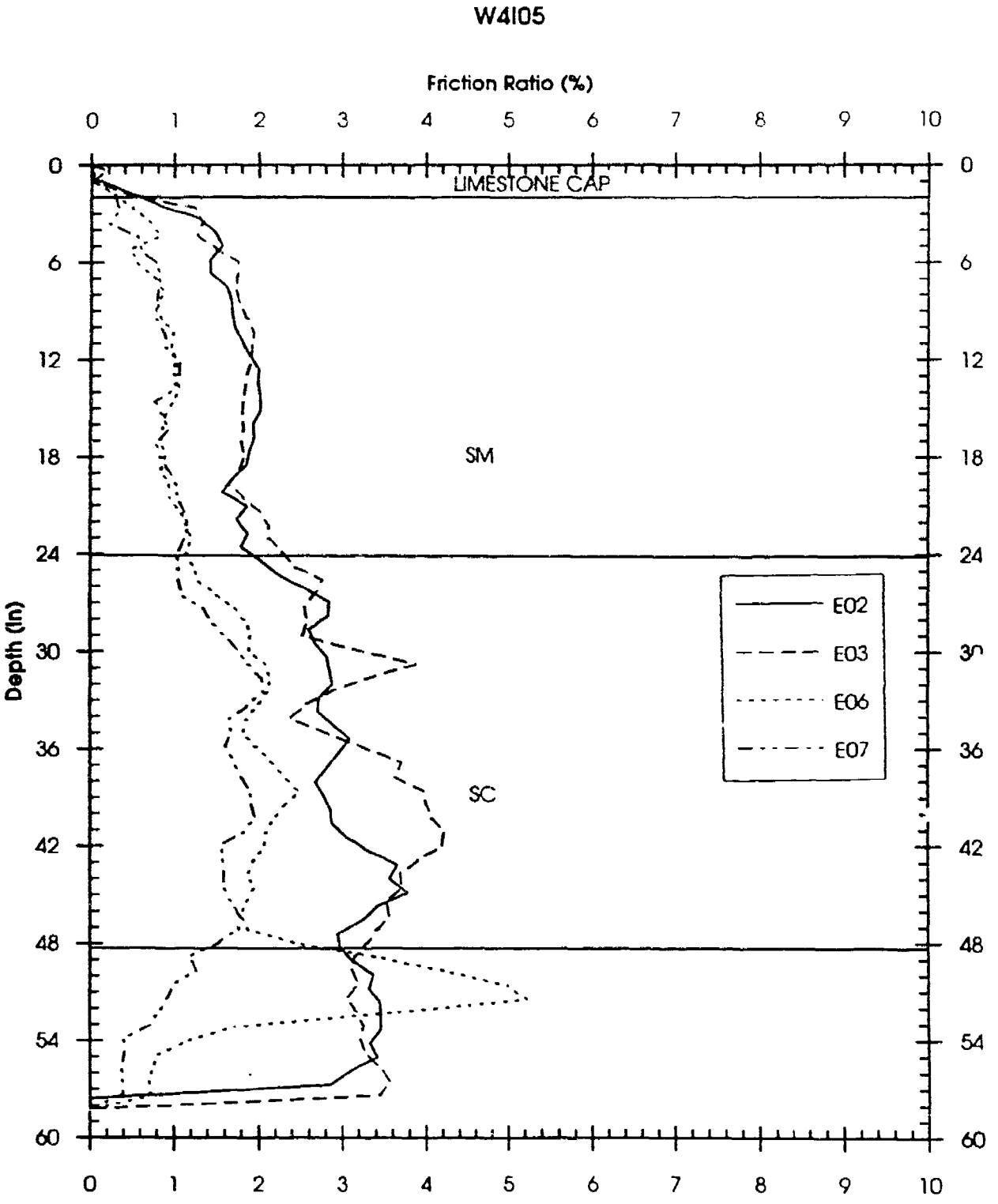

Figure F34. ECP FR versus depth for W4105

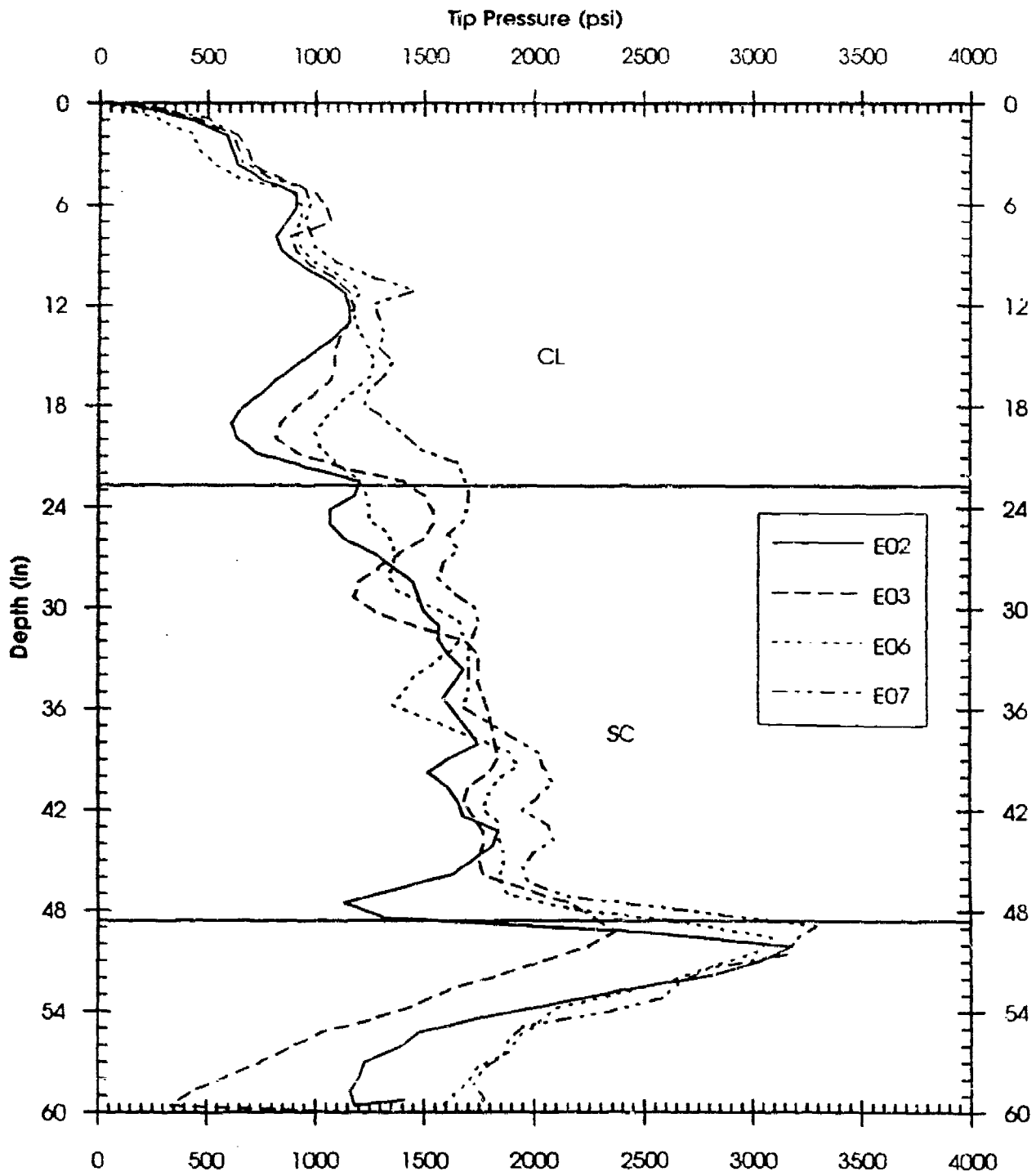

Figure F35. ECP TP versus depth for W4106

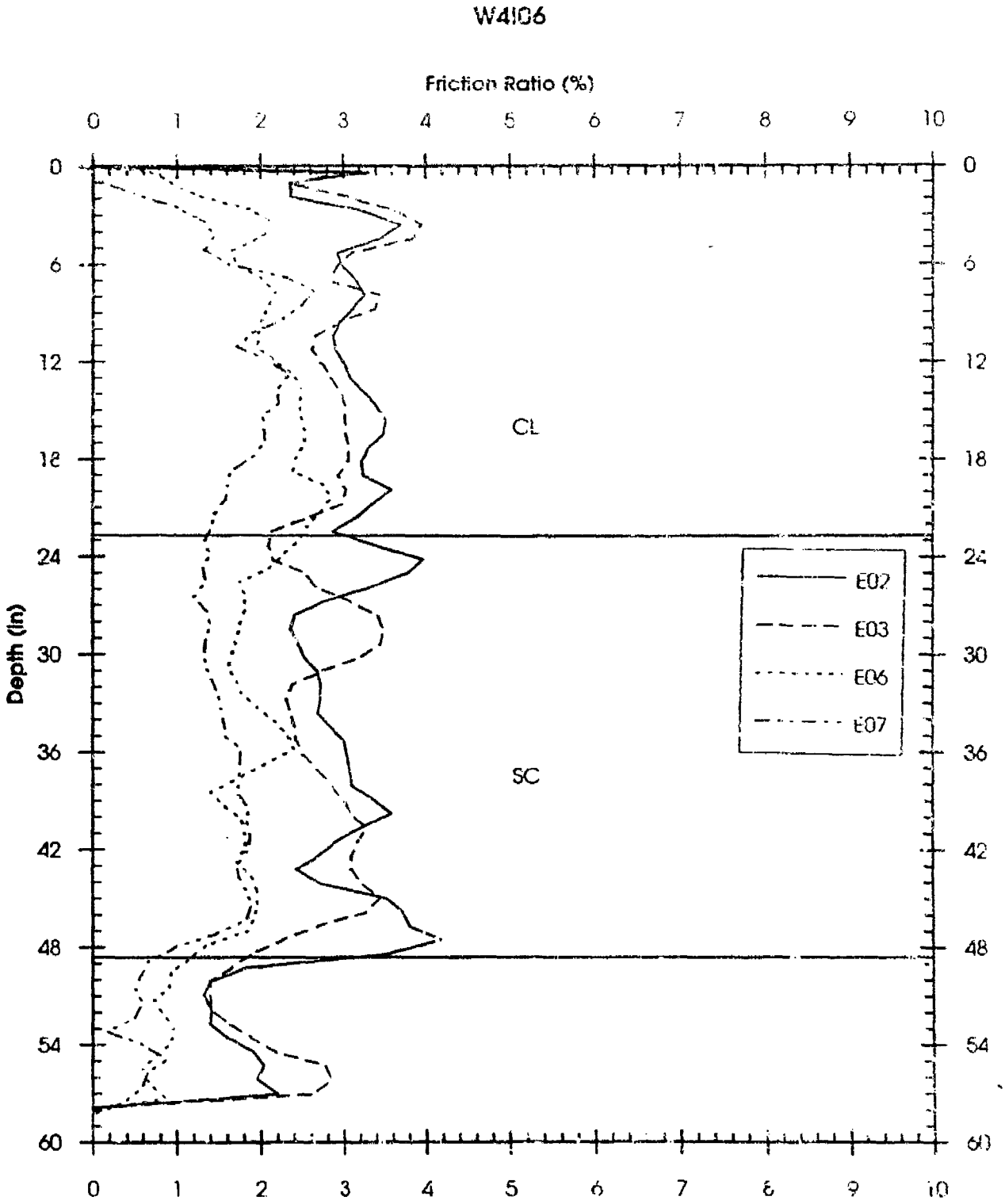

Figure F36. ECP FR versus depth for W4106

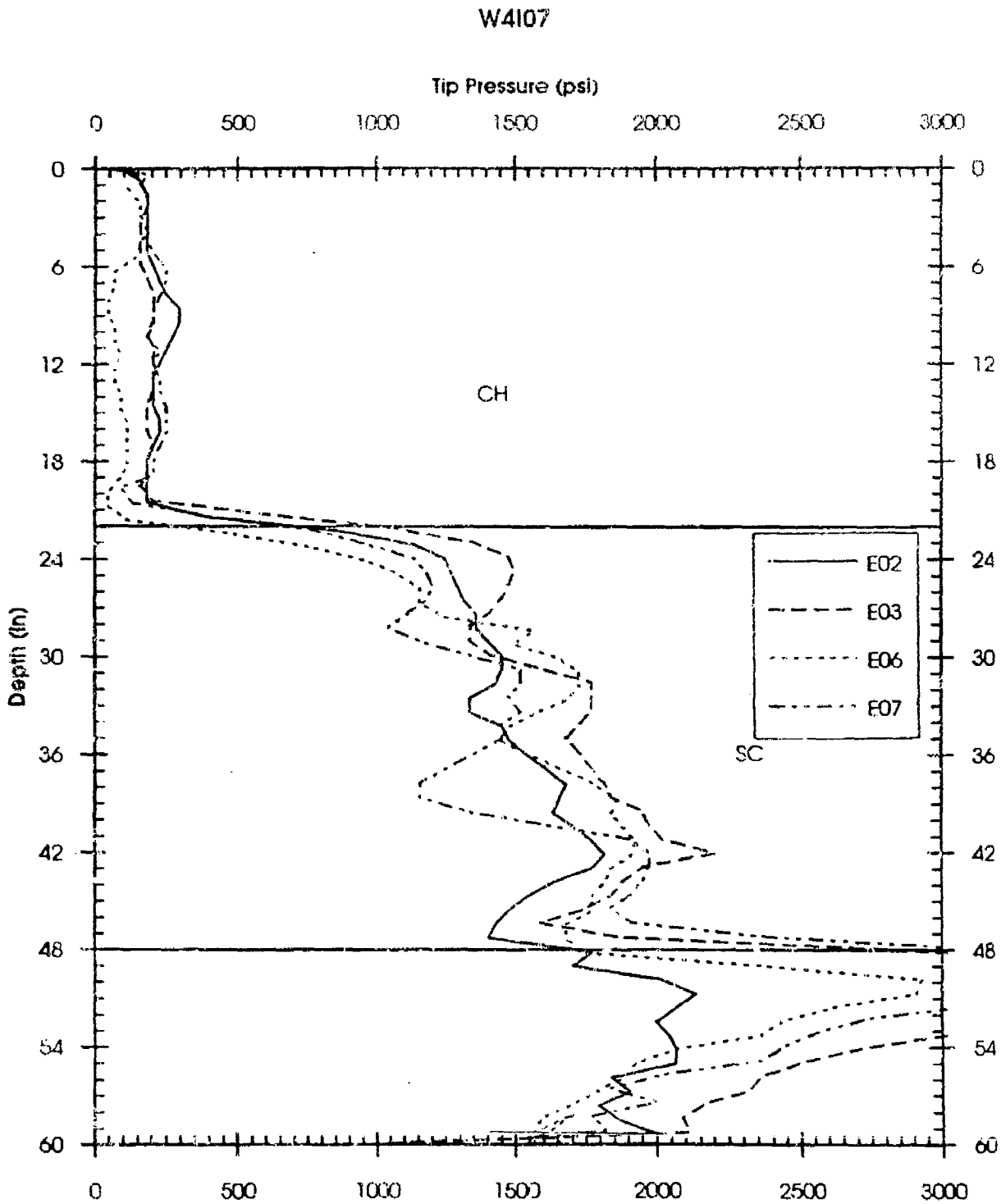

Figure F37. ECP TP versus depth for W4107

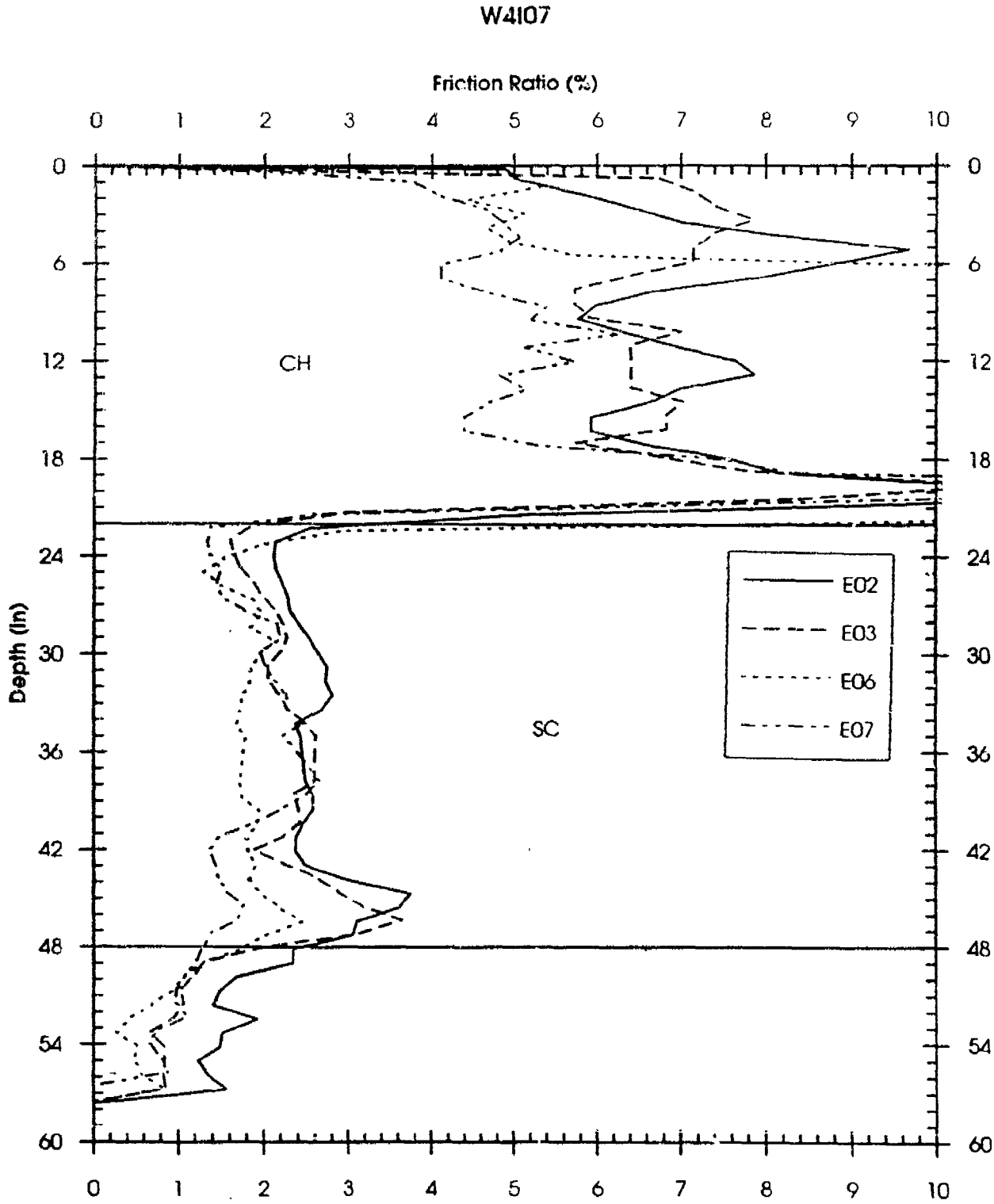

Figure F38. ECP FR versus depth for W4107

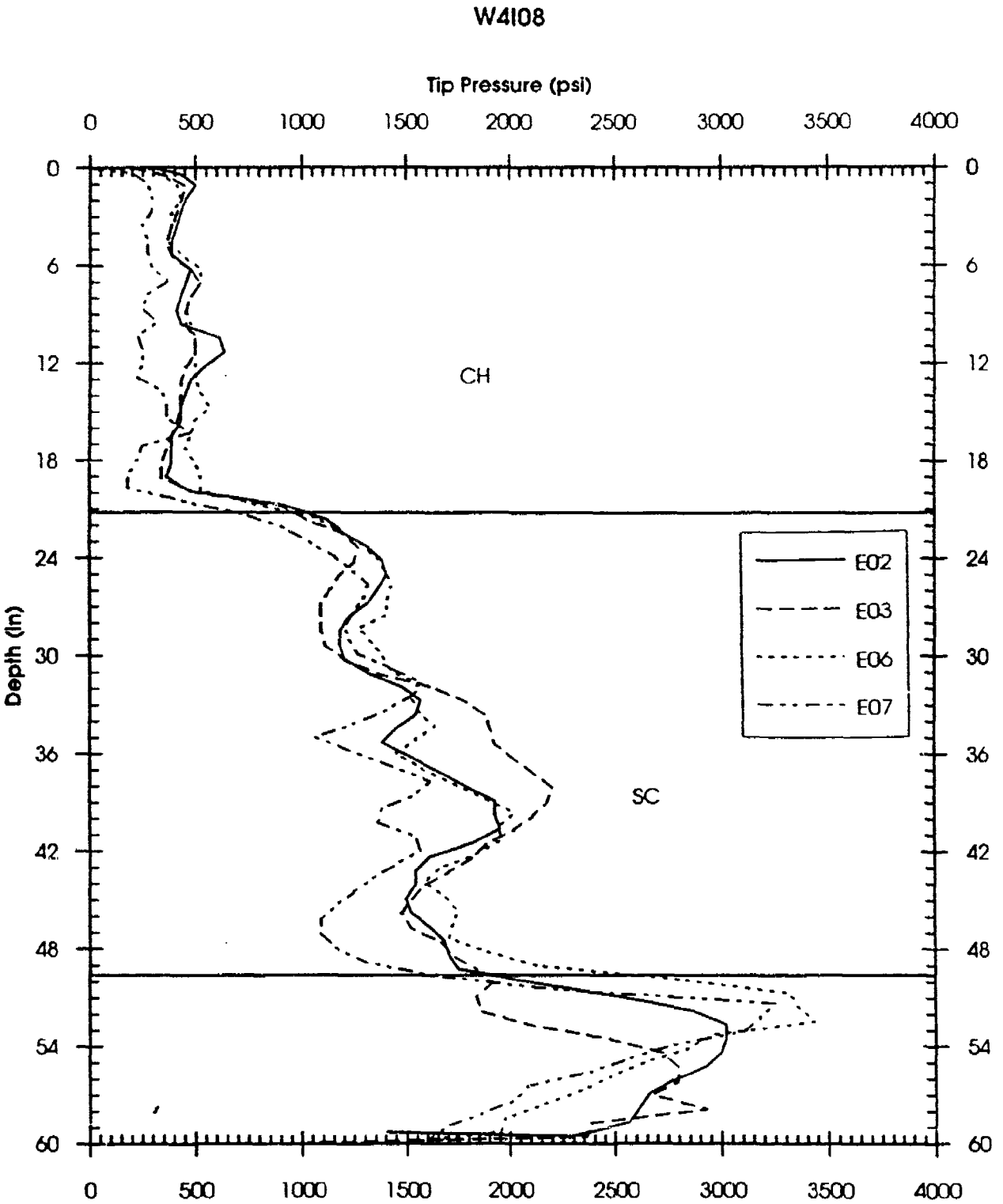

Figure F39. ECP TP versus depth for W4108

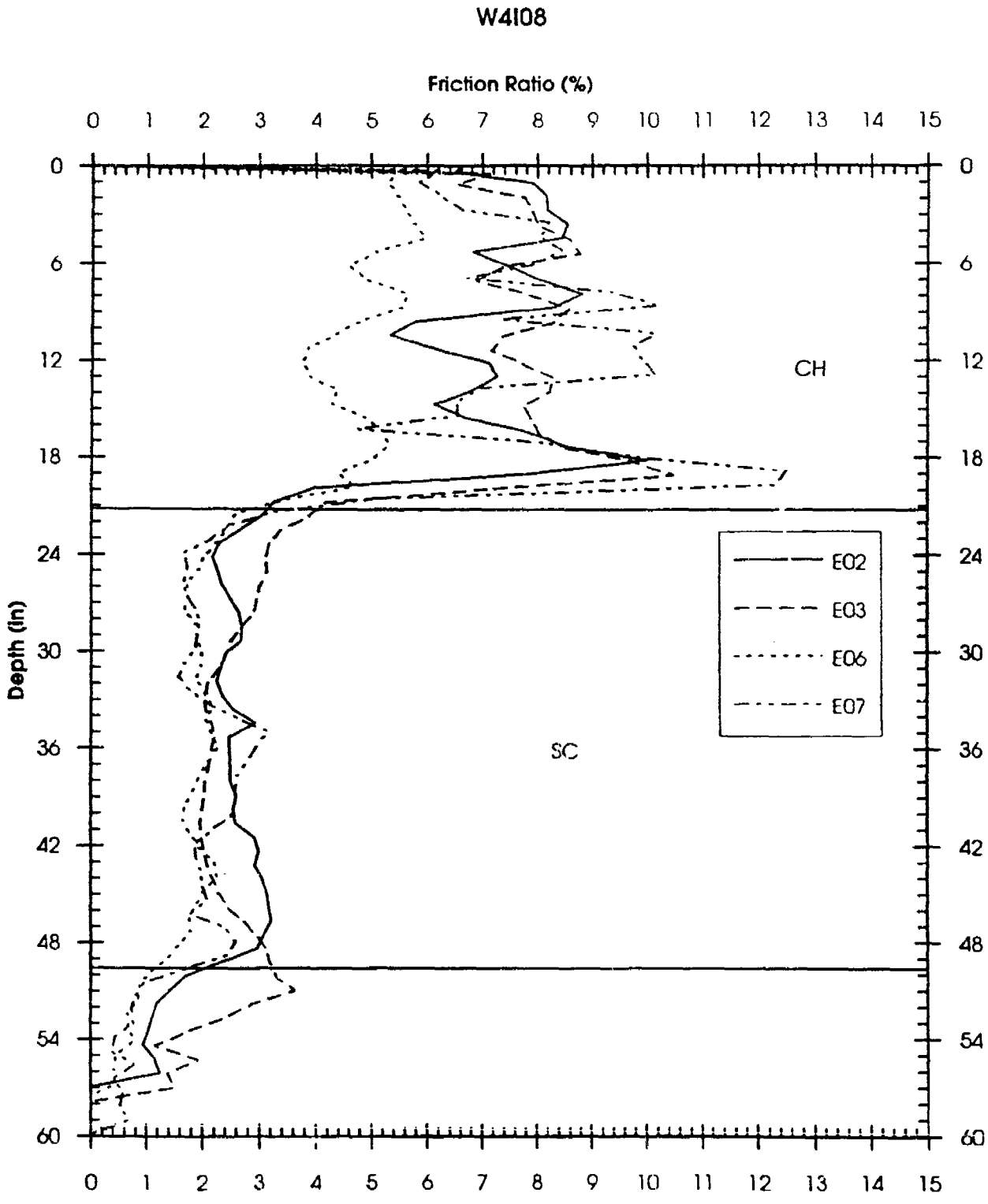

Figure F40. ECP FR versus depth for W4108

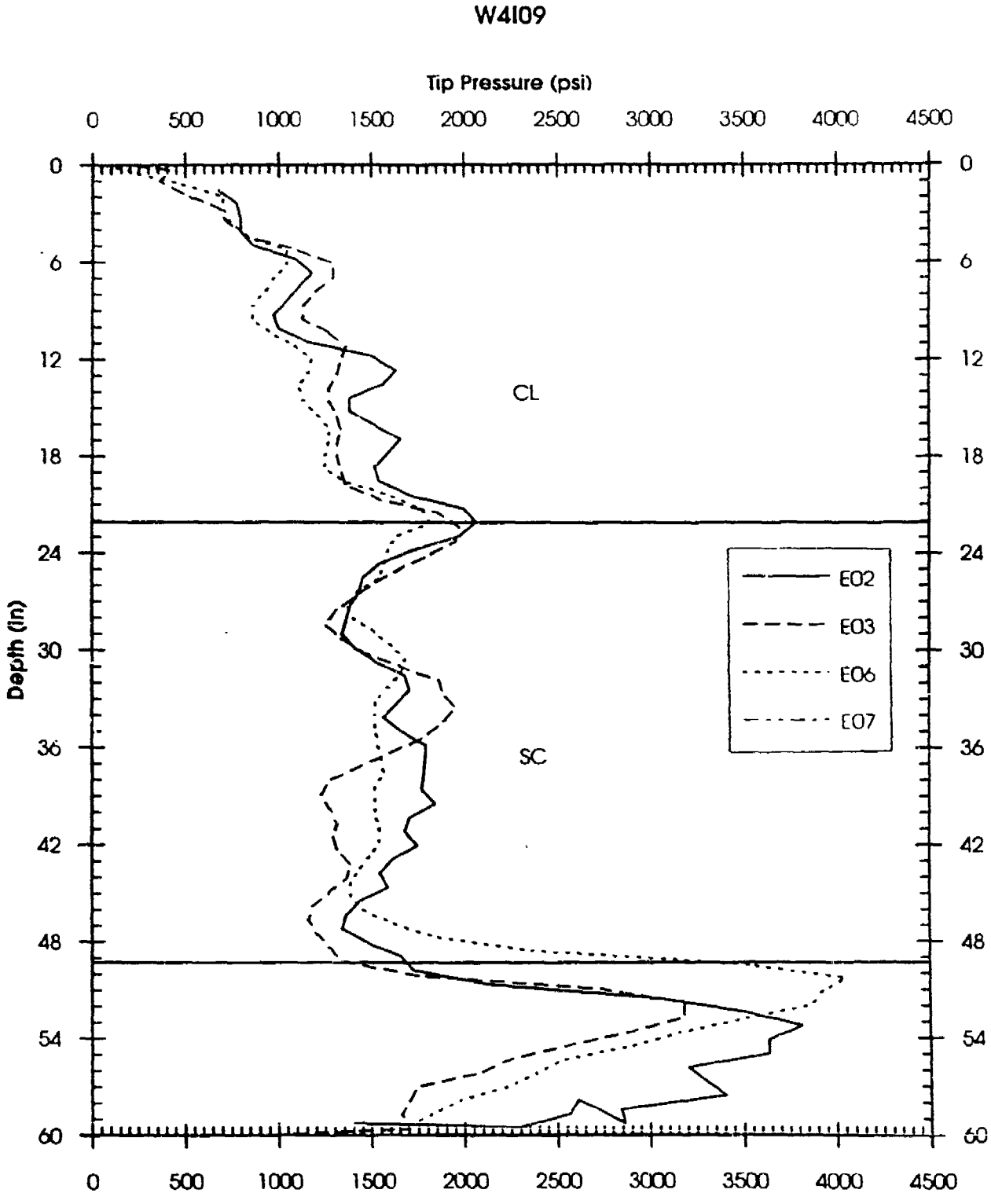

Figure F41. ECP TP versus depth for W4109

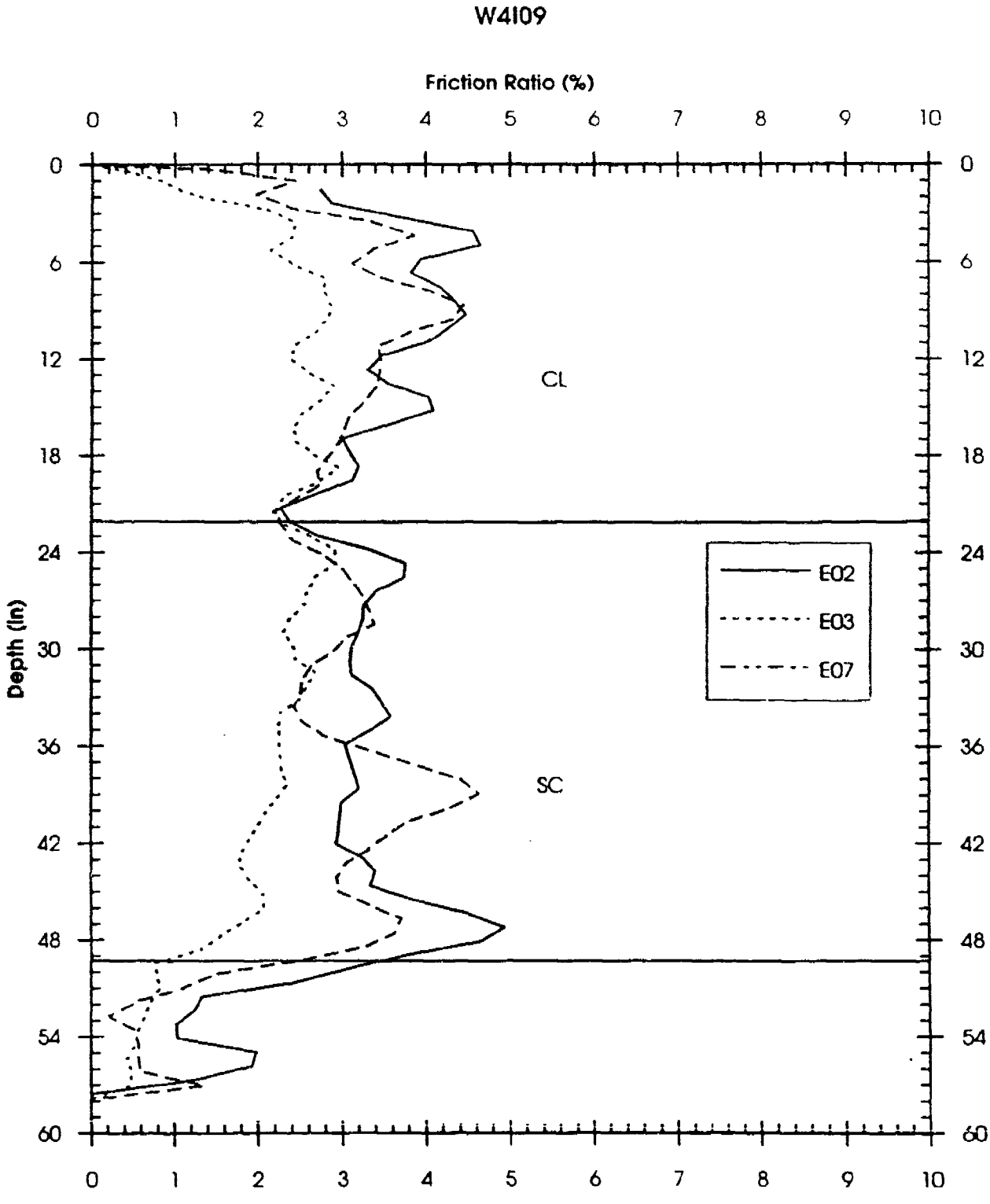

Figure F42. ECP FR versus depth for W409

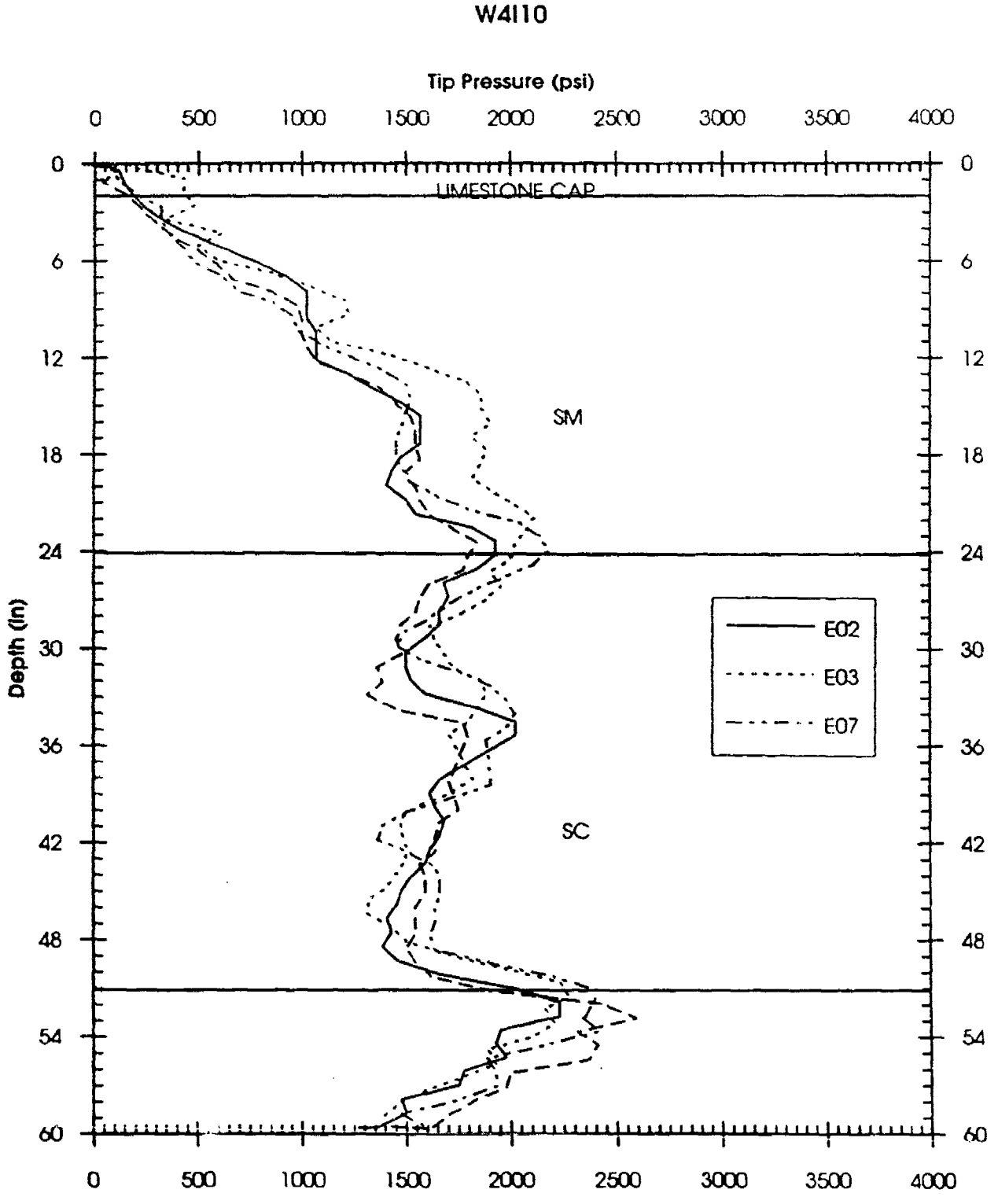

Figure F43. ECP TP versus depth for W4I10

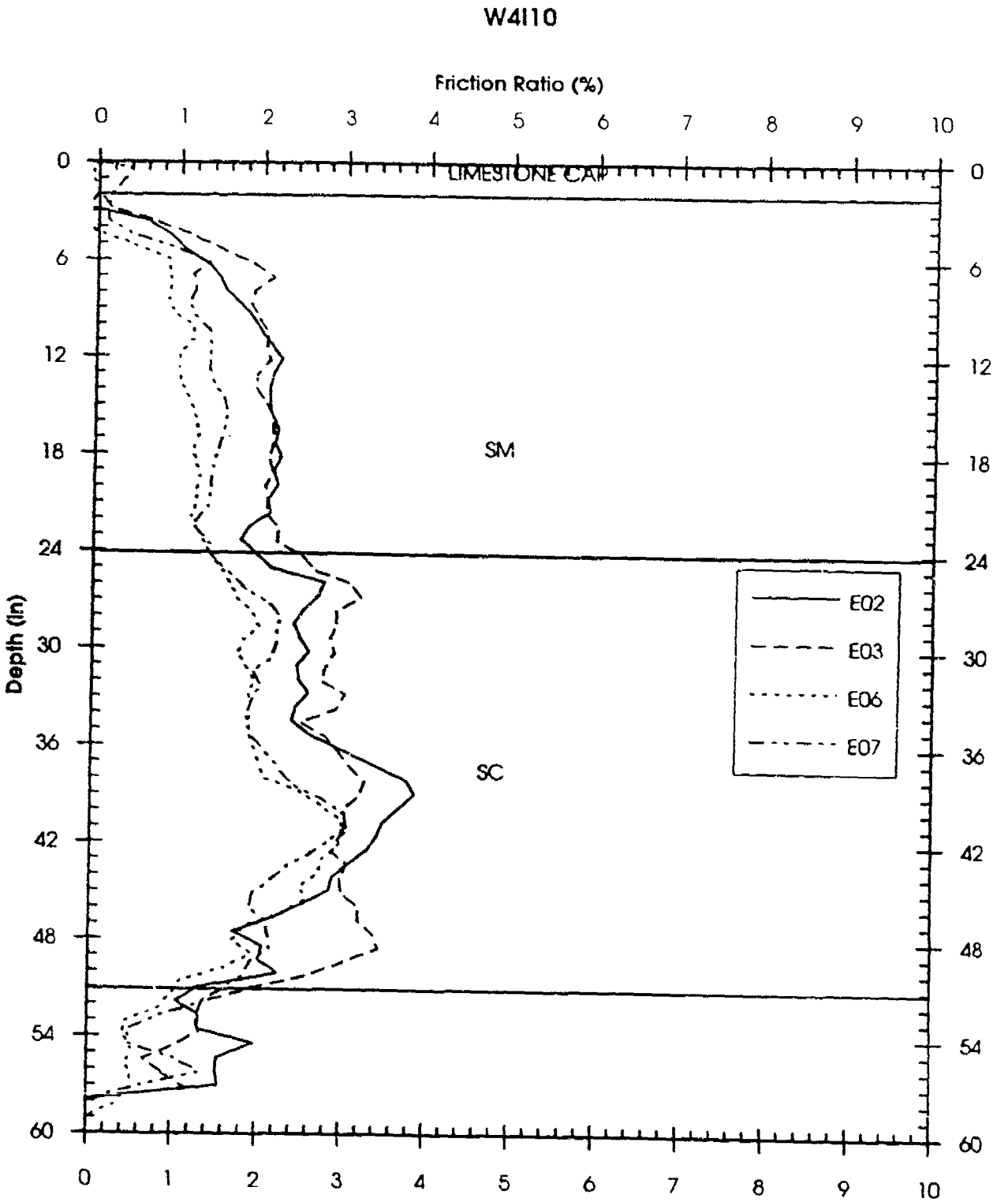

Figure F44. ECP FR versus depth for W4I10

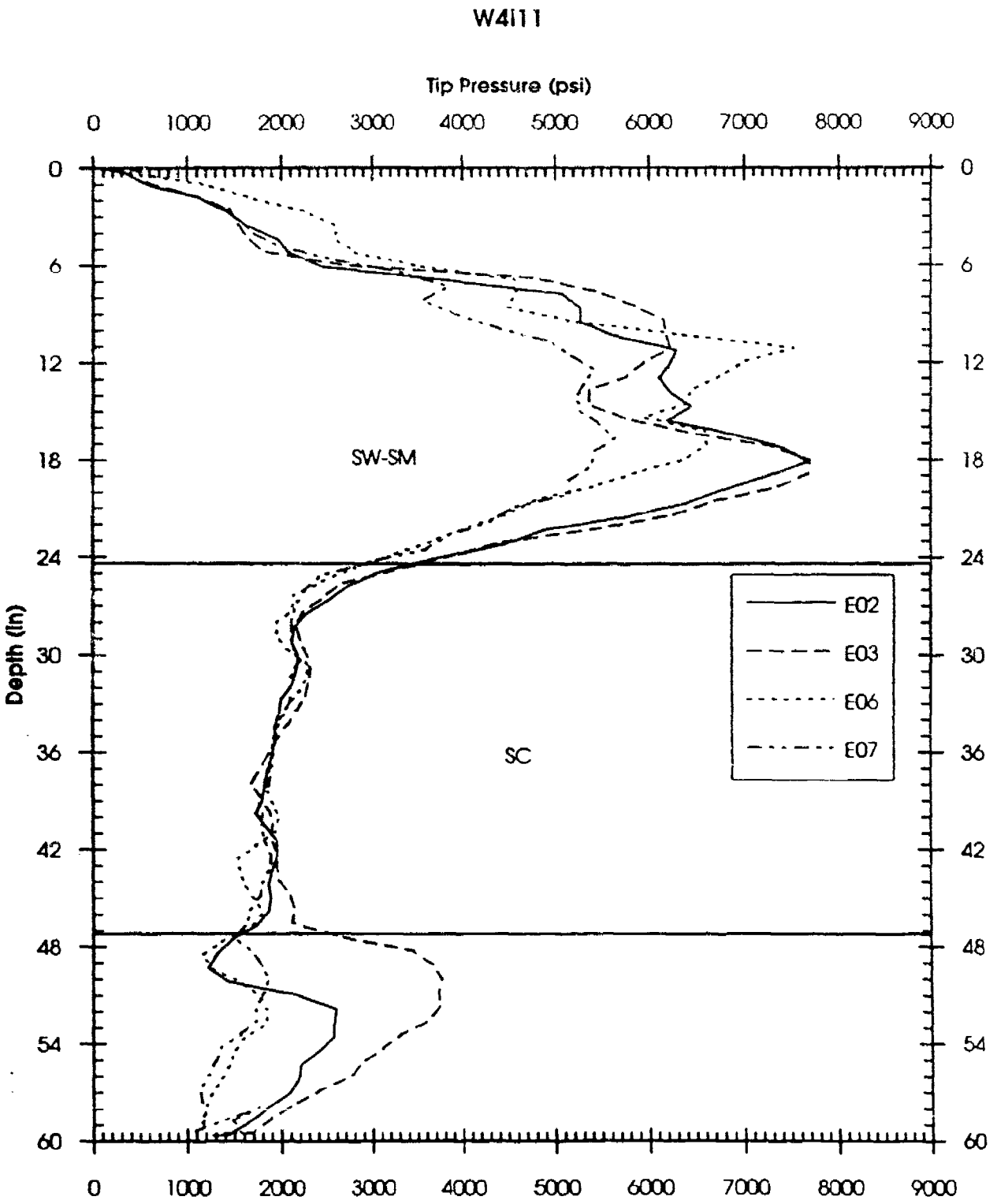

Figure F45. ECP TP versus depth for W4I11

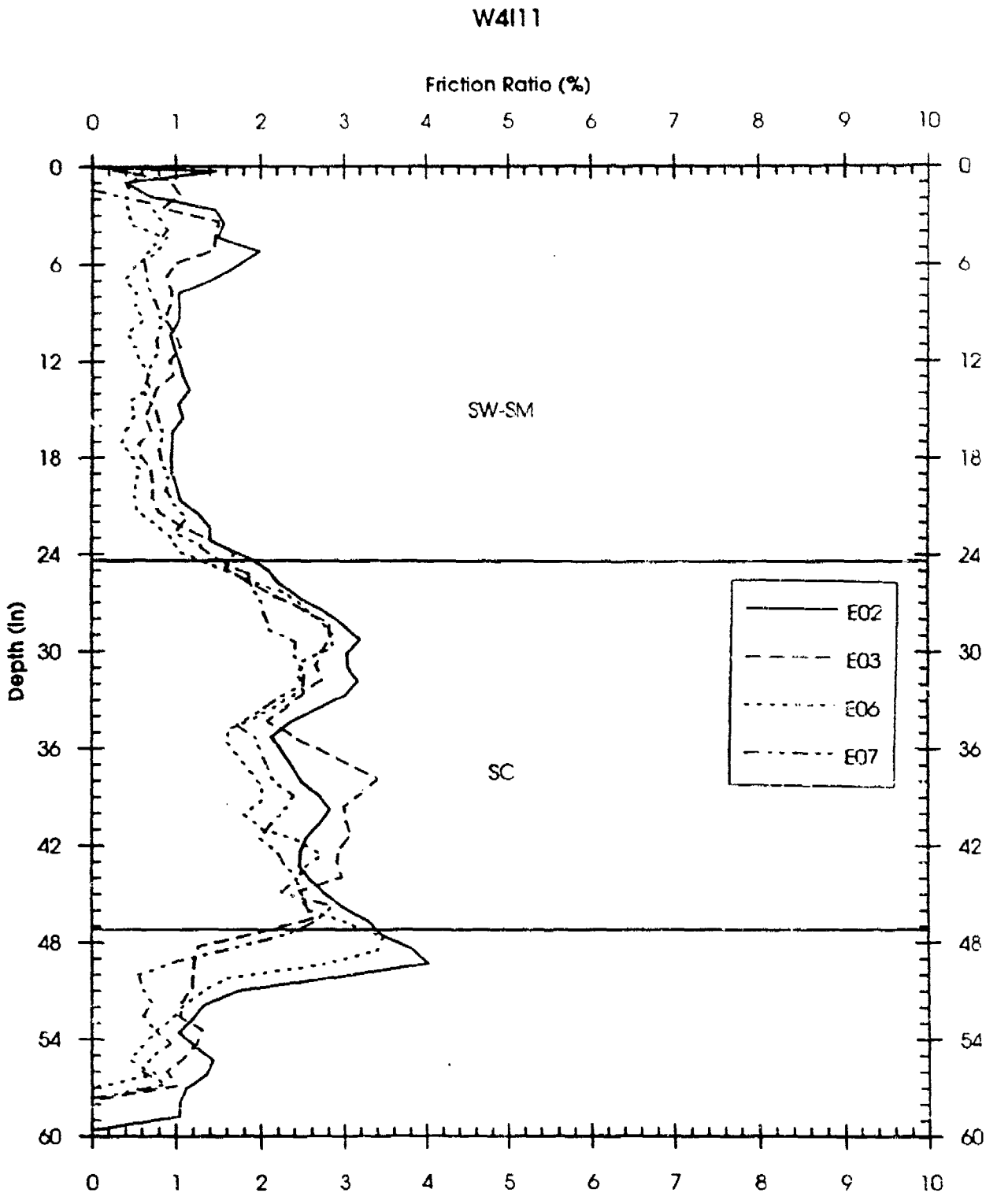

Figure F46. ECP FR versus depth for W4I11

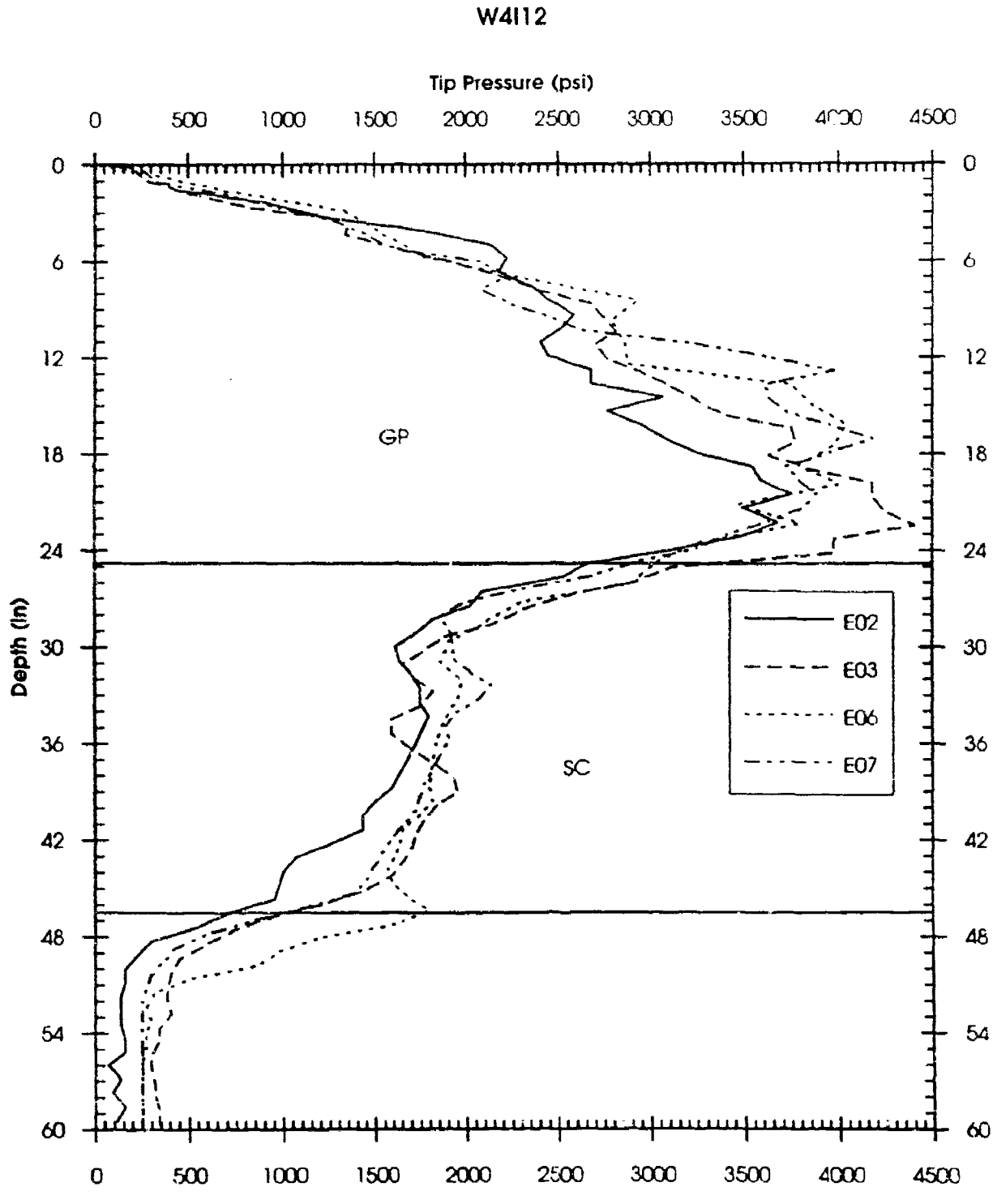

Figure F47. ECP TP versus depth for W4I12

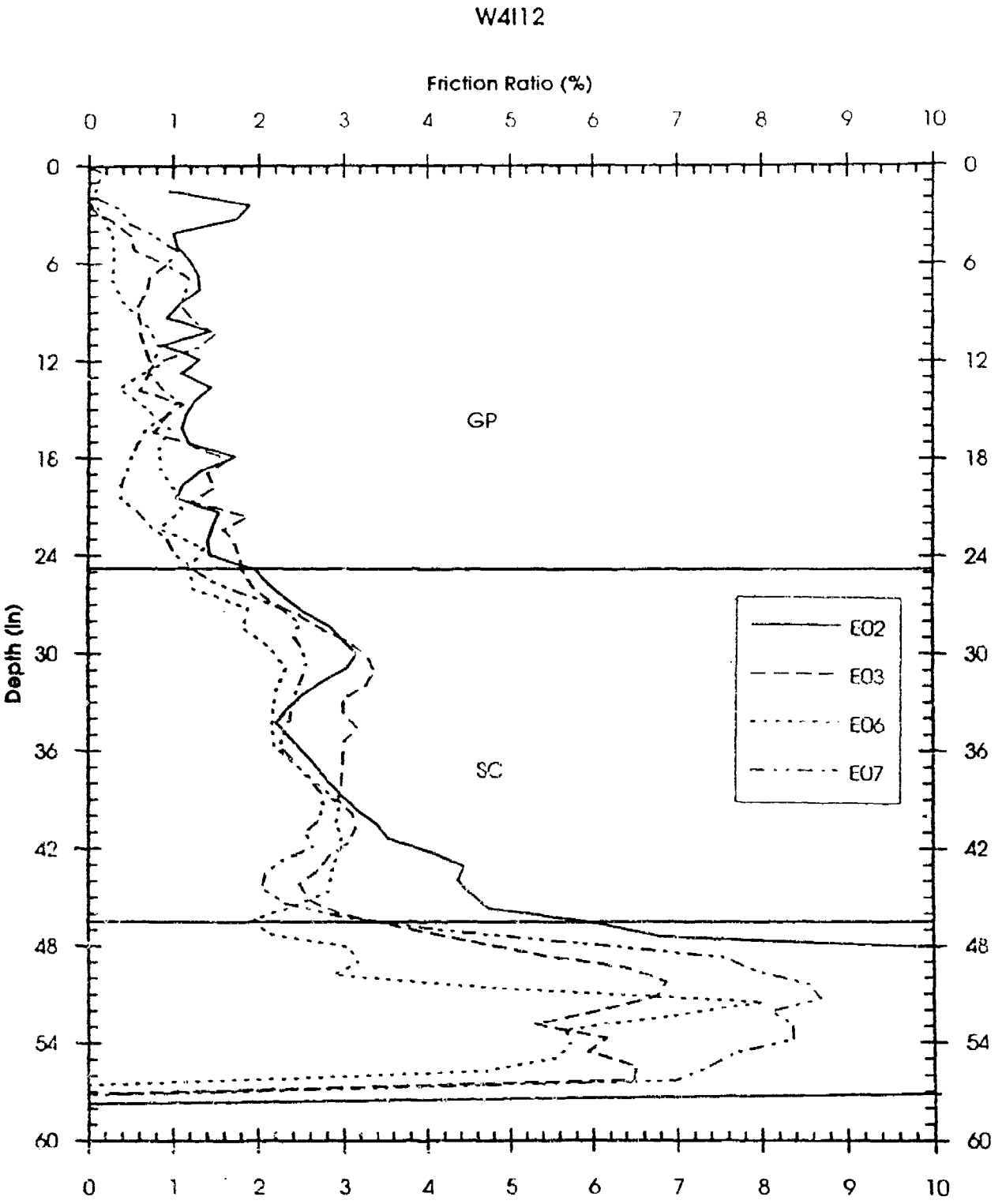

Figure F48. ECP FR versus depth for W4121

Appendix G
ECP Versus CBR Correlations, Predicted Versus Observed CBR and Normal Probability Plots

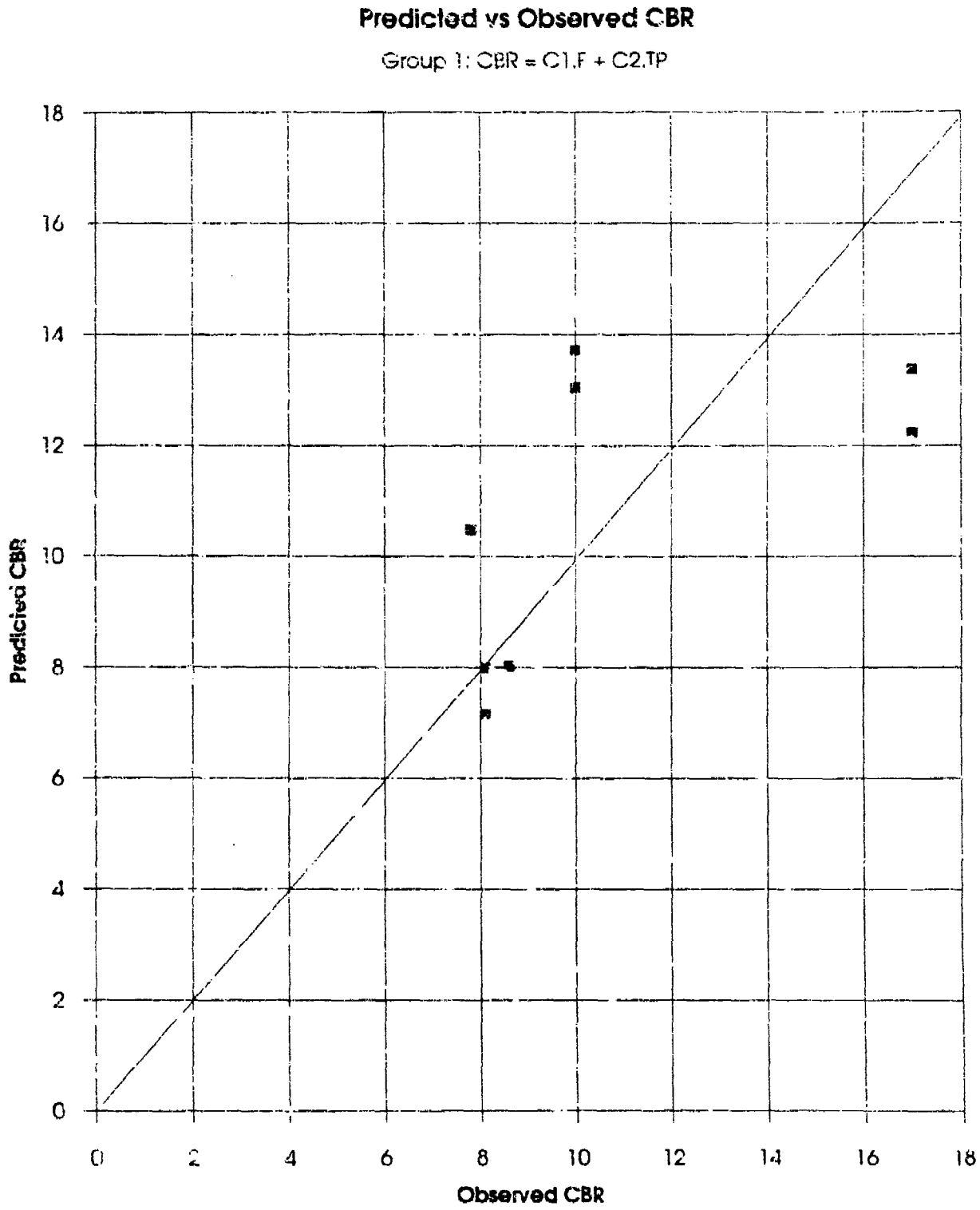

Figure G1. Group 1 predicted versus observed CBR

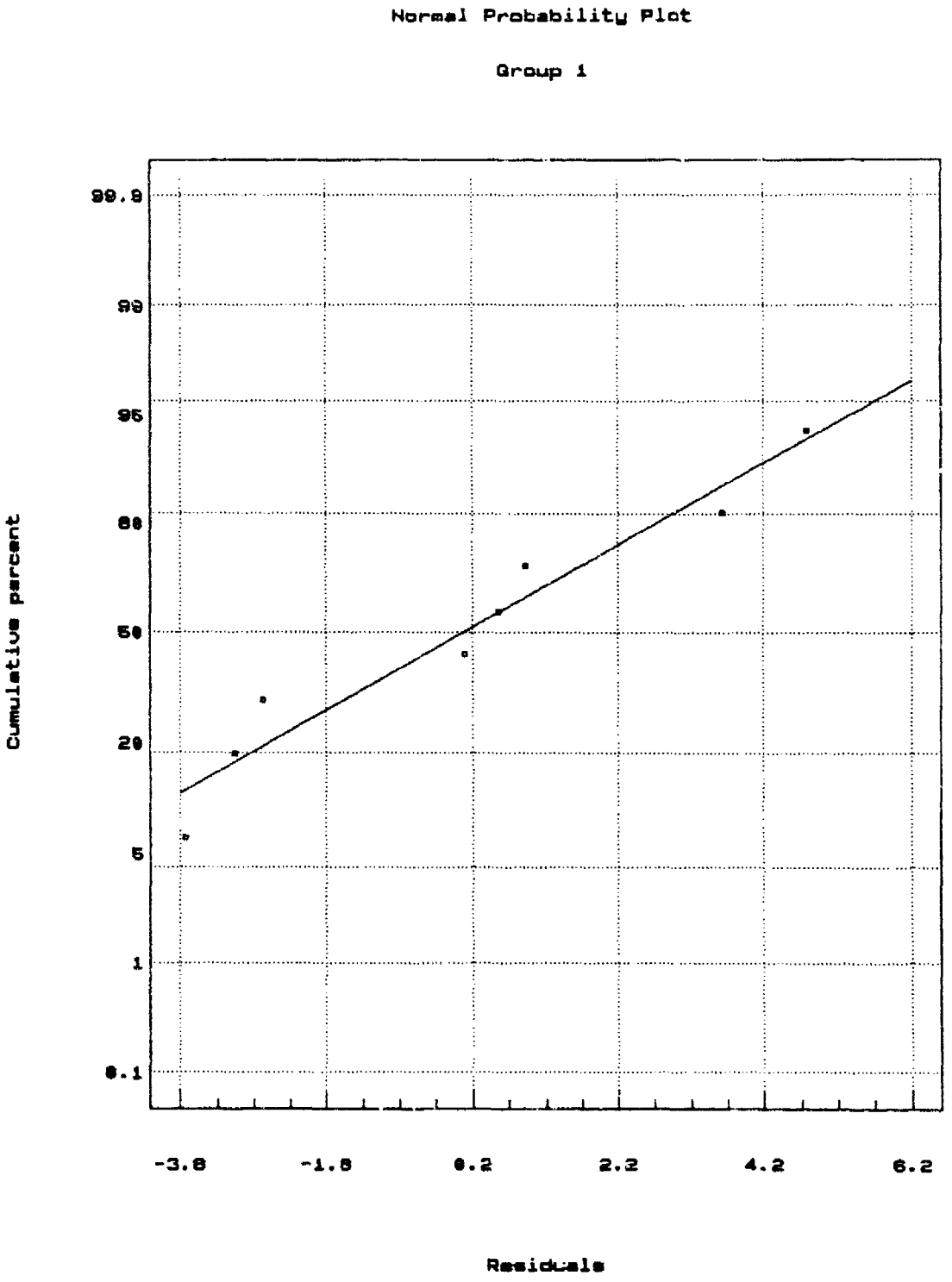

Figure G2: Group 1 normal probability plot

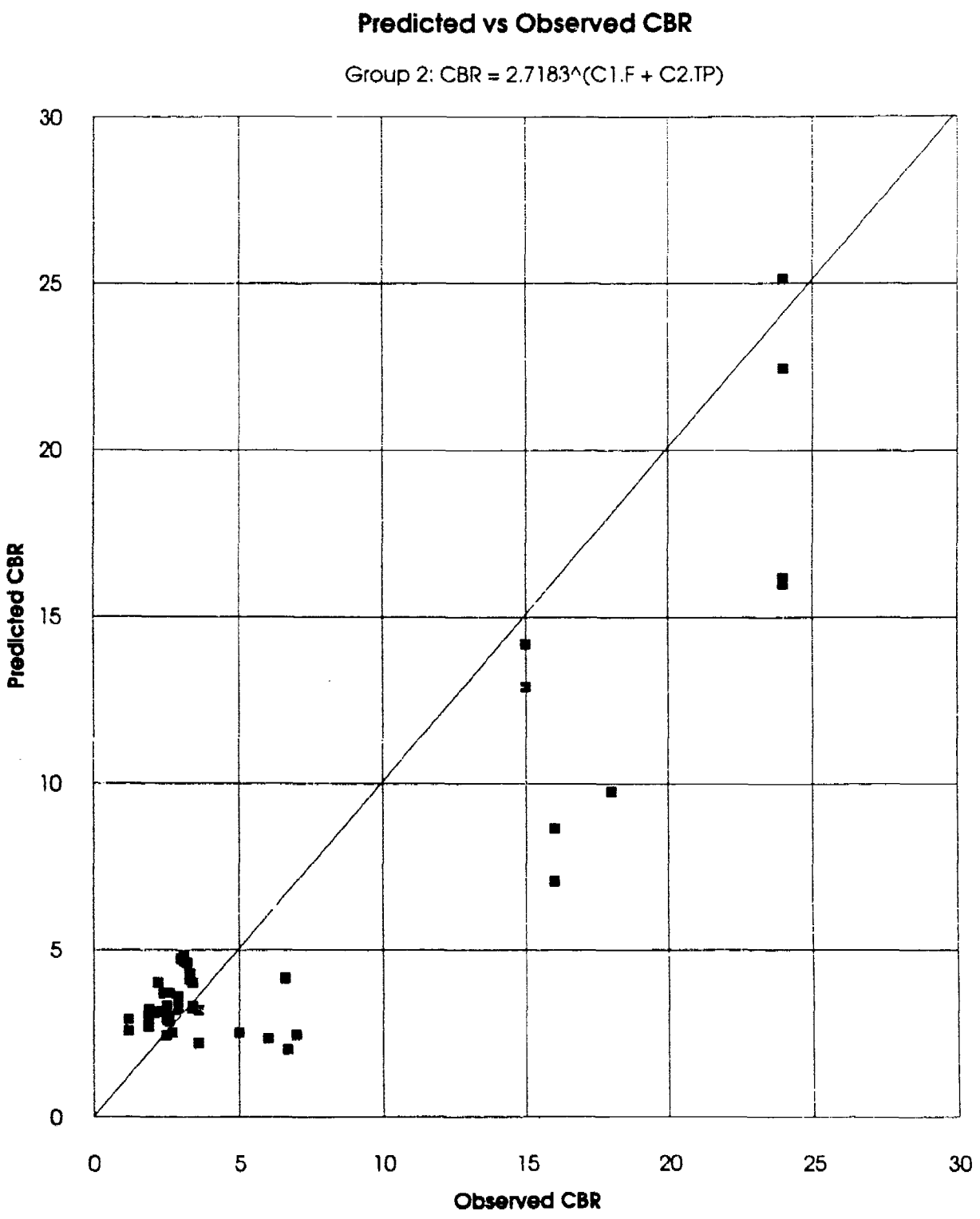

Figure G3. Group 2 predicted versus observed CBR

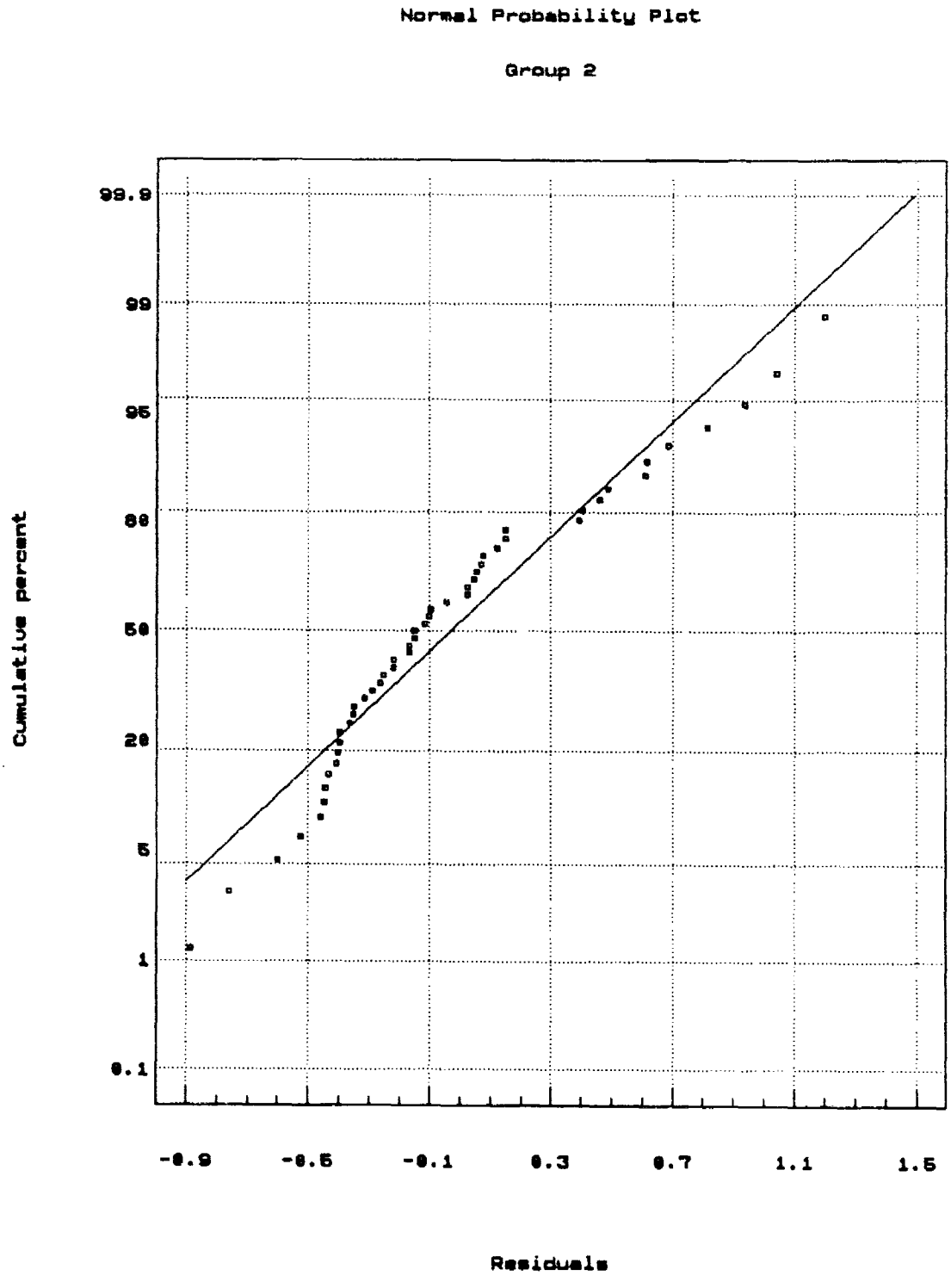

Figure G4: Group 2 normal probability plot

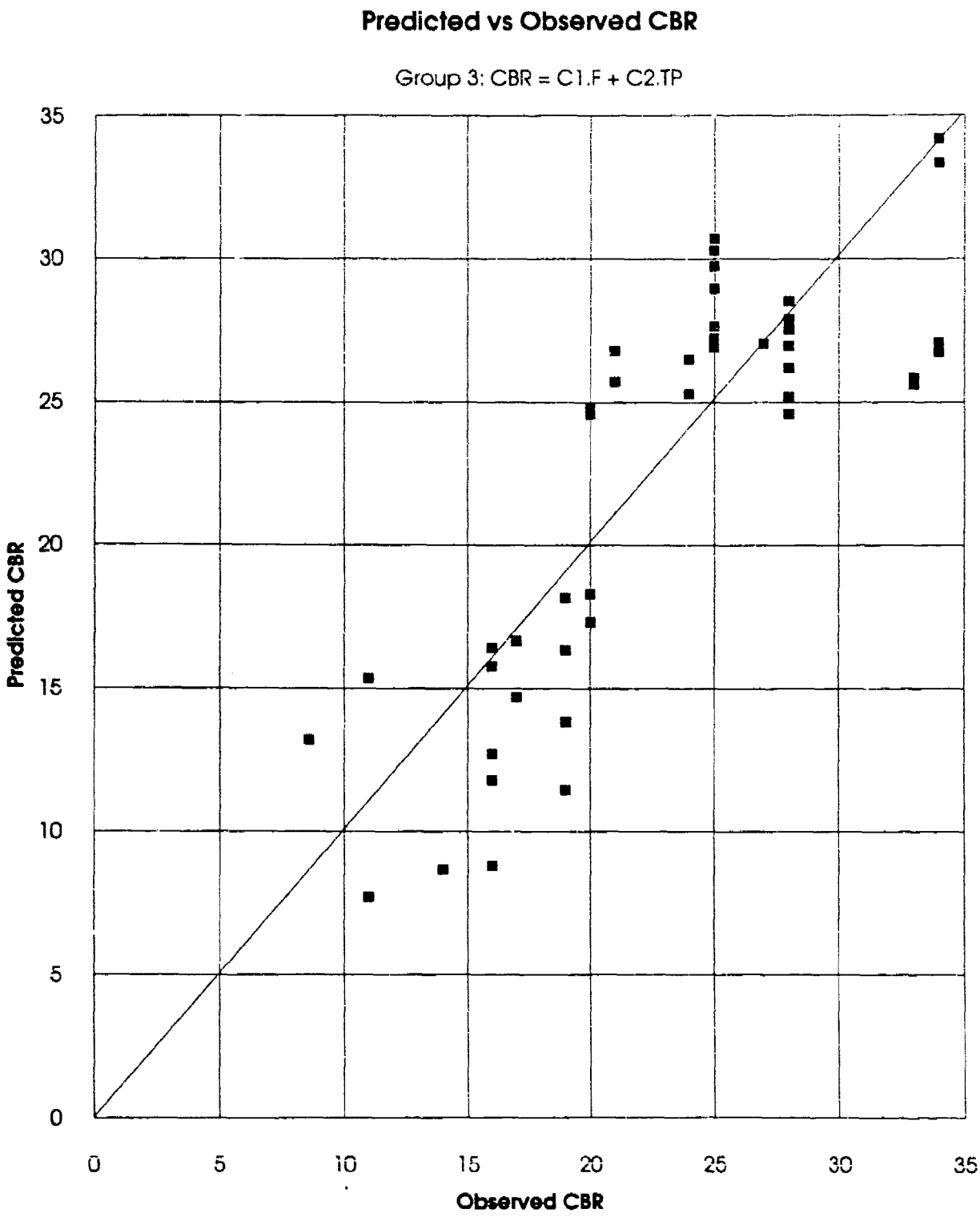

Figure G5. Group 3 predicted versus observed CBR

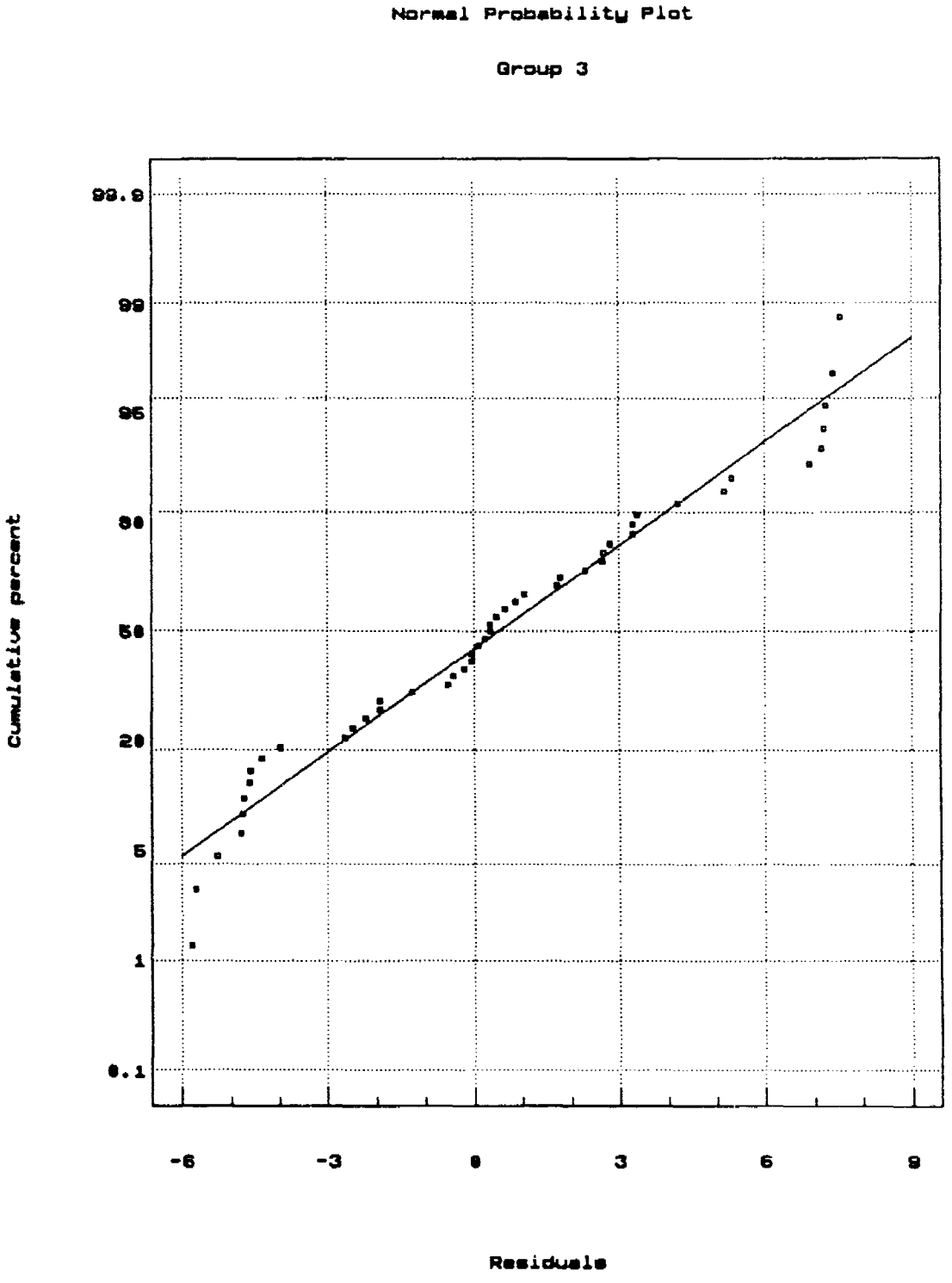

Figure G6: Group 3 normal probability plot

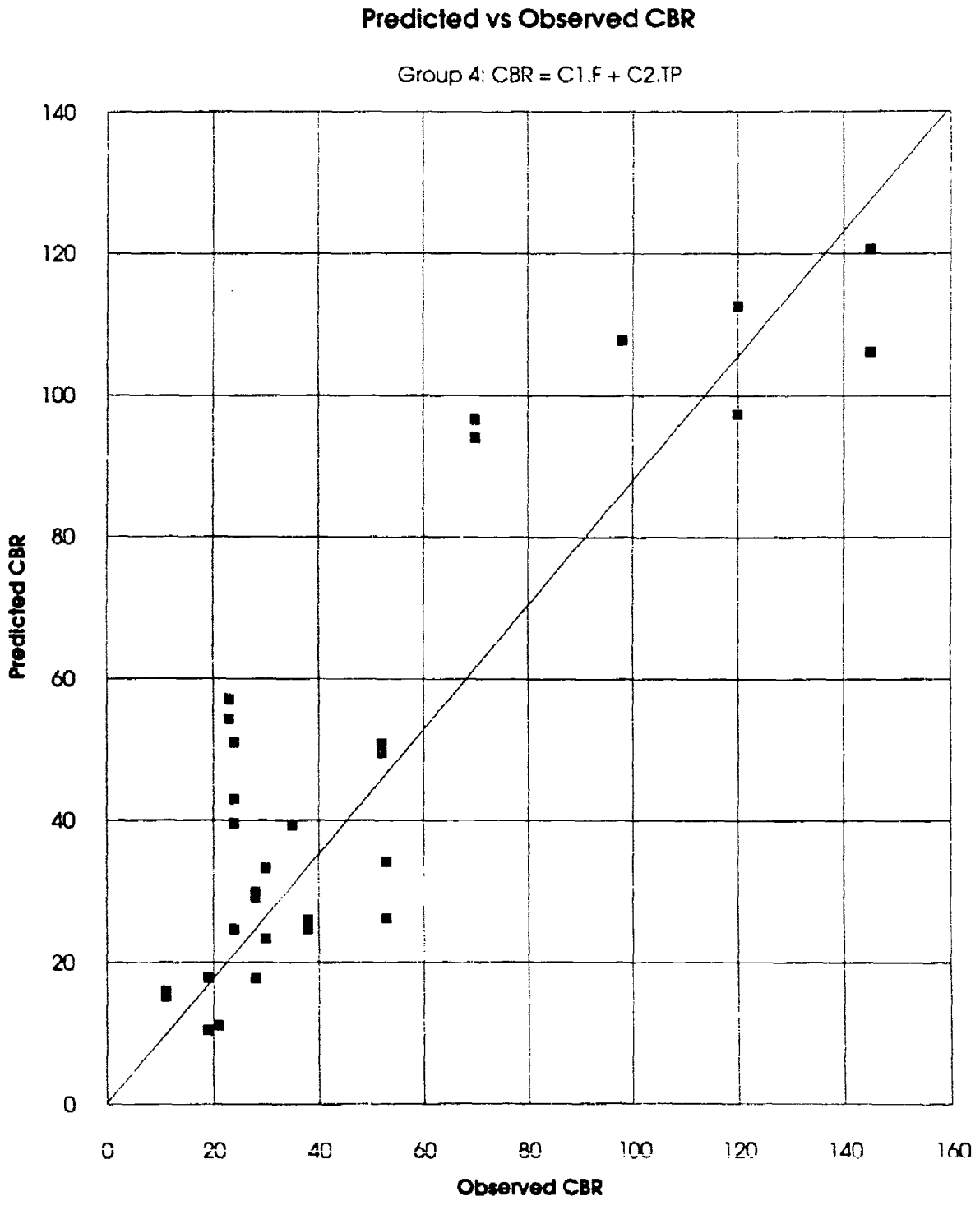

Figure G7. Group 4 predicted versus observed CBR

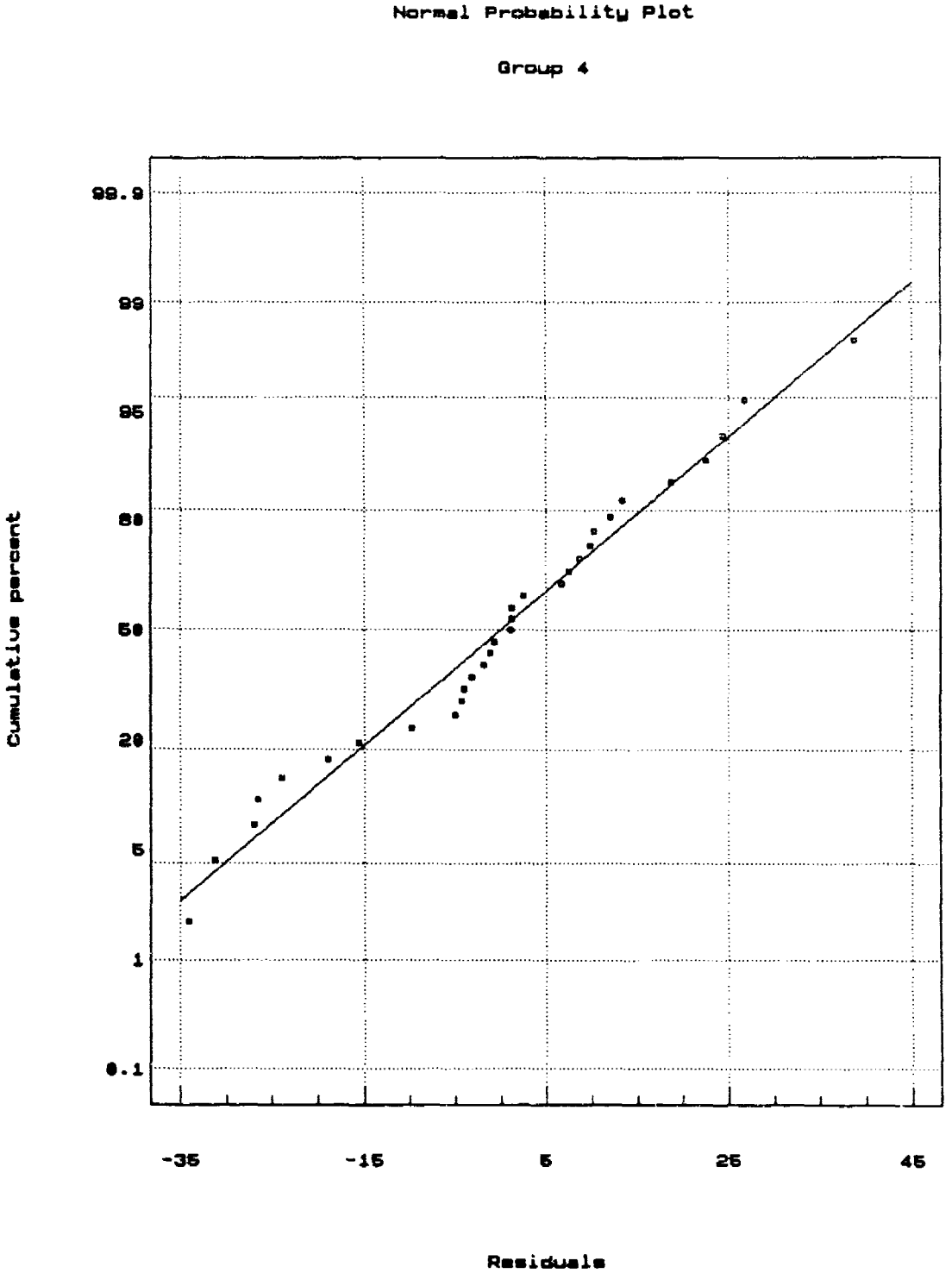

Figure G8: Group 4 normal probability plot

REPORT DOCUMENTATION PAGE

Form Approved
OMB No 0704-0188

1. AGENCY USE ONLY (Leave blank)	2. REPORT DATE	3. REPORT TYPE AND DATES COVERED
	April 1994	Final report

4. TITLE AND SUBTITLE
Force Projection Site Evaluation Using the Electric Cone Penetrometer (ECP) and the Dynamic Cone Penetrometer (DCP)

5. FUNDING NUMBERS

6. AUTHOR(S)
Steve L. Webster, Randall W. Brown, Jonathan R. Porter

7. PERFORMING ORGANIZATION NAME(S) AND ADDRESS(ES)
See reverse.

8. PERFORMING ORGANIZATION REPORT NUMBER
Technical Report
GL-94-17

9. SPONSORING / MONITORING AGENCY NAME(S) AND ADDRESS(ES)
United States Air Force
Headquarters, Air Force Civil Engineering Support Agency
Tyndall AFB, FL

10. SPONSORING / MONITORING AGENCY REPORT NUMBER

11. SUPPLEMENTARY NOTES
Available from National Technical Information Service, 5285 Port Royal Road, Springfield, VA 22161.

12a. DISTRIBUTION / AVAILABILITY STATEMENT
Approved for Public Release, Distribution is Unlimited.

12b. DISTRIBUTION CODE

13. ABSTRACT *(Maximum 200 words)*

World political and economic changes over the last decade have dictated the United States Air Force (USAF) to alter its concept of operations from prepositioning forces to projecting forces into the needed area. This force projection concept generates a requirement for rapid, accurate assessment of an unfamiliar airfield's load-carrying capability with minimum logistical support. USAF development of dynamic cone penetrometer (DCP) and electric cone penetrometer (ECP) capabilities have aided in meeting this requirement.

This study is to develop better correlations between ECP results and California Bearing Ratio (CBR) and DCP results and CBR. These correlations are essential since current evaluation charts relate allowable aircraft loads and passes to CBR. Field tests were conducted on existing airfield pavements at Maxwell AFB, AL. In addition, 28 test items reflecting a broad spectrum of materials, densities, and water contents were constructed and tested at the U.S. Army Engineer Waterways Experiment Station. This report presents the correlations developed between ECP results and CBR and between DCP results and CBR. Other significant findings of the study were (a) the ECP is an effective tool for classifying soils, (b) both the ECP and DCP can produce strength versus depth profiles, and (c) both the ECP and DCP are capable of identifying layer interfaces.

14. SUBJECT TERMS		15. NUMBER OF PAGES
California Bearing Ratio	Layer interfaces	172
Dynamic cone penetrometer	Prepositioning forces	16. PRICE CODE
Electric cone penetrometer	Projecting forces	

17. SECURITY CLASSIFICATION OF REPORT	18. SECURITY CLASSIFICATION OF THIS PAGE	19. SECURITY CLASSIFICATION OF ABSTRACT	20. LIMITATION OF ABSTRACT
UNCLASSIFIED	UNCLASSIFIED		

7. Concluded

U.S. Army Engineer Waterways Experiment Station
3909 Halls Ferry Road
Vicksburg, MS 39180-6199

Department of Civil Engineering
USAF Academy, CO

Wright Laboratory
Tyndall AFB, FL